UNIVERSITY OF CALIFORNIA SAN DIEGO

Annelids and Mollusks from Chemosynthetic Environments of the Pacific Ocean

A dissertation submitted in partial satisfaction of the
requirements for the degree Doctor of Philosophy

in

Marine Biology

by

Marina McCowin

Committee in charge:

Professor Gregory Rouse, Chair
Professor Ronald Burton
Professor Lisa Levin
Professor Deirdre Lyons
Professor Kaustuv Roy

2022

The Dissertation of Marina McCowin is approved, and it is acceptable in quality and form for publication on microfilm and electronically.

University of California San Diego

2022

DEDICATION

To Em.

TABLE OF CONTENTS

LIST OF FIGURES

LIST OF TABLES

LIST OF SUPPLEMENTARY FILES

ACKNOWLEDGEMENTS

To Dr. Greg Rouse: Thank you so much for sharing your expertise and support over the years. From the very first class I took of yours as an undergraduate, I was inspired by your teaching skills and passion for your research–thank you for bringing me into your lab that first summer back in 2015. I have learned so much from working with you in our lab, and have so enjoyed working with you and learning from you as a TA. I feel so lucky to have gotten the chance to work with such a passionate and skilled scientist and lecturer, and to be exposed to so many new and fascinating molecular techniques in the lab. Your support and advocacy for me, your encouragement of my pursuit of teaching opportunities and industry work, and more have meant so incredibly much to me. Thank you for all your work as my advisor.

To Dr. Ron Burton: Thank you so much for your support, your patience, and your willingness to answer questions. Your molecular ecology and genomics seminar courses were two of my absolute favorites during my graduate career–I enjoyed and learned so much from them and from you.

To Dr. Lisa Levin: I am so inspired by you and your incredible work and advocacy for deep-sea animals and environments. Thank you so much for your encouragement, your passion, and reminders to look at the big picture. I have enjoyed and been so stimulated by our conversations and your questions, and am truly grateful to have been able to interact with and learn from you so much in person during the course of my program.

To Dr. Dede Lyons: Thank you so much for your support, kindness, and encouragement over the years. You inspire me and remind me of the power of women scientists, and your kindness and acceptance have helped me to feel like I belong here.

To Dr. Kaustuv Roy: Thank you so much for your advice and support. Your approach to science inspires me and your encouragement has been so important to my confidence as a researcher.

To the Rouse Lab (past and present): Thank you to all of you for the wonderful support and community that we have built together over the years. Special thanks to Avery Hiley for

your boundless enthusiasm, labwork solidarity, and our many lunch chats about our research. I am so grateful for your love and support, especially over the last few years when things were tough. Thank you to Charlotte Seid for your collection management expertise (so many samples and so much cataloguing over these last five years), and also for your friendship, support, and encouragement to maintain some work-life-balance. Thank you to Jose Carvajal, Josefin Stiller, Ekin Tilic, and Nicolas Mongiardino-Koch–I have learned so much from all of you and your support has meant the world to me. Thank you to all of my "invertemates" at the Rouse Lab, and especially to Chrissy Tustison, Cassandra Koga, Gabriella Berman, Sonja Huc,and Tiffany Wong as we figured things out during the pandemic together. Every member of the Rouse Lab, new and old, has brought me so much joy during my time here–thank you all so much.

To the SIO Grad Office: Thank you so much for your assistance and patience, and especially to Gilbert Bretado, Shelley Weisel, and Maureen McGreevy. You are all deeply appreciated. Thank you also to our Facilities Specialist Dejan Ristic–so grateful to you for everything you've done for our lab and it's always a joy to see you around Hubbs.

To my friends at SIO, UCSD, and beyond: Thank you to all of you for your support and solidarity. Thanks especially to Beverly French, Erica Bender, Erica Mason, and Haley McInnis–your camaraderie and community were a real driving force that helped me dig deep and finish. I am so grateful to all of you, and so proud to know you and call you my friends.

To my mother and grandmother: Mom–thank you so much for the myriad ways in which you've supported me, from raising me to be a strong and resilient woman, to your constant support and encouragement to find and do what brings me joy. I will never forget our many long talks on the phone, your advice, and your help navigating through tough times. Grandma–you have always been such an inspiration for me to find balance and happiness. I am so grateful for our quiet talks over laundry, for our comfortable silence together, and for your incredibly healing hugs. I am so lucky to be the daughter and granddaughter of such strong and inspiring women, and would never have finished a PhD program without you two. Thank you both for your love and support.

To Em: Your love and support over these wild five years have meant everything. We have grown so much together, and you have sacrificed so much for me so I could follow this dream–I would not be here now without you. I cannot thank you enough for all the late nights, cooking, listening, and reminders to be human, your love and acceptance even in my worst moments, and your endless support when the road got rough. I can't wait to continue on to our next great adventure together. TMD.

Chapter 1, in full, is a reprint of the material as it appears in *Deep-Sea Research Part I: Oceanographic Research Papers*. McCowin, Marina F., Feehery, Caitlin, and Rouse, Greg W. (2020). Spanning the depths or depth-restricted: Three new species of *Bathymodiolus* (Bivalvia, Mytilidae) and a new record for the hydrothermal vent *Bathymodiolus thermophilus* at methane seeps along the Costa Rica margin. *Deep-Sea Research Part I: Oceanographic Research Papers* 164, 103322. The dissertation author was the primary investigator and author of this paper.

Chapter 2, in full, is a reprint of the material as it appears in *Zookeys*. McCowin, Marina F. and Rouse, Greg W. (2018). Phylogeny of hydrothermal vent Iphionidae, with the description of a new species (Aphroditiformia, Annelida). *Zookeys* 779: 89-107. The dissertation author was the primary investigator and author of this paper.

Chapter 3, in full, is a reprint of the material as it appears in *Zootaxa*. McCowin, Marina F. and Rouse, Greg W. (2018). A new *Lamellibrachia* species and confirmed range extension for *Lamellibrachia barhami* (Siboglinidae, Annelida) from Costa Rica methane seeps. Zootaxa 4504(1): 1-22. The dissertation author was the primary investigator and author of this paper.

Chapter 4, in full, is a reprint of the material as it appears in *Marine Biodiversity Records*. McCowin, Marina F., Rowden, Ashley A., and Rouse, Greg W. (2019). A new record of *Lamellibrachia columna* (Siboglinidae, Annelida) from cold seeps off New Zealand, and an assessment of its presence in the western Pacific Ocean. *Marine Biodiversity Records* 12 (10): 12. The dissertation author was the primary investigator and author of this paper.

Chapter 5 is being prepared for publication of the material. McCowin, Marina F., Collins, Patrick C., and Rouse, Greg W. The dissertation author was the primary researcher and author of

this material.

VITA

2015 Bachelor of Science in Marine Biology, University of California San Diego

2022 Doctor of Philosophy in Marine Biology, University of California San Diego

PUBLICATIONS

McCowin, Marina F., Feehery, Caitlin, and Rouse, Greg W. (2020). Spanning the depths or depth-restricted: Three new species of *Bathymodiolus* (Bivalvia, Mytilidae) and a new record for the hydrothermal vent *Bathymodiolus thermophilus* at methane seeps along the Costa Rica margin. *Deep-Sea Research Part I: Oceanographic Research Papers* 164, 103322.

McCowin, Marina F., Rowden, Ashley A., and Rouse, Greg W. (2019). A new record of *Lamellibrachia columna* (Siboglinidae, Annelida) from cold seeps off New Zealand, and an assessment of its presence in the western Pacific Ocean. *Marine Biodiversity Records* 12 (10): 12.

McCowin, Marina F. and Rouse, Greg W. (2018). A new *Lamellibrachia* species and confirmed range extension for *Lamellibrachia barhami* (Siboglinidae, Annelida) from Costa Rica methane seeps. *Zootaxa* 4504(1): 1-22.

McCowin, Marina F. and Rouse, Greg W. (2018). Phylogeny of hydrothermal vent Iphionidae, with the description of a new species (Aphroditiformia, Annelida). *Zookeys* 779: 89-107.

ABSTRACT OF THE DISSERTATION

Annelids and Mollusks from Chemosynthetic Environments of the Pacific Ocean

by

Marina McCowin

Doctor of Philosophy in Marine Biology

University of California San Diego, 2022

Professor Gregory Rouse, Chair

This dissertation utilized molecular methods to reveal new species of annelids and mollusks from chemosynthetic environments in the Pacific Ocean and examined their biogeography and evolutionary history. Sanger sequencing revealed three new species of *Bathymodiolus* mussels that are partially restricted by depth at seeps along the Costa Rica Margin, and confirmed the presence of *B. thermophilus* at a seep with molecular data for the first time. New species of the iphionid *Thermiphione* and vestimentiferan tube worm *Lamellibrachia* are also described using a combination of Sanger-sequenced molecular data and morphological data. The close relationship of the new *Lamellibrachia* species with relatives across the Panama Isthmus suggests a vicariant event post-radiation of *Lamellibrachia* into the Atlantic. Sanger-sequencing also revealed two

putative new species of the vestimentiferan tube worm *Alaysia*. High-throughput sequencing and mitochondrial genome skimming provided the data necessary to place these new species, as well as the vestimentiferan genera *Alaysia* and *Arcovestia* into the phylogeny of Vestimentifera for the first time. Additional sequencing of whole mitochondrial genomes in this group provided the data necessary to generate the most complete mitogenomic phylogeny of Vestimentifera to date. The resulting topology suggests the most recent common ancestor of Vestimentifera was a vent-inhabitant of the Pacific Ocean.

Introduction

While the deep sea (greater than 200m depth) remains the least explored habitat on earth, the past fifty years of research have been underscored by the discovery of chemosynthetic environments, including hydrothermal vents, cold seeps, and organic falls. Prior to the discovery of these environments, the deep sea was thought to be generally nutrient-poor and heterotrophic (Gage, 2003). However, chemosynthetic environments provide unique chemical resources that support primary production by bacteria and archaea, which utilize the inorganic compounds present to produce energy (Boetius et al., 2000; Jørgensen & Boetius, 2007). Not only have these discoveries completely changed scientific understanding of primary production in the deep sea, but they have also revealed a unique diversity of fauna endemic to these habitats and dependent on chemosymbioses with bacteria for survival (Dubilier, Bergin, & Lott, 2008; Van Dover, 2000). Some of these chemosymbiotic fauna, like annelids and mollusks, play crucial roles in their environments.

Chemosymbiotic annelids and mollusks often occur in large densities at chemosynthetic environments (Bergquist et al., 2003; Levin et al., 2012; Shank et al., 1998). Some Vestimentifera (deep-sea tubeworms within Annelida), such as *Riftia* Jones, 1981, *Lamellibrachia* Webb, 1969, and *Alaysia* Southward, 1991, grow in vast columns or bushes: their tubes extend over meters, covered in limpets, snails, and other animals that depend on them for habitat (Levin et al., 2012). Mollusks such as *Bathymodiolus* Kenk and Wilson, 1985 mussels also grow in large densities and provide a similar service, creating attachment substrate and shelter for other animals (Govenar, 2010; Vrijenhoek, 2010; Xu, Feng, Tao, & Qiu, 2019b). Both Vestimentifera and *Bathymodiolus* act as ecosystem engineers in the habitats they live in by creating shelter and sustenance for other

organisms that contribute to the biodiversity of their environment (Samadi et al., 2015). While both of these groups serve fundamental roles in their ecosystems, there are still many questions about their life histories, biogeography, and evolution that remain unanswered.

The challenges surrounding deep-sea exploration and sampling play an essential role in the knowledge gaps surrounding the unique fauna at chemosynthetic environments. These environments can be difficult to find and even more difficult to sample, often requiring costly submersibles with limited sampling volumes. In addition, cryptic biodiversity and morphological plasticity of some species make it difficult to delimit species based on morphology (Southward et al., 1995; see also Chapters 1, 3, 4). While the study of biodiversity at chemosynthetic environments began with morphological descriptions of new species, molecular methods have drastically increased scientific understanding of the relationships between fauna and made it possible to address numerous questions about their biodiversity, life history, and evolution. For example, Vestimentifera, now a rank-free taxon used to describe deep-sea chemosymbiotic tube worms within Siboglinidae Caullery, 1914 , was once shrouded in past debate regarding its placement in the tree of life. This debate likely resulted from challenges assessing the worms' strange morphology (majority of the body not segmented, segmented parts easily lost in sampling, lack of a mouth or gut, difficulty assigning dorsal and ventral orientation, etc) (Bright & Lallier, 2010; Pleijel, Dahlgren, & Rouse, 2009). The first Vestimentifera described, *Lamellibrachia barhami* Webb, 1969, was placed in the phylum Pogonophora, then separate from Annelida (Webb, 1969). Some morphological examinations (such as the discovery of posterior segments with chaetae) and observations of early development provided evidence that Vestimentifera may be within Annelida, and the first molecular phylogeny involving a vestimentiferan (Kojima et al., 1993) lent major support to this hypothesis. Additional molecular data obtained with Sanger sequencing (Black et al., 1997; Halanych, Feldman, & Vrijenhoek, 2001; Mchugh, 1997; Rousset, Rouse, Siddall, Tillier, & Pleijel, 2004) and morphological examination culminated in referring Pogonophora (and Vestimentifera) to Siboglinidae within Annelida (see Pleijel et al., 2009 for further details). Molecular methods like Sanger sequencing (Sanger et al., 1977)

continue to facilitate phylogenetic inference for both annelids and mollusks in the deep sea. Many new species have been described at chemosynthetic environments since they were discovered in the 1970's (Baker et al., 2010; Corliss, Dymond, Gordon, & Al., 1979; German et al., 2011), and new species of annelids and mollusks are still being described from chemosynthetic environments today (e.g., *Lamellibrachia sagami* Kobayashi, 2015 and *Gigantidas haimensis* Xu, 2019). As a result, the taxonomy of annelids and mollusks at chemosynthetic environments continues to undergo revision as new molecular data become available (e.g., Cowart et al., 2014; Xu et al., 2019).

While Sanger sequencing is frequently useful for the establishment of new annelid species, genes like COI and 16S sometimes shows low levels of variation in various members of Vestimentifera, which is reflected in poor phylogenetic support in past studies utilizing these markers (Cowart et al., 2014, 2013). However, whole mitochondrial genomes provide a much larger nucleotide dataset and have begun to play a key role in the phylogenetics of Vestimentifera. The mitochondrial genomes of sixteen members of Siboglinidae (including nine Vestimentifera) have already proven valuable in resolving the siboglinid phylogeny (Li et al., 2015; Patra, Kwon, Kang, Fujiwara, & Kim, 2016; Sun et al., 2018).

In this dissertation, I use a combination of molecular methods, including Sanger sequencing and next-generation sequencing (genome skimming for mitochondrial genomes), to delimit deep-sea annelid and mollusk species from chemosynthetic environments and examine their genetic connectivity and biogeography in the Pacific Ocean. Small numbers of mitochondrial and nuclear markers were Sanger-sequenced to assess phylogenetic relationships and describe new species of *Bathymodiolus*, *Thermiphione*, and *Alaysia*. The combination of these molecular methods with morphological data allowed for the official description of new species and some exploration of their connectivity, evolutionary history, and biogeography. Next-generation sequencing methods, (mitochondrial genome skimming) were utilized to place *Alaysia spiralis* Southward, 1991and *Arcovestia ivanovi* Southward and Galkin, 1997 into the context of the vestimentiferan phylogeny and further resolve phylogenetic relationships between Vestimentifera.

In **Chapter 1**, we investigate three putative new species of bathymodiolin mussels from seeps along the Costa Rica margin. We assess their phylogenetic position, as well as the presence of *Bathymodiolus thermophilus* Kenk and Wilson, 1985 at the Costa Rica margin seeps with genetic data. We provide a time-calibrated phylogeny of this group using fossils, an ancestral state reconstruction of habitat, and compare shell morphologies with the genetic data we have collected. Phylogenetic analyses revealed three new *Bathymodiolus* species and confirmed the presence of *B. thermophilus* at the Costa Rica margin seeps. A principal component analysis revealed that only one species could be reliably differentiated from the remaining species based on shell morphology alone, underlying the importance of molecular data for biodiversity assessments. Analyses also revealed that the new species showed some stratification by depth, and that one of the new species may differ in evolutionary origin from the other two.

In **Chapter 2**, we provide genetic and morphological data for a new species of iphionid scaleworm from hydrothermal vents in the East Pacific. We use a combination of nuclear and mitochondrial loci to conduct phylogenetic analyses that include Maximum Likelihood, Bayesian Inference, and Maximum Parsimony analyses, distance analyses, and haplotype networks. These analyses reveal a new iphionid species and demonstrate the paraphyly of *Thermiphione* Hartmann-Schroder, 1992 which is resolved in this study.

In **Chapter 3**, we describe a new species of *Lamellibrachia* (Siboglinidae, Annelida) and assess its phylogenetic position. This new species differs genetically and morphologically from all congeneric species and is currently known only from 1,000 m at the Costa Rica margin. Despite its close geographic proximity to *Lamellibrachia barhami* at the Costa Rica margin, the new species is recovered inside an Atlantic clade of *Lamellibrachia*, suggesting its existence there may be the result of a vicariant event post-Atlantic-radiation of *Lamellibrachia*.

In **Chapter 4**, we genetically identify *Lamellibrachia* specimens sampled from cold seeps of the Hikurangi Margin off the Northern Island of New Zealand as *L. columna* Southward, 1991. We also discover close genetic affinities of *L.* sp. L2 and *L. sagami* Kobayashi et al., 2015 specimens from seeps of southern and eastern Japan to *L. columna*. We suggest that *L. sagami* is

a junior synonym of *L. columna* and confirm that *L. columna* is found at both vents and seeps over a large geographic range in the West Pacific Ocean.

In **Chapter 5**, we describe a new species of *Alaysia* and use mitochondrial genome skimming to place this new species, as well as the type species *Alaysia spiralis* Southward, 1991 into the vestimentiferan phylogeny with high confidence for the first time. A total of ten new mitochondrial genomes are sequenced to further resolve relationships among Vestimentifera in this phylogeny, including *Arcovestia ivanovi* Southward and Galkin, 1997, various *Lamellibrachia* species, and a new species of *Oasisia* Jones, 1985. A well-supported 16-gene phylogeny of Vestimentifera reveals a potential Pacific origin of the clade, and a most recent common ancestor that was likely a vent inhabitant. This document is not intended to act as an official description or publication of the new *Alaysia* species under the International Code of Zoological Nomenclature (ICZN).

References

Baker, M. C., Ramirez-Llodra, E. Z., Tyler, P. A., German, C. R., Boetius, A., Cordes, E. E., ... Warén, A. (2010). Biogeography, Ecology, and Vulnerability of Chemosynthetic Ecosystems in the Deep Sea. Life in the World's Oceans: Diversity, Distribution, and Abundance, (October), 161–182. https://doi.org/10.1002/9781444325508.ch9

Bergquist, D. C., Ward, T., Cordes, E. E., McNelis, T., Howlett, S., Kosoff, R., ... Fisher, C. R. (2003). Community structure of vestimentiferan-generated habitat islands from Gulf of Mexico cold seeps. Journal of Experimental Marine Biology and Ecology, 289(2), 197–222. https://doi.org/10.1016/S0022-0981(03)00046-7

Black, M. B., Halanych, K. M., Maas, P. A. Y., Hoeh, W. R., Hashimoto, J., Desbruyères, D., ... Vrijenhoek, R. C. (1997). Molecular systematics of vestimentiferan tubeworms from hydrothermal vents and cold-water seeps. Marine Biology, 130(2), 141–149. https://doi.org/10.1007/s002270050233

Boetius, A., Ravenschlag, K., Schubert, C. J., Rickert, D., Widdel, F., Gieseke, A., ... Pfannkuche, O. (2000). A marine microbial consortium apparently mediating anaerobic oxidation of methane. Nature, 407, 623–626. https://doi.org/10.1038/35036572

Bright, M., & Lallier, F. (2010). The Biology of Vestimentiferan Tubeworms. Oceanography and

Marine Biology: An Annual Review, 48, 213–265. https://doi.org/10.1201/EBK1439821169-c4

Caullery, M. (1914). Sur les Siboglinidae, type nouveau d'invertébrés receuillis par l'expédition du Siboga. Comptes Rendus Hebdomadaires Des Séances de l'Académie Des Sciences, 158, 2014–2017.

Corliss, J. B., Dymond, J., Gordon, J., & Al., E. (1979). Submarine Thermal Springs on the Galápagos Rift. Science, 1073–1083.

Cowart, D. A., Halanych, K. M., Schaeffer, S. W., & Fisher, C. R. (2014). Depth-dependent gene flow in Gulf of Mexico cold seep *Lamellibrachia* tubeworms (Annelida, Siboglinidae). Hydrobiologia, 736, 139–154. https://doi.org/10.1007/s10750-014-1900-y

Cowart, D. A., Huang, C., Arnaud-Haond, S., Carney, S. L., Fisher, C. R., & Schaeffer, S. W. (2013). Restriction to large-scale gene flow vs. regional panmixia among cold seep *Escarpia* spp. (Polychaeta, Siboglinidae). Molecular Ecology, 22(16), 4147–4162. https://doi.org/10.1111/mec.12379

Dubilier, N., Bergin, C., & Lott, C. (2008). Symbiotic diversity in marine animals: The art of harnessing chemosynthesis. Nature Reviews Microbiology, 6(10), 725–740. https://doi.org/10.1038/nrmicro1992

Gage, J. (2003). Food inputs, utilisation, carbon flow and energetics. In P. Tyler (Ed.), Ecosystems of the World: Ecosystems of the Deep Ocean (pp. 313–426). Amsterdam: Elsevier.

German, C. R., Ramirez-Llodra, E., Baker, M. C., Tyler, P. A., Baco-Taylor, A., Boetius, A., ... Warén, A. (2011). Deep-water chemosynthetic ecosystem research during the census of marine life decade and beyond: A proposed deep-ocean road map. PLoS ONE, 6(8). https://doi.org/10.1371/journal.pone.0023259

Govenar, B. (2010). Shaping Vent and Seep Communities: Habitat Provision and Modification by Foundation Species. In Steffen Kiel (Ed.), The Vent and Seep Biota: Aspects from Microbes to Ecosystems (pp. 403–432). https://doi.org/10.1007/978-90-481-9572-5

Halanych, K. M., Feldman, R. A., & Vrijenhoek, R. C. (2001). Molecular Evidence that *Sclerolinum brattstromi* Is Closely Related to Vestimentiferans, not to Frenulate Pogonophorans (Siboglinidae, Annelida). Biological Bulletin, 201(1), 65–75. https://doi.org/10.2307/1543527

Hartmann-Schroder, G. (1992). Zur Polychaetenfauna in rezenten hydrothermalen Komplexmassivsulfiderzen ("Schwarze Raucher") am Ostpazifischen Rucken bei 21 30 S. Helgolander Meeresuntersuchungen, 46(4), 389–403. https://doi.org/10.1007/BF02367206

Jones, M. L. (1985). On the Vestimentifera, new phylum: six new species, and other taxa, from hydrothermal vents and elsewhere. Bulletin of the Biological Society of Washington, (6), 117–158.

Jones, M. L. (1981). *Riftia pachyptila*, new genus, new species, the vestimentiferan worm from the Galápagos Rift geothermal vents. Biological Society of Washington, 93(4), 1295–1313.

Jørgensen, B. B., & Boetius, A. (2007). Feast and famine — microbial life in the deep-sea bed. Nature Reviews Microbiology, 5(10), 770–781. https://doi.org/10.1038/nrmicro1745

Kenk, V. C., & Wilson, B. R. (1985). A new mussel (Bivalvia, Mytilidae) from hydrothermal vents in the Galapagos rift zone. Malacologia, 26(1–2), 253–271. Retrieved from https://www.biodiversitylibrary.org/pdf4/095854300047334

Kobayashi, G., Miura, T., & Kojima, S. (2015). *Lamellibrachia sagami* sp. nov., a new vestimentiferan tubeworm (Annelida: Siboglinidae) from Sagami Bay and several sites in the northwestern Pacific Ocean. Zootaxa, 4018(1), 97–108. https://doi.org/10.11646/zootaxa.4018.1.5

Kojima, S., Hashimoto, T., Hasegawa, M., Murata, S., Ohta, S., Seki, H., & Okada, N. (1993). Close phylogenetic relationship between vestimentifera (tube worms) and annelida revealed by the amino acid sequence of elongation factor-lalpha. Journal of Molecular Evolution, 37(1), 66–70. https://doi.org/10.1007/BF00170463

Levin, L. A., Orphan, V. J., Rouse, G. W., Rathburn, A. E., Ussler, W., Cook, G. S., … Strickrott, B. (2012). A hydrothermal seep on the Costa Rica margin: middle ground in a continuum of reducing ecosystems. Proceedings of the Royal Society B: Biological Sciences, 279, 2580–2588. https://doi.org/10.1098/rspb.2012.0205

Li, Y., Kocot, K. M., Schander, C., Santos, S. R., Thornhill, D. J., & Halanych, K. M. (2015). Mitogenomics reveals phylogeny and repeated motifs in control regions of the deep-sea family Siboglinidae (Annelida). Molecular Phylogenetics and Evolution, 85(February), 221–229. https://doi.org/10.1016/j.ympev.2015.02.008

Mchugh, D. (1997). Molecular evidence that echiurans and pogonophorans are derived annelids. Proceedings of the National Academy of Sciences of the United States of America, 94, 8006–8009. https://doi.org/10.1073/pnas.94.15.8006

Patra, A. K., Kwon, Y. M., Kang, S. G., Fujiwara, Y., & Kim, S. J. (2016). The complete mitochondrial genome sequence of the tubeworm *Lamellibrachia satsuma* and structural conservation in the mitochondrial genome control regions of Order Sabellida. Marine Genomics, 26, 63–71. https://doi.org/10.1016/j.margen.2015.12.010

Pleijel, F., Dahlgren, T. G., & Rouse, G. W. (2009). Progress in systematics: from Siboglinidae to Pogonophora and Vestimentifera and back to Siboglinidae. Comptes Rendus Biologies,

332, 140–148. https://doi.org/10.1016/J.CRVI.2008.10.007

Rousset, V., Rouse, G. W., Siddall, M. E., Tillier, A., & Pleijel, F. (2004). The phylogenetic position of Siboglinidae (Annelida) inferred from 18S rRNA, 28S rRNA and morphological data. Cladistics, 20, 518–533. https://doi.org/10.1111/j.1096-0031.2004.00039.x

Samadi, S., Puillandre, N., Pante, E., Boisselier, M. C., Corbari, L., Chen, W. J., … Hourdez, S. (2015). Patchiness of deep-sea communities in Papua New Guinea and potential susceptibility to anthropogenic disturbances illustrated by seep organisms. Marine Ecology, 36(S1), 109–132. https://doi.org/10.1111/maec.12204

Sanger, F., Air, G. M., Barrell, B. G., Brownt, N. L., Coulson, A. R., Fiddes, J. C., … Smith, M. (1977). Nucleotide sequence of bacteriophage. Nature, 265, 687–695.

Shank, T. M., Fornari, D. J., Von Damm, K. L., Lilley, M. D., Haymon, R. M., & Lutz, R. A. (1998). Temporal and spatial patterns of biological community development at nascent deep-sea hydrothermal vents (9° 50'N, East Pacific Rise). Deep-Sea Research II, 45, 465–515. https://doi.org/10.1016/S0967-0645(97)00089-1

Southward, E.C. (1991). Three new species of Pogonophora, including two vestimentiferans, from hydrothermal sites in the Lau Back-arc Basin (Southwest Pacific Ocean). Journal of Natural History, 25(4), 859–881. https://doi.org/10.1080/00222939100770571

Southward, E.C., & Galkin, S. V. (1997). A new vestimentiferan (Pogonophora: Obturata) from hydrothermal vent fields in the Manus Back-arc Basin (Bismarck Sea, Papua New Guinea, Southwest Pacific Ocean). Journal of Natural History, 31(1), 43–55. https://doi.org/10.1080/00222939700770041

Southward, Eve C., Tunnicliffe, V., & Black, M. (1995). Revision of the species of *Ridgeia* from northeast Pacific hydrothermal vents, with a redescription of *Ridgeia piscesae* Jones (Pogonophora: Obturata = Vestimentifera). Canadian Journal of Zoology, 73, 282–295. https://doi.org/10.1139/z95-033

Sun, Y., Liang, Q., Sun, J., Yang, Y., Tao, J., Liang, J., … Qian, P.-Y. (2018). The mitochondrial genome of the deep-sea tubeworm *Paraescarpia echinospica* (Siboglinidae, Annelida) and its phylogenetic implications. Mitochondrial DNA Part B, 3(1), 131–132. https://doi.org/10.1080/23802359.2018.1424576

Van Dover, C. L. (2000). The Ecology of Deep-Sea Hydrothermal Vents. New Jersey: Princeton University Press.

Vrijenhoek, R. C. (2010). Genetics and Evolution of Deep-Sea Chemosynthetic Bacteria and Their Invertebrate Hosts. In S. Kiel (Ed.), The Vent and Seep Biota, Topics in Geobiology (pp. 15–49). https://doi.org/10.1007/978-90-481-9572-5_2

Webb, M. (1969). Lamellibrachia barhami, gen. nov., sp. nov. (Pogonophora), from the Northeast Pacific. Bulletin of Marine Science, 19(1), 18–47.

Xu, T., Feng, D., Tao, J., & Qiu, J.-W. (2019). A new species of deep-sea mussel (Bivalvia: Mytilidae: Gigantidas) from the South China Sea: morphology, phylogenetic position, and gill-associated microbes. Deep-Sea Research Part I: Oceanographic Research Papers, 146, 79–90. https://doi.org/10.1016/j.dsr.2019.03.001

Chapter 1

Spanning the depths or depth-restricted: Three new species of *Bathymodiolus* (Bivalvia, Mytilidae) and a new record for the hydrothermal vent *Bathymodiolus thermophilus* at methane seeps along the Costa Rica margin

Marina F. McCowin[1], Caitlin Feehery[1] and Greg W. Rouse[1]

[1]Scripps Institution of Oceanography, University of California San Diego, USA

Deep–Sea Research I 164 (2020) 103322

Contents lists available at ScienceDirect

Deep-Sea Research Part I

journal homepage: http://www.elsevier.com/locate/dsri

Spanning the depths or depth-restricted: Three new species of *Bathymodiolus* (Bivalvia, Mytilidae) and a new record for the hydrothermal vent *Bathymodiolus thermophilus* at methane seeps along the Costa Rica margin

Marina F. McCowin [*], Caitlin Feehery, Greg W. Rouse [**]

Scripps Institution of Oceanography, University of California San Diego, La Jolla, CA, 92093-0202, USA

ARTICLE INFO

Keywords:
Bathymodiolinae
Cold seeps
New species
East pacific

ABSTRACT

Bathymodiolus Kenk and Wilson, 1985 includes fourteen currently recognized species from deep-sea chemosynthetic environments in the Pacific, Atlantic, and Indian oceans. In this study, phylogenetic analyses of mytilid mussels sampled from seeps along the Costa Rica margin reveal the presence of three new *Bathymodiolus* species, sampled from depths across ~1000–1900 m. *Bathymodiolus billschneideri* n. sp., *B. earlougheri* n. sp., and *B. nancyschneiderae* n. sp. differ genetically from congeneric species of *Bathymodiolus* and show some stratification by depth. The depth ranges of *Bathymodiolus billschneideri* n. sp., *B. nancyschneiderae* n. sp., and *B. earlougheri* n. sp. were ~1400–1900 m, 1000–1100 m, and ~1000–1900m, respectively. *Bathymodiolus billschneideri* n. sp. and *B. earlougheri* n. sp. were found to be closely related to *Bathymodiolus thermophilus* Kenk and Wilson, 1985, while *B. nancyschneiderae* n. sp. exhibited closer relationships to non-East-Pacific taxa. *Bathymodiolus thermophilus* was the first *Bathymodiolus* mussel discovered, sampled from a vent along the Galápagos Rift Zone in 1985 and later recorded along much of the East Pacific Rise. This study confirms the presence of *B. thermophilus* at the Costa Rica margin, representing the first DNA and morphological samples of *B. thermophilus* at a seep environment. Analysis of habitat evolution suggests that *B. thermophilus* and its closest relative, *B. antarcticus* Johnson and Vrijenhoek, 2013, are of seep ancestry.

1. Introduction

Bathymodiolinae Kenk and Wilson, 1985 is a subfamily of the Mytilidae mussel group whose members inhabit reducing environments worldwide (Kiel, 2010; Taylor and Glover, 2010). Within Bathymodiolinae, the eight currently accepted genera contain over fifty named species (Kenk and Wilson, 1985; Olu-Le Roy et al., 2007; Taylor and Glover, 2010): *Adipicola* Dautzenberg, 1927, *Bathymodiolus* Kenk and Wilson, 1985, *Benthomodiolus* Dell, 1987, *Gigantidas* Cosel and Marshall, 2003, *Idas* Jeffreys, 1876, *Tamu* Gustafson, Turner, Lutz & Vrijenhoek, 1998, *Terua* Dall, Bartsch and Rehder, 1938 and *Vulcanidas* Cosel and Marshall, 2010. Many of these mussels, such as *Bathymodiolus*, are chemosymbiotic, relying on sulphide and/or methane-oxidizing symbionts in the ctenidia for much of their nutritional requirements (Fisher et al., 1993; Duperron et al., 2008; Taylor and Glover, 2010). *Bathymodiolus* are restricted to deep-sea chemosynthetic environments such as vents and seeps, where they often serve as foundational species and dominate the community biomass, creating essential habitat space for other organisms (Govenar, 2010; Vrijenhoek, 2010; Xu et al., 2019). *Bathymodiolus* currently includes 14 accepted species, distributed in the Atlantic, Pacific, and Indian oceans, as well as the Caribbean and Gulf of Mexico (Cosel et al., 1999; Cosel and Olu, 1998; Gustafson et al., 1998; Hashimoto, 2001). However, molecular data suggests that *Bathymodiolus* is not monophyletic (Cosel and Marshall, 2003; Jones et al., 2006; Lorion et al., 2010).

Historically, Bathymodiolinae species were described based on morphological characteristics such as shell dimensions and internal anatomy (Kenk and Wilson, 1985), but molecular data has greatly changed the understanding of the group's internal relationships. For example, DNA sequence data suggested that both *Bathymodiolus* and

* Corresponding author.
** Corresponding author.
E-mail addresses: marruda@ucsd.edu (M.F. McCowin), grouse@ucsd.edu (G.W. Rouse).

https://doi.org/10.1016/j.dsr.2020.103322
Received 29 January 2020; Received in revised form 7 May 2020; Accepted 19 May 2020
Available online 16 July 2020

Gigantidas were paraphyletic or polyphyletic (Jones et al., 2006). The paraphyly of *Gigantidas* has been recently resolved (see summary in Xu et al., 2019), while the paraphyly of *Bathymodiolus* has yet to be remedied. *Bathymodiolus manusensis* Hashimoto and Furuta, 2007 and *B. aduloides* Hashimoto and Okutani, 1994 are clearly not members of the *Bathymodiolus* clade containing the type species for the genus, so we have placed their names in quotation marks, echoing the treatment by Gustafson et al. (1998), to indicate the nomenclatural problems regarding these taxa. While the taxonomy of *Bathymodiolus* needs some revision, new species of Bathymodiolinae are still being described (e.g. *Gigantidas haimaensis* Xu et al., 2019).

This study focuses on mussels collected from deep-sea seeps at various depths along the Costa Rica margin in the eastern Pacific Ocean (Fig. 1). These collections include unidentified *Bathymodiolus* and *B. thermophilus* Kenk and Wilson, 1985 specimens that had been noted previously at these seeps (Levin et al., 2012, 2015). The Costa Rica margin in the East Pacific represents a biodiverse and variable seep habitat for many chemosymbiotic fauna, with over 40 seeps discovered along the margin since 2008 (Sahling et al., 2008; Levin et al., 2012, 2015). *Bathymodiolus thermophilus* is well-known from hydrothermal vents along the East Pacific Rise, but had not been previously sampled outside of the East Pacific Rise or Galápagos Rift, or at any seep environments, until it was observed at the Jaco Scar seep (which exhibits some vent-like characteristics) on the Costa Rica margin (Levin et al., 2012). Here we combine newly generated DNA data for *Bathymodiolus* mussels sampled from five seep sites in Costa Rica (999–1891 m) with previously published DNA data (Table 1) to substantiate the presence of *B. thermophilus* (as reported in Levin et al., 2012) and reveal three new species of *Bathymodiolus* at seeps along the Costa Rica margin, which are described here.

2. Methods

2.1. Sampling

Bathymodiolus mussels were collected and subsampled for DNA on several dives by the HOV *Alvin* and ROV *SuBastian* between 2009 and 2019 along the Costa Rica margin at the following dive sites between 999 and 1891 m: Mound 12, Jaco-1000, The Thumb, Parrita Seep (formerly "Mound Quepos" (Levin et al., 2015) and "Quepos Seep" (Lindgren et al., 2019; McCowin and Rouse, 2018)), and Jaco Scar (Fig. 1, Table 1, Supplementary Table 1). Four *Bathymodiolus thermophilus* specimens were also collected and subsampled for DNA in 2017 and 2019. Three *B. thermophilus* specimens from the East Pacific Rise (collected between 1985 and 2007) were also used for the morphological analyses in this study, and two *"B." manusensis* specimens from the Snowcap dive site in the Manus Basin (collected in 2000) were used in the phylogenetic analyses in this study (Table 1, Supplementary Tables 1 and 3).

For molecular analyses, a portion of the foot was cut and preserved in 95% ethanol (details of individual samples are noted in Material Examined). Specimens were photographed post-preservation with a

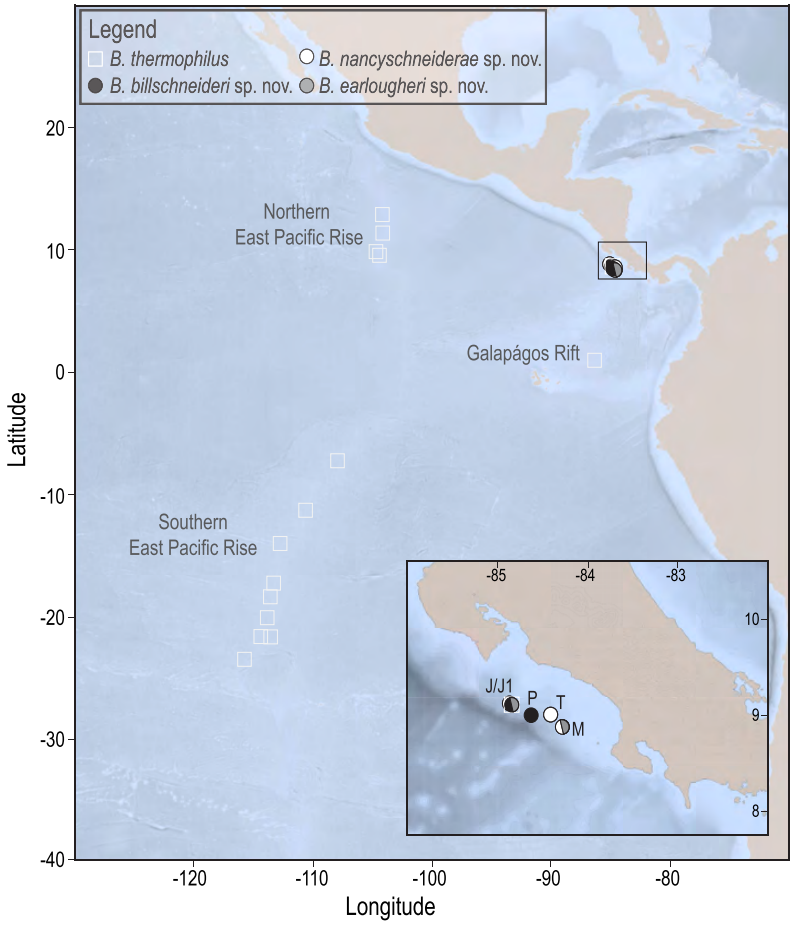

Fig. 1. Distribution of *Bathymodiolus thermophilus* (squares) and three new *Bathymodiolus* species (circles) in the eastern Pacific and along the Costa Rica margin: *Bathymodiolus thermophilus* (white square), *Bathymodiolus billschneideri* n. sp. (black circle), *Bathymodiolus earlougheri* n. sp. (grey circle), *Bathymodiolus nancyschneiderae* n. sp. (white circle). Detailed map of sampling at Costa Rica margin lower right: Jaco Scar (J), Jaco-1000 (J1), Parrita Seep (P), The Thumb (T), Mound 12 (M).

Table 1
Origin of sequenced terminals, vouchers, and GenBank accession numbers used in final concatenated analyses (8 genes). New sequences are set in bold.

Scientific Name	Origin	Habitat	COI	16S	HSP70	ND4	ANT	18S	28S	HH3	Voucher or Reference
"Bathymodiolus "aduloides	Kikajima Island	vent	AB170057	–	–	AB175326	–	–	–	–	Iwasaki et al., 2006
Bathymodiolus antarcticus	EPR	vent	AF456317	–	–	AY649809	–	AY649823	AY781140	–	Won et al., 2003; Jones et al., 2006
Bathymodiolus azoricus	Menez Gwen (Atl.)	vent	AY649795	KF611758	KF720580	–	KF720540	AY649822	AY781148	KF720621	Jones et al., 2006; Thubaut et al., 2013
Bathymodiolus billschneideri n. sp.	**Jaco Scar, CR**	**seep**	**MN986781**	**MN977821**	**-**	**-**	**-**	**MN978735**	**MN978745**	**MN986898**	**SIO-BIC M14535**
Bathymodiolus billschneideri n. sp.	**Jaco Scar, CR**	**seep**	**MN904638**	**MN977822**	**-**	**-**	**-**	**MN978736**	**-**	**-**	**SIO-BIC M12078–04**
Bathymodiolus billschneideri n. sp.	**Jaco Scar, CR**	**seep**	**MN986815**	**MN977823**	**MN986906**	**-**	**MN974019**	**MN978737**	**-**	**-**	**SIO-BIC M16792**
Bathymodiolus boomerang	Barbados Accretionar Prism	seep	FJ890503	KF611759	KF720579	–	KF720541	–	FJ890505	KF720622	Lorion et al., 2010; Thubaut et al., 2013
Bathymodiolus brevior	Mariana Trough	vent	AY649799	–	–	AY649806	–	AY649824	AY781150	–	Jones et al., 2006
Bathymodiolus brooksi	West Florida Escarpment	seep	AY649798	–	–	AY649805	–	AY649825	AY781135	–	Jones et al., 2006
Bathymodiolus earlougheri n. sp.	**Jaco Scar, CR**	**seep**	**MN986856**	**-**	**-**	**-**	**-**	**-**	**-**	**-**	**SIO-BIC M12080**
Bathymodiolus earlougheri n. sp.	**Mound 12, CR**	**seep**	**MN986865**	**MN977824**	**-**	**MN986913**	**-**	**MN978738**	**MN978746**	**MN986899**	**SIO-BIC M14487**
Bathymodiolus earlougheri n. sp.	**Mound 12, CR**	**seep**	**MN986851**	**MN977825**	**MN986907**	**MN986914**	**-**	**MN978739**	**MN978747**	**MN986900**	**SIO-BIC M18326 (M11974–05)**
Bathymodiolus heckerae	West Florida Escarpment	seep	AY649794	–	–	AY130246	–	AF221639	AY781138	–	Jones et al., 2006; Distel et al., 2000
"Bathymodiolus" manusensis	**Manus Basin**	**vent**	**MN986850**	**-**	**-**	**-**	**-**	**MN978740**	**MN978748**	**MN986901**	**SAM D19368.13**
"Bathymodiolus" manusensis	Manus Basin	vent	GU966637	HF545059	KF720556	–	KF720537	KF611718	GU966642	KF720618	Lorion et al., 2010, 2013; Thubaut et al., 2013
Bathymodiolus marisindicus	Edmond, CIR	vent	AY275543	–	–	AY046279	–	AY649818	AY781147	–	Smith et al., 2004; Van Dover et al., 2001; Jones et al., 2006
Bathymodiolus nancyschneiderae n. sp.	**Mound 12, CR**	**seep**	**MN895199**	**-**	**MN986908**	**MN986915**	**-**	**-**	**-**	**-**	**SIO-BIC M18327 (M11979–07)**
Bathymodiolus nancyschneiderae n. sp.	**Mound 12, CR**	**seep**	**MN895191**	**MN977826**	**MN986909**	**MN986916**	**-**	**MN978741**	**MN978749**	**MN986902**	**SIO-BIC M11974–18**
Bathymodiolus nancyschneiderae n. sp.	**Mound 12, CR**	**seep**	**MN895215**	**MN977827**	**MN986910**	**MN986917**	**-**	**MN978742**	**MN978750**	**MN986903**	**SIO-BIC M14471**
Bathymodiolus nancyschneiderae n. sp.	**Jaco-1000, CR**	**seep**	**MN895206**	**MN977828**	**MN986911**	**MN986918**	**MN974020**	**MN978743**	**MN978751**	**MN986904**	**SIO-BIC M12032**
Bathymodiolus puteoserpentis	Snake Pit, MAR	vent/seep	AY649796	–	–	AF128533	–	AF221640	AY781151	–	Maas et al., 1999; Distel et al., 2000; Jones et al., 2006
Bathymodiolus septemdierum	Nankai Trough	seep	AB170052	–	–	AB175298	–	–	–	–	Iwasaki et al., 2006
Bathymodiolus thermophilus	EPR	vent	AF456285	–	–	AY649807	–	AF221638	AY781141	–	Won et al., 2003; Jones et al., 2006; Distel et al., 2000
Bathymodiolus thermophilus	EPR	vent	GU966639	KF611760	–	–	FJ842134	–	GU966640	KF720623	Lorion et al., 2010; Thubaut et al., 2013; Audzijonyte and Vrijenhoek, 2010

(*continued on next page*)

Table 1 (*continued*)

Scientific Name	Origin	Habitat	COI	16S	HSP70	ND4	ANT	18S	28S	HH3	Voucher or Reference
Bathymodiolus thermophilus	**Jaco Scar, CR**	**seep**	**MN986846**	**-**	**MN986912**	**MN986919**	**-**	**MN978744**	**-**	**MN986905**	**SIO-BIC M14568**
Benthomodiolus geikotsucola	Japan	organic substrate	HF545103	HF545049	–	–	–	–	HF545023	HF545149	Lorion et al. (2013)
Benthomodiolus lignocola	New Zealand	organic substrate	AY275545	HF545050	–	AY649817	–	AF221648	AY781131	KF720596	Smith et al., 2004; Lorion et al., 2013; Jones et al., 2006; Distel et al., 2000; Thubaut et al., 2013
Benthomodiolus lignocola	South Atlantic	organic substrate	KF611691	KF611733	KF720560	–	–	KF611703	KF611698	KF720593	Thubaut et al., 2013
Gigantidas childressi	Alaminos Canyon (Atl.)	seep	AY649800	–	–	AY130248	–	AF221641	AY781137	–	Jones et al., 2006; Won et al., 2003; Distel et al., 2000
Gigantidas crypta	Philippines	organic substrate	EU702319	KF611750	KF720563	–	KF720531	KF611714	EU683298	KF720612	Lorion et al., 2009;Thubaut et al., 2013
Gigantidas gladius	Rumble III (WP)	vent	AY649802	–	–	AY649813	–	AY649821	AY781149	–	Jones et al., 2006
Gigantidas hirtus	Kuroshima Knoll	seep	AB170047	–	–	AB175301	–	–	–	–	Iwasaki et al., 2006
Gigantidas japonicus	Mid-Okinawa Trough	seep	AB101422	HF545081	–	AB175281	–	–	HF545039	HF545154	Miyazaki et al., 2004; Lorion et al., 2013; Iwasaki et al., 2006
Gigantidas mauritanicus	West Africa	seep	AY649801	–	–	AY649810	–	AY649828	AY781144	–	Jones et al., 2006
Gigantidas mauritanicus	Barbados Accretionar Prism	seep	FJ890502	KF611747	KF720565	–	KF720528	KF611712	FJ890504	KF720609	Lorion et al., 2010; Thubaut et al., 2013
Gigantidas platifrons	Sagami Bay	vent/seep	AB101420	–	–	AB175286					Miyazaki et al., 2004; Iwasaki et al., 2006
Gigantidas securiformis	Nankai Trough	seep	AB170052	–	–	AB175298	–	–	–	–	Iwasaki et al., 2006
Gigantidas taiwanensis	Okinawa Arc	seep	GU966638	KF611746	KF720566	–	KF720527	KF611711	GU966641	KF720608	Lorion et al., 2010; Thubaut et al., 2013
Gigantidas tangaroa	New Zealand	seep	AY608439	KF611748	KF720572	AY649811	KF720529	AY649820	AY781134	KF720610	Smith et al., 2004; Thubaut et al., 2013; Jones et al., 2006
Idas macdonaldi	Gulf of Mexico	seep	AY649804	–	–	AY649816	–	–	AY781145	–	Jones et al., 2006
Idas washingtonius	Monterey Bay	organic substrate	AY275546	HF545073	–	AY649815	–	AF221645	AY781146	–	Smith et al., 2004; Lorion et al., 2013; Jones et al., 2006; Distel et al., 2000
Tamu fisheri	Garden Banks, GoM	seep	AY649803	–	–	AY649814	–	AF221642	AY781132	–	Jones et al., 2006; Distel et al., 2000
Terua arcuatilis	New Zealand	organic substrate	FJ937033	KF611756	KF720584	–	KF720538	KF611719	GU065879	KF720619	Lorion et al., 2010; Thubaut et al., 2013
Vulcanidas insolatus	Kermadec Ridge, NZ	vent	FJ767936	KF611739	KF720558	–	KF720520	KF611706	FJ767937	KF720601	Lorion et al., 2010; Thubaut et al., 2013
Vulcanidas insolatus (sp. 3)	Kermadec Ridge, NZ	vent	AY608440	–	–	AY649812	–	AY649819	AY781133	–	Smith et al., 2004; Jones et al., 2006

Canon Rebel camera. After subsampling, the holotypes were fixed in 8% formalin. Most of the remaining specimens were cleaned and their shells were dried for preservation. Three paratypes are deposited at the Museo de Zoología, Universidad de Costa Rica, San Jose, Costa Rica (MZUCR), and the holotypes, remaining paratypes, and other collected specimens are deposited in the Scripps Institution of Oceanography Benthic Invertebrate Collection (SIO-BIC), La Jolla, California, USA.

2.2. DNA extraction, amplification, and sequencing

DNA was extracted from 271 *Bathymodiolus* specimens with the Zymo Research DNA-Tissue Miniprep kit, following the protocol supplied by the manufacturer. Approximately 550 bp of the mitochondrial gene cytochrome oxidase subunit I (COI) were amplified for each specimen using the *Bathymodiolus* primers BathCOIF and BathCOIR (Olu-Le Roy et al., 2007), (Supplementary Table 1). For a subset of 12 specimens, up to three additional mitochondrial genes (16S rRNA [16S], NADH dehydrogenase subunit 4 [ND4], and heat shock protein 70 [HSP70]) and up to four nuclear genes (18S rRNA [18S], 28S rRNA [28S], histone H3 [HH3], and adenine nucleotide ADP/ATP translocase [ANT]) were amplified for genetic analysis (Table 1). Amplification details for each gene can be found in Table 2. Fast PCR reactions (COI, 16S, ND4, HSP70, 18S, 28S, HH3) were carried out with the following approximate temperature profiles shown in Table 2, and touchdown PCR was conducted to amplify the ANT gene (same temperature and duration as the Fast PCR for denaturation and extension, but with an annealing temperature that decreased from 55 to 48°/45s; Table 2). All PCR products were purified with the ExoSAP-IT protocol (USB, Affymetrix) and sequencing was performed by Eurofins Genomics (Louisville, KY).

2.3. Molecular analyses

In order to control for doubly uniparental inheritance (DUI), known in some Mytilidae (Breton et al., 2007; Passamonti et al., 2011; Zouros et al., 1994), COI and additional gene sequences for multiple specimens of each species were used in preliminary phylogenetic analyses (Table 1, Supplementary Table 1). We compared sequences from multiple specimens of each species to confirm that there were no "divergent or highly heterogeneous DNA sequences" among the replicates (Fujita et al., 2009; Iwasaki et al., 2006; Kyuno et al., 2009; Miyazaki et al., 2010) that might be indicative of DUI. After this preliminary analysis, a single representative was chosen to represent each species in the final phylogenetic analyses (with a few exceptions where biogeographical relationships were of interest, e.g. *B. thermophilus*). The newly generated sequences plus available sequence data from GenBank for other *Bathymodiolus* species (Table 1) were aligned with MAFFT with default settings (Katoh and Standley, 2013). Poorly-aligned regions of the 16S, 18S, and 28S noncoding genes were removed using Gblocks version 0.91b (Catresana, 2000), with least stringent settings. 93% of sites were retained by Gblocking for 16S, 98% for 18S, and 82% for 28S. This resulted in two alignments for each of these genes, as well as two concatenated alignments, referred to here as complete and Gblocked.

Best-fit models for individual gene alignments (complete and Gblocked, if applicable) were selected using the Akaike information criterion (AIC) in jModelTest 2 (Darriba et al., 2012; Guindon and Gascuel, 2003). All partition models assigned by jModelTest 2 are reported in associated figure legends. Maximum likelihood (ML) analyses were conducted on individual gene alignments (complete and Gblocked, if applicable) separately using the RAxML-HPC2 Workflow on XSEDE v. 8.2.12 in the CIPRES Science Gateway v. 3.3 (Miller et al., 2010; Stamatakis, 2014). A mitochondrial concatenated analysis (COI, 16S, HSP70, ND4; complete and Gblocked) and a nuclear concatenated analysis (18S, 28S, HH3, ANT; complete and Gblocked) were also conducted in RAxML. An ML analysis was conducted for each of the eight-gene concatenated datasets using the same RAxML workflow (and the GTR + G + I model). Node support was assessed via a thorough bootstrapping (1000 replicates) for all ML analyses. Bayesian Inference (BI) analyses were conducted on the complete and Gblocked eight-gene concatenated datasets using MrBayes on XSEDE v. 3.2.x in the CIPRES Science Gateway v. 3.3 (Miller et al., 2010; Ronquist et al., 2012). Each gene partition was assigned the appropriate best-fit model selected by jModelTest 2. Maximum parsimony (MP) analyses were also conducted for the complete and Gblocked eight-gene concatenated datasets using PAUP* v. 4.0a.165 (Swofford, 2002), using heuristic searches with the tree-bisection-reconnection branch-swapping algorithm and 100 random addition replicates. Support values for the MP analyses were determined using 100 bootstrap replicates.

An Approximately Unbiased Test (Shimodaira, 2002) was conducted to test whether one placement of *Bathymodiolus nancyschneiderae* n. sp. in the phylogenetic trees was more likely than the other. A constraint tree placing *B. nancyschneiderae* n. sp. with the clade containing *B. thermophilus*, *B. antarcticus* Johnson and Vrijenhoek, 2013, *B. billschneideri* n. sp., and *B. earlougheri* n. sp. was made using Mesquite v. 3.6 (Maddison and Maddison, 2018) and RAxML v.1.5. Subsequently, IQ-Tree v.1.6.12 (Chernomor et al., 2016) was used to conduct the AU test with 20,000 replicates to generate likelihood scores for the constrained tree and the unconstrained tree (the unconstrained tree from the eight-gene concatenated ML analysis can be seen in Fig. 2). The AU test was also conducted with PAUP* with 10,000 replicates, and the corresponding likelihood scores and p-value were compared with the IQ-Tree results.

Table 2
Amplification details (fragment size, primers and associated references, and amplification programs) for each locus amplified in this study. Touchdown PCR was used to amplify ANT (annealing temperature decreased from 55 to 48 °C over 40 cycles of Denaturation, Annealing Extension. Fast PCR was used to amplify all other loci (30–40 cycles Denaturation, Annealing, Extension). Abbreviations: m - minutes, s - seconds.

Locus	Primers	Approx. Fragment Size (bp)	Initial Denaturation	Denaturation	Annealing	Extension	Final Extension	Reference
COI	BathCOIF, BathCOIR	550	94 °C/4m	94 °C/40s	50 °C/50s	72 °C/1m	72/10m	Olu-Le Roy et al., 2007
16S	Idas16SA, IdasLRJ12864	455	94 °C/4 m	94 °C/40s	55 °C/50s	72 °C/1m	72 °C/10m	Baco-Taylor, 2002; Thubaut et al., 2013
ND4	ND46S, ND47A	490	94 °C/2–4m	94 °C/ 30–40s	52–56.5 °C/ 10–50s	72–74 °C/ 40–60s	72 °C/10m	Kyuno et al., 2009
HSP70	HSP70F, HSP70R	885	94 °C/4m	94 °C/40s	55 °C/50s	72 °C/1m	72 °C/10m	Thubaut et al., 2013
18S	18S1F, 18S5R; 18S9R, 18Sa2.0	1190	94 °C/3m	94 °C/30s	49 °C/30s	72 °C/1m	72 °C/8m	Giribet et al., 1996; Whiting et al., 1997
18S	18S3F, 18Sbi	590	95 °C/3m	95 °C/30s	52 °C/30s	72 °C/90s	72 °C/8m	Giribet et al., 1996; Whiting et al., 1997
28S	28SC1, 28SD2	795	95 °C/3m	95 °C/30s	55 °C/40s	72 °C/75s	72 °C/5m	Jovelin and Justine, 2001
HH3	H3F, H3R	330	95 °C/3m	94 °C/30s	53 °C/45s	72 °C/45s	72 °C/5m	Colgan et al., 1998
ANT	ANTF, ANTR1, ANTR2	500	94 °C/3m	94 °C/30s	55-48 °C/45s	72 °C/1m	72 °C/10m	Audzijonyte and Vrijenhoek, 2010

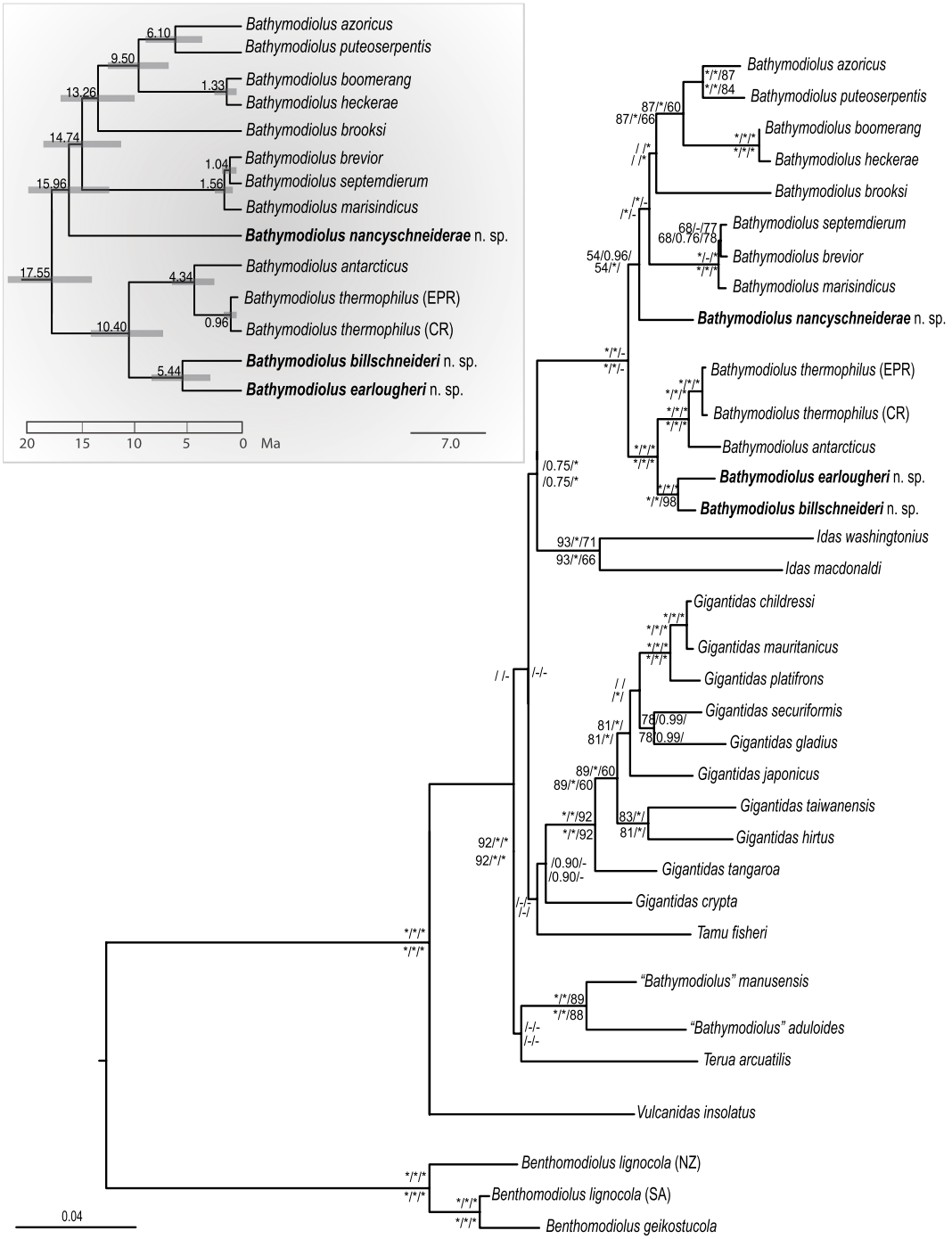

Fig. 2. Maximum likelihood tree of the combined analysis from four mitochondrial (COI, 16S, ND4, HSP70) and four nuclear (18S, 28S, HH3, ANT) genes, conducted in RAxML with best-fit model GTR + G + I. Support values for the complete analysis aligned with MAFFT listed above nodes, support values for the Gblocked analysis listed below nodes. Bootstrap support percentages from Maximum Likelihood analysis, Bayesian posterior probabilities, and bootstrap support percentages from Maximum Parsimony analysis separated by slashes. Support values of 95%/1 or greater for each analysis are indicated by asterisks, support values less than 50%/0.9 are left blank, and nodes not recovered in one of the analyses are indicated by a hyphen. **Inset**. Results of molecular dating analyses (Bayesian inference tree generated with BEAST) for *Bathymodiolus* clade (excluding *"B." aduloides* and *"B." manusensis*), with best-fit models assigned to individual genes (see Supplementary Figs. 2-3 for details). Node ages are indicated above nodes and node bars in light grey indicate 95% HPD).

A subset of the *Bathymodiolus* COI dataset including the new species holotypes and a selection of relevant sequences from GenBank was used to calculate uncorrected and model-corrected (HKY + G) distances and serve as a representative sample (Table 3). Minimum uncorrected pairwise distances were calculated for the entire COI dataset (~400 bp) with PAUP* (Supplementary Table 2). A model-corrected distance analysis for a reduced COI dataset containing the three new *Bathymodiolus* species discussed in this paper and their sister clades (supported by the phylogenetic analyses) was also conducted with the best-fit model, HKY + G (Hasegawa et al., 1985), which was selected via AIC in jModelTest 2 (minimum corrected distances represented by bold values in Supplementary Table 2).

Haplotype networks were created using the COI dataset (terminals listed in Supplementary Table 1) for each of the three new *Bathymodiolus* species and *Bathymodiolus thermophilus* with PopART v.1.7 (Bandelt et al., 1999; Leigh and Bryant, 2015) using the median-joining option with epsilon set at 0 for each analysis.

The complete eight-gene concatenated ML phylogeny was also used in an ancestral state reconstruction of habitat. A habitat character with three states, vent, seep, and organic fall, was mapped onto the ML phylogeny using the Mk-1 likelihood model in Mesquite. Where individual taxa had been reported at multiple habitats, multiple states were coded (e.g., vent/seep for a single taxon reported from both habitats).

The complete eight-gene concatenated alignment was used for molecular dating with BEAST2 (v.2.4.8) (Bouckaert et al., 2019) with the same parameter settings as the most recent molecular dating analysis of Bathymodiolinae by Lorion et al. (2013). The tree was minimally constrained to match the complete concatenated ML tree at nodes of interest for molecular dating. A Yule speciation model was used as a tree prior, with rate variation modelled among lineages by an uncorrelated lognormal relaxed clock, with the mean substitution rate fixed to 1. Three fossils were used as calibrations per Lorion et al. (2013) and implemented as prior distributions for node ages in the tree. These fossils include *Vulcanidas goederti* (Kiel and Little, 2006; Lorion et al., 2013), which was dated to the Middle Eocene, 45 Myr (Kiel and Little, 2006); *Gigantidas coseli* (Lorion et al., 2013; Saether et al., 2010), which was dated to the Middle Miocene, 12.7–15.1 Myr (Saether et al., 2010); and *Bathymodiolus heretaunga* (Lorion et al., 2013; Saether et al., 2010), which was dated to the Early Miocene, 21.7–25.2 Myr (Saether et al., 2010). As in Lorion et al. (2013), we modelled the divergence time of the most inclusive clade containing *Vulcanidas insolatus* Cosel and Marshall (2010) using an exponential prior with a hard minimum bound of 45 Myr and a mean of 1.2 Myr, we modelled the divergence time of the most inclusive clade containing *Gigantidas crypta* (Dall et al., 1938) using an exponential prior with a minimum bound of 15.1 Myr and a mean of 1.3 Myr, and we modelled the divergence time of the most inclusive clade containing *Gigantidas childressi* Gustafson et al. (1998) using an exponential prior with a minimum bound of 25.2 Myr and a mean of 0.7 Myr (Lorion et al., 2013). A minimum of four runs of 20 million Markov chain Monte Carlo (MCMC) steps and a 4000-step subsampling of individual runs was used for the analysis. Each of the fossil calibrations was used in a separate analysis to check whether specific fossils had significant influences on the resulting dates (four to eight runs per fossil until a minimum of four runs converged), then a combined analysis with all three calibrations at once was conducted with a total of seven runs: four of these runs converged and were used (3 reached stationarity at a poorer likelihood plateau and were not used). Burn-in was determined to be 15% using Tracer v.1.7 (Rambaut et al., 2018). Runs were combined in LogCombiner and trees were annotated in TreeAnnotator (BEAST v.2.4.8). The combined individual runs and the single combined run yielded nearly identical results. The divergence times of clades of interest were compared with those found in the Lorion et al. (2013) and Johnson et al. (2013) analyses.

Table 3
Uncorrected and corrected distances for a subset of the COI data (new *Bathymodiolus* species holotypes and other relevant *Bathymodiolus* species). Corrected distances (HKY + G) for are set in bold.

	B. billschneideri n. sp.	*B. earlougheri* n. sp.	*B. nancyschneiderae* n. sp.	*B. thermophilus* (EPR)	*B. thermophilus* (CR)	*B. antarcticus*	*B. azoricus*	*B. boomerang*	*B. heckerae*	*B. marisindicus*
B. billschneideri n. sp.	–	**0.0959**	**0.1393**	**0.1022**	**0.1264**	**0.1334**	**0.2191**	**0.2137**	**0.2476**	**0.1797**
B. earlougheri n. sp.	0.0624	–	**0.1672**	**0.1519**	**0.1658**	**0.1737**	**0.2035**	**0.2451**	**0.2561**	**0.1798**
B. nancyschneiderae n. sp.	0.0812	0.0904	–	**0.1805**	**0.1734**	**0.2125**	**0.1846**	**0.1499**	**0.1703**	**0.1583**
B. thermophilus (EPR)	0.0674	0.0851	0.0952	–	**0.0137**	**0.0550**	**0.2723**	**0.2792**	**0.3299**	**0.2139**
B. thermophilus (CR)	0.0763	0.0895	0.0933	0.0127	–	**0.0601**	**0.2448**	**0.2926**	**0.3379**	**0.2172**
B. antarcticus	0.0795	0.0918	0.1037	0.0421	0.0450	–	**0.3022**	**0.2780**	**0.2970**	**0.2158**
B. azoricus	0.1131	0.1069	0.1019	0.1264	0.1194	0.1325	–	**0.1242**	**0.1548**	**0.2614**
B. boomerang	0.1071	0.1152	0.0887	0.1241	0.1261	0.1242	0.0772	–	**0.0131**	**0.2447**
B. heckerae	0.1165	0.1191	0.0963	0.1341	0.1358	0.1280	0.0914	0.0123	–	**0.2296**
B. marisindicus	0.0997	0.1003	0.0902	0.1084	0.1101	0.1098	0.1213	0.1140	0.1119	–
B. septemdierum	0.1133	0.1047	0.0929	0.1128	0.1060	0.1061	0.1187	0.1115	0.1146	0.0220

2.4. Morphological analyses

Identification of the *Bathymodiolus* mussels from Costa Rica seeps by morphology alone was difficult, so morphological identifications were confirmed with DNA sequencing (minimally COI). Of the DNA-confirmed specimens, a subset of the largest shells for each species were used for morphological analyses. Electric calipers (Mitutoyo) accurate to 0.01 mm were used to measure 23 shells of *B. billschneideri* n. sp., 22 shells of *B. nancyschneiderae* n. sp., 13 shells of *B. earlougheri* n. sp., and 7 shells of *B. thermophilus* (including the three specimens from the East Pacific Rise that had been previously identified without DNA evidence). Shell length, shell width, and shell height were measured according to Kenk and Wilson (1985) (Supplementary Table 3) for each specimen. When possible, both valves were measured separately and averaged for each specimen, but for specimens with only a single valve preserved, that valve only was measured (since the taxa measured in this study are equivalve). Prior to any analysis, all data was standardized and zero-centered (z-scores) in RStudio v.1.2.1335 to remove size-related variation in shell shape. Following standardization, a principle component analysis (PCA) was conducted in RStudio using ggplot2 (Wickham, 2016), ggfortify (Tang et al., 2016), factoextra (Kassambara and Mundt, 2019), and FactoMineR (Le et al., 2008) to explore the morphometric data by comparing the three shell morphological measurements.

3. Results

3.1. Molecular analyses

The ML and BI analyses for the complete and Gblocked eight-gene concatenated datasets (Fig. 2) were nearly identical, with some variation at poorly supported nodes. The complete and Gblocked MP analyses yielded similar results to the ML and BI analyses but differed from them at poorly supported nodes. All analyses recovered a *Gigantidas* clade and a *Bathymodiolus* clade (excluding *"B." manusensis* and *"B." aduloides*). The concatenated mitochondrial phylogeny differed noticeably (Supplementary Fig. 1); however, there was also conflict between individual gene trees: not all mitochondrial gene trees agreed with one another or the concatenated mitochondrial tree, and not all nuclear gene trees agreed with one another or the concatenated nuclear tree (Supplementary Figs. 1-3). Interspecific uncorrected pairwise distances among *Bathymodiolus* species (excluding *"B." manusensis* and *"B." aduloides*) ranged from 2.09 to 18.37% and the corrected pairwise distances ranged from 2.35 to 35.98% (Supplementary Table 2).

All concatenated analyses (ML, BI, MP) consistently placed *Bathymodiolus billschneideri* n. sp. sister to *B. earlougheri* n. sp. with high support (Fig. 2). This clade was recovered as sister to the clade containing *B. thermophilus* and *B. antarcticus* with maximal support in all concatenated analyses. The concatenated mitochondrial, concatenated nuclear, and individual gene trees also consistently recovered the close sister relationship between *B. billschneideri* n. sp. and *B. earlougheri* n. sp. (Supplementary Figs. 1-3). Most gene trees also recovered the close relationship between *B. thermophilus* and either/both *B. billschneideri* n. sp. and *B. earlougheri* n. sp. (COI, 16S, ND4, HSP70, 18S, 28S, HH3; Supplementary Figs. 2-3). Uncorrected pairwise distances for the COI dataset showed that *B. billschneideri* n. sp. and *B. earlougheri* n. sp. had a minimum divergence of 5.65% from one another (Supplementary Table 2) and the holotypes were 6.24% divergent from one another (Table 3). Both *B. billschneideri* n. sp. and *B. earlougheri* n. sp. also exhibited small uncorrected distances from *B. thermophilus* (9°N haplotype): minimally 6.85% and 8.08% respectively (Table 3, Supplementary Table 2). Model-corrected pairwise distances for a subset of the COI data (*Bathymodiolus* clade only) revealed similar, though larger, relative distances (Table 3, Supplementary Table 2). *Bathymodiolus billschneideri* n. sp. and *B. earlougheri* exhibited a next-closest relationship to *B. thermophilus* (Table 3, Supplementary Table 2). *Bathymodiolus antarcticus*, the sister taxon to *B. thermophilus,* was also closely related to *B. billschneideri* n. sp. and *B. earlougheri* n. sp. (Table 3, Supplementary Table 2).

The ML and BI (concatenated) analyses recovered *Bathymodiolus nancyschneiderae* n. sp. as sister, with low support, to a clade of mixed Pacific, Atlantic, and Indian Ocean taxa that was distinctly separate from the East Pacific taxa, (Fig. 2). The placement of *B. nancyschneiderae* n. sp. was variable across the gene trees (Supplementary Figs. 1-3). The concatenated mitochondrial tree (Supplementary Fig. 1A) recovered *B. nancyschneiderae* as sister to the clade containing the East Pacific taxa *B. thermophilus*, *B. antarcticus*, *B. billschneideri* n. sp., and *B. earlougheri* n. sp. In contrast, the concatenated nuclear tree (Supplementary Fig. 1B) recovered the same placement of *B. nancyschneiderae* n. sp. as the ML and BI analyses. There was not a consistent topology trend associated with mitochondrial or nuclear loci and disagreements between loci were at nodes with poor support. However, most gene trees showed a close relationship between *B. billschneideri* n. sp. and *B. earlougheri* n. sp. that was distinctly separate from *B. nancyschneiderae* n. sp. (Supplementary Figs. 1-3). Since the placement of *B. nancyschneiderae* n. sp. in the eight-gene concatenated ML tree (with the non-East-Pacific taxa) differed from its placement in the concatenated mitochondrial analysis and some of the gene trees, an Approximately Unbiased Test (AU Test), was conducted to compare the original ML tree (seen in Fig. 2) with a constrained ML tree that placed *B. nancyschneiderae* n. sp. with the East Pacific clade. Two AU tests, conducted independently in IQ-Tree and PAUP*, recovered no significant difference between the trees, with p-values of 0.201 and 0.223, respectively. Uncorrected pairwise distances for the COI dataset revealed that *B. nancyschneiderae* n. sp. was minimally 7.52% and 8.08% divergent from *B. billschneideri* n. sp. and *B. earlougheri* n. sp. respectively (Supplementary Table 2). The *B. nancyschneiderae* n. sp. holotype was 8.12% and 9.04% divergent from the *B. billschneideri* n. sp. and *B. earlougheri* n. sp. holotypes respectively (Table 3). *Bathymodiolus nancyschneiderae* n. sp. also exhibited a small uncorrected distance from *B. boomerang* (Table 3, Supplementary Table 2). Model-corrected pairwise distances for the COI data subset revealed similar relationships to the uncorrected dataset for *B. nancyschneiderae* n. sp. (Table 3, Supplementary Table 2): *B. nancyschneiderae* n. sp. was minimally 11.39% and 12.84% divergent from *B. billschneideri* n. sp. and *B. earlougheri* n. sp. respectively (holotypes 13.93% and 16.72% divergent respectively) (Table 3, Supplementary Table 2). Though *B. billschneideri* n. sp. exhibited a smallest minimum corrected distance from *B. nancyschneiderae* n. sp. (above), *B. marisindicus* was also very close to *B. nancyschneiderae* n. sp. (minimum corrected distance of 13.37%) (Supplementary Table 2).

Bathymodiolus thermophilus was recovered as sister to *B. antarcticus* with maximal support in all concatenated analyses (Fig. 2). This clade was recovered as sister to *B. billschneideri* n. sp. and *B. earlougheri* n. sp. also with high support in all concatenated analyses (Fig. 2). *Bathymodiolus thermophilus* samples from Costa Rica were recovered as sister to a confirmed *B. thermophilus* specimen from the East Pacific Rise with a very short branch length and maximal support from all concatenated analyses (Fig. 2) and in all gene trees for which there was sequence data available for both terminals (Supplementary Figs. 2-3). The uncorrected distance analysis (based on the COI dataset) revealed that the *B. thermophilus* specimens sampled from Costa Rica were 0–2.11% divergent from the other *B. thermophilus* sequences (from the East Pacific Rise and the Galápagos Rift) (Table 3, Supplementary Table 2). The corrected distance analysis (based on a subset of the COI data) revealed similar distances (Table 3, Supplementary Table 2). Measurements of the shells of *B. thermophilus* specimens from Costa Rica and the East Pacific Rise resulted in a slight extension of the previously recorded shell measurements for this species. The mean ratio of height to length in specimens from Costa Rica was 0.416; range 0.391–0.430 (previously 0.475, range 0.428–0.513). The mean ratio of width to length in specimens from Costa Rica was 0.137; range 0.124–0.147 (previously 0.208; range of 0.185–0.230).

Haplotype networks generated from the COI data (sequences 450–520 bp in length) for each new species revealed similar network

shapes: within each species there was a single dominant haplotype, with other haplotypes varying by just a few base pairs (Fig. 3). In total, there were 66 *B. billschneideri* n. sp. sequences, 150 *B. nancyschneiderae* n. sp. sequences, 45 *B. earlougheri* n. sp. sequences, and 41 *B. thermophilus* sequences. The COI haplotype network for *B. billschneideri* n. sp. showed that the majority of specimens shared a single haplotype regardless of locality/depth, with a few specimens differing by at most a few base pairs (Fig. 3). However, *B. billschneideri* n. sp. appeared to be restricted to two localities/depths: Jaco Scar (1800 m) and Parrita Seep (1400 m). The *B. earlougheri* n. sp. haplotype network exhibited a similar structure with a single haplotype shared by the majority of specimens regardless of locality (Fig. 3). *Bathymodiolus earlougheri* n. sp. was present at the shallower sampling sites Mound 12 (1000 m) and The Thumb (1060 m), as well as the deepest sampling site, Jaco Scar (1800 m), but not at Parrita Seep (1400 m) (Fig. 3). *Bathymodiolus nancyschneiderae* n. sp. shared the same network shape but was not sampled below 1100 m; it was only present at the three shallowest sampling sites: Mound 12 (1000 m), The Thumb (1070 m) and Jaco-1000 (1060 m) (Fig. 3). The haplotype network generated from the COI data for *B. thermophilus* (Fig. 4, ~400 bp), which included a subset of sequences from East Pacific Rise and Galápagos Rift (Johnson et al., 2013) revealed that the five Costa Rican seep *B. thermophilus* sequences were either of two previously established dominant haplotypes from Johnson et al. (2013). One of the haplotypes (including four Costa Rica specimens) was shared with *B. thermophilus* sequences from vents at the northern East Pacific Rise and southern East Pacific Rise, while the other dominant haplotype (including one Costa Rica specimen) was shared with *B. thermophilus* sequences from vents at the Galápagos Rift, northern East Pacific Rise, and southern East Pacific Rise. These two haplotypes diverged by approximately six base pairs from one another (Fig. 4).

The maximum clade credibility tree created with the Bayesian relaxed-clock analysis (calibrated using fossils at three nodes; converged runs that were conducted with individual fossils did not vary significantly from the combined runs) resulted in an estimated mean age for the most recent common ancestor for *Bathymodiolus* (excluding *"B." manusensis* and *"B." aduloides*) of 17.5 Myr (95% HPD interval: 13.67–21.47) (Fig. 2 inset; see Supplementary Fig. 4 for full time tree). Our analysis calculated an estimated mean age of 4.34 Myr (95% HPD interval: 2.47–6.44 Myr) for the divergence of *B. thermophilus* and *B. antarcticus*, which was previously calculated by Lorion et al. (2013) and Johnson et al. (2013) to be approximately 5 Myr and 2.1–4.3 Myr, respectively. The estimated mean age for the divergence of *B. billschneideri* n. sp. and *B. earlougheri* n. sp. from the *B. thermophilus/antarcticus* clade was 10.4 Myr (95% HPD interval: 7.23–13.94). The estimated mean age for the divergence of *B. billschneideri* n. sp. from *B. earlougheri* n. sp. was 5.44 Myr (95% HPD interval: 2.85–8.30), and the estimated mean age for the divergence of *B. nancyschneiderae* n. sp. from the other *Bathymodiolus* clade (including *B. marisindicus* and *B. azoricus* Cosel and Comtet, 1999) was 15.95 Myr (95% HPD interval: 12.22–19.74) (Supplementary Fig. 4).

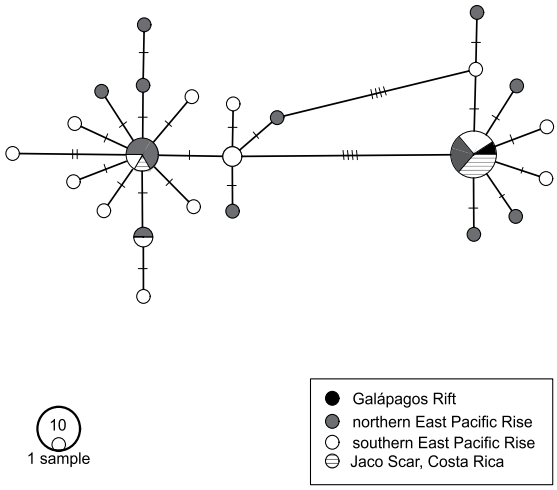

Fig. 4. Haplotype network from COI data for *Bathymodiolus thermophilus*. Color-coded according to locality.

The likelihood ancestral state reconstruction revealed that a seep origin was most likely for the most recent common ancestor of the *Bathymodiolus* clade, excluding *"B." manusensis* and *"B."aduloides* (Fig. 5). Within *Bathymodiolus*, the East Pacific Rise clade containing *B. thermophilus*, *B. antarcticus*, *B. billschneideri* n. sp., and *B. earlougheri* n. sp. was also most likely to have had an ancestor with a seep origin, similarly to its sister clade containing various *Bathymodiolus* species from the Atlantic, West Pacific, Indian Ocean, Caribbean, Gulf of Mexico, and *B. nancyschneiderae* n. sp. from the East Pacific. The habitat

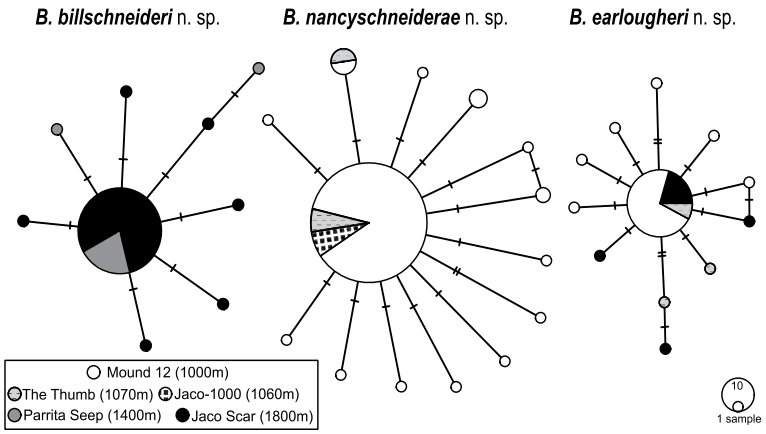

Fig. 3. Haplotype networks from COI data for *Bathymodiolus billschneideri* n. sp., *B. nancyschneiderae* n. sp., and *B. earlougheri* n. sp. Color-coded according to locality/depth of sampling.

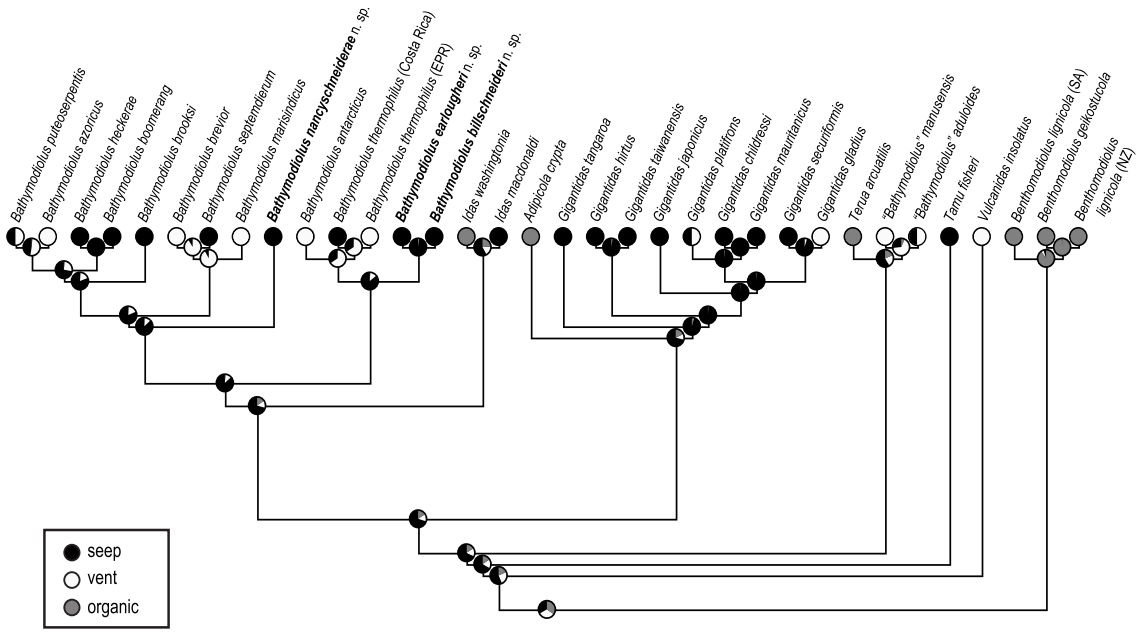

Fig. 5. Likelihood ancestral state reconstruction of habitat (vent, seep, organic fall) mapped onto the complete concatenated ML phylogeny.

of the most recent common ancestor of Bathymodiolinae was ambiguous (Fig. 5).

3.2. Morphological analyses

A morphological examination of the shells of the three new species revealed that *B. earlougheri* n. sp. had a distinguishable shape and color from the other *Bathymodiolus* species sampled from the seeps along the Costa Rica margin. *Bathymodiolus earlougheri* n. sp. shells had a distinct golden-yellow color in all specimens, with a noticeably shorter shell length (relative to shell height and width) and more compact shape than *B. billschneideri* n. sp., *B. nancyschneiderae* n. sp, and *B. thermophilus* (Figs. 6–9). *Bathymodiolus billschneideri* n. sp., *B. nancyschneiderae* n. sp., and *B. thermophilus* could not be reliably differentiated morphologically

Fig. 6. Photographs of shells of *Bathymodiolus thermophilus*. **A.** SIO-BIC M14586, right valve exterior, sampled from Costa Rica (Jaco Scar). **B.** SIO-BIC M14568, right valve exterior, sampled from Costa Rica (Jaco Scar). **C.** SIO-BIC M16462, left valve exterior, sampled from East Pacific Rise. **D.** SIO-BIC M8223, right valve exterior, sampled from Galápagos Rise. Scale bars indicate 20 mm.

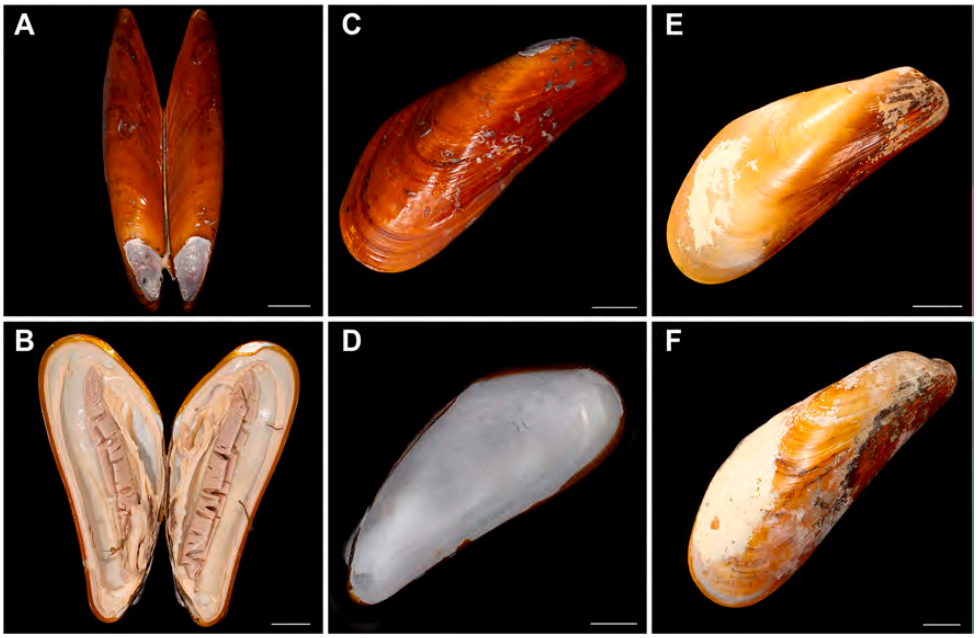

Fig. 7. Photographs of shells and internal anatomy of Bathymodiolus billschneideri n. sp. A. Holotype (SIO-BIC M12074), dorsal exterior. B. Holotype, internal anatomy, ventral view. **C.** Holotype, right valve exterior. **D.** Holotype, right valve interior. **E.** Paratype (SIO-BIC M16763), right valve exterior. **F.** Paratype (SIO-BIC M16793) right valve exterior. Scale bars indicate 20 mm.

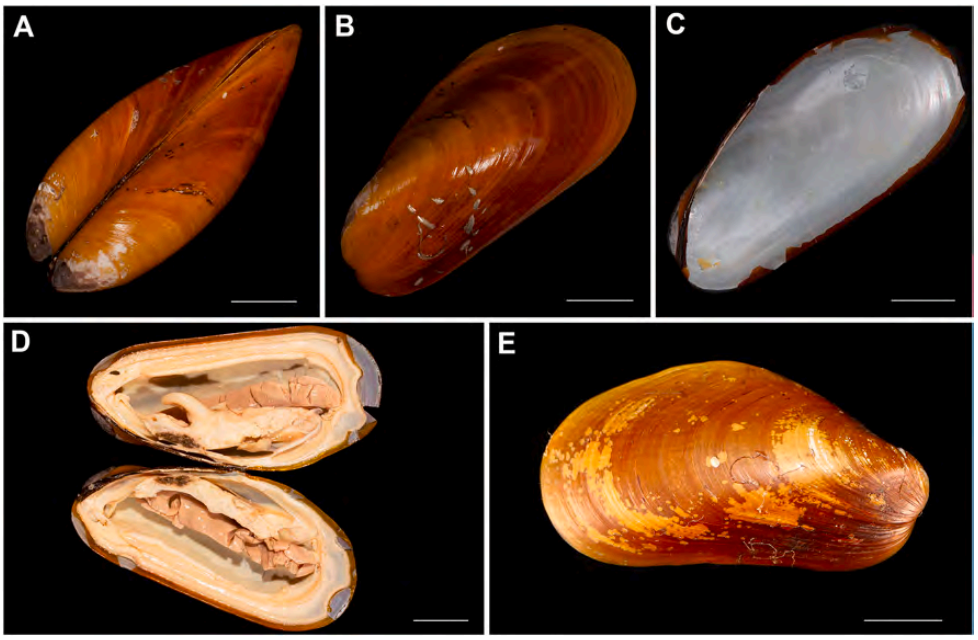

Fig. 8. Photographs of shells and internal anatomy of *Bathymodiolus earlougheri* n. sp. **A.** Holotype (SIO-BIC M12076), dorsal exterior. **B.** Holotype, left valve exterior. **C.** Holotype, right valve interior. **D.** Holotype, internal anatomy, ventral view. **E.** Paratype (SIO-BIC M14479), right valve exterior. Scale bars indicate 20 mm.

and molecular data was required for identification. A Principal Component Analysis (PCA) confirmed the results of the morphological examination, showing that *B. earlougheri* n. sp. could be differentiated reliably from the other two new *Bathymodiolus* species by its more compact shape and golden-yellow color, but that *B. billschneideri* n. sp., *B. nancyschneiderae* n. sp., and *B. thermophilus* could not be differentiated from one another based on shell length, width, or height (Fig. 10). The PCA explained nearly all of the variation (approximately 96%) in the morphological measurements for the shells (shell length, height, and width) of *Bathymodiolus billschneideri* n. sp., *B. earlougheri* n. sp.,

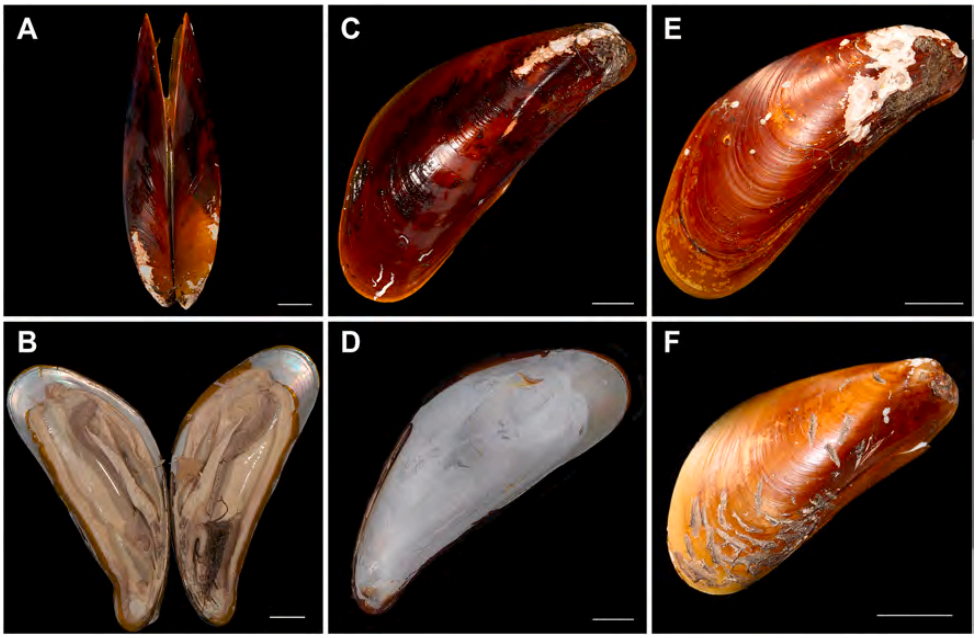

Fig. 9. Photographs of shells and internal anatomy of *Bathymodiolus nancyschneiderae* n. sp. A. Holotype (SIO-BIC M12032), dorsal exterior. B. Holotype, internal anatomy, ventral view. **C.** Holotype, right valve exterior. **D.** Holotype, right valve exterior. **E.** Paratype (SIO-BIC M14531), right valve exterior. **F.** Paratype (SIO-BIC M14530), right valve exterior. Scale bars indicate 20 mm.

B. nancyschneiderae n. sp., and *B. thermophilus* (Fig. 10). PC1 explained approximately 80.1% of the data, and PC2 explained approximately 16.4% of the data (Fig. 10). The relative contributions of shell length, height, and width were 33.3%, 27.1%, and 39.6% (respectively) to PC1, and 33.3%, 1.9%, and 64.8% (respectively) to PC2. *Bathymodiolus thermophilus* (Fig. 6) formed two clusters in the PCA: one that was closer to *B. earlougheri* n. sp. (composed of specimens from the East Pacific Rise) and one that was mixed with *B. billschneideri* n. sp. and *B. nancyschneiderae* n. sp. (specimens from Costa Rica).

4. Discussion

4.1. Molecular analyses

The phylogenetic and distance analyses supported the recognition of three new *Bathymodiolus* species: *B. billschneideri* n. sp., *B. earlougheri* n. sp., and *B. nancyschneiderae* n. sp. (formally described in Taxonomy section) and confirmed the presence of *B. thermophilus* at the Costa Rica seeps. The eight-gene concatenated analyses (ML, BI, MP; complete and Gblocked; Fig. 2) from this study were largely consistent with previous concatenated analyses where nodes were well-supported (Lorion et al., 2013; Thubaut et al., 2013; Xu et al., 2019). The respective monophyly of *Gigantidas* (established by Samadi et al., 2015; Thubaut et al., 2013; Xu et al., 2019) and *Bathymodiolus* (Xu et al., 2019), excluding *"B." manusensis* and *"B." aduloides*, were recovered in all concatenated analyses (Fig. 2). However, our analyses showed some deviation from previous ones at poorly supported nodes. *Bathymodiolus brooksi* Gustafson et al. (1998), *B. brevior*, and *B. azoricus* were always recovered in *Bathymodiolus* and were consistent with Lorion et al. (2013), but their placement within *Bathymodiolus* received low support, varied between analyses, and deviated from Thubaut et al. (2013) and Xu et al. (2019). The placement of *B. nancyschneiderae* n. sp. sister to the non-East-Pacific *Bathymodiolus* species (including *B. azoricus* and *B. septemdierum*) was not well-supported in the ML or MP analyses but was well-supported by the BI analyses (complete and Gblocked). The results of the AU test also showed that the placement of *B. nancyschneiderae* n. sp. sister to the non-East-Pacific *Bathymodiolus* species was not significantly more likely than its placement sister to the East Pacific *Bathymodiolus* species (recovered in the concatenated mitochondrial tree, Supplementary Fig. 1A). This lack of phylogenetic support makes it difficult to ascertain the exact placement of *B. nancyschneiderae* n. sp. in the phylogeny of Bathymodiolinae. However, the phylogeny and minimum distances between *B. nancyschneiderae* n. sp. and its close relatives support its recognition as a new species.

The inclusion of the *Bathymodiolus thermophilus* sample from Costa Rica within *B. thermophilus* was supported by all phylogenetic analyses, distance analyses, and haplotype networks. The samples from Costa Rica exhibited small uncorrected and corrected distances from other available *B. thermophilus* sequences (East Pacific Rise and Galápagos Rift) that were within the expected range for the intraspecific variation of *B. thermophilus*. The COI haplotype network (Fig. 4) of *B. thermophilus* revealed that the Jaco Scar specimens shared two haplotypes with previously sampled specimens from the Galápagos Rift and the East Pacific Rise (940–2300 km away, respectively). This is unsurprising given that *B. thermophilus* specimens from a variety of locations (spanning ~4000 km) along the East Pacific Rise and Galápagos Rift have been shown to share single haplotypes (Johnson et al., 2013), and that *Bathymodiolus* have the capacity for long-distance distance dispersal (Arellano and Young, 2009; Kyuno et al., 2009; Johnson et al., 2013; Arellano et al., 2014). We now confirm records of *B. thermophilus* from the Jaco Scar seep (9.1175°N, 84.8395°W), at depths of 1794–1817 m (Levin et al., 2012).

4.2. Habitat, biogeography, and evolutionary origins of Costa Rica *Bathymodiolus*

The haplotype networks for each of the new species revealed some separation of species by depth along the Costa Rica margin. *Bathymodiolus nancyschneiderae* n. sp. was present only at the shallower dive sites around 1000 m, despite its geographic proximity (less than 1 km) to

deeper sites like Jaco Scar. *Bathymodiolus billschneideri* n. sp. was present at both intermediate sites (Parrita Seep ~1400 m) and deep sites, (Jaco Scar ~1800 m), but was never found at any of the shallower dive sites (Mound 12, The Thumb, Jaco-1000), despite their geographic proximity. *Bathymodiolus earlougheri* n. sp. was present at some of the shallowest sites (1000–1070 m) and deepest sites (1800 m) (Fig. 3) but was not found at any intermediate depths. Each of the haplotype networks for the new *Bathymodiolus* species exhibited a star-shape in which a single haplotype was much more frequent than the others, which is suggestive of a past evolutionary bottleneck (Bazin et al., 2006; Plouviez et al., 2009). In contrast, the reduced-representation haplotype network of *B. thermophilus* (Fig. 4) showed two closely related haplotypes that were more frequent than the others. This finding is consistent with the COI haplotype networks for *B. thermophilus* by Johnson et al. (2013).

The separation of *B. nancyschneiderae* n. sp. from *B. billschneideri* n. sp./*B. earlougheri* n. sp. indicated by some of the molecular analyses suggests it may have a different biogeographic origin from the other *Bathymodiolus* species at the Costa Rica margin. *Bathymodiolus billschneideri* n. sp. and *B. earlougheri* n. sp. were grouped with high support into a clade with *B. thermophilus* and *B. antarcticus* that is sister to the other *Bathymodiolus* species, (Fig. 2). This clearly suggests a Pacific origin for *B. billschneideri* n. sp. and *B. earlougheri* n. sp. However, *B. nancyschneiderae* appeared in the ML and BI analyses to be more closely related to taxa from a variety of other places, including the Atlantic, Indian, and West Pacific oceans. The stratification by depth of *B. nancyschneiderae* n. sp. (only found at ~1000 m) versus *B. billschneideri* n. sp. (only found at 1400–1900 m) may also represent evidence of a different origin. Some of the taxa that *B. nancyschneiderae* n. sp. is closely related to are prevalent in the Gulf of Mexico (*B. brooksi*, *B. heckerae* Gustafson et al., 1998), Caribbean (*B. boomerang*), and Mid-Atlantic Ridge (*B. puteoserpentis* Cosel, Métivier & Hashioto, 1994; *B. azoricus*). Other taxa that exhibit this phylogenetic pattern, such as the vesicomyid *Abyssogena* Krylova, Sahling & Janssen, 2010, the ampharetid *Amphisamytha fauchaldi* Solis-Weiss and Hernandez-Alcantara, 1994, and the annelid *Lamellibrachia donwalshi* McCowin and Rouse, 2018, are hypothesized to have had ancestors that spanned the open seaway between the Pacific and Atlantic and speciated during the shoaling up of deep water that occurred as the Panama Isthmus began to form (Stiller et al., 2013; O'Dea et al., 2016; LaBella et al., 2017). *Amphisamytha fauchaldi*, which was sampled from seeps along the East Pacific margin including Costa Rica, was shown to have a sister taxon from as far as the Mid-Atlantic Ridge (Stiller et al., 2013). Four species of polynoid scaleworms belonging to *Branchipolynoe* Pettibone, 1984 were recently described, and are all symbionts of the *Bathymodiolus* mussels described here (Lindgren et al., 2019). There was no distinct correlation between the divergence patterns of the scaleworms and their mussel hosts. Two of these scaleworms were shown to be most closely related to another species of *Branchipolynoe* from the Gulf of Mexico, rather than to Pacific *Branchipolynoe,* but they are not specific to *B. nancyschneiderae* n. sp. However, the *Bathymodiolus* clade that *B. nancyschneiderae* n. sp. was recovered as sister to also contains taxa sampled from the Central Indian Ridge (*B. marisindicus*) and the Northwest Pacific (*B. septemdierum*, *B. brevior*). It is possible, given the known long larval duration and dispersal capabilities of some Bathymodiolinae (e.g., *G. childressi* (Arellano et al., 2014; Arellano and Young, 2009)) that an ancestor of these taxa and *B. nancyschneiderae* n. sp. could have dispersed across the Pacific and/or from the Central Indian Ridge. However, due to the uncertainty of the placement of *B. nancyschneiderae* n. sp. in the phylogeny, more molecular data is needed to resolve the evolutionary origin of *B. nancyschneiderae* n. sp. While the genetic and depth separation between *B. nancyschneiderae* n. sp. and the other *Bathymodiolus* species at the Costa Rica margin is compelling, additional genetic loci will be needed to refine the placement of *B. nancyschneiderae* n. sp. in Bathymodiolinae.

Bathymodiolus thermophilus was sampled from a single seep site at the Costa Rica margin, Jaco Scar. This represents confirmation with genetic data of *B. thermophilus* at a seep environment first reported in Levin et al. (2012). *Bathymodiolus thermophilus* had previously been thought to be a vent-endemic, so its appearance at a seep is of interest. The ancestral state reconstruction of habitat for the Bathymodiolinae in this study suggests that *B. thermophilus*, which had been previously observed only at vents (Won et al., 2003; Johnson et al., 2013), may have had a seep origin (Fig. 5). The most recent common ancestor of the *Bathymodiolus* clade (excluding "*B.*" *manusensis* and *"B." aduloides*) is most likely to be of seep origin as well (Fig. 5). Jaco Scar has been previously reported to have temperature anomalies of up to 3 °C above ambient seawater in areas of "shimmering water" where *B. thermophilus* mussels were sampled (Levin et al., 2012). According to Levin et al. (2012), Jaco Scar may represent an intermediate environment with both vent and seep characteristics (a "hydrothermal seep"). It is possible that intermediate environments like these facilitated the dispersal of *B. thermophilus* to both vent and seep environments, though it has not yet been reported at any of the other seep environments along the Costa Rica margin.

This study represents the first documentation of three sympatric *Bathymodiolus* species at a single dive site, Jaco Scar (as well as four species within approximately 1 km of each other). Current sampling suggests that the three newly discovered *Bathymodiolus* species are unique to this area. Other taxa that were reported at the Costa Rica margin seep sites have been reported and confirmed with genetic data at other seeps and vents north of Costa Rica, such as Vestimentifera (e.g. *Lamellibrachia barhami* (McCowin and Rouse, 2018)), Ampharetidae (e.g., *Amphisamytha fauchaldi* (Stiller et al., 2013)), Amphinomidae (e.g., *Archinome levinae* (Borda et al., 2013)), and Vesicomyidae (*Archivesica gigas* (Levin et al., 2012; Breusing et al., 2019)). However, no Bathymodiolinae have been reported at any vent sites north of 13°N on the East Pacific Rise (Johnson et al., 2013), even though surface dispersal and long duration of larval stages should make it possible for these mussels to disperse long distances (Arellano et al., 2014; Arellano and Young, 2009; Kyuno et al., 2009). Seeps are known to exist along the continental margin south of Costa Rica as far as Chile (Sellanes et al., 2008; Zapata-Hernández et al., 2014; Kobayashi and Araya, 2018), and reports of Bathymodiolinae have been made there, but little deep-sea exploration has been conducted along the coast of South America. While the dispersal capabilities of the new *Bathymodiolus* species at Costa Rica have not been directly tested, given the known dispersal capabilities of their close relatives (Arellano et al., 2014), we believe that it is likely that their range extends south of Costa Rica. Future sampling in the East Pacific, especially along the South American coast, is needed to confirm this.

4.3. Morphology and the importance of molecular data

While the molecular analyses in this study clearly revealed three new *Bathymodiolus* species from seeps at the Costa Rica margin, morphological examination did not yield this same result. Only two new species were reported in initial observations from the Costa Rica margin (Levin et al., 2012) because the four species actually present could not be differentiated morphologically (confirmed by the PCA, Fig. 10), while there was clear genetic evidence for three new mussel species and *B. thermophilus* in the molecular dataset. The disparity between the morphological and molecular data underscores the importance of molecular data for future biological and ecological studies along the Costa Rica margin. Without molecular data, the number of mussel species, the stratification of those species by depth, and the resulting evolutionary and biogeographical hypotheses for *Bathymodiolus* mussels from the Costa Rica margin would have been lost. Data like these will be important for future ecological studies and conservation efforts, which cannot hope to accurately portray ecological relationships at seeps along the Costa Rica margin without the species-level information that can only be obtained from molecular data.

5. Conclusion

This study revealed three new species of *Bathymodiolus* and confirmed the presence of *B. thermophilus* at seeps along the Costa Rica margin. While morphological data alone could not discriminate four species, molecular analyses (including phylogenies based on four mitochondrial and four nuclear genes, distance analyses, and haplotype networks) provided strong support for the three new species *B. billschneideri* n. sp., *B. earlougheri* n. sp., and *B. nancyschneiderae* n. sp., and for the presence of *B. thermophilus* at the Costa Rica margin. Our molecular analyses also revealed the depth stratification of some of the mussel species (*B. billschneideri* n. sp. restricted to deeper sites and *B. nancyschneiderae* n. sp. restricted to shallower sites).

6. Taxonomy

6.1. Family: Bathymodiolinae *Kenk and Wilson, 1985*.

Bathymodiolus Kenk and Wilson, 1985.
Type species: *Bathymodiolus thermophilus* Kenk and Wilson, 1985.

6.2. *Bathymodiolus billschneideri n sp.*

(Figs. 3 and 7; Supplementary Fig. 5A).
urn:lsid:zoobank.org:act:C0B4867B-1900-4CE9-A27F-1DD187153152
Bathymodiolus n. sp. Levin et al., (2012), p. 2583.
Bathymodiolus sp. Levin et al., (2015), supplemental data.
Bathymodiolus sp. 1 Lindgren et al., (2019), p. 153.

6.2.1. Material Examined

Holotype: SIO-BIC M12074, collected on March 7, 2009 from Jaco scar, HOV *Alvin* Dive 4513, 1817 m depth; 9.1167°N, 84.8351°W. Collected by G. Rouse and D. Huang. Subsample of foot preserved in 95% ethanol for molecular analyses; remainder of specimen fixed in 8% formalin and preserved in 50% ethanol.

Paratypes: SIO-BIC M14533 and SIO-BIC M14534 collected on May 26, 2017 from Jaco Scar, HOV *Alvin* Dive 4911, 1891 m depth; 9.1151°N, 84.8468°W. Subsample of foot preserved in 95% ethanol, 1 valve cleaned for dry preservation. SIO-BIC M16763 and SIO-BIC M16793 collected on October 18, 2018 from Jaco Scar, HOV *Alvin* Dive 4972, 1784 m depth; 9.1178°N, 84.8395°W. Subsample of foot preserved in 95% ethanol, 1 valve cleaned for dry preservation. SIO-BIC M17000 collected on November 5, 2018 from Parrita Seep, HOV Alvin Dive 4990, 1400 m depth; 9.0318°N, 84.6205°W. Subsample of foot preserved in 95% ethanol, 1 valve cleaned for dry preservation. MZUCR 8578 collected on March 3, 2009 from Jaco Scar, HOV *Alvin* Dive 4509, 1783 m depth; 9.1172°N, 84.8417°W. Subsample of foot preserved in 95% ethanol for molecular analyses; remainder of specimen fixed in 8% formalin and preserved in 50% ethanol.

Other Material Examined: See Table 1 and Supplementary Table 1 for genetic data and Supplementary Table 3 for additional morphological data.

6.2.2. Description

Shell large, up to 189.14 mm (Supplementary Table 3), thin but sturdy, elongate modioliform, equivalve, slightly variable in outline. Shell height to length ratio 0.35–0.56, width to length ratio 0.12–0.24. Shell height gradually increasing anteriorly, curved dorsoventrally, most inflated at the middle, with a broadly rounded ridge extending from umbonal region to posterior-ventral margin. Anterior margin short and narrow but evenly rounded; ventral margin slightly concave. Posterior margin broadly rounded; posterio-dorsal angulation well defined, broadly rounded, situated anteriorly to the posterior adductor scar. Dorsal margin markedly convex, slightly curved to straight over the span of the ligament, highest part of the valve situated along middle of ligament. Umbones fairly narrow and flattened, situated 5–10% posteriorly from anterior margin, subterminal, prosogyrate; eroded with nacreous layer free in larger specimens (Fig. 7).

Ligament plate narrow, slightly convex to straight. Exterior smooth except for well-developed, irregular commarginal growth lines and very faint and irregularly spaced radial striae in periostracum running from the umbo to the posterior/dorsal margin. Periostracum smooth, glossy, thick and yellow to brown, lightest in umbonal and posterior margin regions, darkest on anterior-dorsal slope, curving over shell edge. Byssal hairs and byssal endplates of other specimens often scattered over surface. Shell dull-white to grey under periostracum (Fig. 7). Ligament opisthodetic, long and narrow, extending over four-fifths to five-sixth of the

Postero-dorsal margin in front of the postero-dorsal corner, ending posteriorly with a slight taper. Hinge edentulous, hinge thickened below and anterior to umbo. Hinge denticles absent in smallest specimens.

Anterior adductor scar small and rounded but truncated posteriorly, situated medially/dorsally in the anterior part of the valve, partly below and partially anterior to umbo, distant to antero-ventral margin. Anterior byssal-pedal retractor scar oval, located high within umbonal cavity behind umbo. Posterior adductor scar rounded-rectangular. Posterior byssal-pedal retractor muscles form two separate scars with large gap between them, anterior one elongate-elliptical, located high, and close to posterior end of ligament, second one elliptical and located antero-dorsally to but contiguous with posterior adductor scar to form a joint comma-shaped scar. Pallial line distinct, extending ventrally from anterior adductor to posterior adductor, parallel to ventral margin (Supplementary Fig. 5A).

Animal with long, narrow ctenida, 100 mm long and 11 mm broad in holotype; outer demibranchs anteriorly slightly shorter than inner demibranch; both demibranchs end abruptly anteriorly, taper posteriorly (Fig. 7B). Filaments broad and fleshy, ventral edges lack food grooves. Foot medium sized, 27 mm long (byssus orifice included) in holotype. Foot thick, flattened, slightly terminally swollen; byssal groove running along ventral surface almost to tip. Byssal threads sparce, usually emerging as separate strands from orifice, strands thick and strong. Foot-byssus retractor complex moderately prolongated like the shell. Posterior byssal retractors in two roughly equal main bundles arising together at base of byssus but diverge and attach separately to shell. Posterior pedal retractors thick, arising from base of foot anterior to origin of posterior byssal retractors, passing dorsally on both inner and outer sides of most anterior bundles of posterior retractors (Fig. 7B).

6.2.3. Etymology

This species is named for William (Bill) Schneider, a San Diego native and lover of all marine life including molluscs, and a great supporter of the Benthic Invertebrate Collection at Scripps Institution of Oceanography.

6.2.4. Distribution

Bathymodiolus billschneideri n. sp. is known from Jaco Scar (1783–1891 m) and Parrita Seep (1400 m).

6.2.5. Variation

Bathymodiolus billschneideri n. sp. specimens differ genetically by at most a few base pairs (COI, Fig. 3); there is considerable color variation between specimens, from dark brown to gold and yellow (Fig. 7E–F).

6.2.6. Remarks

The shells of *Bathymodiolus billschneideri* n. sp. most closely resemble those of *B. nancyschneiderae* n. sp., with the PCA unable to separate the two species morphologically (Supplemental Fig. 5). Overall size ranges, umbone location, ligament length, and muscle scars of the two species were also very similar. The two species are separated by approximately 400–800 m, with *B. billschneideri* n. sp. occurring at depths of approximately 1400–1800 m and *B. nancyschneiderae* n. sp. occurring at depths

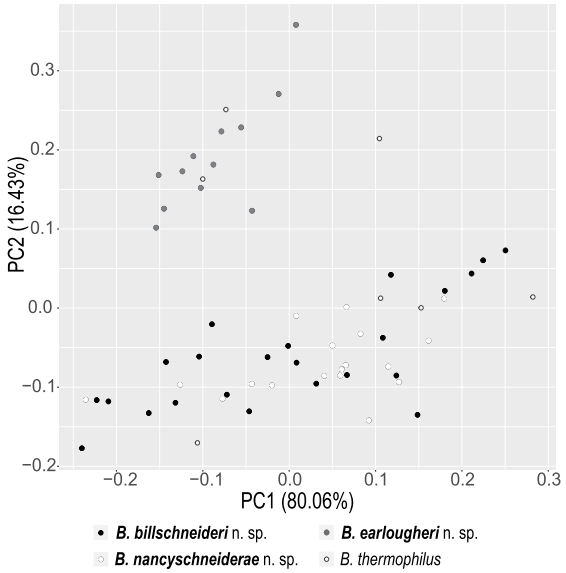

Fig. 10. Principal component analysis of shell length, shell width, and shell height of *Bathymodiolus billschneideri* n. sp., *B. earlougheri* n. sp., *B. nancyschneiderae* n. sp., and *B. thermophilus*.

of approximately 1000–1100 m. *Bathymodiolus billschneideri* n. sp. is often slightly lighter in coloration than *B. nancyschneiderae* n. sp., has a less angular postero-dorsal corner, a wider posterior part, and a more evenly concave ventral margin. The shell of *B. billschneideri* n. sp. also resembles *B. thermophilus*. The two species can sometimes be differentiated by color: the darker brown specimens of *B. billschneideri* n. sp. can be differentiated from the golden-yellow *B. thermophilus* (Figs. 6 and 7). However, the yellow *B. billschneideri* n. sp. specimens could not be differentiated from *B. thermophilus* specimens from Costa Rica (Fig. 6A–B, 7), but tended to have a more elongate shell shape that allowed them to be differentiated from *B. thermophilus* specimens from the East Pacific Rise (Fig. 6C–D, 7).

6.3. *Bathymodiolus earlougheri n sp.*

(Figs. 3 and 8; Supplementary Fig. 5B).

urn:lsid:zoobank.org:act:CDD83187-F83C-4FAE-A730-026A3C3EC989

Bathymodiolus sp. Aguado and Rouse (2011), p. 114.
Bathymodiolus n. sp. Levin et al., (2012), p. 2583.
Bathymodiolus sp. Levin et al., (2015), supplemental data.
Bathymodiolus sp. 3 Lindgren et al., (2019), p. 153.

6.3.1. *Material Examined*

Holotype: SIO-BIC M12076 collected on March 7, 2009 from Jaco Scar, HOV *Alvin* Dive 4513, 1817m depth; 9.1167°N, 84.8351°W. Collected by G. Rouse and D. Huang. Subsample of foot preserved in 95% ethanol for molecular analyses; remainder of specimen fixed in 8% formalin and preserved in 50% ethanol.

Paratypes: SIO-BIC M12080 collected on March 7, 2009 from Jaco Scar, HOV *Alvin* Dive 4513, 1817 m depth; 9.1167°N, 84.8351°W. Subsample of foot preserved in 95% ethanol, 1 valve cleaned for dry preservation. SIO-BIC M14479 collected on May 22, 2017 from Mound 12, HOV *Alvin* Dive 4907, 999 m depth; 8.9304°N, 84.3128°W. Subsample of foot preserved in 95% ethanol, 1 valve cleaned for dry preservation. MZUCR 8579 collected on March 7, 2009 from Jaco Scar, HOV *Alvin* Dive 4513, 1817 m depth; 9.1167°N, 84.8351°W. Subsample of foot preserved in 95% ethanol for molecular analyses; remainder of specimen fixed in 8% formalin and preserved in 50% ethanol.

Other Material Examined: See Table 1 and Supplementary Table 1 for genetic data and Supplementary Table 3 for additional morphological data.

6.3.2. *Description*

Shell medium sized, up to 119.9 mm, short and stout modioliform, thin but fairly sturdy, equivalve, very inflated, elliptical in immature specimens, becoming increasingly arculate in larger, older specimens. Shell height to length ratio 0.44–0.56, shell width to height ratio 0.2–0.24. Shell height increasing posteriorly, exhibiting somewhat trapezoid outline. Anterior margin narrowly rounded, posterior margin broadly rounded, ventral margin straight to very slightly concave. Dorsal margin convex, postero-dorsal corner indistinct and gently rounded. Umbones prosogyrate low, broad and flattened, subterminal to nearly terminal in some specimens, situated 3–7% posteriorly from anterior margin, eroded in larger specimens with nacreous layer free. An indistinct, raised, and broadly rounded ridge extends from the umbonal region to the postero-ventral margin (Fig. 8).

Exterior smooth except for faint, irregular commarginal growth lines. Periostracum smooth, dull to somewhat glossy, thin and golden brown to copper brown to golden, occasionally byssal endplates and hair present from other specimens. Shell dull-white under periostracum. Ligament plate narrow, slightly convex to straight. Ligament opisthodetic, extending posteriorly from umbones to occupy ~40% of dorsal margin. Posterior end of ligament tapering, subligamental shell ridge strong and angular. Adult hinge edentulous, thickened below and anterior to umbo (Fig. 8).

Muscle scars and pallial line fairly indistinct. Anterior adductor muscle scar small and oblong, tapering posteriorly, situated more ventrally in the anterior part of the valve, partly below and partially posterior to umbo. Posterior adductor scar round, contiguous dorsaly with single posterior byssal-pedal retractor scar; posterior byssal retractors forming continuous scar extending from directly beneath posterior end of ligament to antero-dorsal edge of posterior adductor scar. Ventral pallial line straight, paralleling the ventral shell margin and extending from postero-ventral edge of anterior adductor scar to posterior adductor (Supplementary Fig. 5B).

Animal with long, wide ctenida, 86 mm long and 7 mm broad in holotype; outer demibranchs anteriorly slightly shorter than inner demibranch; both demibranchs end abruptly anteriorly (Fig. 8D). Filaments broad and fleshy, ventral edges lack food grooves. Foot small sized, 13 mm long (byssus orifice included) in holotype. Foot fairly thick, rounded, terminally tapered; byssal groove running along ventral surface almost to tip. Byssus sparse, usually emerging as separate strands from orifice, strands thick and strong. Foot-byssus retractor complex moderately prolongated like the shell. Posterior byssal retractors in two roughly equal main bundles arising together at base of byssus but diverge and attach separately to shell. Posterior pedal retractors thick, arising from base of foot anterior to origin of posterior byssal retractors, passing dorsally on both inner and outer sides of most anterior bundles of posterior retractors (Fig. 8).

6.3.3. *Etymology*

This species is named in memory of Robert Charles "Chuck" Earlougher in recognition of the support of the SIO Collections by his daughter Jan and her husband Jim Hawkins.

6.3.4. *Distribution*

Bathymodiolus earlougheri n. sp. is known from Jaco Scar (1812–1891 m), The Thumb (1073 m), and Mound 12 (999–1008 m).

6.3.5. *Variation*

Bathymodiolus earlougheri n. sp. specimens differ genetically by at most a few base pairs (COI, Fig. 3) and show less morphological

variation in shell color and shape than *B. billschneideri* n. sp. specimens (Fig. 8).

6.3.6. Remarks

Bathymodiolus earlougheri n. sp. morphologically resembles *B. azoricus* and B. *thermophilus* (East Pacific Rise specimens). *Bathymodiolus earlougheri* n. sp. is stouter, wider, more wedge shaped, and lighter and more golden in color than *B. azoricus*. *Bathymodiolus earlougheri* n. sp. shells also closely resemble *B. thermophilus* specimens that are under ~10 cm long, sharing a similar wedge modioliform shape and straight to slightly concave ventral margin. However, the umbones are more anteriorly situated in *B. earlougheri* n. sp., and larger specimens are more elongate with a concave ventral margin and therefore easily distinguishable. *Bathymodiolus earlougheri* n. sp. also shares the two-bundle foot byssus retractor complex with *B. thermophilus*. *Bathymodiolus earlougheri* n. sp. is easily morphologically distinguishable from the two other new seep species, *B. billschneideri* n. sp. and *B. nancyschneiderae* n. sp., by its golden color and compact shape (Figs. 8 and 10).

6.4. *Bathymodiolus nancyschneiderae n sp.*

(Figs. 3 and 9; Supplementaary Fig. 5C).

urn:lsid:zoobank.org:act:FCC9AAEF-BCD6-48DB-85F8-3069C95DFE20

Bathymodiolus n. sp. Levin et al., (2012), p. 2583.

Bathymodiolus sp. Levin et al., (2015), supplemental data.

Bathymodiolus sp. 2 Lindgren et al., (2019), p. 153.

6.4.1. Material Examined

Holotype: SIO-BIC M12032, collected on March 3, 2009 from Jaco-1000, HOV *Alvin* Dive 4509, 1063 m depth; 9.1172°N, 84.8417°W. Collected by G. Rouse and D. Huang. Subsample of foot preserved in 95% ethanol for molecular analyses; remainder of specimen fixed in 8% formalin and preserved in 50% ethanol.

Paratypes: SIO-BIC M14530 and SIO-BIC M14531 collected on May 24, 2017 from Mound 12, HOV Alvin Dive 4909, 1000 m depth; 8.9305°N, 84.3125°W. Subsample of foot preserved in 95% ethanol, 1 valve cleaned for dry preservation. SIO-BIC M16778 collected on October 21, 2018 from Mound 12, HOV *Alvin* Dive 4975, 1000 m depth; 8.9337°N, 84.3067°W. Subsample of foot preserved in 95% ethanol, 1 valve cleaned for dry preservation. MZUCR 8577 collected on March 3, 2009 from Jaco-1000, HOV *Alvin* Dive 4509, 1063 m depth; 9.1172°N, 84.8417°W. Fixed in 8% formalin and preserved in 50% ethanol.

Other Material Examined: See Table 1 and Supplementary Table 1 for genetic data and Supplementary Table 3 for additional morphological data.

6.4.2. Description

Shell large up to 181.67 mm, thick sturdy, elongate modioliform, equivalve, slightly variable in outline. Shell height to length ratio 0.37–0.42, shell width to shell length ratio 0.13–0.15. Shell height gradually increasing anteriorly, curved dorsoventrally, most inflated at the middle, with a broadly rounded ridge extending from umbonal region to postero-ventral margin. Anterior margin short and narrow but evenly rounded; ventral margin markedly concave, with most concave part located far anteriorly. Posterior margin broadly rounded; posterio-dorsal angulation ill-defined, very broadly rounded, situated anteriorly to the posterior adductor scar. Dorsal margin markedly convex, slightly curved to straight over the span of the ligament, highest part of the valve situated along middle of ligament. Umbones fairly narrow and flattened, situated 9–13% posteriorly from anterior margin, subterminal, prosogyrate; eroded with nacreous layer free in larger specimens (Fig. 9).

Ligament plate narrow, slightly convex to straight. Exterior smooth except for well-developed, irregular commarginal growth lines and very faint and irregularly spaced radial striae in periostracum running from the umbo to the posterior/dorsal margin. Periostracum smooth, glossy, thick and brown to dark brown, lightest in umbonal and posterior margin regions, darkest on anterior-dorsal slope, curving over shell edge. Byssal hairs and byssal endplates of other specimens often scattered over the surface, polychaete tubes often present. Shell dull-white to grey under periostracum (Fig. 9). Ligament opisthodetic, long and narrow, extending over ~80% of the postero-dorsal margin in front of the postero-dorsal corner, ending posteriorly with a slight taper. Hinge edentulous in large specimens, hinge thickened below and anterior to umbo. Hinge denticles absent in smallest specimens.

Anterior adductor scar medium and rounded, situated medially/dorsally in the anterior part of the valve, partly below and partially anterior to umbo, distant to antero-dorsal margin. Anterior byssal-pedal retractor scar elliptical, located within umbonal cavity behind umbo; posterior adductor scar rounded and elongate; posterior byssal-pedal retractor muscles form two separate scars with gap between them, anterior one elongate-elliptical, located high, and close to posterior end of ligament, second one elliptical and located antero-dorsally to but contiguous with posterior adductor scar to form a joint comma-shaped scar. Pallial line distinct, extending ventrally from anterior adductor to posterior adductor, parallel to ventral margin (Supplementary Fig. 5C).

Animal with long, narrow ctenida, 138 mm long and 12 mm broad in holotype; outer demibranchs anteriorly slightly shorter than inner demibranch; both demibranchs end abruptly anteriorly. Filaments broad and fleshy, ventral edges lack food grooves. Foot medium sized, 24 mm long (byssus orifice included) in holotype. Foot thick, rounded, terminally tapered; byssal groove running along ventral surface almost to tip. Byssus abundant, usually emerging as separate strands from orifice, strands dark, thick and strong. Foot-byssus retractor complex moderately prolongated like the shell. Posterior byssal retractors in two roughly equal main bundles arising together at base of byssus but diverge and attach separately to shell. Posterior pedal retractors thick, arising from base of foot anterior to origin of posterior byssal retractors, passing dorsally on both inner and outer sides of most anterior bundles of posterior retractors (Fig. 9).

6.4.3. Etymology

This species is named for Nancy Schneider, a San Diego native and lover of all marine life including molluscs, and a great supporter of the Benthic Invertebrate Collection at Scripps Institution of Oceanography.

6.4.4. Distribution

Bathymodiolus nancyschneiderae n. sp. is known from Mound 12 (999–1008 m), Jaco-1000 (1063 m), and The Thumb (1072–1073 m).

6.4.5. Variation

Bathymodiolus nancyschneiderae n. sp. specimens differ genetically by at most a few base pairs (COI, Fig. 3) and tend to have less color variation than *B. billschneideri* n. sp. specimens. However, some smaller *B. nancyschneiderae* n. sp. specimens have a more golden-brown color (similar to *B. billschneideri* n. sp.) than the larger adults (Fig. 9E–F).

6.4.6. Remarks

The shell of *B. nancyschneiderae* n. sp. most closely resembles that of *B. billschneideri* n. sp., with the PCA unable to separate the two species morphologically (Fig. 10). Overall size ranges, umbone location, ligament length, and muscle scars of the two species are also very similar. The two species do not co-occur at a single dive site but are found at different depths within 1 km of each other (Jaco-1000 and Jaco Scar, approximately 1000 m and 1800 m, respectively). *Bathymodiolus nancyschneiderae* n. sp. tends to have a darker periostracum than *B. billschneideri* n. sp., and a rounder and wider postero-dorsal corner, a narrower posterior part, and the most concave part of the ventral margin is not in the middle of the shell as in *B. billschneideri* n. sp. but more anteriorly situated. The shell of *B. nancyschneiderae* n. sp. also resembles

B. azoricus, *B. brooksi*, and *B. heckerae*. It is distinguished from *B. azoricus* by a markedly more concave ventral margin, more pronounced umbones, and a more elongate form. Both *B. heckerae* and *B. brooksi* have the same periostracal coloration as *B. nancyschneiderae* n. sp., but both have a straighter ventral margin, more posteriorly situated umbones, and a more posteriorly situated postero-dorsal corner.

Declaration of competing interest

The authors declare that they have no known competing financial interests or personal relationships that could have appeared to influence the work reported in this paper.

Acknowledgements

Many thanks to Chief Scientists Lisa Levin and Erik Cordes, the captain and crew of the *R/V Atlantis* and the *R/V Falkor*, and the pilots of the HOV *Alvin* and ROV *SuBastian* for crucial assistance in specimen collection on cruises to Costa Rica. Thanks also to Charlotte Seid for collection management at SIO-BIC. We would also like to thank Shirley Sorokin and the South Australian Museum (SAM) for curation of samples. We thank Bill and Nancy Schneider and Jan and Jim Hawkins for their support of the SIO Collections and the Schmidt Ocean Institute for ship time support and publishing costs. This project was supported by the US National Science Foundation (NSF OCE-0826254, OCE-0939557, OCE-1634172).

Appendix A. Supplementary data

Supplementary data to this article can be found online at https://doi.org/10.1016/j.dsr.2020.103322.

References

Aguado, M.T., Rouse, G.W., 2011. Nautiliniellidae (Annelida) from costa rican cold seeps and a western pacific hydrothermal vent, with description of four new species. Syst. Biodivers. 9, 109–131. https://doi.org/10.1080/14772000.2011.569033.

Arellano, S.M., Van Gaest, A.L., Johnson, S.B., Vrijenhoek, R.C., Youn, C.M., 2014. Larvae from deep-sea methane seeps disperse in surface waters. Proc. R. Soc. B Biol. Sci. 281, 8. https://doi.org/10.1098/rspb.2013.3276.

Arellano, S.M., Young, C.M., 2009. Spawning, development, and the duration of larval life in a deep-sea cold-seep mussel. Biol. Bull. 216, 149–162. https://doi.org/10.2307/25470737.

Audzijonyte, A., Vrijenhoek, R.C., 2010. Three nuclear genes for phylogenetic, SNP and population genetic studies of molluscs and other invertebrates. Mol. Ecol. Resour. 10, 200–204. https://doi.org/10.1111/j.1755-0998.2009.02737.x.

Baco-Taylor, A.R., 2002. Food-web structure, succession and phylogenetics on deep-sea whale skeletons. PhD Thesis. The University of Hawaii.

Bandelt, H., Forster, P., Röhl, A., 1999. Median-joining networks for inferring intraspecific phylogenies. Mol. Biol. Evol. 16, 37–48.

Bazin, E., Glemin, S., Galtier, N., 2006. Population size does not influence mitochondrial genetic diversity in animals. Science 84 312, 570–572. https://doi.org/10.1126/science.1122033.

Borda, E., Kudenov, J.D., Chevaldonne, P., Blake, J.A., Desbruyeres, D., Fabri, M.-C., Hourdez, S., Pleijel, F., Shank, T.M., Wilson, N.G., Schulze, A., Rouse, G.W., 2013. Cryptic species of *Archinome* (Annelida: amphinomida) from vents and seeps. Proc. R. Soc. B Biol. Sci. 280, 9. https://doi.org/10.1098/rspb.2013.1876.

Bouckaert, R., Vaughan, T.G., Barido-Sottani, J., Duchêne, S., Fourment, M., Gavryushkina, A., Heled, J., Jones, G., Kühnert, D., De Maio, N., Matschiner, M., Mendes, F.K., Müller, N.F., Ogilvie, H.A., du Plessis, L., Popinga, A., Rambaut, A., Rasmussen, D., Siveroni, I., Suchard, M.A., Wu, C.H., Xie, D., Zhang, C., Stadler, T., Drummond, A.J., 2019. Beast 2.5: an advanced software platform for Bayesian evolutionary analysis. PLoS Comput. Biol. 15 (4), 28. https://doi.org/10.1371/journal.pcbi.1006650 e1006650.

Breton, S., Beaupré, H.D., Stewart, D.T., Hoeh, W.R., Blier, P.U., 2007. The unusual system of doubly uniparental inheritance of mtDNA: isn't one enough? Trends Genet. 23, 465–474. https://doi.org/10.1016/j.tig.2007.05.011.

Breusing, C., Johnson, S.B., Vrijenhoek, R.C., Young, C.R., 2019. Host hybridization as a potential mechanism of lateral symbiont transfer in deep-sea vesicomyid clams. Mol. Ecol. 1–12. https://doi.org/10.1111/mec.15224.

Catresana, J., 2000. Selection of conserved blocks from multiple alignments for their use in phylogenetic analysis. Mol. Biol. Evol. 17, 540–522.

Chernomor, O., Von Haeseler, A., Minh, B.Q., 2016. Terrace aware data structure for phylogenomic inference from supermatrices. Syst. Biol. 65, 997–1008. https://doi.org/10.1093/sysbio/syw037.

Colgan, D.J., McLauchlan, A., Wilson, G.D.F., Livingston, S.P., Edgecombe, G.D., Macaranas, J., Cassis, G., Gray, M.R., 1998. Histone H3 and U2 snRNA DNA sequences and arthropod molecular evolution. Aust. J. Zool. 46 (5), 419–437. https://doi.org/10.1071/ZO98048.

Cosel, R. von, Comtet, T., Krylova, E.M., 1999. *Bathymodiolus* (Bivalvia: Mytilidae) from hydrothermal vents on the Azores triple junction and the Logatchev hydrothermal field. Veliger 42, 218–248.

Cosel, R. von, Marshall, B.A., 2010. A new genus and species of large mussel (Mollusca: Bivalvia: Mytilidae) from the Kermadec Ridge. TUHINGA 21, 59–73.

Cosel, R. Von, Marshall, B.A., 2003. Two new species of large mussels (Bivalvia: Mytilidae) from active submarine volcanoes and a cold seep off the eastern North Island of New Zealand, with description of a new genus. Nautilus 117, 31–46.

Cosel, R. von, Olu, K., 1998. Gigantism in Mytilidae: a new *Bathymodiolus* from cold seeps on the Barbados accretionary prism. Comptes-Rendus de l'Académie des Sciences, ser. 3. Sci. la Vie 321, 655–663.

Dall, W.H., Bartsch, P., Rehder, H.A., 1938. A manual of the recent and fossil marine pelecypod mollusks of the Hawaiian Islands. Bish. Museum Bull. 153, 233.

Darriba, D., Taboada, G.L., Doallo, R., Posada, D., 2012. jModelTest 2: more models, new heuristics and parallel computing. Nat. Methods 9. https://doi.org/10.1038/nmeth.2109, 772–772.

Dautzenberg, P., 1927. Mollusques provenant des campagnes scientifiques du Prince Albert Ier de Monaco dans l'Océan Atlantique et dans le Golfe de Gascogne. Résultats des Campagnes Sci. Accompl. sur son Yacht par Albert Ier Prince Souver. Monaco 72, 401.

Dell, R.K., 1987. Mollusca of the family Mytilidae (Bivalvia) associated with organic remains from deep water off New Zealand, with revisions of the genera *Adipicola* Dautzenberg, 1927 and *Idasola* Iredale, 1915. Natl. Museum New Zeal. Rec. 3, 17–36.

Distel, D.L., Baco, A.R., Chuang, E., Morrill, W., Cavanaugh, C., Smith, C.R., 2000. Do mussels take wooden steps to deep-sea vents? Nature 403, 725–726.

Duperron, S., Halary, S., Lorion, J., Sibuet, M., Gaill, F., 2008. Unexpected co-occurrence of six bacterial symbionts in the gills of the cold seep mussel *Idas* sp. (Bivalvia: Mytilidae). Environ. Microbiol. 10, 433–445. https://doi.org/10.1111/j.1462-2920.2007.01465.x.

Fisher, C.R., Brooks, J.M., Vodenichar, J.S., Zande, J.M., Childress, J.J., Burke Jr., R.A., 1993. The co-occurrence of methanotrophic and chemoautotrophic sulfur-oxidizing bacterial symbionts in a deep-sea mussel. Mar. Ecol. 14, 277–289. https://doi.org/10.1111/j.1439-0485.1993.tb00001.x.

Fujita, Y., Matsumoto, H., Fujiwara, Y., Hashimoto, J., Galkin, S.V., Ueshima, R., Miyazaki, J.-I., 2009. Phylogenetic relationships of deep-sea *Bathymodiolus* mussels to their Mytilid relatives from sunken whale carcasses and wood. Venus 67, 123–134.

Giribet, G., Carranza, S., Baguna, J., Riutort, M., Ribera, C., 1996. First molecular evidence for the existence of a Tardigrada plus Arthropoda clade. Mol. Biol. Evol. 13 (1), 76–84. https://doi.org/10.1093/oxfordjournals.molbev.a025573.

Govenar, B., 2010. Shaping vent and seep communities: habitat provision and modification by foundation species. In: Kiel, S. (Ed.), The Vent and Seep Biota: Aspects from Microbes to Ecosystems. Springer, pp. 403–432. https://doi.org/10.1007/978-90-481-9572-5.

Guindon, S., Gascuel, O., 2003. A simple, fast and accurate method to estimate large phylogenies by maximum-likelihood. Syst. Biol. 52, 696–704.

Gustafson, R.G., Turner, R.D., Lutz, R.A., Vrijenhoek, R.C., 1998. A new genus and five new species of mussels (Bivalvia: Mytilidae) from deep-sea sulfide/hydrocarbon seeps in the Gulf of Mexico. Malacologia 40, 63–112.

Hasegawa, M., Kishino, H., Yano, T. aki, 1985. Dating of the human-ape splitting by a molecular clock of mitochondrial DNA. J. Mol. Evol. 22, 160–174. https://doi.org/10.1007/BF02101694.

Hashimoto, J., 2001. A new species of *Bathymodiolus* (Bivalvia: Mytilidae) from hydrothermal vent communities in the Indian Ocean. Venus 60, 141–149.

Hashimoto, J., Furuta, M., 2007. A new species of *Bathymodiolus* (Bivalvia: Mytilidae) from hydrothermal vent communities in the Manus Basin, Papua New Guinea. Venus 66, 57–68.

Iwasaki, H., Kyuno, A., Shintaku, M., Fujita, Y., Fujiwara, Y., Fujikura, K., Hashimoto, J., Martins, L. de O., Gebruk, A., Miyazaki, J.-I., 2006. Evolutionary relationships of deep-sea mussels inferred by mitochondrial DNA sequences. Mar. Biol. 149, 1111–1122. https://doi.org/10.1007/s00227-006-0268-6.

Jeffreys, J.G., 1876. New and peculiar Mollusca of the Pecten, Mytilus and Arca families, procured in the Valorous expedition. Ann. Mag. Nat. Hist. 18, 424–436.

Johnson, S.B., Won, Y.-J., Harvey, J.B., Vrijenhoek, R.C., 2013. A hybrid zone between *Bathymodiolus* mussel lineages from eastern Pacific hydrothermal vents. BMC Evol. Biol. 13, 18. https://doi.org/10.1186/1471-2148-13-21.

Jones, W.J., Won, Y.-J., Maas, P.A.Y., Smith, P.J., Lutz, R.A., Vrijenhoek, R.C., 2006. Evolution of habitat use by deep-sea mussels. Mar. Biol. 148, 841–851. https://doi.org/10.1007/s00227-005-0115-1.

Jovelin, R., Justine, J.-L., 2001. Phylogenetic relationships within the polyopisthocotylean monogeneans (Platyhelminthes) inferred from partial 28S rDNA sequences. Int. J. Parasitol. 31 (4), 393–401. https://doi.org/10.1016/S0020-7519(01)00114-X.

Kassambara, A., Mundt, F., 2019. Factoextra: Extract and Visualize the Results of Multivariate Data Analyses.

Katoh, K., Standley, D.M., 2013. MAFFT multiple sequence alignment software version 7: improvements in performance and usability. Mol. Biol. Evol. 30, 772–780. https://doi.org/10.1093/molbev/mst010.

Kenk, V.C., Wilson, B.R., 1985. A new mussel (Bivalvia, Mytilidae) from hydrothermal vents in the Galapagos rift zone. Malacologia 26, 253–271.

Kiel, S. (Ed.), 2010. The Vent and Seep Biota: Aspects from Microbes to Ecosystems. Springer. https://doi.org/10.1007/978-90-481-9572-5.
Kiel, S., Little, C.T.S., 2006. Cold-seep mollusks are older than the general marine mollusk fauna. Science 313 (5792), 1429–1431. https://doi.org/10.1126/science.1126286.
Kobayashi, G., Araya, J.F., 2018. Southernmost records of *Escarpia spicata* and *Lamellibrachia barhami* (Annelida: siboglinidae) confirmed with DNA obtained from dried tubes collected from undiscovered reducing environments in northern Chile. PloS One 13 (10), 1–13. https://doi.org/10.1371/journal.pone.0204959 e0204959.
Krylova, E., Sahling, H., Janssen, R., 2010. *Abyssogena*: a new genus of the family Vesicomyidae (Bivalvia) from deep water vents and seeps. J. Molluscan Stud. 76, 107–132.
Kyuno, A., Shintaku, M., Fujita, Y., Matsumoto, H., Utsumi, M., Watanabe, H., Fujiwara, Y., Miyazaki, J.-I., 2009. Dispersal and differentiation of deep-sea mussels of the genus *Bathymodiolus* (Mytilidae, Bathymodiolinae). J. Mar. Biol. 15. https://doi.org/10.1155/2009/625672, 2009.
LaBella, A.L., Van Dover, C.L., Jollivet, D., Cunningham, C.W., 2017. Gene flow between Atlantic and Pacific Ocean basins in three lineages of deep-sea clams (Bivalvia: Vesicomyidae: Pliocardiinae) and subsequent limited gene flow within the Atlantic. Deep. Res. Part II Top. Stud. Oceanogr. 137, 307–317. https://doi.org/10.1016/j.dsr2.2016.08.013.
Le, S., Josse, J., Husson, F., 2008. FactoMineR: an R package for multivariate analysis. J. Stat. Software 25, 1–18. https://doi.org/10.18637/jss.v025.i01.
Leigh, J., Bryant, D., 2015. PopART: full-feature software for haplotype network construction. Methods Ecol. Evol. 6, 1110–1116.
Levin, L.A., Mendoza, G.F., Grupe, B.M., Gonzalez, J.P., Jellison, B., Rouse, G., Thurber, A.R., Waren, A., 2015. Biodiversity on the rocks: macrofauna inhabiting authigenic carbonate at Costa Rica methane seeps. PloS One 10 (7), e0131080. https://doi.org/10.1371/journal.pone.0131080.
Levin, L.A., Orphan, V.J., Rouse, G.W., Rathburn, A.E., Ussler, W., Cook, G.S., Goffredi, S. K., Perez, E.M., Waren, A., Grupe, B.M., Chadwick, G., Strickrott, B., 2012. A hydrothermal seep on the Costa Rica margin: middle ground in a continuum of reducing ecosystems. Proc. R. Soc. B Biol. Sci. 279, 2580–2588. https://doi.org/10.1098/rspb.2012.0205.
Lindgren, J., Hiley, A.S., Hourdez, S., Rouse, G.W., 2019. Phylogeny and biogeography of *Branchipolynoe* (Polynoidae, Phyllodocida, Aciculata, Annelida), with descriptions of five new species from methane seeps and hydrothermal vents. Diversity 11, 153.
Lorion, J., Buge, B., Cruaud, C., Samadi, S., 2010. New insights into diversity and evolution of deep-sea Mytilidae (Mollusca: Bivalvia). Mol. Phylogenet. Evol. 57, 71–83. https://doi.org/10.1016/j.ympev.2010.05.027.
Lorion, J., Duperron, S., Gros, O., Cruaud, C., Samadi, S., 2009. Several deep-sea mussels and their associated symbionts are able to live both on wood and on whale falls. Proc. R. Soc. B Biol. Sci. 276, 177–185. https://doi.org/10.1098/rspb.2008.1101.
Lorion, J., Kiel, S., Faure, B., Kawato, M., Ho, S.Y.W., Marshall, B., Tsuchida, S., Miyazaki, J.-I., Fujiwara, Y., 2013. Adaptive radiation of chemosymbiotic deep-sea mussels. Proc. R. Soc. B Biol. Sci. 280 (1770), 20131243. https://doi.org/10.1098/rspb.2013.1243, 10.
Maas, Paula A.Y., O'Mullan, Gregory D., Lutz, Richard A., Vrijenhoek, Robert C., 1999. Genetic and morphometric characterization of mussels (Bivalvia: Mytilidae) from Mid-Atlantic hydrothermal vents. Biol. Bull. 196, 265–272. https://doi.org/10.2307/1542951.
Maddison, W.P., Maddison, D.R., 2018. Mesquite: a modular system for evolutionary analysis. Version 3.51. http://www.mesquiteproject.org.
McCowin, M.F., Rouse, G.W., 2018. A new *Lamellibrachia* species and confirmed range extension for *Lamellibrachia barhami* (Siboglinidae, Annelida) from Costa Rica methane seeps. Zootaxa 4504, 1–22. https://doi.org/10.11646/zootaxa.4504.1.1.
Miller, M.A., Pfeiffer, W., Schwartz, T., 2010. Creating the CIPRES Science Gateway for inference of large phylogenetic trees. In: Proceedings of the Gateway Computing Environments Workshop (GCE). New Orleans, LA, pp. 1–8.
Miyazaki, J.-I., Martins, L. de O., Fujita, Y., Matsumoto, H., Fujiwara, Y., 2010. Evolutionary process of deep-sea *Bathymodiolus* mussels. PloS One 5 (4), 11. https://doi.org/10.1371/journal.pone.0010363 e10363.
Miyazaki, J.-I., Shintaku, M., Kyuno, A., Fujiwara, Y., Hashimoto, J., Iwasaki, H., 2004. Phylogenetic relationships of deep-sea mussels of the genus *Bathymodiolus* (Bivalvia: Mytilidae). Mar. Biol. 144 (3), 527–535. https://doi.org/10.1007/s00227-003-1208-3.
O'Dea, A., Lessios, H.A., Coates, A.G., Eytan, R.I., Restrepo-moreno, S.A., Cione, A.L., Collins, L.S., Queiroz, A. De, Farris, D.W., Norris, R.D., Stallard, R.F., Woodburne, M. O., Aguilera, O., Aubry, M., Berggren, W.A., Budd, A.F., Cozzuol, M.A., Coppard, S. E., Duque-caro, H., Finnegan, S., Gasparini, G.M., Grossman, E.L., Johnson, K.G., Keigwin, L.D., Knowlton, N., Leigh, E.G., Leonard-pingel, J.S., Marko, P.B., Pyenson, N.D., Rachello-dolmen, P.G., Soibelzon, E., Soibelzon, L., Todd, J.A., Vermeij, G.J., Jackson, J.B.C., 2016. Formation of the Isthmus of Panama. Sci. Adv. 2, 11. https://doi.org/10.1126/sciadv.1600883.
Olu-Le Roy, K., Cosel, R. von, Hourdez, S., Carney, S.L., Jollivet, D., 2007. Amphi-Atlantic cold-seep *Bathymodiolus* species complexes across the equatorial belt. Deep. Res. Part I Oceanogr. Res. Pap. 54, 1890–1911. https://doi.org/10.1016/j.dsr.2007.07.004.
Passamonti, M., Ricci, A., Milani, L., Ghiselli, F., 2011. Mitochondrial genomes and doubly uniparental inheritance: new insights from *Musculista senhousia* sex-linked mitochondrial DNAs (Bivalvia Mytilidae). BMC Genom. 12, 19. https://doi.org/10.1186/1471-2164-12-442.
Pettibone, M.H., 1984. A new scale-worm commensal with deep-sea mussels on the Galapagos hydrothermal vent (Polychaeta: polynoidae). Proc. Biol. Soc. Wash. 97, 226–239.
Plouviez, S., Shank, T.M., Faure, B., Daguin-Thiebaut, C., Viard, F., Lallier, F.H., Jollivet, D., 2009. Comparative phylogeography among hydrothermal vent species along the East Pacific Rise reveals vicariant processes and population expansion in the South. Mol. Ecol. 18, 3903–3917. https://doi.org/10.1111/j.1365-294X.2009.04325.x.
Rambaut, A., Drummond, A.J., Xie, D., Baele, G., Suchard, M.A., 2018. Posterior summarization in Bayesian phylogenetics using Tracer 1.7. Syst. Biol. 67, 901–904. https://doi.org/10.1093/sysbio/syy032.
Ronquist, F., Teslenko, M., van der Mark, P., Ayres, D., Darling, A., Hohna, S., Larget, B., Liu, L., Suchard, M., Huelsenbeck, J., 2012. Efficient Bayesian phylogenetic inference and model choice across a large model space. Syst. Biol. 61, 539–542.
Saether, K.P., Little, C.T.S., Campbell, K.A., Marshall, B.A., Collins, M., Alfaro, A.C., 2010. New fossil mussels (Bivalvia: Mytilidae) from Miocene hydrocarbon. Zootaxa 2577, 1–45.
Sahling, H., Masson, D.G., Ranero, C.R., Hühnerbach, V., Weinrebe, W., Klaucke, I., Bürk, D., Brückmann, W., Suess, E., 2008. Fluid seepage at the continental margin offshore Costa Rica and southern Nicaragua. G-cubed 9, Q05S05. https://doi.org/10.1029/2008GC001978.
Samadi, S., Puillandre, N., Pante, E., Boisselier, M.-C., Corbari, L., Chen, W.J., Maestrati, P., Mana, R., Thubaut, J., Zuccon, D., Hourdez, S., 2015. Patchiness of deep-sea communities in Papua New Guinea and potential susceptibility to anthropogenic disturbances illustrated by seep organisms. Mar. Ecol. 36, 109–132. https://doi.org/10.1111/maec.12204.
Sellanes, J., Quiroga, E., Neira, C., 2008. Megafauna community structure and trophic relationships at the recently discovered Concepción Methane Seep Area, Chile, ~36°S. ICES J. Mar. Sci. 65, 1102–1111. https://doi.org/10.1093/icesjms/fsn099.
Shimodaira, H., 2002. An approximately unbiased test of phylogenetic tree selection. Syst. Biol. 51, 492–508. https://doi.org/10.1080/10635150290069913.
Smith, P.J., McVeagh, S.M., Won, Y., Vrijenhoek, R.C., 2004. Genetic heterogeneity among New Zealand species of hydrothermal vent mussels (Mytilidae: Bathymodiolus). Mar. Biol. 144, 537–545. https://doi.org/10.1007/s00227-003-1207-4.
Solis-Weiss, V., Hernandez-Alcantara, P., 1994. *Amphisamytha fauchaldi*: a new species of Ampharetid (Annelida: polychaeta) from the hydrothermal vents at Guaymas Basin, Mexico. Bull. South Calif. Acad. Sci. 93, 127–134.
Stamatakis, A., 2014. RAxML version 8: a tool for phylogenetic analysis and post-analysis of large phylogenies. Bioinformatics 30, 1312–1313. https://doi.org/10.1093/bioinformatics/btu033.
Stiller, J., Rousset, V., Pleijel, F., Chevaldonné, P., Vrijenhoek, R.C., Rouse, G.W., 2013. Phylogeny, biogeography and systematics of hydrothermal vent and methane seep *Amphisamytha* (Ampharetidae, Annelida), with descriptions of three new species. Syst. Biodivers. 11, 35–65. https://doi.org/10.1080/14772000.2013.772925.
Swofford, D.L., 2002. Phylogenetic Analysis Using Parsimony (*and Other Methods), fourth ed. Sinauer Associates, Inc, Sunderland, MA.
Tang, Y., Horikoshi, M., Li, W., 2016. ggfortify: unified interface to visualize statistical result of popular R packages. R J 8.
Taylor, J.D., Glover, E.A., 2010. Chemosymbiotic bivalves. In: Kiel, S. (Ed.), The Vent and Seep Biota: Aspects from Microbes to Ecosystems. Springer. https://doi.org/10.1007/978-90-481-9572-5.
Thubaut, J., Puillandre, N., Faure, B., Cruaud, C., Samadi, S., 2013. The contrasted evolutionary fates of deep-sea chemosynthetic mussels (Bivalvia, Bathymodiolinae). Ecol. Evol. 3, 4748–4766. https://doi.org/10.1002/ece3.749.
Van Dover, C.L., Humphris, S.E., Fornari, D., Cavanaugh, C.M., Collier, R., Goffredi, S.K., Hashimoto, J., Lilley, M.D., Reysenbach, A.L., Shank, T.M., Von Damm, K.L., Banta, A., Gallant, R.M., Gotz, D., Green, D., Hall, J., Harmer, T.L., Hurtado, L.A., Johnson, P., McKiness, Z.P., Meredith, C., Olson, E., Pan, I.L., Turnipseed, M., Won, Y., Young III, C.R., Vrijenhoek, R.C., 2001. Biogeography and ecological setting of Indian Ocean hydrothermal vents. Science 294, 818–823. https://doi.org/10.1126/science.1064574.
Vrijenhoek, R.C., 2010. Genetic diversity and connectivity of deep-sea hydrothermal vent metapopulations. Mol. Ecol. 19, 4391–4411. https://doi.org/10.1111/j.1365-294X.2010.04789.x.
Whiting, Michael F., Carpenter, James C., Wheeler, Quentin D., Wheeler, Ward C., 1997. The Stresiptera problem: Phylogeny of the holometabolous insect orders inferred from 18S and 28S ribosomal DNA sequences and morphology. Syst. Biol. 46 (1), 1–68. https://doi.org/10.2307/2413635.
Wickham, H., 2016. ggplot2: Elegant Graphics for Data Analysis. Springer-Verlag, New York.
Won, Y., Young, C.R., Lutz, R.A., Vrijenhoek, R.C., 2003. Dispersal barriers and isolation among deep-sea mussel populations (Mytilidae: *Bathymodiolus*) from eastern Pacific hydrothermal vents. Mol. Ecol. 12, 169–184. https://doi.org/10.1046/j.1365-294X.2003.01726.x.
Xu, T., Feng, D., Tao, J., Qiu, J.-W., 2019. A new species of deep-sea mussel (Bivalvia: Mytilidae: *Gigantidas*) from the South China Sea: morphology, phylogenetic position, and gill-associated microbes. Deep. Res. Part I Oceanogr. Res. Pap. 146, 79–90. https://doi.org/10.1016/j.dsr.2019.03.001.
Zapata-Hernández, G., Sellanes, J., Thurber, A.R., Levin, L.A., 2014. Trophic structure of the bathyal benthos at an area with evidence of methane seep activity off southern Chile (~45°S). J. Mar. Biol. Assoc. U. K. 94, 659–669. https://doi.org/10.1017/S0025315413001914.
Zouros, E., Ball, A.O., Saavedra, C., Freeman, K.R., 1994. An unusual type of mitochondrial DNA inheritance in the blue mussel *Mytilus*. Proc. Natl. Acad. Sci. U.S. A. 91, 7463–7467. https://doi.org/10.1073/pnas.91.16.7463.

1.1 Acknowledgements

Chapter 1 in full, is a reprint of the material as it appears in *Deep-Sea Research Part I: Oceanographic Research Papers*. McCowin, Marina F., Feehery, Caitlin, and Rouse, Greg W. (2020). Spanning the depths or depth-restricted: Three new species of *Bathymodiolus* (Bivalvia, Mytilidae) and a new record for the hydrothermal vent *Bathymodiolus thermophilus* at methane seeps along the Costa Rica margin. *Deep-Sea Research Part I: Oceanographic Research Papers* 164, 103322. The dissertation author was the primary investigator and author of this paper.

Chapter 2

Phylogeny of hydrothermal vent Iphionidae, with the description of a new species (Aphroditiformia, Annelida)

Marina F. McCowin[1] and Greg W. Rouse[1]

[1]Scripps Institution of Oceanography, University of California San Diego, USA

ZooKeys 779: 89–107 (2018)
doi: 10.3897/zookeys.779.24781
http://zookeys.pensoft.net

RESEARCH ARTICLE

A peer-reviewed open-access journal
ZooKeys
Launched to accelerate biodiversity research

Phylogeny of hydrothermal vent Iphionidae, with the description of a new species (Aphroditiformia, Annelida)

Marina F. McCowin[1], Greg W. Rouse[1]

1 *Scripps Institution of Oceanography, University of California San Diego, La Jolla, CA 92093-0202, USA*

Corresponding authors: *Marina F. McCowin* (marruda@ucsd.edu); *Greg W. Rouse* (grouse@ucsd.edu)

Academic editor: *C. Glasby* | Received 2 March 2018 | Accepted 15 June 2018 | Published 2 August 2018

http://zoobank.org/7ED3734C-37F7-4ABF-89B6-A12A2A56B216

Citation: McCowin MF, Rouse GW (2018) Phylogeny of hydrothermal vent Iphionidae, with the description of a new species (Aphroditiformia, Annelida). ZooKeys 779: 89–107. https://doi.org/10.3897/zookeys.779.24781

Abstract

The scale-worm family Iphionidae consists of four genera. Of these, *Thermiphione* has two accepted species, both native to hydrothermal vents in the Pacific Ocean; *T. fijiensis* Miura, 1994 (West Pacific) and *T. tufari* Hartmann-Schröder, 1992 (East Pacific Rise). *Iphionella* is also known from the Pacific, and has two recognized species; *Iphionella risensis* Pettibone, 1986 (East Pacific Rise, hydrothermal vents) and *I. philippinensis* Pettibone, 1986 (West Pacific, deep sea). In this study, phylogenetic analyses of Iphionidae from various hydrothermal vent systems of the Pacific Ocean were conducted utilizing morphology and mitochondrial (COI and 16S rRNA) and nuclear (18S and 28S rRNA) genes. The results revealed a new iphionid species, described here as *Thermiphione rapanui* **sp. n.** The analyses also demonstrated the paraphyly of *Thermiphione*, requiring *Iphionella risensis* to be referred to the genus, as *Thermiphione risensis* (Pettibone, 1986).

Keywords

East Pacific Rise, Pacific Ocean, polychaete, systematics, scale-worm

Introduction

Annelid scale-worms (Aphroditiformia) are a particularly common and diverse group at hydrothermal vents (Desbruyères et al. 2006). Most of this diversity is within Polynoidae Kinberg, 1856, but there have been several records of another aphroditiform family, Iphionidae Kinberg, 1856, which currently includes four genera and 13 accepted species

(Read and Fauchald 2018). Iphionidae had been regarded as a subfamily of Polynoidae, until Norlinder et al. (2014) gave it family rank, as it appears it is actually most closely related to Acoetidae (Gonzalez et al. 2018). In addition to DNA sequence data, the monophyly of Iphionidae is supported by the presence of feathered notochaetae, areolae on elytra, and the absence of a median antenna (Gonzalez et al. 2018). The majority of the known diversity of iphionids are within *Iphione* Kinberg, 1856, and these are mostly shallow-water taxa. However, three genera of deep-sea hydrothermal vent iphionids have been described: *Iphionella* McIntosh, 1885 and *Thermiphione* Hartmann-Schröder, 1992, each with two species, and *Iphionides* Hartmann-Schröder, 1977, containing only *I. glabra* Hartmann-Schröder, 1977.

With regards to the hydrothermal vent-associated iphionids, *Iphionella risensis* Pettibone, 1986 was erected for specimens collected from the East Pacific Rise at 20°50'N. Similar to *I. philippinensis*, this species has 13 pairs of elytra. *Thermiphione tufari* Hartmann-Schröder, 1992, was described for specimens also collected from the East Pacific Rise at 21°30'S, well to the south of the type locality of *I. risensis*. A new genus, *Thermiphione* Hartmann-Schröder, 1992, was erected for this species. *Thermiphione* was distinguished from *Iphionella* by the presence of 14 pairs of elytra instead of 13, as well as by having a greater number of segments (Hartmann-Schröder 1992). *Thermiphione fijiensis* Miura, 1994 was subsequently described from hydrothermal vents from the western Pacific (North Fiji Basin), also with 14 pairs of elytra (Miura 1994).

This paper focuses on new deep-sea collections of Iphionidae from Pacific Ocean hydrothermal vents. DNA data was previously published for *Thermiphione fijiensis* (as *Thermiphione* sp.) in Norlinder et al. (2012); herein we add additional DNA data for this species and for the other two known hydrothermal vent Iphionidae. Furthermore, we describe a new vent-associated iphionid species from the East Pacific Rise and assess some morphological and taxonomic issues for Iphionidae.

Materials and methods

Sample collection

Sampling was conducted over several years and at multiple localities (Figure 1, Tables 1, 2). *Thermiphione rapanui* sp. n. and *T. tufari* were collected on several dives by the manned submersible *Alvin* in 2005 at hydrothermal vents of the southern East Pacific Rise (Table 2). *Thermiphione fijiensis* was collected from the Lau Back-arc Basin in 2005 utilizing the ROV *Jason II* (Table 2). *Iphionella risensis* was collected in 2012 using the ROV *Doc Ricketts* from the Alarcon Rise in the Gulf of California, just north of its type locality (Table 2). All specimens are deposited in the Scripps Institution of Oceanography Benthic Invertebrate Collection (SIO-BIC), La Jolla, California, USA. Whole specimens were photographed prior to preservation using Leica MZ8 or MZ9.5 stereomicroscopes. Post-preservation, specimens were examined and photographed using Leica S8 APO and DMR HC microscopes.

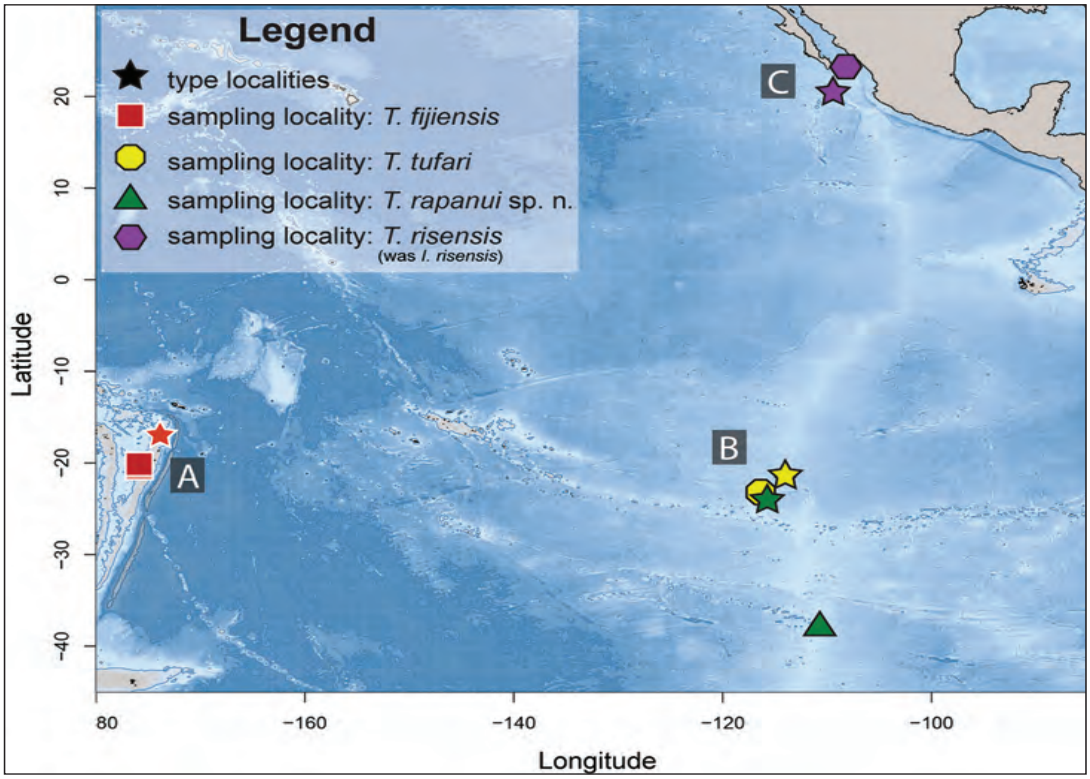

Figure 1. Map of sampling localities for iphionids in this study. Species differentiated by color and shape, type localities represented by stars. **A** *Thermiphione fijiensis* type (star) and sampling (square) localities **B** *Thermiphione tufari* type (star) and sampling (octagon) localities, as well as *Thermiphione rapanui* sp. n. localities (triangle) **C** *Thermiphione risensis* (was *Iphionella risensis*) type (star) and sampling (hexagon) localities.

DNA extraction and amplification

DNA extraction of specimens from the aforementioned collection sites was conducted with the Zymo Research DNA-Tissue Miniprep kit, following the protocol supplied by the manufacturer. Up to 645 bp of mitochondrial cytochrome subunit I (COI) were amplified using the primer set HCO2198 and LCO1490 (Folmer et al. 1994) for multiple specimens in Table 2 and 16S rRNA, 18S rRNA, and 28S rRNA were amplified for a subset of these specimens. Up to 527 bp of 16S rRNA (16S) were amplified using the primer set 16SbrH and 16SarL (Palumbi 1996). 18S rRNA was amplified in three fragments using 18S1F, 18S3F, 18S9R, 18S5R, 18Sbi, and 18Sa2.0 (Giribet et al., 1996; Whiting et al. 1997), resulting in sequence lengths up to 1927 bp. Up to 973 bp of 28S rRNA were amplified using Po28F1 and Po28R4 (Struck et al. 2006). Amplification was carried out with 12.5µl Apex 2.0x Taq RED DNA Polymerase Master Mix (Genesee Scientific), 1µl each of the appropriate forward and reverse primers (10µM), 8.5µl of ddH_2O, and 2µl eluted DNA. The PCR reactions were carried out in a thermal cycler

Table 1. Origin of sequenced terminals, vouchers, and GenBank accession numbers. New sequences in bold. Family assignments follow Zhang et al. (2018).

Scientific name	Origin	Voucher	18S	28S	16S	COI
Panthalis oerstedi	Sweden	SMNH118954	AY839572	JN852845	JN852881	AY839584
Iphione cf. *treadwelli*	Eilat, Israel	–	KY823447	–	KY823478	KY823494
Iphione sp. 1	Hong Kong	–	KY753852	KY753852	KY753835	KY753835
Iphione sp. 2	Papua New Guinea	SMNH118972	JN852819	–	JN852886	JN852921
***Iphione* sp. 3**	Lord Howe Island, Australia	SIO-BIC A8708	–	–	–	**MH389786**
Thermiphione risensis (was *Iphionella risensis)*	Gulf of California	SIO-BIC A6326	**MG994954**	**MH000396**	**MG994947**	**MG981037**
Thermiphione tufari	East Pacific Rise	SIO-BIC A7973	**MG994958**	**MH000401**	**MG994951**	**MG981042**
Thermiphione sp. *(fijiensis)*	Fiji, Lau Basin	SMNH118982	JN852820	JN852849	JN852887	JN852922
Thermiphione fijiensis	Lau back-arc Basin	SIO-BIC A7975	**MG994960**	**MH000402**	**MG994953**	**MG981044**
***Thermiphione rapanui* sp. n.**	East Pacific Rise	SIO-BIC A7969	**MG994955**	**MH000397**	**MG994948**	**MG981038**

Table 2. Sampling localities and GenBank COI accession numbers for all specimens collected and sequenced for this study.

Specimen	Voucher	Locality	Latitude	Longitude	Depth (m)	COI Accession No.
Iphionella risensis	SIO-BIC A6326	Alarcon Rise, Gulf of California	23°22'37"N	108°31'52"W	2,309	MG981037
Thermiphione rapanui sp. n.	SIO-BIC A7969	Pacific Antarctic Ridge	37°47'60"S	110°55'0"W	2,216	MG981038
Thermiphione rapanui sp. n.	SIO-BIC A7970	Pacific Antarctic Ridge	37°47'60"S	110°55'0"W	2,216	MG981039
Thermiphione rapanui sp. n.	SIO-BIC A8557	Pacific Antarctic Ridge	37°47'60"S	110°55'0"W	2,216	–
Thermiphione rapanui sp. n.	SIO-BIC A7971	East Pacific Rise	23°32'47"S	115°34'11"W	2,595	MG981040
Thermiphione rapanui sp. n.	SIO-BIC A7972	East Pacific Rise	23°32'47"S	115°34'11"W	2,595	MG981041
Thermiphione tufari	SIO-BIC A7973	East Pacific Rise	23°32'47"S	115°34'11"W	2.595	MG981042
Thermiphione tufari	SIO-BIC A7974	East Pacific Rise	23°32'47"S	115°34'11"W	2.595	MG981043
Thermiphione fijiensis	SIO-BIC A7975	Lau Back-Arc Basin	20°19'0"S	176°9'0"W	2,719	MG981044
Thermiphione fijiensis	SIO-BIC A8510	Kilo Moana, Lau Back-Arc Basin	20°3'0"S	176°9'0"W	2,657	MG981045
Iphione sp. 3	SIO-BIC A8708	Lord Howe Island, Australia	31°31.603'S	159°4.518'E	5	MH389786

(Eppendorf). The COI temperature profile was as follows: 94 °C/180 s – (94 °C/30 s – 47 °C/45 s – 72 °C/60 s) * 5 cycles – (94 °C/30 s – 52 °C/45 s – 72 °C/60 s) * 30 cycles – 72 °C/300 s. The 16S temperature profile was as follows: 95 °C/180 s – (95 °C/40 s – 50 °C/40 s – 72 °C/50 s) * 35 cycles – 72 °C/300 s. The 18S1F/18S5R temperature profile was as follows: 95 °C/180 s – (95 °C/30 s – 50 °C/30 s – 72 °C/90 s) * 40 cycles – 72 °C/480 s. The 28S temperature profile was as follows: 95 °C/180 s – (95 °C/30 s – 55 °C/40 s – 72 °C/75 s) * 40 cycles – 72 °C/300 s. The PCR product was purified with the ExoSap-it protocol (USB, Affimetrix) and sequencing was performed by Eurofins Genomics (Louisville, KY).

Phylogenetic analyses

Alignments of the newly generated sequences, along with sequence data from GenBank for the four genes presented in Table 1 and published in the most recent aphroditiform phylogeny (Zhang et al. 2018) were performed using MAFFT (Katoh and Standley 2013). Poorly-aligned regions of the three rDNA genes were removed using Gblocks v.0.91b (Catresana 2000), with least stringent settings. This resulted in two concatenated alignments, referred to here as complete and Gblocked. Maximum likelihood (ML) analyses were conducted on the two datasets using RaXML v.8.2.10 (Stamatakis 2014) with each partition assigned the GTR+G model. Node support was assessed via thorough bootstrapping (1000 replicates). Bayesian Inference (BI) analyses were also conducted using MrBayes v.3.2.6 (Rohnquist et al. 2012). Best-fit models for these partitions were selected using the Akaike information criterion (AIC) in jModelTest 2 (Darriba et al. 2012; Guindon and Gascuel 2003). Maximum parsimony (MP) analyses were conducted using PAUP* v.4.0a161 (Swofford 2002), using heuristic searches with the tree-bisection-reconnection branch-swapping algorithm and 100 random addition replicates. Support values were determined using 100 bootstrap replicates. The acoetid *Panthalis oerstedi* Kinberg, 1856, was selected as the outgroup based on recent phylogenomic analyses that place Acoetidae as the sister clade to Iphionidae (Zhang et al., 2018). Uncorrected pairwise distances were calculated for the COI dataset with PAUP* v.4.0a161 (Swofford 2002). Median-joining haplotype networks (Bandelt et al. 1999) for *Thermiphione rapanui* sp. n. and *T. fijiensis* were created with PopART v.1.7 (Leigh and Bryant 2015).

Morphology

Most parsimonious reconstructions for a few relevant characters were mapped onto the molecular phylogeny of Iphionidae using Mesquite v.3.4 (Maddison and Maddison 2018). No DNA data is presently available for *Iphionella philippinensis*, or *Iphionides glabra*, and they are not included in this study. Their eventual phylogenetic placement in Iphionidae will influence the inferred transformations found in this study. Morphological characters used were:

1. Elytra. Thirteen pairs of elytra are found in *Iphionella* (Pettibone, 1986), while *Thermiphione* has 14 pairs (Hartmann-Schröder 1992). Members of *Iphione* have 13 pairs of elytra (Pettibone 1986). The monotypic *Iphionides* has up to 20 pairs (Hartmann-Schröder 1977). Other Aphroditiformia, including the outgroup Acoetidae, normally have many elytral pairs. States, **0**. Many pairs; **1**. 13 pairs; **2**. 14 pairs.
2. Palps. Within Iphionidae, *Iphione* have papillate palps, while all other Iphionidae and the outgroup have smooth palps (Pettibone 1986, Gonzalez et al. 2018). States, **0**. Smooth; **1**. Papillate.
3. Eyes. Within Iphionidae, *Thermiphione* and *Iphionella risensis* lack obvious eyes, while all other Iphionidae and the outgroup have them (Pettibone 1986, Gonzalez et al. 2018). States, **0**. Present; **1**. Absent.
4. Antennae. In general, Aphroditiformia have a median antenna, while most have lateral antennae (Gonzalez et al. 2018). Acoetidae have lateral and median antennae. A median antenna is absent in all Iphionidae, while the presence of lateral antennae varies. In *Iphione*, lateral antennae are present, while they are absent in *Iphionella*, *Iphionides* and *Thermiphione* (Pettibone 1986, Hartmann-Schröder 1992, Miura 1994). States, **0**. Present; **1**. Absent.

Taxonomic note

Iphionella was erected by McIntosh (1885) as a new genus of Polynoidae for a specimen collected from ~900 meters depth from off Philippines, identified as *Iphione cimex* Quatrefages, 1866. This species was therefore the type species for *Iphionella* by monotypy. Pettibone (1986) determined that this identification by McIntosh as *Iphione cimex* was incorrect as the type of *Iphione cimex*, described from the Malacca Strait, actually belonged to Polynoidae and should be placed in a new genus, *Gaudichaudius* Pettibone, 1986, and so it was referred to as *G. cimex* (Quatrefages, 1866). Pettibone (1986) then redescribed the specimen McIntosh (1885) had used to erect *Iphionella* as a new species, *Iphionella philippinensis* Pettibone, 1986. This was not in accordance with the International Code on Zoological Nomenclature at the time (see Art. 70.3; ICZN, 1999). According to 70.3.1, the correct type species name for *Iphionella* was *Iphione cimex* Quatrefages, which should have become *Iphionella cimex* (Quatrefages, 1866). Furthermore, since *Iphione cimex* is the type species of *Gaudichaudia*, then *Gaudichaudia* should become a junior synonym of *Iphionella*. As a result of this, *Iphionella* should be referred to Polynoidae, and the two currently accepted species of *Iphionella*, *I. philippinensis* and *I. risensis* Pettibone, 1986 are in the incorrect genus and require new names. While technically correct, we regard this as not being in accordance of a goal of taxonomic nomenclature to provide stability of names. We therefore endorse Pettibone's (1986) non-ICZN-compliant actions. In order to preserve stability, the type species of *Iphionella* is now fixed here (under Art. 70.3.2 of the ICZN) as *Iphionella philippinensis* Pettibone, 1986, misidentified as *Iphione cimex* in the original designation by McIntosh (1885).

Results

The complete and Gblocked ML, BI and MP analyses (Figure 2) were congruent, showing the same topology for relationships and generally similar high support values within Iphionidae (Figure 2), except for relationships within *Iphione*. The *Iphione* terminals formed a sister clade to a well-supported clade comprised of all the iphionids from hydrothermal vents.

The two known *Thermiphione* species, *T. fijiensis* and *T. tufari*, formed a grade with respect to *Iphionella risensis* (Figure 2). The new species, *Thermiphione rapanui* sp. n., was the well-supported sister group to the sympatric *T. tufari*. The three East Pacific Rise taxa, *I. risensis*, *T. tufari* and *T. rapanui* sp. n. were recovered as the sister group to the western Pacific *T. fijiensis*. The taxonomic implications of the paraphyly of *Thermiphione* and our rationale for the generic placement of the new species are discussed below. The analysis of uncorrected pairwise COI distances (Table 3) showed that *T. rapanui* sp. n. was ~10.5% divergent from its sister taxon, *T. tufari*, and 13–15% divergent from *I. risensis* and *T. fijiensis* (Table 3). For the four specimens of *T. rapanui* sp. n. that we obtained COI sequences for there were three haplotypes that varied from each other by only two base pairs (Figure 4B).

The parsimony reconstruction of ancestral states revealed an unambiguous convergent appearance of 14 pairs of elytra in *Thermiphione fijiensis* and *Thermiphione tufari* and that an elytral number of 13 represents the plesiomorphic state for Iphionidae. The absences of eyes and lateral antennae may be apomorphies for *Thermiphione* (but see below) (Figs 2, 3). The presence of papillate palps was apomorphic for *Iphione* (Figure 3).

Taxonomy

Iphionidae Kinberg, 1856

Thermiphione Hartmann-Schröder, 1992, emended

http://zoobank.org/7BC3CE3F-4C9B-476A-A263-B8B77B961467

Type species. *Thermiphione tufari* Hartmann-Schröder, 1992

Diagnosis (emended). Ventrally flattened, short, oval-shaped body. Between 28 and 32 segments in adults, with 13 or 14 pairs of elytra on segments 2, 4, 5, 7, 9, 11, 13, 15, 17, 19, 21, 23, 26 (and 27, if 14 pairs) that cover dorsal side. Elytra rounded, covered with polygonal and/or hexagonal areas with lattice-like areolae; may exhibit papillae along elytral margins and on elytral surface near margins. Bilobed prostomium square to oval, merged with segment 1, with short, smooth, bulbous palps. Lateral and median antennae absent. Eyes absent. Segment 1 with paired enlarged anterior cirri (*sensu* Rouse and Pleijel 2001; = tentacular cirri), bearing each pair on a tentaculophore with an acicula and capillary chaetae. Mouth anterior, not ventral. Eversible pharynx with papillae and two pairs of jaws. Segment 2 bears first pair of elytra and parapodia,

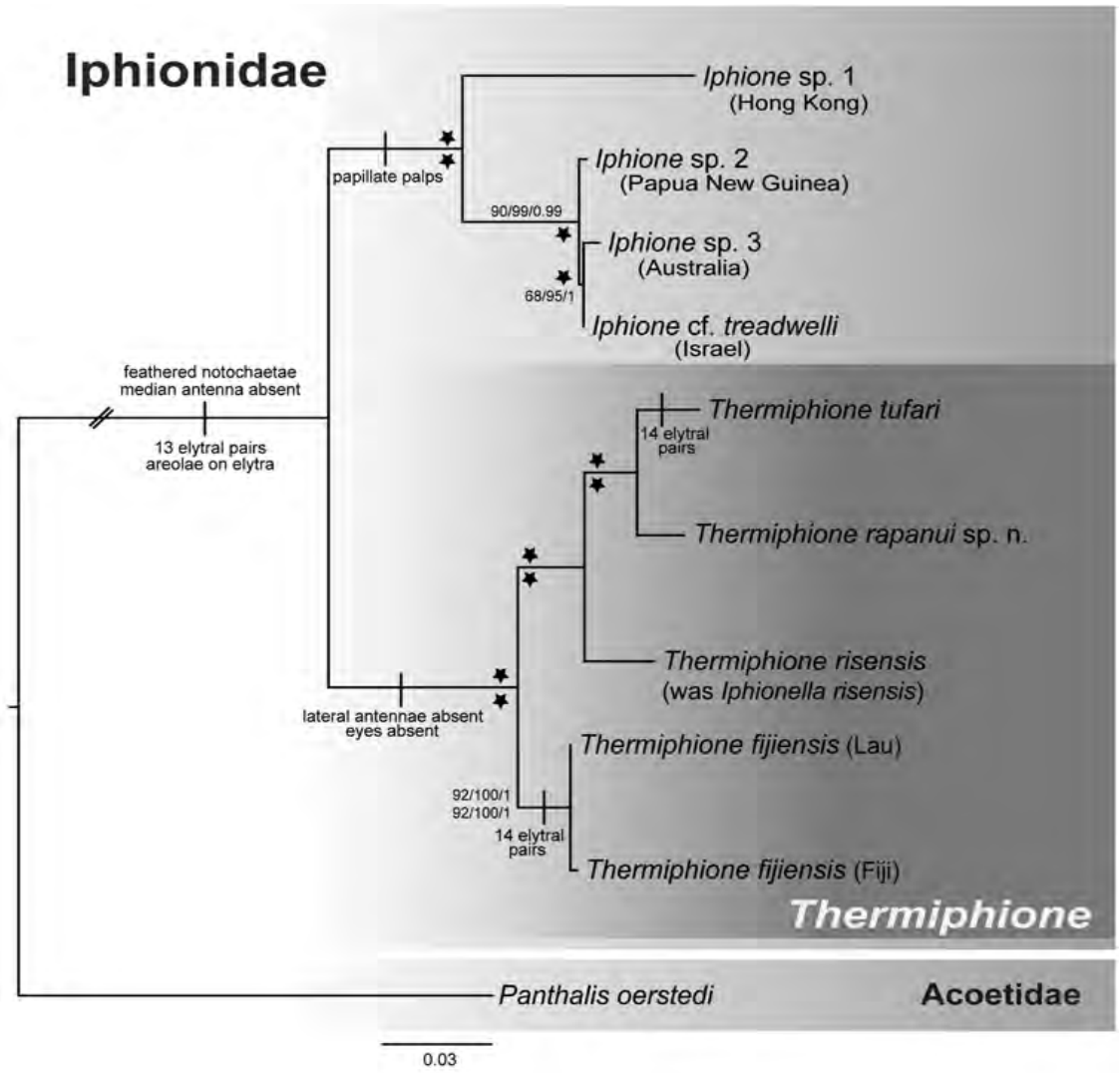

Figure 2. Maximum likelihood tree of the combined analysis from four genes (28S, 18S, 16S, COI) aligned with MAFFT and then concatenated (No Gblocks). Numbers above nodes are bootstrap support percentages from RAxML and Maximum Parsimony analyses (separated by slashes), followed by Bayesian posterior probabilities from the complete dataset alignment (no Gblocks) and below nodes from Gblocks. Support values of 95% or greater for all analyses are indicated by stars.

spherical papillae. Segment 3 barely visible dorsally, with parapodia wedged between segments 2 and 4. Segments 4 and 7 bear spherical ventral papillae. All parapodia biramous: notopodia rounded and much smaller than neuropodia, with bundles of thin, feathered notochaetae; neuropodia large with thicker, single-tipped neurochaetae. Dorsal cirri with short papillae and cylindrical cirrophores. Ventral cirri much smaller than dorsal cirri, short and cirriform. Pygidium inconspicuous, lacking anal cirri.

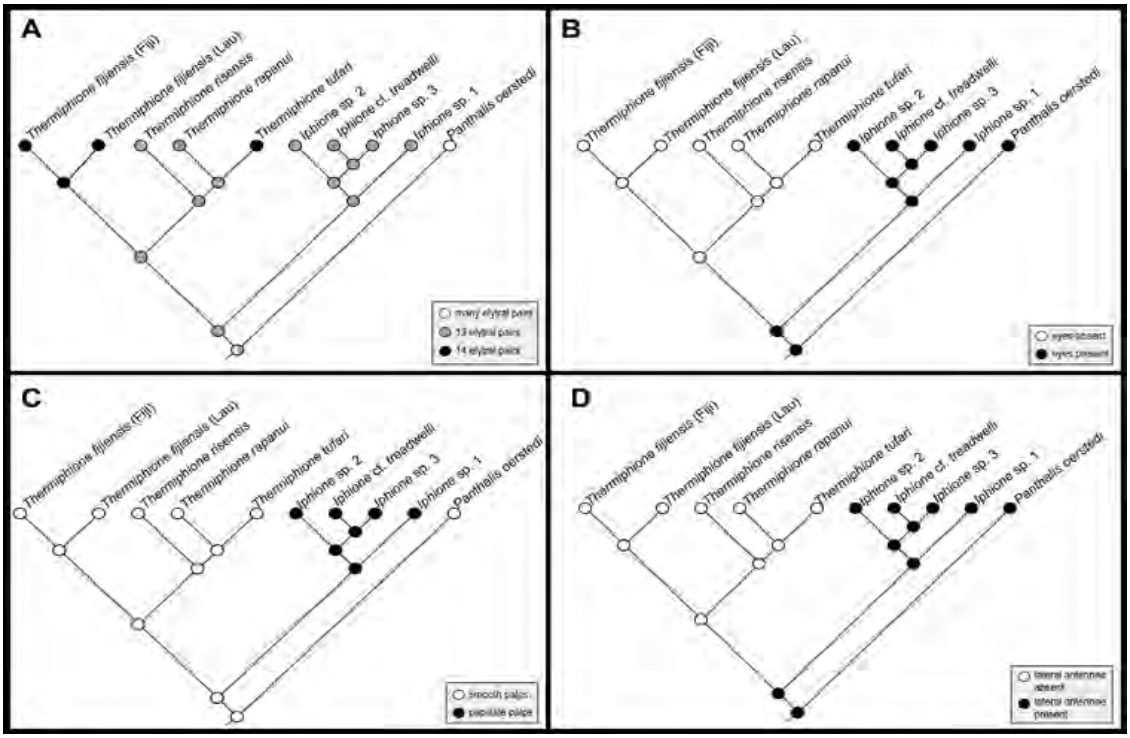

Figure 3. Most parsimonious reconstructions of four traits mapped onto the molecular phylogeny (complete dataset). **A** Elytral pairs **B** Eyes **C** Palps **D** Lateral antennae.

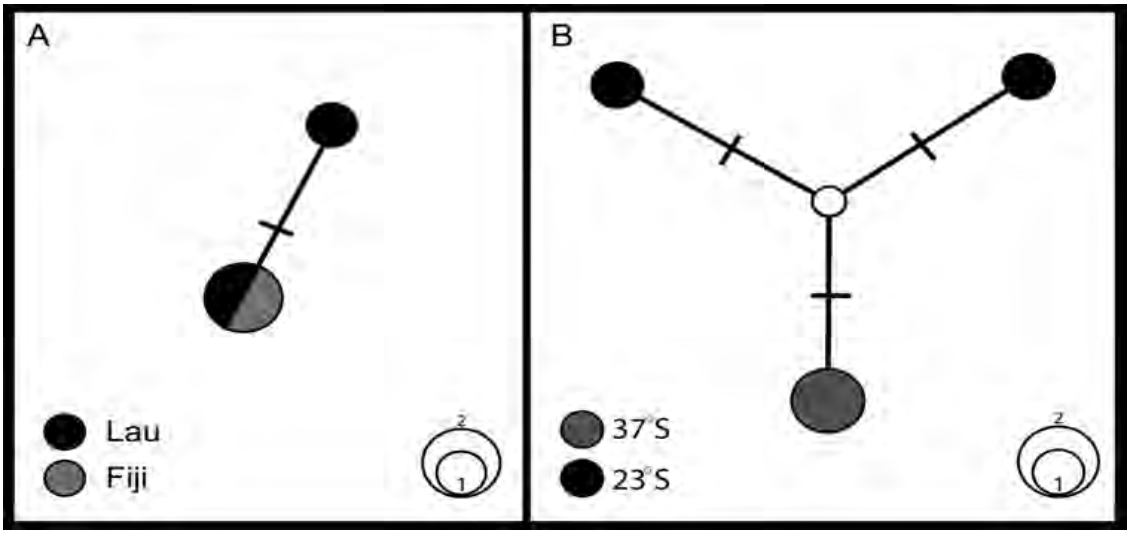

Figure 4. Haplotype networks from COI data: **A** *Thermiphione fijiensis* network includes two sequences from specimens from the Lau Back-Arc Basin (black), and one from the type locality in Fiji (grey) **B** *Thermiphione rapanui* sp. n. network includes two sequences from 23°S (black) and two from 37°S (grey).

Table 3. Uncorrected pairwise distances for COI data, generated with PAUP*.

	***Thermiphione rapanui* sp. n.**	***Thermiphione tufari***	***Thermiphione fijiensis***	***Thermiphione* (*Iphionella*) *risensis***	***Iphione* cf. *treadwelli***	***Iphione* sp. 1**	***Iphione* sp. 2**
Thermiphione tufari	10.48%	–	–	–	–	–	–
Thermiphione fijiensis	15.39%	16.67%	–	–	–	–	–
Thermiphione (*Iphionella*) *risensis*	13.39%	14.25%	14.79%	–	–	–	–
Iphione cf. *treadwelli*	18.14%	19.88%	17.27%	19.23%	–	–	–
Iphione sp. 1	21.75%	19.73%	20.39%	21.52%	18.78%	–	–
Iphione sp. 2	23.81%	24.01%	21.66%	24.00%	23.35%	24.73%	–
Iphione sp. 3	18.49%	19.92%	17.42%	19.06%	0.76%	19.75%	23.14%

Remarks. Hartmann-Schröder's (1992) diagnosis of *Thermiphione* has been amended to accommodate the inclusion of *Iphionella risensis* and *Thermiphione rapanui* sp. n. The genus now comprises *Thermiphione fijiensis* (Figure 5A, D), *T. risensis* (Figure 5B, E), *T. tufari* (Figure 5C), and *T. rapanui* sp. n (Figs 6–9). The morphology of these taxa and phylogenetic evidence suggests that segment and elytral numbers are more variable than in the previous diagnosis. *Thermiphione* all have smooth palps, but this is plesiomorphic for Iphionidae. The absence of eyes may be an apomorphic state, depending on the eventual placement of *Iphionella philippinensis*, which was not included here owing to the lack of material for DNA sequencing. Similarly, the loss of lateral antennae may also be an apomorphy for *Thermiphione* once the position of *Iphionella philippinensis* and *Iphionides glabra*, which also lack them, is resolved.

Thermiphione rapanui sp. n.

http://zoobank.org/D201192A-0569-4C3E-8B22-4C3C3C6A27D7
Figures 6–9

Type-locality. German Flats, hydrothermal vents of Pacific Antarctic Ridge, 110°55'W, 37°48'S.

Material Examined. *Type specimens.* Holotype (SIO-BIC A8557) from German Flats, hydrothermal vents of Pacific Antarctic Ridge, (type locality above), HOV *Alvin* Dive 4088, 2216m depth, 22 March 2005; fixed in 10% SW formalin, preserved in 50% ethanol. The holotype was not sequenced directly to avoid damage but was morphologically identical to sequenced specimens from the same locality. Post-preservation, holotype 10 mm long, 8.5 mm wide including parapodia, 31 segments.

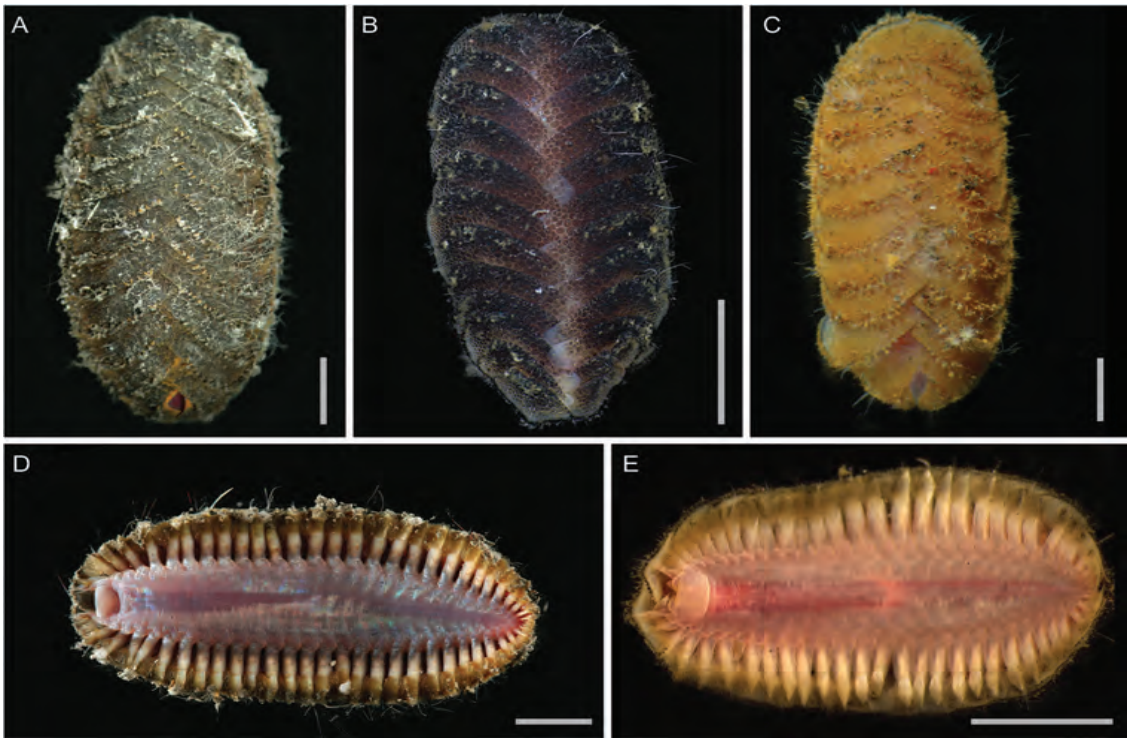

Figure 5. Dorsal and ventral micrographs of species in *Thermiphione*. Scale bars represent 5 mm. **A** *Thermiphione fijiensis* (SIO-BIC A7975), dorsal **B** *Thermiphione risensis* (SIO-BIC A6326, was *Iphionella risensis*), dorsal **C** *Thermiphione tufari* (SIO-BIC A7973), dorsal **D** *Thermiphione fijiensis* (SIO-BIC A7975), ventral **E** *Thermiphione risensis* (SIO-BIC A6326), ventral.

Paratypes: 1 specimen (SIO-BIC A7969) fixed and preserved in 95% ethanol, same location as holotype, post-preservation 9 mm long, 7 mm wide, 29 segments; 1 specimen (SIO-BIC A7970) from same location as holotype: anterior of specimen (approximately 14 segments) fixed in 10% SW formalin and preserved in 50% ethanol and posterior (approximately 14 segments) fixed and preserved in 95% ethanol; 2 specimens (SIO-BIC A7971, juvenile; SIO-BIC A7972) from the western flank of the Easter Microplate, East Pacific Rise, 115°34'W, 23°32'S, HOV *Alvin* Dive 4096, 2595m depth, 6 April 2005. SIO-BIC A7971 fixed and preserved in 95% ethanol, post-preservation 7 mm long, 4 mm wide, 19 segments; SIO-BIC A7972: anterior of specimen (approximately 20 segments) fixed in 10% SW formalin and preserved in 50% ethanol and posterior (approximately 9 segments) fixed and preserved in 95% ethanol.

Diagnosis. Ventrally flattened, oval-shaped body. Between 29 and 31 segments, with 13 pairs of elytra on segments covering dorsum. Elytra covered completely by polygonal areas enclosing areolae, with marginal papillae covering edges. Prostomium bilobed and slightly rounded. Eyes absent. Lateral and median antennae absent. Segment 1 with

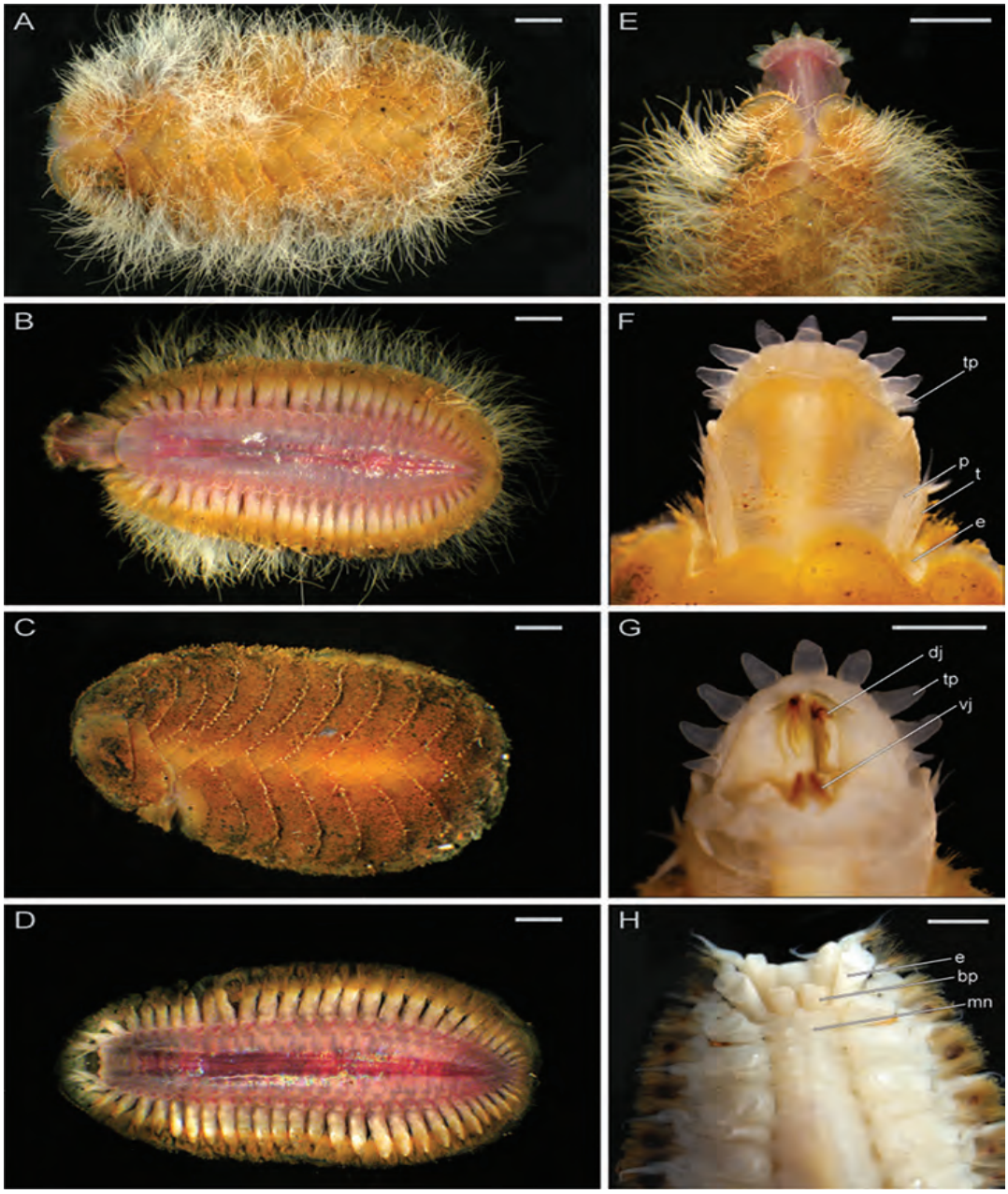

Figure 6. Micrographs of live *Thermiphione rapanui*, sp. n., holotype (SIO-BIC A8557) and paratype (SIO-BIC A7969). Scale bars in A–E represent 1 mm, and scale bars in F–H represent 0.5 mm. **A** Dorsal view of whole body, holotype **B** Ventral view of whole body with pharynx everted, holotype **C** Dorsal view of whole body, paratype **D** Ventral view of whole body, paratype **E** Dorsal view of anterior region with scales, holotype **F** Dorsal view of anterior region with 2 pairs of scales removed, holotype. Abbreviations as follows: *tp*, terminal papilla; *p*, palp; *t*, tentaculophore; *e*, elytrophore **G** Ventral view of anterior region with pharynx and jaws everted/visible, holotype. Abbreviations: *dj*, dorsal jaw; *tp*, terminal papilla; *vj*, ventral jaw **H** Dorsal view of anterior region, paratype. *e*, elytrophore; *bp*, prostomium (bilobed); *mn*, medial nodule.

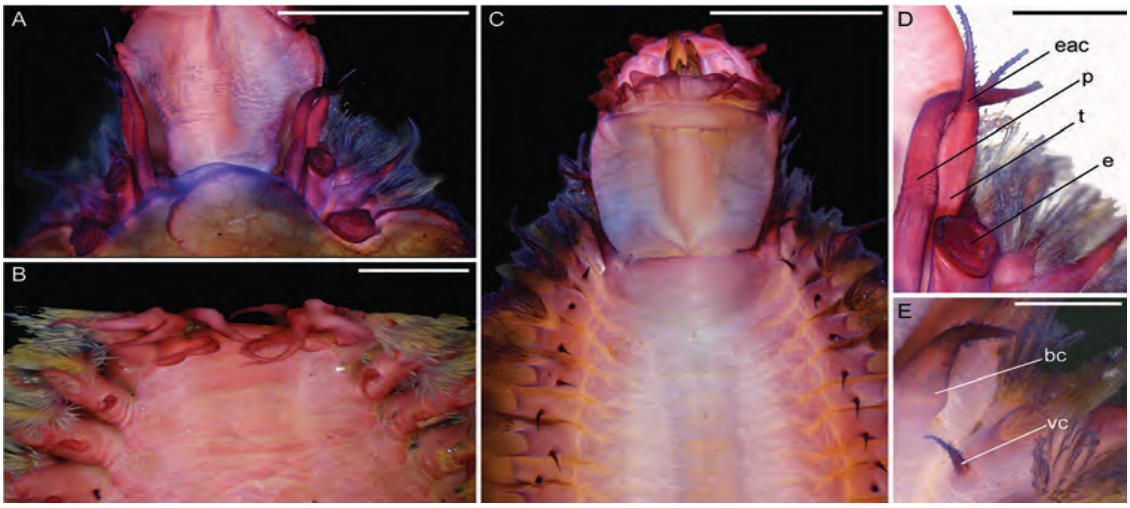

Figure 7. Micrographs of *Thermiphione rapanui* sp. n. holotype (SIO-BIC A8557) and paratype (SIO-BIC A7971), stained with Shirlastain-A. Scale bars in A–C represent 1 mm, and scale bars in D–E represent 0.25 mm. **A** Dorsal view of anterior with 2 pairs of scales removed, holotype **B** Ventral view of anterior showing palps tentaculophore and cirri, paratype. **C** Ventral view of anterior with pharynx everted and jaws visible, holotype **D** Magnified dorsal view of anterior right side, holotype. Abbreviations as follows: *e,* elytrophore; *p,* palp; *t,* tentaculophore; *eac,* enlarged anterior cirrus **E** Magnified ventral view of left anterior parapodia and ventral cirri on segments 2 and 3, holotype. Abbreviations: *bc*, buccal cirrus; *vc*, ventral cirrus.

pair of smooth palps and pair of tentaculophores plus enlarged anterior cirri (tentacular cirri). Mouth anterior with eversible pharynx. Segment 2 with buccal cirri. Segment 3 with dorsal tubercles. Dorsal cirri long with short styles. Ventral cirri short. Anus dorsal. Parapodia biramous with dense bundles of feathered notochaetae and less dense hooked neurochaetae.

Description. In life, elytra pale brown with yellow tinge, becoming slightly paler after preservation. Body ventrally flattened, slightly tapered at anterior and posterior ends (Figure 6A–D). Holotype with 31 segments, 13 pairs of elytra, bacterial filaments on elytra (Figure 6A, B). One mature paratype SIO-BIC A7969, 29 segments, 13 pairs of elytra (Figure 6C, D). One juvenile paratype (SIO-BIC A7971), 19 segments, eight pairs of elytra (identified by scars; elytra lost in sampling).

Pharynx everted anteriorly in holotype, with 9 pairs terminal papillae, and dorsal and ventral pairs of hook-shaped jaws (Figs 6E–G, 7A–C). Prostomium bilobed, slightly rounded; eyes lacking (Figure 6H). Dorsal small circular medial nodules on segments 4 (1), and 5–8 (2 per segment) (Figure 6H). Lateral and median antennae lacking (Figs 6F–H, 7A–C). Pair of smooth palps, longer than pair of tentaculophores plus enlarged anterior cirri (tentacular cirri) (Figs 6F, 7A–B, D). Tentaculophores extending laterally to prostomium (Figs 6F, 7A–B, D), each with single acicula and very thin, short capillary chaetae on inner side. Enlarged anterior cirri, dorsal cirri, and ventral cirri with papillae (Figure 7). Buccal cirri on segment 2, also papillate, appearing larger than

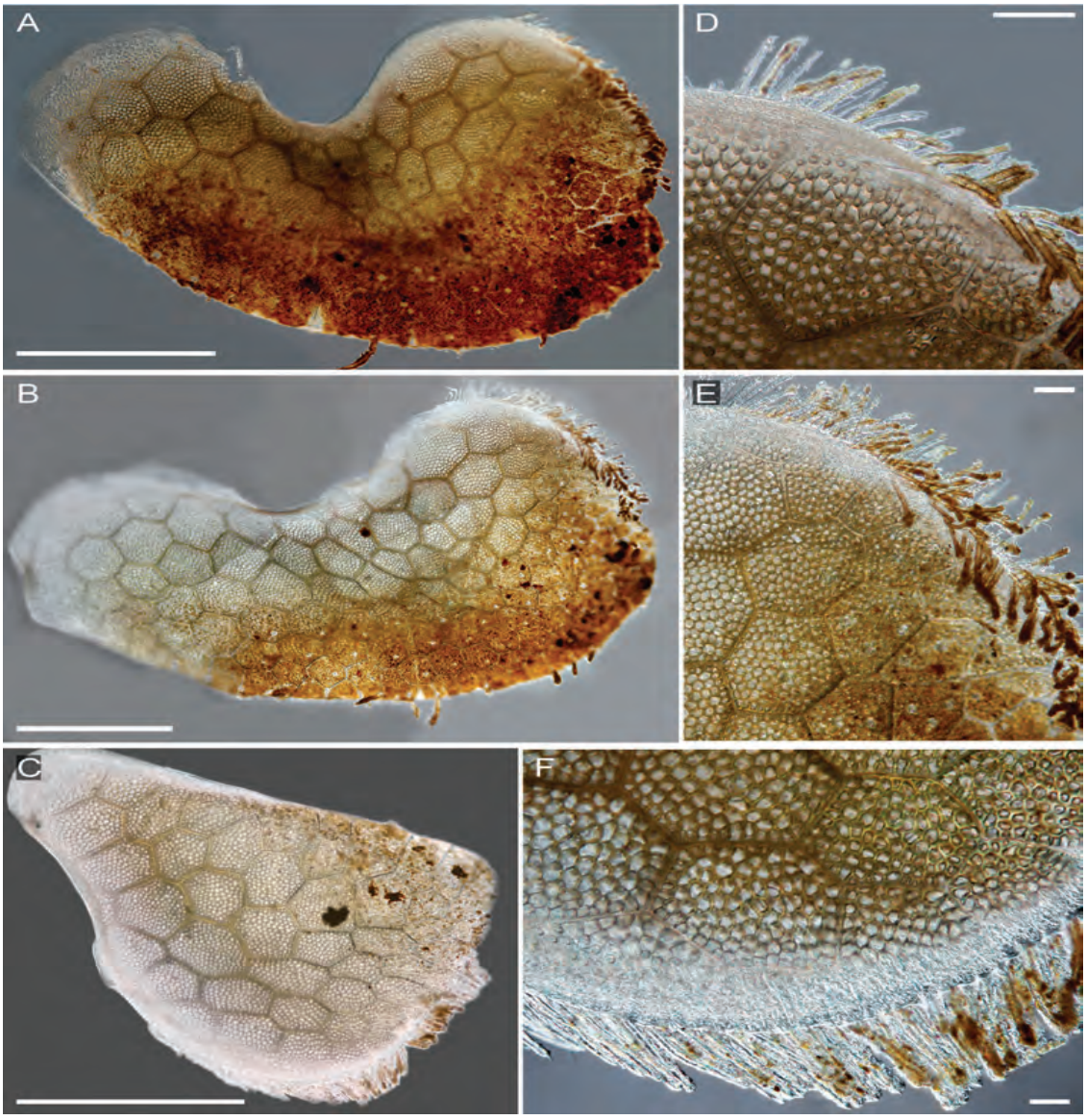

Figure 8. Interference contrast micrographs of *Thermiphione rapanui* sp. n elytra, paratype (SIO-BIC A7969). Scale bars in A–C represent 1mm, and scale bars in D–F represent 0.1 mm. **A** Right elytron 1 **B** Right elytron 3 **C** Left elytron 13 **D** Right elytron 1 margin **E** Right elytron 3 margin **F** Left elytron 13 margin.

remaining ventral cirri (Figure 7C, E). Thirteen pairs of elytra covering dorsum and oval in shape, on segments 2, 4, 5, 7, 9, 11, 13, 15, 17, 19, 21, 23, 26 (Figure 8). First pair of elytra slightly compressed (Figure 8A); last pair much smaller in size and tapered at one end compared to other elytra (Figure 8B–C). Elytra covered completely by polygonal (generally hexagonal) areas enclosing areolae (Figure 8D–F). Thin, rounded marginal

papillae covering lateral edges of elytra, sometimes sparsely extending towards posterior edges of elytra (Figure 8D-F). Remaining segments cirrigerous. Dorsal tubercles and dorsal cirri on segment 3, alternating on segments 6–29, with short, clavate papillae; anal cirri on segments 30, 31 (Figure 6B, D). Dorsal cirri long with short styles, usually extending to near tips of neurochaetae. Ventral cirri much shorter and smaller than dorsal cirri, present on segments 2–29 (Figure 7B–C, E). Anus dorsal; short ventral anal cirri similar to posterior dorsal cirri. Parapodia biramous (Figure 9), with short, subconical notopodia anterodorsal to larger neuropodia (Figure 9). Dense bundles of slender feathered notochaetae, shorter than neurochaetae (Figure 9F, H, J, L). Longer, simple, or slightly hooked neurochaetae, less dense but more numerous than notochaetae (Figure 9G, I, K). Upper neurochaetae generally longer than lower neurochaetae, with length of neurochaetae gradually decreasing towards dorsal and ventral edges (Figure 9).

Variation. Paratypes vary in segment number from holotype and were observed with fewer bacterial filaments on elytra.

Genetic distance. Paratype specimens from the 23°S sampling locality varied by two nucleotide bases from the holotype specimen, 37°S (Figure 4B). This genetic distance is so small that they are certainly all the same species. Unfortunately, our sampling was too limited for any analyses of connectivity.

Etymology. *Thermiphione rapanui* sp. n. is named after the traditional Polynesian name for Easter Island (Rapa Nui), which lies near one of the paratype localities. Neither of the specimens from near Easter Island were chosen as the holotype as they were in poor condition.

Remarks. *Thermiphione rapanui* sp. n. was collected from hydrothermal vents across 15 degrees of latitude, with the northernmost samples collected from the western flank of the Easter Microplate region at 23°S latitude, and the samples from further south collected on the East Pacific Rise at 37°S. The northernmost samples of *Thermiphione rapanui* sp. n. were collected from the same locality as samples of its sister taxon, *T. tufari*, which previously has only been recorded from slightly further north at 21°30'S (Hartmann-Schröder 1992).

Thermiphione rapanui sp. n. differs from its sister taxon *T. tufari* in that it has 13 pairs of elytra instead of 14 pairs of elytra and the last pair of elytra are on segment 26 instead of segment 27 (compare dorsal photos of each in Figs 6A and 5C, respectively). Like *T. tufari*, the new species also has up to 31 segments (Hartmann-Schröder 1992). Both *T. tufari* and *T. fijiensis* (Figure 5A) have 14 pairs of elytra and 30–31 segments (Pettibone, 1986), so elytral number may be convergent (Figure 3). *Thermiphione* was erected by Hartmann-Schröder (1992) and distinguished from other Iphionidae largely based on the presence of 14 pairs of elytra and 30–31 segments, but *Iphionella risensis* (Figure 5B), which nests within the *Thermiphione* (Figure 2), and *Thermiphione rapanui* sp. n. have 13 elytral pairs (Pettibone 1986). However, the two latter species differ in that *I. risensis* has 28–29 segments (Pettibone 1986) and *T. rapanui* sp. n. has 29–31 segments. *T. rapanui* sp. n. also differs from *I. risensis* in the presence of medial nodules on segments 6–8 in *T. rapanui* sp. n., which are absent on these segments in *I. risensis* (Pettibone 1986).

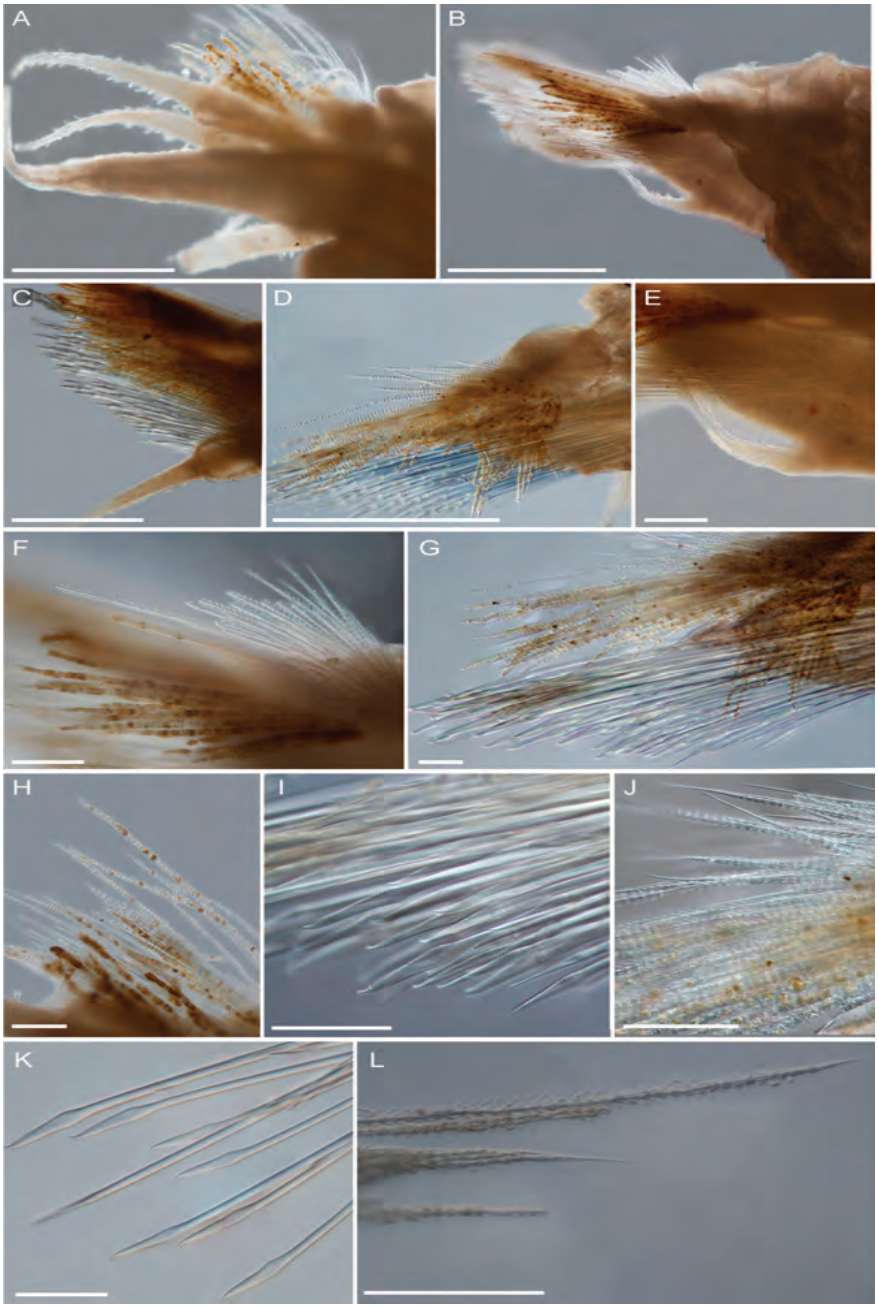

Figure 9. Interference contrast micrographs of *Thermiphione rapanui* sp. n. parapodia, (paratype SIO-BIC A7969). Scale bars in A–D represent 0.5 mm, and scale bars in E–L represent 0.1 mm. **A** Right parapodium 1 **B** Right parapodium 2 **C** Right parapodium 13 **D** Right parapodium 25 **E** Enlarged view of ventral cirrus (parapodium 2) **F** Feathered notochaetae (parapodium 2) **G** Chaetae of parapodium 25 **H** Notochaetae of right parapodium 2. **I** Slightly hooked neurochaetae (right parapodium 25) **J** Feathered notochaetae of parapodium 25 **K** Simple neurochaetae (some slightly hooked) from right parapodium 13. **L** Feathered notochaetae from right parapodium 13.

Discussion

The topologies of the likelihood and parsimony phylogenies are similar to those recovered in the recent analyses of Norlinder et al. (2012), Gonzalez et al. (2018), and Zhang et al. (2018) and support the maintenance of Iphionidae as a family distinct from Polynoidae.

The phylogeny demonstrates that our newly generated sequences for *Thermiphione fijiensis* represent the same species as the *Thermiphione* sp. published in Norlinder et al. (2012). These specimens were collected on the same cruise as the Norlinder et al. (2012) specimen. The *Thermiphione* sp. (Norlinder) specimen was collected at the White Lady hydrothermal vent, near the type locality for *Thermiphione fijiensis*. It is therefore identified here as *T. fijiensis*. The two specimens of *Thermiphione fijiensis* collected from the Lau Back-Arc basin, varied at most by a single base pair from the Norlinder et al. (2012) sequences (Figure 4A).

The distribution of the three East Pacific Rise iphionids sampled in this study (Table 2) and the phylogenetic results (Figure 2) indicate that *Iphionella risensis* forms a northern sister clade to the more southern *Thermiphione rapanui* sp. n. and *T. tufari* clades. This combined eastern Pacific clade is then sister group to *Thermiphione fijiensis* (Figure 2). The placement of *Iphionella risensis* makes *Thermiphione*, as currently formulated, paraphyletic. To resolve the paraphyly of *Thermiphione, Iphionella risensis* should be placed within *Thermiphione* and we do so here by amending the diagnosis for *Thermiphione* to allow for the presence of 13 or 14 pairs of elytra and 28–31 segments (see below). No DNA data currently exists for the type species of *Iphionella*, *I. philippinensis*.

Acknowledgements

Many thanks to Robert Vrijenhoek (MBARI) for inviting Greg Rouse on cruises to various Pacific hydrothermal vent localities. Thanks also to Nerida Wilson for help with sorting the samples that included *T. rapanui* n. sp., to Geoff Read who gave valuable advice on resolving *Iphionella* nomenclature, and to Charlotte Seid for her collections support. The crews of the R/V *Melville*, R/V *Western Flyer*, and the pilots of the ROVs *Jason II* and *Doc Ricketts* provided essential expertise, for which we are grateful. We would also like to thank an anonymous reviewer and Christina Piotrowski, as well as Zookeys editor Chris Glasby. Analysis of the specimens for this project was funded by the US National Science Foundation (NSF OCE-1634172).

References

Bandelt H, Forster P, Röhl A (1999) Median-joining networks for inferring intraspecific phylogenies. Molecular Biology and Evolution 16(1): 37–48. https://doi.org/10.1093/oxfordjournals.molbev.a026036

Catresana J (2000) Selection of conserved blocks from multiple alignments for their use in phylogenetic analysis. Molecular Biology and Evolution 17: 540–522. https://doi.org/10.1093/oxfordjournals.molbev.a026334

Darriba D, Taboada GL, Doallo R, Posada D (2012) jModelTest 2: more models, new heuristics and parallel computing. Nature Methods 9(8): 772. https://doi.org/10.1038/nmeth.2109

Desbruyères D, Segonzac M, Bright M (2006) Handbook of Deep-Sea Hydrothermal Vent Fauna. Biologiezentrum der Oberösterreichische Landesmuseen, Linz, Austria, 565 pp.

Folmer O, Black M, Hoeh W, Lutz R, Vrijenhoek R (1994) DNA primers for amplification of mitochondrial cytochrome c oxidase subunit I from diverse metazoan invertebrates. Molecular Marine Biology and Biotechnology 3(5): 294–299. https://www.mbari.org/wp-content/uploads/2016/01/Folmer_94MMBB.pdf

Giribet G, Carranza S, Baguna J, Riutort M, Ribera C (1996) First molecular evidence for the existence of a Tardigrada plus arthropoda clade. Molecular Biology and Evolution 13: 76–84. https://doi.org/10.1093/oxfordjournals.molbev.a025573

Gonzalez BC, Martínez A, Borda E, Iliffe TM, Eibye-Jacobsen D, Worsaae K (2018) Phylogeny and systematics of Aphroditiformia. Cladistics 34: 225–259. https://doi.org/10.1111/cla.12202

Guindon S, Gascuel O (2003) A simple, fast and accurate method to estimate large phylogenies by maximum-likelihood. Systematic Biology 52: 696–704. https://doi.org/10.1080/10635150390235520

Hartmann-Schröder G (1977) Die Polychaeten der Kubanisch-Rumänischen Biospeologischen Expedition nach Kuba 1973. Résultats des expéditions biospéologiques cubano-roumaines à Cuba 2: 51–63.

Hartmann-Schröder G (1992) Zur Polychaetenfauna in rezenten hydrothermalen Komplexmassivsulfiderzen ("Schwarze Raucher") am Ostpazifischen Rucken bei 21°30'S. Helgolander Meeresuntersuchungen 46: 389–403. https://doi.org/10.1007/BF02367206

Katoh K, Standley DM (2013) MAFFT multiple sequence alignment software version 7: Improvements in performance and usability. Molecular Biology and Evolution 30: 772–780. https://doi.org/10.1093/molbev/mst010

Kinberg J (1856) Nya slägten och arter af Annelider, Öfversigt af Kongl. Vetenskaps-Akademiens Förhhandlingar Stockholm 12: 381–388.

Maddison WP, Maddison DR (2018). Mesquite: a modular system for evolutionary analysis. Version 3.40 http://mesquiteproject.org

McIntosh WC (1885) Report on the Annelida Polychaeta collected by H.M.S. Challenger during the years 1873–1876. Ser. Zoology 12: 1–554.

Miura T (1994) Two new scale-Worms (Polynoidae: Polychaeta) from the Lau Back-Arc and North Fiji Basins, South Pacific Ocean. Proceedings of the Biological Society of Washington 107: 532–543.

ICZN (1999) International Code of Zoological Nomenclature. Fourth Edition. The International Trust for Zoological Nomenclature, London, UK. http://www.iczn.org/iczn/index.jsp

Norlinder E, Nygren A, Wiklund H, Pleijel F (2012) Phylogeny of scale-worms (Aphroditiformia, Annelida), assessed from 18SrRNA, 28SrRNA, 16SrRNA, mitochondrial cytochrome c

oxidase subunit I (COI), and morphology. Molecular Phylogenetics and Evolution 65: 490–500. https://doi.org/10.1016/j.ympev.2012.07.002

Palumbi SR (1996) Nucleic acid II: the polymerase chain reaction. In: Hillis DM, Moritz C, Mable BK (Eds) Molecular Systematics. 2nd ed, Sinauer Associates, Inc, Sunderland, MA, 205–247.

Pettibone MH (1986) Review of the Iphioninae (Polychaeta: Polynoidae) and revision of *Iphione cimex* Quatrefages, *Gattyana deludens* Fauvel, and *Harmothoe iphionelloides* Johnson (Harmothoinae). Smithsonian Contribution to Zoology 428: 1–43. https://doi.org/10.5479/si.00810282.428

Quatrefages A de (1866) Histoire naturelle des Annelés marins et d'eau douce. Annélides et Géphyriens. Librarie Encyclopédique de Roret, Paris, France, 588 pp.

Read G, Fauchald K (Eds) (2018) World Polychaeta database. Iphionidae Kinberg, 1856. http://www.marinespecies.org/polychaeta/aphia.php?p=taxdetails&id=155222 [on 2018-05-23]

Rouse GW, Pleijel F (2001) Polychaetes. Oxford University Press, London, 354 pp.

Ronquist F, Teslenko M, Mark P van der, Ayres DL, Darling A, Höhna S, Larget B, Liu L, Suchard MA, Huelsenbeck JP (2012) MrBayes 3.2: Efficient Bayesian phylogenetic inference and model choice across a large model space. Systematic Biology 61: 539–542. https://doi.org/10.1093/sysbio/sys029

Stamatakis A (2014) RAxML version 8: A tool for phylogenetic analysis and post-analysis of large phylogenies. Bioinformatics 30: 1312–1313. https://doi.org/10.1093/bioinformatics/btu033

Struck T, Purschke G, Halanych K (2006) Phylogeny of Eunicida (Annelida) and Exploring Data Congruence Using a Partition Addition Bootstrap Alteration (PABA) Approach. Systematic Biology 55: 1–20. https://doi.org/10.1080/10635150500354910

Swofford DL (2002) Phylogenetic analysis using parsimony (*and other methods) v.4.0a161. Sinauer Associates, Sunderland, Massachusetts.

Whiting MF, Carpenter JC, Wheeler QD, Wheeler WC (1997) The Strepsiptera Problem: Phylogeny of the Holometabolous Insect Orders Inferred from 18S and 28S Ribosomal DNA Sequences and Morphology. Systematic Biology 46: 1–68. https://doi.org/10.2307/2413635

Zhang Y, Sun J, Rouse GW, Wiklund H, Pleijel F, Watanabe HK, Chen C, Qian P, Qiu J (2018) Phylogeny, evolution and mitochondrial gene order rearrangement in scale worms (Aphroditiformia, Annelida). Molecular Phylogenetics and Evolution 125: 220–231. https://doi.org/10.1016/j.ympev.2018.04.002

2.1 Acknowledgements

Chapter 2 in full, is a reprint of the material as it appears in *Zookeys*. McCowin, Marina F. and Rouse, Greg W. (2018). Phylogeny of hydrothermal vent Iphionidae, with the description of a new species (Aphroditiformia, Annelida). *Zookeys* 779: 89-107. The dissertation author was the primary investigator and author of this paper.

Chapter 3

A new *Lamellibrachia* species and confirmed range extension for *Lamellibrachia barhami* (Siboglinidae, Annelida) from Costa Rica methane seeps

Marina F. McCowin[1] and Greg W. Rouse[1]

[1]Scripps Institution of Oceanography, University of California San Diego, USA

Zootaxa 4504 (1): 001–022
http://www.mapress.com/j/zt/

Article

ISSN 1175-5326 (print edition)
ZOOTAXA
ISSN 1175-5334 (online edition)

https://doi.org/10.11646/zootaxa.4504.1.1
http://zoobank.org/urn:lsid:zoobank.org:pub:20345246-E45C-4A1A-A59B-E0300C853707

A new *Lamellibrachia* species and confirmed range extension for *Lamellibrachia barhami* (Siboglinidae, Annelida) from Costa Rica methane seeps

MARINA F. MCCOWIN[1] & GREG W. ROUSE[1]

[1]*Scripps Institution of Oceanography, University of California San Diego, La Jolla, CA 92093-0202, USA*
[2]*Corresponding author. E-mail: marruda@ucsd.edu, grouse@ucsd.edu*

Abstract

Lamellibrachia Webb, 1969 has eight currently recognized species reported from chemosynthetic environments in the Pacific, Atlantic, and Mediterranean. Of these, *Lamellibrachia barhami* Webb, 1969 has been reported in the eastern Pacific from Canada to Costa Rica. In this study, phylogenetic analyses of *Lamellibrachia* tubeworms sampled from the Costa Rica margin confirm the large geographic range of *L. barhami* and reveal a new *Lamellibrachia* species from a single methane seep between 999 and 1,040 meters. *Lamellibrachia donwalshi* **sp. nov.** differs genetically and morphologically from all congeneric species. Despite its geographic proximity to the eastern Pacific *L. barhami*, *L. donwalshi* **sp. nov.** formed a clade with Atlantic and Mediterranean *Lamellibrachia* species. This suggests a vicariant event may have occurred after an Atlantic radiation of *Lamellibrachia*.

Key words: Vestimentifera, cold seeps, new species, deep sea, East Pacific

Introduction

The first Vestimentifera described, *Lamellibrachia barhami* Webb, 1969, was from southern California and placed in the phylum Pogonophora. Webb (1969) also erected the Order Vestimentifera in the same paper owing to the unusual morphology of *L. barhami*. Pogonophora (and Vestimentifera) is now referred to as the family Siboglinidae Caullery, 1914, within Annelida, though *Lamellibrachia* Webb, 1969 and its relatives are still often placed in the rank-free taxon Vestimentifera, within Siboglinidae; see Pleijel *et al.* (2009) for details of this complex story. Members of Vestimentifera lack a mouth and gut as adults, instead relying on organic compounds supplied by endosymbiotic chemoautotrophic bacteria for nutrition (Bright & Lallier 2010). Their generally large size (up to 2.4 meters in *Riftia pachyptila* Jones, 1981), high densities in some chemosynthetic environments (Bergquist *et al.* 2003; Levin *et al.* 2012; Shank *et al.* 1998), and their unusual features make them compelling organisms to study.

Of the ten vestimentiferan genera, the majority are known from hydrothermal vents in the Pacific: *Alaysia* Southward, 1991*, Arcovestia* Southward & Galkin, 1997, *Oasisia* Jones, 1985*, Paraescarpia* Southward, Schulze & Tunnicliffe, 2002*, Ridgeia* Jones, 1985*, Riftia* Jones, 1981 and *Tevnia* Jones, 1985*. Escarpia* Jones, 1985 and *Lamellibrachia* are also known from sedimented vents in the Pacific, and *Escarpia* has been reported from whale bones (Feldman *et al.* 1998), but they are primarily seep-associated genera (Bright & Lallier 2010; Kobayashi *et al.* 2015; Nishijima *et al.* 2010; Watanabe *et al.* 2010). There are five seep-associated genera, *Alaysia*, *Escarpia, Lamellibrachia*, *Paraescarpia* and *Seepiophila* Gardiner, McMullin & Fisher, 2001. *Seepiophila* is only known from the Gulf of Mexico, while *Lamellibrachia* and *Escarpia* contain species present in the Pacific or Atlantic/Caribbean/Mediterranean. *Paraescarpia* has been reported in the West Pacific and the very eastern margin of the Indian Ocean (Southward *et al.* 2002; McMullin *et al.* 2003).

Eight *Lamellibrachia* species have been described to date, making the genus the most speciose and one of the most widely spread vestimentiferan clades (distribution shown in Fig. 1). The majority of the diversity of *Lamellibrachia* lies in the Pacific with five of the eight currently accepted species (*L. barhami*, *L. columna*

Accepted by W. Magalhaes: 10 Sept. 2018; published: 23 Oct. 2018

Southward, 1991, *L. satsuma* Miura, 1997, *L. juni* Miura & Kojima, 2006, and *L. sagami* Kobayashi, Miura & Kojima, 2015), four of which occur in the West Pacific (Fig. 1). *Lamellibrachia anaximandri* Southward, Andersen & Hourdez, 2011 was described from the Mediterranean, while in the West Atlantic and Caribbean there are two described species: *L. luymesi* van der Land & Nørrevang, 1975, off Guyana, and *L. victori* Mañé-Garzón & Montero, 1985, off Uruguay (Fig. 1, Table 1). Despite being a moderate distance from either type locality, specimens sampled from the Gulf of Mexico have been identified morphologically as *L. luymesi* (Jones 1985; Gardiner & Hourdez 2003; McMullin *et al.* 2003), and *L. victori* was considered "questionably distinct" by Jones (1985) and Gardiner & Hourdez (2003). However, Miglietta *et al.* (2010) and Cowart *et al.* (2014) showed through DNA sequencing that there were several distinct species in the northern Gulf of Mexico, and it remains unclear whether these are *L. luymesi*, *L. victori*, or other species altogether, and the validity of *L. victori* remains in question.

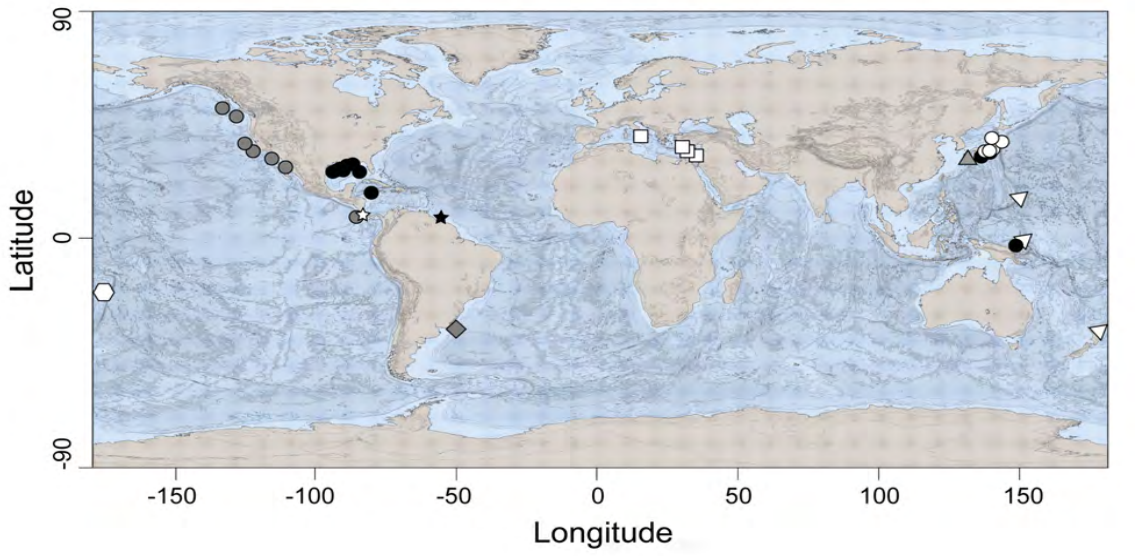

FIGURE 1. Distribution of *Lamellibrachia*. *Lamellibrachia anaximandri* (white square), *Lamellibrachia barhami* (grey circle), *Lamellibrachia columna* (white hexagon), *Lamellibrachia donwalshi* **sp. nov.** (white star), *Lamellibrachia juni* (white triangle), *Lamellibrachia luymesi* (black star), *Lamellibrachia sagami* (grey triangle), *Lamellibrachia satsuma* (white circle), *Lamellibrachia victori* (grey diamond), unresolved *Lamellibrachia* species (black circles): *L.* sp. 1/cf. *luymesi*, *L.* sp. 2, *L.* sp. L4, *L.* sp. L5, *L.* sp. L6.

TABLE 1. Type localities for the eight currently accepted *Lamellibrachia* species.

Name	Region	Locality	Year	Depth (m)	Citation
L. barhami	East Pacific	California coast	1969	1125	Webb, 1969
L. luymesi	South Atlantic	Guyana coast	1975	500	van der Land & Nørrevang, 1975
L. victori	South Atlantic	Uruguay coast	1985	300	Mañé-Garzón & Montero, 1985
L. columna	West Pacific	Lau Basin	1991	1859	Southward, 1991
L. satsuma	Northwest Pacific	Kagoshima Bay	1997	98	Miura, 1997
L. juni	South Pacific	Brothers Caldera	2006	1604	Miura & Kojima, 2006
L. anaximandri	Eastern Mediterranean	Anaximander Mountains	2011	672	Southward, Andersen & Hourdez, 2011
L. sagami	Northwest Pacific	Sagami Bay	2015	853	Kobayashi, Miura & Kojima, 2015

This paper focuses on deep-sea collections of *Lamellibrachia* from the Pacific Ocean off the Costa Rican coast, where there are cold seeps at various depths (Levin *et al.* 2012, 2015; Sahling *et al.* 2008). At these seeps, two species of *Lamellibrachia* have been noted, *L. barhami* at 1,800 meters (Levin *et al.* 2012) and an unidentified *Lamellibrachia* at 1,000 meters (Levin *et al.* 2015). We combine newly generated DNA data for *Lamellibrachia* samples from these sites with previously published DNA data (Braby *et al.* 2007; Cowart *et al.* 2014; Kobayashi *et al.* 2015; Kojima *et al.* 2001, 2006; Li *et al.* 2015, 2017; McMullin *et al.* 2003; Miglietta *et al.* 2010; Sun *et al.*, 2018) and confirm that there is a previously undescribed species of *Lamellibrachia*, which we describe here. This new species has a sister group in the Atlantic (Gulf of Mexico) and the biogeography of *Lamellibrachia* is discussed.

Materials and methods

Sampling and morphological analyses. Sampling was conducted over several years at multiple localities (Fig. 2, Table 2). *Lamellibrachia donwalshi* **sp. nov.** was collected on several dives by the HOV *Alvin* between 2009 and 2017 near Costa Rica at the Mound 12 dive site (1,000 meters) and Mound 11 dive site (1,040 meters). *Lamellibrachia barhami* was also collected on several dives by *Alvin* near Costa Rica at the Quepos Seep (1,400 meters), Jaco Scar (1,800 meters), and Parrita Scar (2,200 meters) dive sites. One specimen of *L. barhami* was collected from a Guaymas Basin seep, referred to as Pinkie's Vent (1,565 meters, see Paull *et al.* 2007), in 2012 via the ROV *Doc Ricketts*.

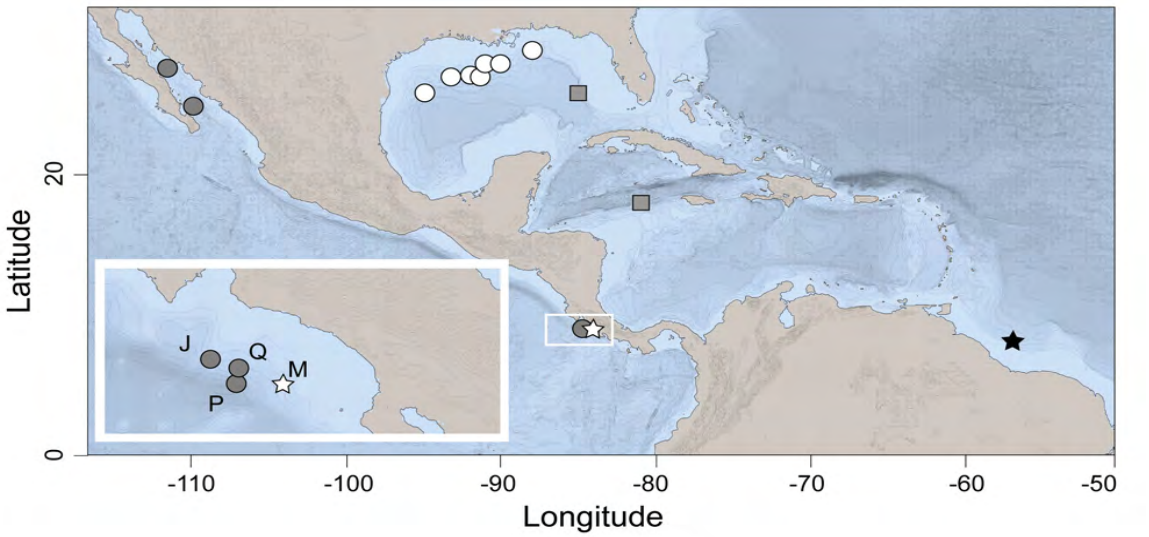

FIGURE 2. *Lamellibrachia* distribution in the Gulf of Mexico, Caribbean, and Costa Rica margin. *Lamellibrachia barhami* (grey circle), *Lamellibrachia donwalshi* **sp. nov.** (white star), *Lamellibrachia luymesi* (black star) *Lamellibrachia* sp. 1/cf. *luymesi* (white circle), *Lamellibrachia* sp. 2 (grey square). Detailed map of sampling at Costa Rica margin within white border: Jaco Scar (J), Quepos Seep (Q), Parrita Scar (P), Mounds 11/12 (M).

For DNA analysis, a portion of the vestimentum and/or trophosome was cut off and preserved in 95% ethanol (details of samples are noted in Material Examined section). One paratype (MZUCR 402-01) is deposited at El Museo de Zoología, Universidad de Costa Rica, San Jose, Costa Rica; the remaining specimens are deposited in the Scripps Institution of Oceanography Benthic Invertebrate Collection (SIO-BIC), La Jolla, California, USA. Whole specimens were photographed prior to preservation using Leica MZ8 or MZ9.5 stereomicroscopes. Post-preservation, specimens were examined and photographed using Leica S8 APO and DMR HC microscopes. Thin pieces of epidermis were cut out from the vestimentum surface near the trunk in the holotype and ten paratypes,

and on the trunk surface near the vestimentum in the holotype and seven paratypes, and placed on a glass slide for observation and measurement of cuticular plaques. A solution of 5% sodium hydroxide in water was added to dissolve tissue and improve observations. Ten plaques from the vestimentum and ten plaques from the trunk were measured from each specimen. Small pieces of the crown (paratype, SIO-BIC A1341), vestimentum (male and putative female paratypes, SIO-BIC A1341), and trunk (male and putative female paratypes, SIO-BIC A1341; holotype SIO-BIC A8382) were embedded in paraffin wax and sectioned on a Spencer '820' microtome. Sections 10µm thick were stained with Azure A for light microscopy. All morphological measurements were made post-preservation. Spearman rank correlations were conducted to test whether certain morphological characteristics (number of sheath lamellae, number of branchial lamellae, vestimental and trunk plaques) were correlated to body size.

DNA extraction, amplification, and sequencing. DNA was extracted from 30 specimens with the Zymo Research DNA-Tissue Miniprep kit, following the protocol supplied by the manufacturer. Approximately 1,050 base pairs (bp) of mitochondrial cytochrome subunit I (COI) were amplified using the polychaete *mtCOI* primer set COIf and COIr (Nelson & Fisher 2000) for multiple specimens in Table 2, and up to 550 bp of 16S rRNA (16S) were amplified using the primer set 16SbrH and 16SarL (Palumbi 1996). The Nelson and Fisher (2000) COIf/COIr primer set did not amplify the COI sequences of a few older specimens, thus these were amplified with the HCO2198 and LCO1490 primer set (Folmer *et al.* 1994) instead. Amplification was carried out with 12.5µl Apex 2.0x Taq RED DNA Polymerase Master Mix (Genesee Scientific), 1µl each of the appropriate forward and reverse primers (10µM), 8.5µl of ddH_2O, and 2µl eluted DNA. The PCR reactions were carried out in a thermal cycler (Eppendorf). The polychaete COI temperature profile was as follows: 95ºC/300s – (94ºC/60s – 55ºC/60s – 72ºC/120s) * 35 cycles – 72ºC/420s. The 16S temperature profile was as follows: 95ºC/180s – (95ºC/40s – 50ºC/40s – 72ºC/50s) * 35 cycles – 72ºC/300s. The universal COI temperature profile was as follows: 94ºC/180s – (94ºC/30s – 47ºC/45s – 72ºC/60s) * 5 cycles – (94ºC/30s – 52ºC/45s – 72ºC/60s) * 30 cycles – 72ºC/300s. The PCR products were purified with the ExoSAP-IT protocol (USB, Affymetrix) and sequencing was performed by Eurofins Genomics (Louisville, KY). The only nuclear gene (18S rRNA [18S]) that has been sequenced for multiple *Lamellibrachia* species has been shown to be uninformative among vestimentiferan species (Halanych *et al.* 2001) and thus was not amplified in this study.

Molecular analyses. Alignments of the newly generated sequences and available sequence data from GenBank for the two genes presented in Table 1 (published in the most recent siboglinid phylogenies [Braby *et al.* 2007; Cowart *et al.* 2014; Kobayashi *et al.* 2015; Kojima *et al.* 2001, 2006; Li *et al.* 2015, 2017; McMullin *et al.* 2003; Miglietta *et al.* 2010; Sun *et al.* 2018]) were performed using MAFFT with default settings (Katoh & Standley 2013) and concatenated with SequenceMatrix v.1.6.7 (Gaurav *et al.* 2011). For those specimens with mitochondrial genomes available on GenBank, 16S and COI genes only were downloaded prior to alignment and concatenation. For species that showed very little variation in COI (*L. anaximandri*, *L.* cf. *luymesi, L. satsuma, L. barhami*), a single individual was chosen to represent that lineage in the phylogenetic analyses. A few terminals included lacked 16S data (Table 1). Maximum likelihood (ML) analyses were conducted on the concatenated dataset using RAxML v.8.2.10 (Stamatakis 2014) with each partition assigned the GTR+G+I model. Node support was assessed via a thorough bootstrapping (1,000 replicates). Bayesian Inference (BI) analyses were also conducted using MrBayes v.3.2.6 (Ronquist *et al.* 2012). Best-fit models for these partitions were selected using the Akaike information criterion (AIC) in jModelTest 2 (Darriba *et al.* 2012; Guindon & Gascuel 2003): GTR+G+I was the best-fit model for both partitions. Maximum parsimony (MP) analyses were conducted using PAUP* v.4.0a161 (Swofford 2002), using heuristic searches with the tree-bisection-reconnection branch-swapping algorithm and 100 random addition replicates. Support values were determined using 100 bootstrap replicates. To check whether different proximate outgroups influenced the topology within *Lamellibrachia*, the previously described analyses were conducted with each of the following outgroups separately: *Escarpia* sp., *Ridgeia piscesae*, and *Riftia pachyptila*. Uncorrected pairwise distances were calculated for the COI dataset (~1275 bp) with PAUP* v.4.0a161 (Swofford 2002). A model-corrected distance analysis for a reduced COI dataset containing *L. donwalshi* **sp. nov.** and its sister clades (supported by the ML analysis) was also conducted with the best-fit model, HKY (Hasegawa *et al.* 1985) selected via AIC in jModelTest 2 (Darriba *et al.* 2012; Guindon & Gascuel 2003). This reduced dataset (n=46) was also analyzed with Automatic Barcoding Gap Discovery (ABGD) (Puillandre *et al.* 2012) with the following settings: p_{min}=0.001, p_{max}=0.1, Steps=20, X=1.5, Nb bins=30. The ABGD analysis was conducted with both Jukes-Cantor and Kimura distances. Haplotype networks of *L. donwalshi* **sp.**

nov., *L. barhami*, *L. anaximandri*, and *L.* sp. 2 were created with PopART v.1.7 (Bandelt *et al.* 1999) using the median-joining option with epsilon set at 0 using the COI dataset (1,177 bp).

Note on some 'Lamellibrachia' sequences on GenBank. Our phylogenetic analyses, which included many sequences from past studies, illuminated a few misidentifications of sequences on GenBank. Though these sequences were identified as *Lamellibrachia*, we found no evidence of their presence in the phylogenetic trees presented in Miglietta *et al.* (2010) (no terminals with matching names or information). We confirmed that the proper identification of these sequences was not *Lamellibrachia* via NCBI BLAST (Altschul *et al.* 1990). These specimens were misidentified as *Lamellibrachia*, and Miglietta *et al.* (2010) did not include them in their *Lamellibrachia* analyses thus we also excluded them from our analyses. Their GenBank accession numbers and approximate identifications are as follows: GU068171 (*Escarpia* sp.), GU059230 (*Seepiophila jonesi*), GU059239 (*Escarpia* sp.), GU059172 (*Seepiophila jonesi*), GU059250 (*Seepiophila jonesi*).

We would also like to note that *Escarpia spicata* (KJ789161) may be a misidentification on GenBank as well: *Escarpia spicata* is known only from the eastern Pacific, while the specimen (KJ789161) identified as *Escarpia spicata* (Li *et al.* 2015) was sampled from the Gulf of Mexico, where only *Escarpia laminata* has been morphologically identified. However, the molecular phylogeny of *Escarpia* lacks the resolution necessary to confirm this with molecular data (Cowart *et al.* 2013) thus we refer to this sequence as *Escarpia* sp.

Results

The ML, BI, and MP analyses of the three different rooting options (*Escarpia* sp., *Riftia pachyptila*, or *Ridgeia piscesae*) were congruent (topology represented in Fig. 3 with the *Ridgeia piscesae* rooting, chosen due to its proximity to *Lamellibrachia* in the recent siboglinid phylogeny by Li *et al.* 2017). *Lamellibrachia juni* was recovered as sister to the remaining *Lamellibrachia* species (ML bootstrap support of 59%) and *L. donwalshi* **sp. nov.** was recovered inside an Atlantic radiation (86%) (Fig. 3). However, the majority of phylogenetic relationships in Fig. 3 were poorly supported, with the exception of the respective sister relationships between *L. columna* and *L. sagami* (100%), and *L.* cf. *luymesi* and *L.* sp. 1 (100%). All analyses (Fig. 3) recovered a grade of Pacific species with respect to the Atlantic species plus *L. donwalshi* **sp. nov.** All analyses also showed *L. donwalshi* **sp. nov.** as sister to a *L.* sp. 2 and *L. anaximandri* (Mediterranean) clade (44%).

Uncorrected pairwise distances for the COI dataset revealed that *L. donwalshi* **sp. nov.** was 2.45% and 2.50% divergent from *L.* sp. 2 (Table 3) and *L. anaximandri* (Table 3), respectively. *Lamellibrachia donwalshi* **sp. nov**. was 5.42% divergent from its geographically nearest relative, *L. barhami* (Table 3). The minimum HKY-corrected distance between *L. donwalshi* **sp. nov.** and *L.* sp. 2 was 1.92%, and the minimum HKY-corrected distance between *L. donwalshi* **sp. nov.** and *L. anaximandri* was 1.81%. Results of the ABGD analyses of COI for the reduced (*L.* sp. 2, *L. anaximandri,* and *L. donwalshi* **sp. nov.**) dataset were identical using either Jukes-Cantor or Kimura distances and showed three distinct clusters, or hypothetical species. Haplotype networks generated for the COI data from *L. donwalshi* **sp. nov.**, *L.* sp. 2, and *L. anaximandri* also showed three distinct species, with some minor variation within each species (Fig. 4). *Lamellibrachia barhami* samples from a variety of depths and localities showed one dominant haplotype in Costa Rica, which was also found in the Gulf of California, Monterey Canyon, and Oregon (Fig. 5).

Taxonomy

Siboglinidae Caullery, 1914

Lamellibrachia Webb, 1969

Lamellibrachia donwalshi sp. nov.

(Figs. 6–11)

urn:lsid:zoobank.org:act:BECD07F4-55CD-499B-B371-32AB404A2DEF
Lamellibrachia sp. (Levin *et al.* 2015)

TABLE 2. Origin of sequenced terminals, vouchers, and GenBank accession numbers. New sequences are set in bold. Sampling sites of new sequences are as follows: Guaymas Basin, 27.59 N, 111.47 W (1,565m); Jaco Scar, 9.12 N, 84.85 W (1,800–1,891m); Quepos Seep, 9.03 N, 84.62 W (1,409m); Parrita Scar, 8.84 N, 84.65W (2,209m); Mound 12, 8.93 N, 84.31 W (999–1,005m); Mound 11, 8.92 N, 84.31 W (1,040m). GM=Gulf of Mexico, CR=Costa Rica, GC=Gulf of California, SP=South Pacific.

Scientific Name	Origin	COI	16S	Voucher or Reference
Escarpia sp.	Mississippi Canyon, GM	KJ789161	KJ789161	Li *et al.* 2015
Lamellibrachia anaximandri	Eastern Mediterranean	EU046616	HM746782	SMH-2007a
Lamellibrachia barhami	Oregon Margin	U74054	-	Black *et al.* 1997
Lamellibrachia barhami	Middle Valley	U74055	-	Black *et al.* 1997
Lamellibrachia barhami	Pescadero Basin, GC	KY581526	-	Goffredi *et al.* 2017
Lamellibrachia barhami	Monterey Canyon	AY129137–38	-	McMullin *et al.* 2003
Lamellibrachia barhami	Oregon	AY129141, AY129145	-	McMullin *et al.* 2003
Lamellibrachia barhami	Vancouver Island Margin	AY129146–47	-	McMullin *et al.* 2003
Lamellibrachia barhami	**Parrita Scar, CR**	**MH670765**	**MH660398**	**SIO-BIC A1564**
Lamellibrachia barhami	**Jaco Scar, CR**	**MH670766–92**	**MH660399**	**SIO-BIC A1824, A1837/A2133, A8305, A8309, A8313–15, A8317–18, A8322–23, A8343–45, A8351, A8375, A8377, A8403–05**
Lamellibrachia barhami	**Guaymas Basin, GC**	**MH670793**	**-**	**SIO-BIC A3433**
Lamellibrachia barhami	**Quepos Seep, CR**	**MH670794–806**	**-**	**SIO-BIC A8432, A8435–40, A8443–45, A8449–50**
Lamellibrachia columna	Fiji-Lau Back Arc Basin	DQ996645	FJ347646	Braby *et al.* 2007
***Lamellibrachia donwalshi* sp. nov.**	**Mound 12, CR**	**MH670826, MH670807–10, MH670813–25, MH670827–34**	**MH664896–MH664918**	**SIO-BIC A1504/A1338, A8266–70, A8272, A8274–77, A8382, A8412, A8416, A1506/A1341**
***Lamellibrachia donwalshi* sp. nov.**	**Mound 11, CR**	**MH670811–12**	**MH664919**	**SIO-BIC A1531**
Lamellibrachia juni	Manus Basin, SP	AB264603	-	Kojima *et al.* 2006
Lamellibrachia luymesi	Green Canyon, GM	GU059225	GU068209	Miglietta *et al.* 2010
Lamellibrachia luymesi	Mississippi Canyon, GM	KJ789163	KJ789163	Li *et al.* 2015
Lamellibrachia sagami	Sagami Bay, Japan	LC064365	-	JAMSTEC 1140043315
Lamellibrachia satsuma	Kagoshima Bay, Japan	KP987801	KP987801	Patra *et al.* 2016
Lamellibrachia sp. 1	GM	GU059165–66, GU059169, GU059227, GU059237	GU068253–54, GU068257, GU068212, GU068227	Miglietta *et al.* 2010
Lamellibrachia sp. 2	GM	GU059173, GU059175–77	GU068265, GU068269	Miglietta *et al.* 2010
Lamellibrachia sp. 2	Mid-Cayman Spreading Center, Caribbean	KM979545	KJ566961	Plouviez *et al.* 2014
Ridgeia piscesae	Hulk, Canada	KJ789165	KJ789165	Li *et al.* 2015
Riftia pachyptila	East Pacific Rise	KJ789166	KJ789166	Li *et al.* 2015

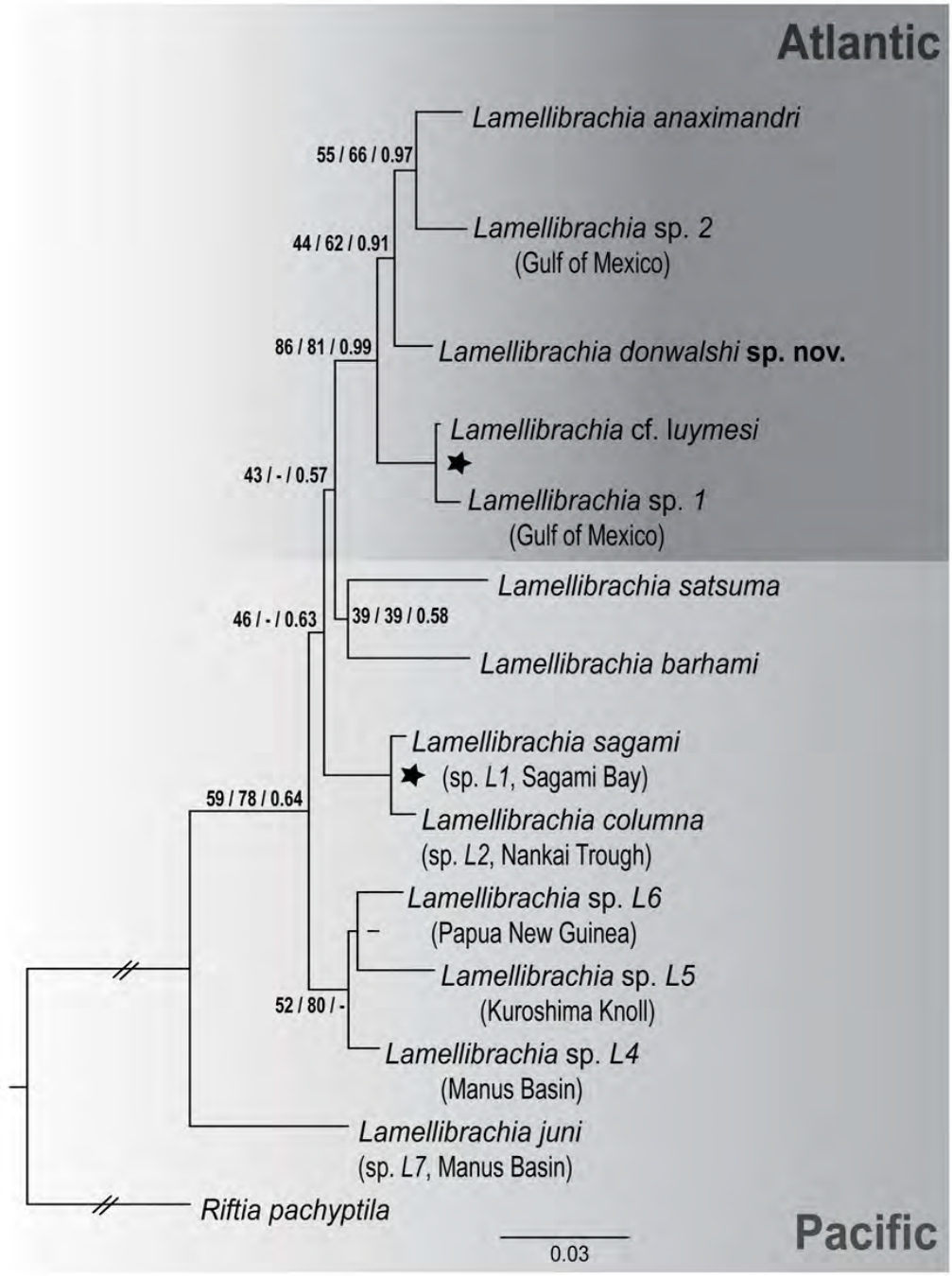

FIGURE 3. Maximum likelihood trees of the combined analysis from two mitochondrial genes (16S, COI) aligned with MAFFT and then concatenated, with three different rooting options: **A** *Escarpia* sp., **B** *Ridgeia piscesae*, **C** *Riftia pachyptila*. Bootstrap support percentages from Maximum Likelihood and Maximum Parsimony analyses (separated by slashes) are followed by Bayesian posterior probabilities. Support values of 95%/0.95 or greater for all analyses are indicated by stars. Nodes with support values less than 50%/0.5 or not recovered in one of the analyses are indicated by a hyphen.

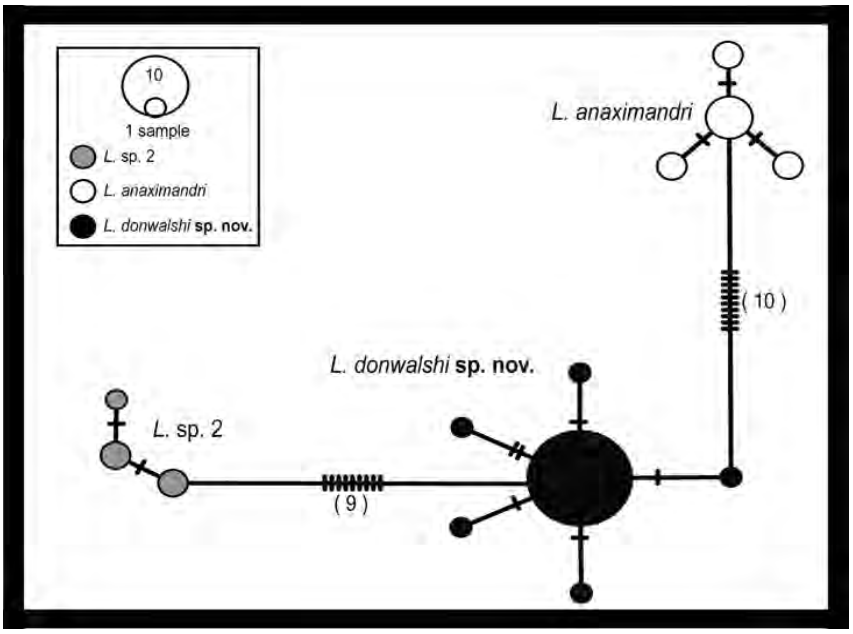

FIGURE 4. Haplotype networks from COI data of *Lamellibrachia* sp. 2 (grey), *Lamellibrachia anaximandri* (white), and *Lamellibrachia donwalshi* **sp. nov.** (black).

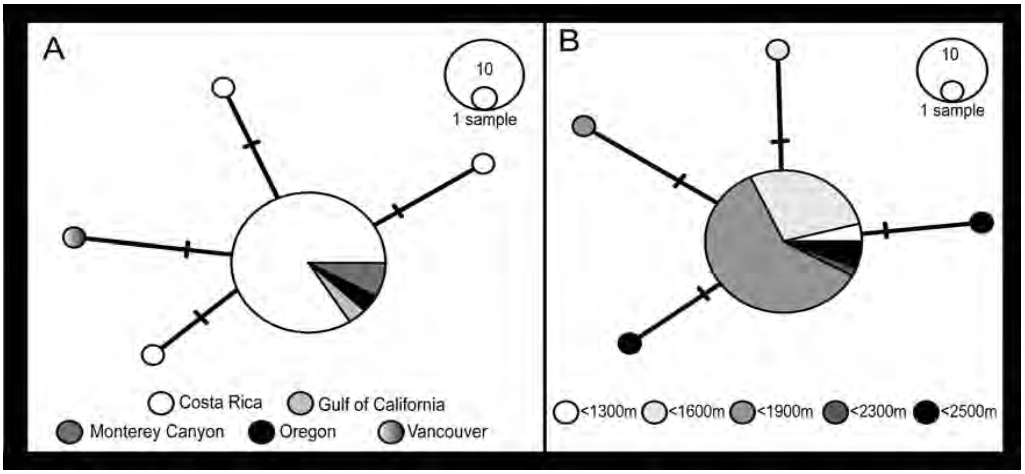

FIGURE 5. Haplotype networks from COI data for *Lamellibrachia barhami* sampled from Costa Rica margin to Vancouver: **A** Color-coded according to sampling locality. **B** Color-coded according to depth of sampling.

Type-locality: Costa Rica, Eastern Pacific, methane seep known as Mound 12, ~1,000 meters depth; 8.93°N, 84.32°W.

Material Examined. Holotype: (SIO-BIC A8382) from type locality, collected by HOV *Alvin,* Dive 4917, 1 June 2016; fixed in 10% SW formalin, preserved in 50% ethanol, putative male.

Paratypes: (SIO-BIC A1341) from type locality, collected by HOV *Alvin* Dive 4503, 24 February 2009; fixed in 10% SW formalin, preserved in 50% ethanol, two males, seven putative females, (see Table 2). One specimen (MZUCR 402-01) from type locality, collected by HOV *Alvin*; fixed in 10% SW formalin, preserved in 50% ethanol.

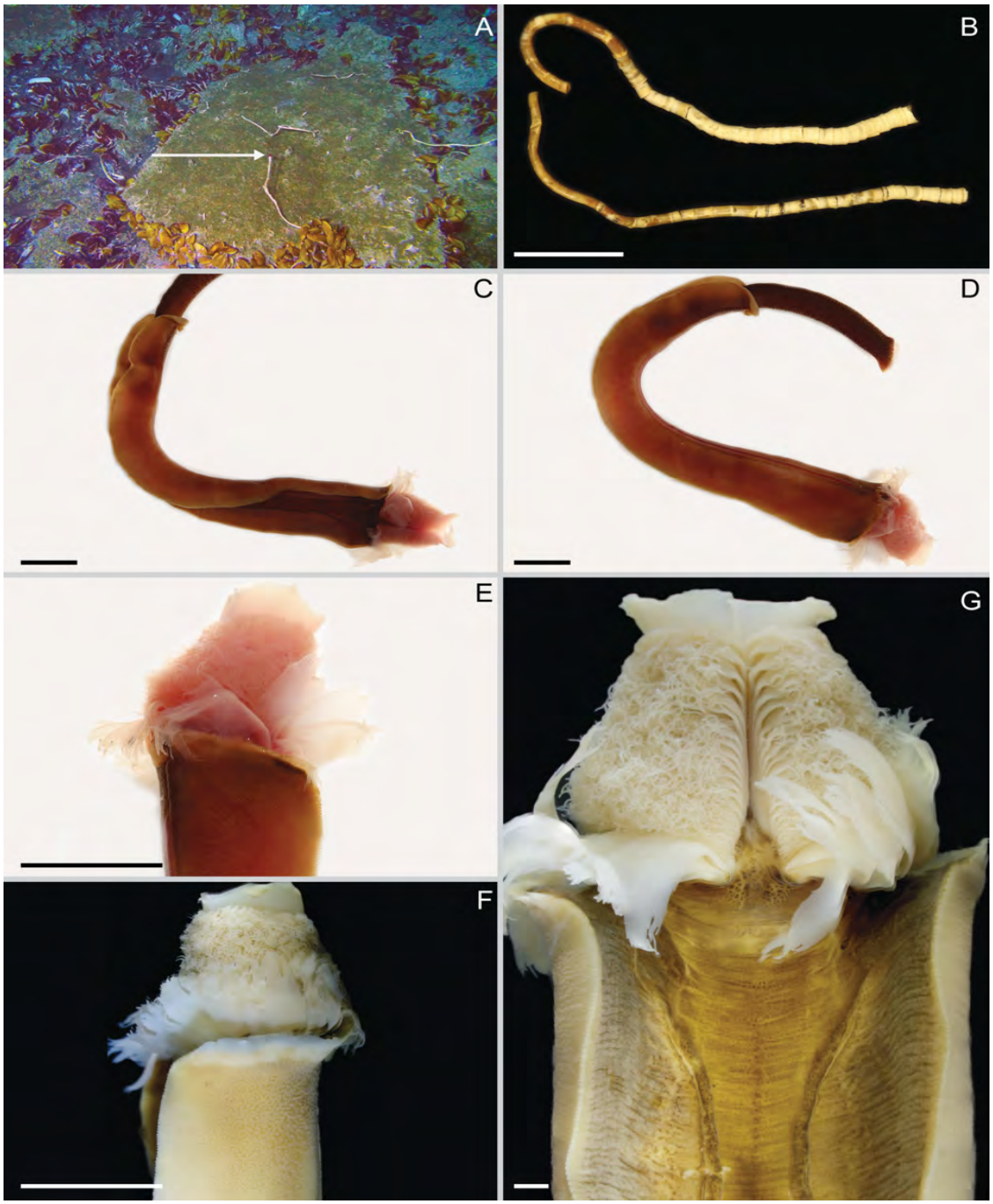

FIGURE 6. *In situ* photograph and micrographs of live *Lamellibrachia donwalshi* **sp. nov. A** In situ photo of *Lamellibrachia donwalshi* **sp. nov.** holotype (SIO-BIC A8382) taken from the HOV *Alvin*, indicated by arrow. **B** Tubes (incomplete) of *Lamellibrachia donwalshi* **sp. nov.** paratypes (SIO-BIC A1341). **C** Holotype, ventro-lateral to dorsal, live. **D** Holotype, ventro-lateral, live. **E** Holotype, left side, live. **F** Holotype, right side, post-preservation. **G** Holotype, dorsal, post-preservation. **G** Holotype, dorsal, post-preservation. Scale bars, B=5cm; C–F=10mm; G=1mm.

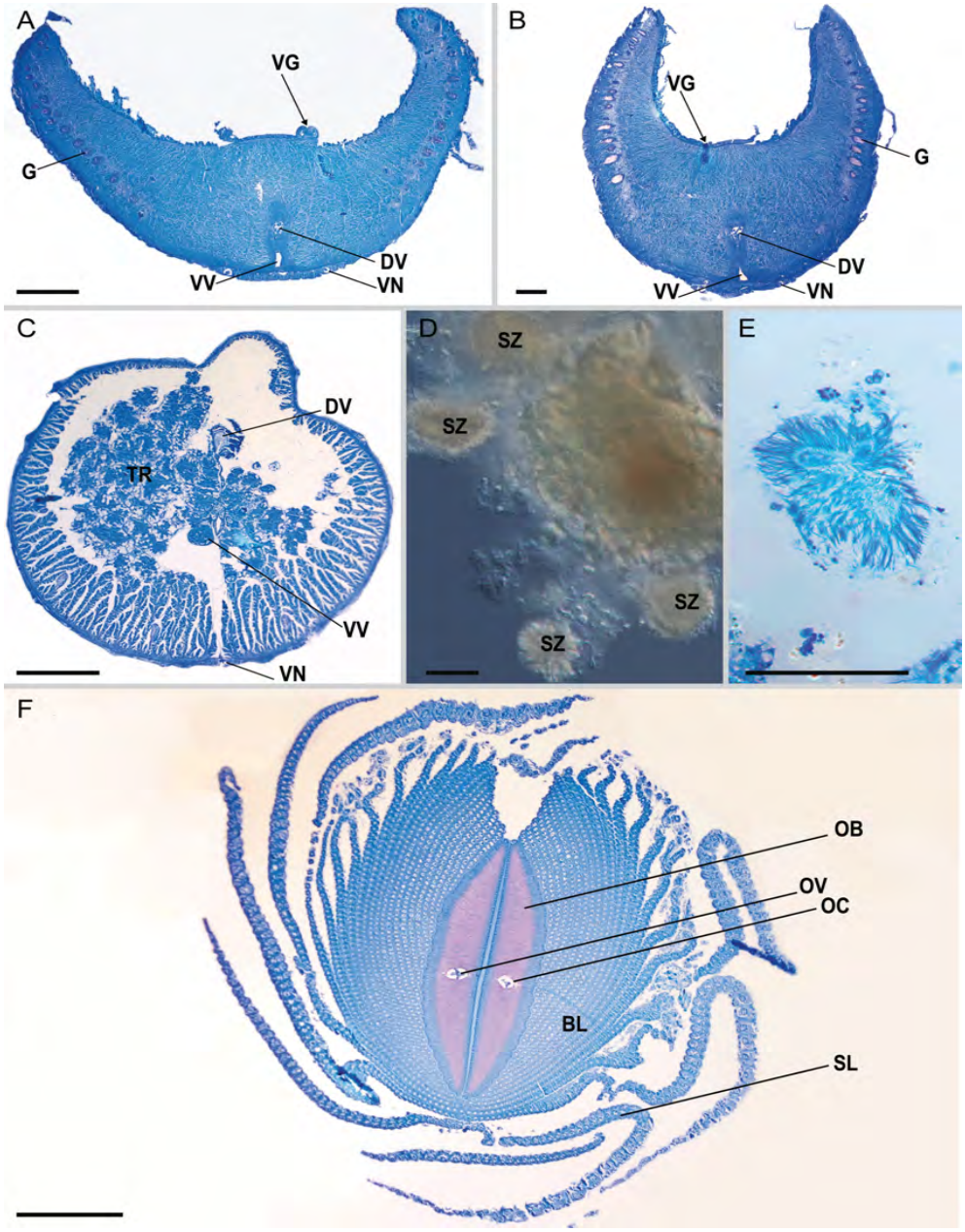

FIGURE 7. Micrographs of vestimental and trunk regions of *Lamellibrachia donwalshi* holotype (SIO-BIC A8382), male paratype (SIO-BIC A1341), and putative female paratype (SIO-BIC A1341). **A** 10 µm transverse section through anterior-middle part of vestimentum, male paratype. **B** 10µm transverse section through anterior-middle part of vestimentum, female paratype. **C** 10µm transverse section through trunk, male paratype. **D** Light micrograph of additional spermatozeugmata dissected from male paratype. **E** Close-up of spermatozeugmata in 10µm transverse section through trunk, male paratype. **F** 10µm transverse section through crown, male paratype. VG, vestimental groove; DV, dorsal blood vessel; VV, ventral blood vessel; VN, ventral nerve cord (Worsaae *et al.* 2016); G, gland; SZ, spermatozeugmata; OB, obturaculum; OV, obturacular blood vessel; OC, coelom of obturacular blood vessel; BL, branchial lamellae; SL, sheath lamellae. Scale bars, A–C=1mm; D=100µm; E–F=1mm.

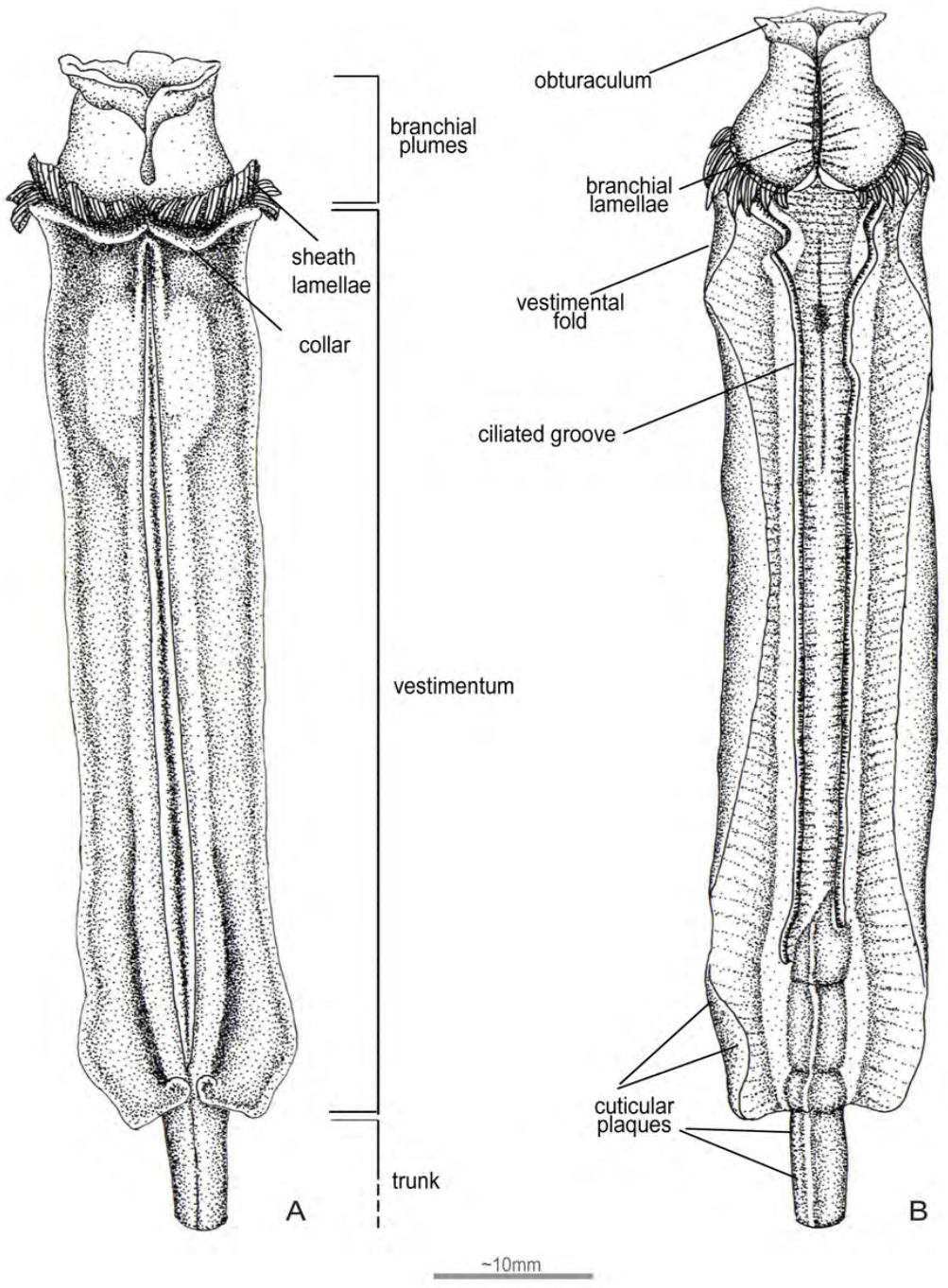

FIGURE 8. Illustration of *Lamellibrachia donwalshi* **sp. nov.** (male), holotype (SIO-BIC A8382). **A** Ventral. **B** Dorsal. Scale bar represents ~10mm.

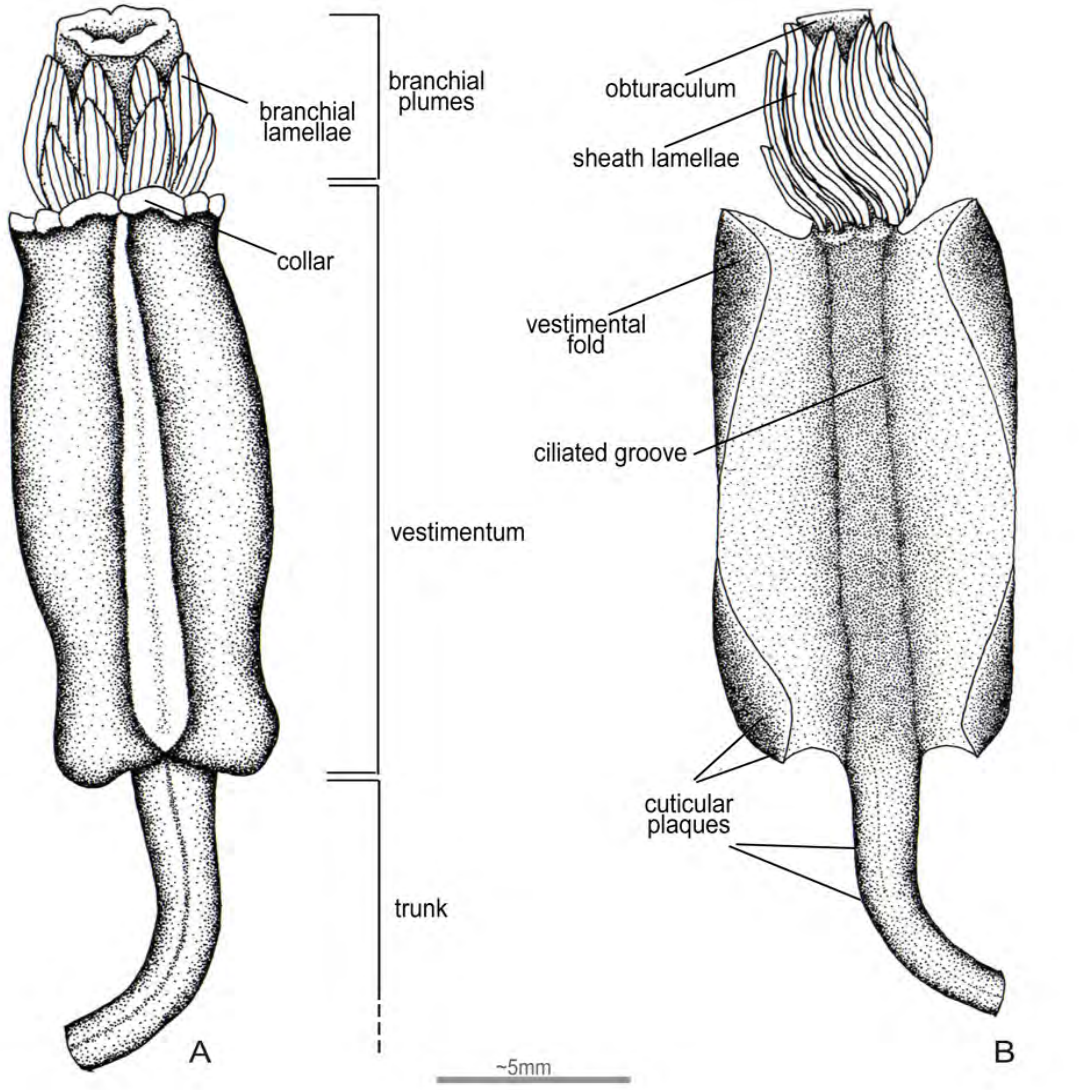

FIGURE 9. Illustration of *Lamellibrachia donwalshi* **sp. nov.** (female), paratype (SIO-BIC A1341). **A** Ventral. **B** Dorsal. Scale bar represents ~5mm.

Description. Tubes incomplete (broken in sampling), 24–26.5cm long, 9–10mm diameter anteriorly (n = 2; photo of tubes in-situ Fig. 6A). Anterior end of tube slightly curved with mostly long tube collars, occasionally interrupted by two or three short tube collars, but varying among specimens (Fig. 6B). Posterior of tubes smooth, curled, without obvious tube collars (Fig. 6B).

Obturaculum length 2.5–9mm (n = 11; holotype 7mm); width 2–8mm (n = 11; holotype 6mm), with bare anterior face, lacking any secreted structures (Figs. 6C–G). Lateral surface of obturaculum surrounded by branchial plumes (Fig. 6E–G). 5–11 pairs sheath lamellae (holotype 11 pairs; Figs 6E–G, 7–9) enclose 10–23 pairs branchial lamellae (holotype 23 pairs; Figs 6G, 8–10) with ciliated pinnules. Ratio of number of branchial lamellae pairs to obturaculum width varied from 1–3.3.

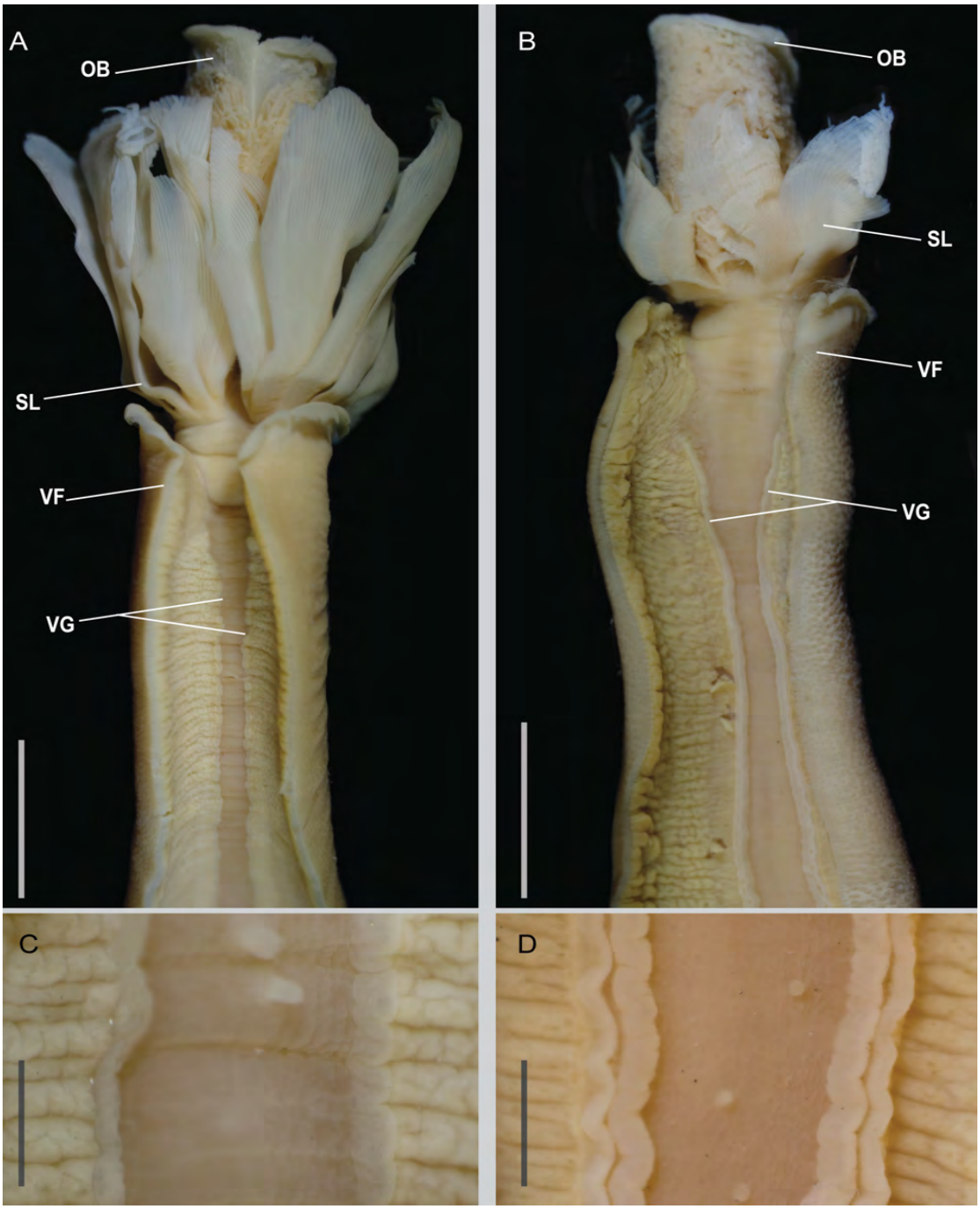

FIGURE 10. Micrographs of *Lamellibrachia donwalshi* **sp. nov.** male and female paratypes (SIO-BIC A1341). **A** Female dorsal anterior and vestimentum. **B** Male dorsal anterior and vestimentum. **C** Female vestimental grooves. **D** Male vestimental grooves. OB, obturaculum; SL, sheath lamellae; VF, vestimental fold; VG, vestimental groove. Scale bars, A–B=5mm; C–D=0.5mm.

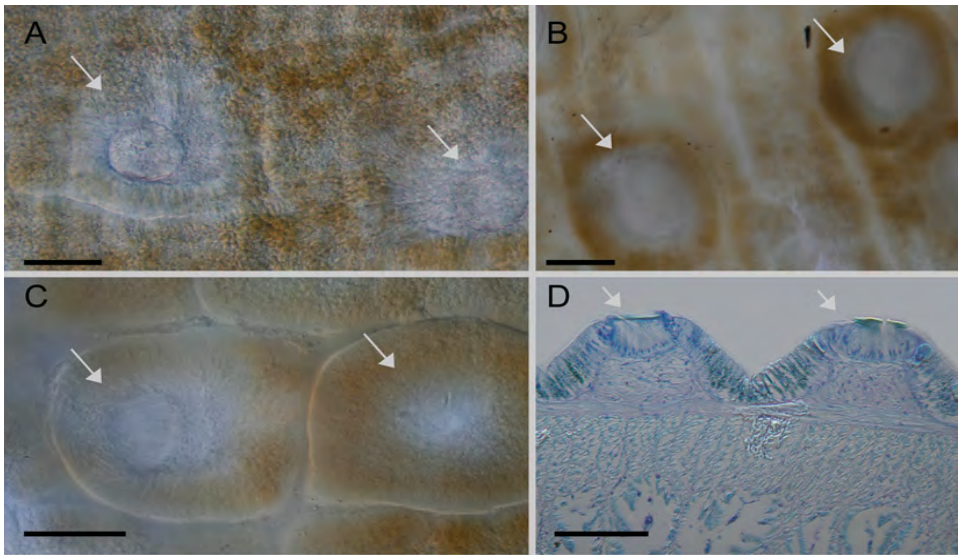

FIGURE 11. Interference contrast micrographs of plaques from *Lamellibrachia donwalshi* **sp. nov.** holotype (SIO-BIC A8382). **A**–**B** vestimental plaques, indicated by arrows. **C** Trunk plaques, indicated by arrows. **D** 10μm transverse section through epidermis showing trunk plaques, indicated by arrows. Scale bars 35μm.

Vestimentum length 22–70mm (holotype 70mm), width 3–12mm with vestimental folds curled (Figs 6C–G, 8A–B, 9B). Anterior vestimentum edge slightly curled forming collar (Figs 8A, 9A); posterior ends of vestimental folds rounded with slight separation at center (Figs 6, 7A–B, 8A, 9A). Dorsal paired vestimental ciliated grooves run down length of vestimentum (Figs 8B, 9B). In males, grooves flanked by ridge-like, conspicuous epidermal folds, spermatozeugmata observed in trunk (Figs 7D–E, 8B); conspicuous epidermal folds not present in putative females (Figs 7A–B, 9B, 10A–D). Both males and females have a few scattered epidermal processes on the internal epidermis of the vestimental cavity (Fig. 10C–D).

All specimens lacking posterior trunks. Anterior portion of trunk (Figs 6C–D, 7C) filled with fragile trophosome tissue (Fig. 7C). Ventral surface of vestimentum covered in cuticular plaques (Figs 11A–B), noticeably smaller than those on trunk (Figs 11C–D). Vestimental plaques measure 33.2–74.7μm in diameter (holotype 41.5–49.8 μm, Fig. 11B). Surface of trunk covered entirely by cuticular plaques, measuring 51.5–83μm in diameter (holotype 41.5–83μm, Fig. 11D). No plaques on middorsal and midventral lines of trunk. Opisthosoma not recovered.

Etymology. Don Walsh was one of the first people to descend to the bottom of the Challenger Deep aboard the bathyscaphe *Trieste* in 1960. He went on to a distinguished career in oceanography and marine policy. We name *Lamellibrachia donwalshi* **sp. nov.** in honor of his contributions to deep sea research and exploration.

Distribution. *Lamellibrachia donwalshi* **sp. nov.** has only been recovered from a single small area (varies by 0.01 N) and depth range of 999 to 1,040 meters. It was previously noted by Levin *et al.* (2015) as *Lamellibrachia* sp.

Remarks. *Lamellibrachia donwalshi* **sp. nov.** differs morphologically from other *Lamellibrachia* species in that it has 5–11 sheath lamellae, 10–23 branchial lamellae, and vestimental plaque diameters of 33.2–74.7μm (Table 4). It is not uncommon for ranges of sheath lamellae, branchial lamellae, and plaque diameters to overlap among *Lamellibrachia* species (Table 4), but no previously described species encompasses the entire range of these morphological traits in *L. donwalshi* **sp. nov.** We found no significant correlation between the body size (length and width of obturaculum and vestimentum) and the number of sheath lamellae, branchial lamellae, or plaque diameters (Spearman rank correlation, 11 specimens, $P > 0.05$). This supports the findings of Kobayashi *et al.* (2015) that the number of lamellae and the diameters of plaques are independent of growth in adults and can be used for morphological comparison across species. Due to a lack of morphological data for *L.* sp. 2, we cannot say

TABLE 3. Uncorrected pairwise distances for COI data (unique taxa only; identical sequences omitted), generated with PAUP*.

	***L.* sp. 1**	***L.* sp. 2**	***L. anaximandri***	***L. barhami***	***L. columna***	***L. juni***	***L.* cf. *luymesi***	***L. donwalshi* sp. nov.**	***L. sagami***	***L.* sp. L4**	***L.* sp. L5**	***L.* sp. L6**
***L.* sp. 2**	3.38	-	-	-	-	-	-	-	-	-	-	-
L. anaximandri	2.50	2.71	-	-	-	-	-	-	-	-	-	-
L. barhami	5.93	4.55	5.52	-	-	-	-	-	-	-	-	-
L. columna	4.92	4.60	5.23	5.68	-	-	-	-	-	-	-	-
L. juni	7.86	7.42	7.79	7.54	7.67	-	-	-	-	-	-	-
L.* cf. *luymesi	1.01	3.36	2.87	6.27	4.28	7.46	-	-	-	-	-	-
***L. donwalshi* sp. nov.**	3.59	2.37	2.50	5.42	4.68	7.25	2.85	-	-	-	-	-
L. sagami	4.49	4.45	4.56	4.99	1.00	6.81	4.14	4.34	-	-	-	-
***L.* sp. L4**	5.16	5.05	5.18	5.09	4.66	6.68	4.09	4.42	4.13	-		-
***L.* sp. L5**	4.71	5.21	4.28	5.30	4.95	6.98	4.47	4.72	4.31	2.62	-	-
***L.* sp. L6**	5.71	5.07	4.74	5.52	4.75	6.70	4.28	4.53	4.00	1.85	2.83	-
L. satsuma	5.94	6.12	6.18	6.06	6.15	8.48	5.12	6.25	5.51	5.69	5.87	5.69

TABLE 4. Morphological characters of *Lamellibrachia donwalshi* **sp. nov.** and congeneric species (1=Kobayashi *et al.* 2015; 2=Southward *et al*. 2011; 3=Miura & Kojima 2006; 4=Gardiner & Hourdez 2003; 5= Miura *et al.* 1997; 6=Southward 1991; 7=Jones 1985; 8=Mañe-Garzón & Montero 1985; 9=van der Land & Nørrevang 1975; 10=Webb 1969; no superscript=this study). OL: obturaculum length, OW: obturaculum width, BL: number of branchial lamellae, SL: number of sheath lamellae, VP: diameter of vestimental plaques, TP: diameter of trunk plaques.

Taxon	**OL (mm)**	**OW (mm)**	**BL**	**SL**	**VP (µm)**	**TP (µm)**
Lamellibrachia anaximandri	5.5–17[2]	1.8–6[2]	8–19[2]	3–9[2]	55–70[2]	60–95[2]
Lamellibrachia barhami	4.5–16[2,7,10]	4.5–12[2,7,10]	?–25[7]/19–25[2,10]	-4[7]/2–5[2,10]	60–150[2]	115–160[2]
Lamellibrachia columna	15–42[2,6]	8–13[2,6]	21[2,6]	8–16[2,6]	65–90[2,6]	70–120[2,6]
***Lamellibrachia donwalshi* sp. nov.**	**2.5–9**	**2–6**	**10–23**	**5–11**	**33.2–74.7**	**53.2–83**
Lamellibrachia juni	6.6–12.9[3]	5.2–8.3[3]	22–35[3]	2–3[3]/-4[2]	87–99[3]	80–98[3]
Lamellibrachia luymesi	13[9]/6.6–16[32,4]	9[9]/3.4–9.7[2,4]	19[9]/15–22[2,4]	6[9]/4–8[2,4]	55–60[2,4]	75–85[2,4]
Lamellibrachia sagami	5.8–22.5[1]	4.4–10.8[1]	19–26[1]	3–6[1]	59–101[1]	67–130[1]
Lamellibrachia satsuma	1.8–9.8[5]	1–5.6[5]	?–19[5]	0–4[5]/4–5[2]	35–63[5]	51–82[5]
Lamellibrachia victori	13[8]	13[2]	7[8]	18[2]	n/a	n/a

at this time whether *L. donwalshi* **sp. nov.** differs morphologically from this close genetic relative (Fig. 3). However, it clearly differs morphologically from its other close relative, *L. anaximandri* (Fig. 3), in having greater numbers of sheath lamellae and branchial lamellae and a shorter obturaculum length (Table 4). *Lamellibrachia donwalshi* **sp. nov.** also demonstrates some of the smallest vestimental plaque diameters reported for the genus (lower bound of 33.2µm, Table 4), though this range is very close to that of *L. sagami* and falls partially within the range of plaque diameters for *L. anaximandri* (also shown in Table 4). *Lamellibrachia donwalshi* **sp. nov.** also closely resembles *L. sagami* in the range of trunk plaque diameters, but numbers of lamellae more closely resemble those of *L. columna* (Table 4).

Discussion

Phylogenetic Support. *Lamellibrachia* shows low levels of variation in the mitochondrial genes 16S and COI and the nuclear gene 18S (Cowart *et al*. 2013, 2014). This is reflected in a number of poorly supported nodes in the phylogenetic analyses conducted with these loci (16S and COI; Fig. 3). The average distance among *Lamellibrachia* species calculated from the uncorrected pairwise distances for taxa in this study was approximately 5%, but several established *Lamellibrachia* species differ by as little as 1–3% (e.g. *L. columna/L. sagami* and *L. anaximandri/L.* sp. 2, respectively). This suggests that the 1.81% and 1.92% minimum distances between *L. donwalshi* **sp. nov.** and its closest relatives *L. anaximandri* and *L.* sp. 2, respectively, is not unusual. The validity of *L. donwalshi* **sp. nov.** is also supported by its geographic separation from its closest relatives, *L. anaximandri* and *L.* sp. 2 by the Panama Isthmus. *Lamellibrachia donwalshi* **sp. nov.** is 5.4% divergent from its sympatric relative, *L. barhami*. While in close proximity, these two species were found at different depths: *L. donwalshi* **sp. nov.** was present only at relatively shallow depths (~1,000m) and at a single location (Mound 12), while *L. barhami* was present at depths of 1,800 meters or greater and multiple sites (Jaco Scar, Parrita Scar, and Quepos Seep).

Gulf of Mexico/Caribbean Taxa. Some *Lamellibrachia* specimens in the upper Gulf of Mexico have often been identified as *L. luymesi*, which was described from much further south off Venezuela at about 500 meters depth. The even more remote Uruguayan species, *L. victori,* trawled from 300 meters depth, has been regarded as "questionably distinct" (Gardiner & Hourdez 2003; Jones 1985). Gardiner & Hourdez (2003) pointed out that the original descriptions of *L. luymesi* and *L. victori* by van der Land & Nørrevang (1975) and Mañé-Garzón & Montero (1985) were based on only one or two specimens. The number of sheath lamellae and the ratio of vestimentum diameter to length for the *L. luymesi* type specimen falls within the ranges reported for the specimens sampled from the Gulf of Mexico. Gardiner & Hourdez (2003) did a detailed morphological study on material collected from less than 1,000 m on the upper Louisiana slope of the Gulf of Mexico and extended the range for *L. luymesi* to that region. Most features of the *L. victori* type specimen (except for vestimentum length and the aperture diameter of the specimen tube) also fall within the range of the sampled Gulf of Mexico specimens, so it was suggested by Gardiner & Hourdez (2003) that *L. victori* may not be distinct from *L. luymesi*. However, the type specimen for *L. victori* differs from the type specimen of *L. luymesi* for most of the features analyzed (numbers of lamellae, obturaculum and vestimentum lengths, etc.) used in Gardiner & Hourdez (2003) and it may still be a valid species. In any case, McMullin *et al.* (2003) reported the *Lamellibrachia* specimens collected from the Louisiana Slope for DNA sequencing as *L.* cf. *luymesi*. The molecular results of Miglietta *et al*. (2010), which included samples from deeper waters in the Gulf of Mexico, then revealed at least two genetically distinct species of *Lamellibrachia*. One included samples studied by McMullin *et al.* (2003), and they referred to this as *L. luymesi*/ sp. 1. There was a second species only found in deeper water, which they called *L.* sp. 2. (Fig. 2). A microsatellite study by Cowart *et al.* (2014) later showed that *L. luymesi/L.* sp. 1 may indeed be distinct species, but we treat them as a single taxon presently based on the mitochondrial data, which does not differentiate the two. The presence of up to three *Lamellibrachia* species in the northern Gulf of Mexico has been corroborated by further sequencing of mitochondrial and nuclear DNA as well as a microsatellite study of Gulf of Mexico *Lamellibrachia* (Cowart *et al.* 2014). No molecular data exists for specimens from either of the type localities of *L. luymesi* or *L. victori* thus until further sampling and DNA sequencing is conducted, there is no way to confirm what the specimens identified as *L.* cf. *luymesi*, *L.* sp. 1, and *L.* sp. 2 from the Gulf of Mexico actually are. Interestingly, *L.* sp. 2 has been recorded south of Cuba at hydrothermal vents at ~2,500 meters in the Mid-Cayman Spreading Center (Plouviez *et al.* 2015).

Biogeographic Implications of Lamellibrachia donwalshi **sp. nov.**. Fig. 3 shows a grade of Pacific species with

respect to Atlantic *Lamellibrachia* species, with the exception of *L. donwalshi* **sp. nov.** (Pacific), which shows a closest relationship with the Atlantic *L.* sp. 2 (Gulf of Mexico) and *L. anaximandri* (Mediterranean) (Fig. 2). As in Southward *et al.* 2011, within the Pacific grade, a West Pacific species (*L. juni*) was recovered as sister to all other *Lamellibrachia*. This suggests a Pacific ancestor for *Lamellibrachia* and may align with the Moalic *et al.* (2012) hypothesis that proposes Atlantic deep-sea chemosynthetic environments were colonized by Pacific deep-sea fauna. The recovery of *L. donwalshi* **sp. nov.** inside the Atlantic clade suggests that a vicariant event may have occurred after an Atlantic radiation of *Lamellibrachia*. The shoaling of deep water as the Panama isthmus began to form (approximately 9–12 Ma [O'Dea *et al.* 2016]) could have shut off the deep-water connection between populations of the *L. donwalshi* **sp. nov.**/*L.* sp. 2/*L. anaximandri* common ancestor. Similar phylogenetic topologies and biogeographic hypotheses have been reported for other deep-sea fauna in chemosynthetic environments in this region, such as the vesicomyids *Pliocardia* Woodring, 1925*, Calyptogena* Dall, 1891, and *Abyssogena* Krylova, Sahling & Janssen 2010 (LaBella *et al.* 2017), and in the annelid *Amphisamytha* Hessle, 1917, which also shows a clear eastern Pacific to Atlantic sister relationship (Stiller *et al.* 2013).

The expanded range of *L. barhami* reported here is also notable. Though originally described from off southern California by Webb in 1969 (sequences not published as yet from the type locality), *L. barhami* has been noted along the Pacific coast of North America from central California to Oregon (Black *et al.* 1997; Suess *et al.* 1985), and as far north as Vancouver Island, Canada (Barry *et al.* 1996; McMullin *et al.* 2003), with DNA sequence data to support this (Black *et al.* 1997; McMullin *et al.* 2003). Sequence data also shows that it occurs in the southern and central Gulf of California (Goffredi *et al*. 2017, present study) and it has been noted as far south as Costa Rica (Han *et al.* 2004; Mau *et al.* 2006; Sahling *et al.* 2008; Southward *et al.* 1996), though until now there been no sequence data to support these southernmost reports. Haplotype networks (Fig. 5) show minimal genetic divergence between *L. barhami* samples from different depths and different localities: Costa Rica (Jaco Scar, Parrita Scar, Quepos Seep), Gulf of California (Guaymas and Pescadero Basins), Monterey Canyon, Oregon, Middle Valley, and Vancouver Island from depths of 1,000–2,416 meters. Though a large proportion of the COI sequences of *L. barhami* were from Costa Rica, even those from as far north as Vancouver Island were identical or differed by at most a single base pair from the most common haplotype, regardless of locality (Fig. 5).

The *Lamellibrachia* phylogeny should also be considered in the context of the phylogeny of Siboglinidae (Rouse 2001; Sun *et al.* 2018). In the Sun *et al.* analysis (2018), generated with 13 mitochondrial genes and two ribosomal RNA genes, all sequenced seep-dwelling Vestimentifera (*Lamellibrachia*, *Escarpia*, *Seepiophila*, and *Paraescarpia*) formed a grade with respect to a vent-dwelling clade (*Riftia*, *Ridgeia, Oasisia*, *Tevnia*). Rouse (2001) showed that the two genera known at that time from seeps (*Lamellibrachia*, *Escarpia*) formed the sister group to the vent clade (*Arcovestia, Alaysia, Riftia*, *Ridgeia, Oasisia*, *Tevnia*) and that, in the context of the overall phylogeny of Siboglinidae, the vent-dwelling clade was derived from seep ancestors. The vent-seep separation is somewhat recurrent geographically: vent Vestimentifera are known only from the Pacific (with the exception of a known occurrence at a submarine volcano north of Sicily [Southward et al. 2011]), with none present at the Mid-Atlantic Ridge (Gebruk *et al.* 1997), Antarctic Ridge (Karaseva *et al.* 2016), or the South-West and Central Indian Ridges (Van Dover *et al.* 2001). The Southern Ocean may act as a barrier to some vent animals (Rogers *et al.* 2012), and at the Central Indian Ridges there is no molecular evidence of a connection between Pacific and Atlantic deep-sea fauna (there are known topographic barriers that could limit dispersal there [Van Dover *et al*. 2001]). However, some non-vestimentiferan taxa inhabiting chemosynthetic environments such as the annelid *Archinome* Kudenov, 1991 and the mussel *Bathymodiolus* Kenk & Wilson, 1985 and two seep vestimentiferan genera (*Lamellibrachia* and *Escarpia*) have distributions in both the Pacific and Atlantic Oceans (Borda *et al.* 2013; Copley *et al.* 2016). The phylogeny of *Escarpia* is not well-resolved and needs further study, but the present results suggest that *Lamellibrachia* originated in the Pacific (Fig. 3). Further molecular data is needed to more clearly elucidate the evolutionary relationships of Pacific and Atlantic seep Vestimentifera.

Acknowledgements

Many thanks to Chief Scientists Lisa Levin, Erik Cordes and Bob Vrijenhoek, the captain and crew of the *R/V Atlantis, R/V Western Flyer*, and the crews of the HOV *Alvin* and ROV *Doc Ricketts* for crucial assistance in specimen collection on cruises to Costa Rica and the Gulf of California. Thanks also to Danwei Huang, Sigrid

Katz, Ben Moran, Charlotte Seid and Nerida Wilson for assistance with samples at sea. Thanks also to Harim Cha and Charlotte Seid for collection management at SIO-BIC, Nicholas Holland for his assistance with histology, Sofia Nahman for her scientific drawings, and Emily Tipton for her photograph editing. We would also like to thank reviewers Genki Kobayashi and Nadezhda Rimskaya-Korsakova, as well as Zootaxa editor Wagner Magalhães. This project was funded by the US National Science Foundation (NSF OCE-0826254, OCE-0939557, OCE-1634172) and a Scripps Institution of Oceanography 1st year Fellowship.

References

Altschul, S.F., Gish, W., Miller, W., Myers, E.W. & Lipman, D.J. (1990) Basic local alignment search tool. *Journal of Molecular Biology*, 215, 403–10.
https://doi.org/10.1016/S0022-2836(05)80360-2

Bandelt, H., Forster, P. & Röhl, A. (1999) Median-joining networks for inferring intraspecific phylogenies. *Molecular Biology and Evolution*, 16, 37–48.
https://doi.org/10.1093/oxfordjournals.molbev.a026036

Barry, J.P., Greene, H.G., Orange, D.L., Baxter, C.H., Robison, B.H., Kochevar, R.E., Nybakken, J.W., Reed, D.L. & McHugh, C.M. (1996) Biologic and geologic characteristics of cold seeps in Monterey Bay, California. *Deep-Sea Research I*, 43, 1739–1762.
https://doi.org/10.1016/S0967-0637(96)00075-1

Bergquist, D.C., Ward, T., Cordes, E.E., McNelis, T., Howlett, S., Kosoff, R., Hourdez, S., Carney, R. & Fisher, C.R. (2003) Community structure of vestimentiferan-generated habitat islands from Gulf of Mexico cold seeps. *Journal of Experimental Marine Biology and Ecology*, 289, 197–222.
http:/dx.doi.org/10.1016/S0022-0981(03)00046-7

Black, M.B., Halanych, K.M., Maas, P.A.Y., Hoeh, W.R., Hashimoto, J., Desbruyères, D., Lutz, R.A. & Vrijenhoek, R.C. (1997) Molecular systematics of vestimentiferan tubeworms from hydrothermal vents and cold-water seeps. *Marine Biology*, 130, 141–149.
https://doi.org/10.1007/s002270050233

Borda, E., Kudenov, J.D., Chevaldonne, P., Blake, J.A., Desbruyeres, D., Fabri, M.-C., Hourdez, S., Pleijel, F., Shank, T.M., Wilson, N.G., Schulze, A. & Rouse, G.W. (2013) Cryptic species of *Archinome* (Annelida: Amphinomida) from vents and seeps. *Proceedings of the Royal Society B: Biological Sciences*, 280, 1–9.
https://doi.org/10.1098/rspb.2013.1876

Braby, C.E., Rouse, G.W., Johnson, S.B., Jones, W.J. & Vrijenhoek, R.C. (2007) Bathymetric and temporal variation among *Osedax* boneworms and associated megafauna on whale-falls in Monterey Bay, California. *Deep-Sea Research I*, 54, 1773–1791.
https://doi.org/10.1016/j.dsr.2007.05.014

Bright, M. & Lallier, F. (2010) The Biology of Vestimentiferan Tubeworms. *Oceanography and Marine Biology: An Annual Review*, 48, 213–265.
https://doi.org/10.1201/EBK1439821169-c4

Caullery, M. (1914) Sur les Siboglinidae, type nouveau d'invertébrés receuillis par l'expédition du Siboga. *Comptes rendus hebdomadaires des séances de l'Académie des sciences*, 158, 2014–2017.

Copley, J.T., Marsh, L., Glover, A.G., Hühnerbach, V., Nye, V.E., Reid, W.D.K., Sweeting, C.J., Wigham, B.D. & Wiklund, H. (2016) Ecology and biogeography of megafauna and macrofauna at the first known deep-sea hydrothermal vents on the ultraslow-spreading Southwest Indian Ridge. *Scientific Reports*, 6, 1–13.
https://doi.org/10.1038/srep39158

Cowart, D.A., Halanych, K.M., Schaeffer, S.W. & Fisher, C.R. (2014) Depth-dependent gene flow in Gulf of Mexico cold seep *Lamellibrachia* tubeworms (Annelida, Siboglinidae). *Hydrobiologia*, 736, 139–154.
https://doi.org/10.1007/s10750-014-1900-y

Cowart, D.A., Huang, C., Arnaud-Haond, S., Carney, S.L., Fisher, C.R. & Schaeffer, S.W. (2013) Restriction to large-scale gene flow vs. regional panmixia among cold seep *Escarpia* spp. (Polychaeta, Siboglinidae). *Molecular Ecology*, 22, 4147–4162.
https://doi.org/10.1111/mec.12379

Darriba, D., Taboada, G.L., Doallo, R. & Posada, D. (2012) jModelTest 2: more models, new heuristics and parallel computing. *Nature Methods*, 9, 772–772.
https://doi.org/10.1038/nmeth.2109

Feldman, R.A., Shank, T.M., Black, M.B., Baco, A.R., Smith, C.R. & Vrijenhoek, R.C. (1998) Vestimentiferan on a Whale Fall. *Biological Bulletin*, 194, 116–119.
https://doi.org/10.2307/1543041

Folmer, O., Black, M., Hoeh, W., Lutz, R. & Vrijenhoek, R. (1994) DNA primers for amplification of mitochondrial cytochrome c oxidase subunit I from diverse metazoan invertebrates. *Molecular Marine Biology & Biotechnology*, 3, 294–

299.
https://doi.org/10.1371/journal.pone.0013102
Gardiner, S.L. & Hourdez, S. (2003) On the occurrence of the vestimentiferan tube worm *Lamellibrachia luymesi* van der Land and Nørrevang, 1975 (Annelida: Pogonophora) in hydrocarbon seep communities in the Gulf of Mexico. *Proceedings of the Biological Society of Washington*, 116, 380–394.
Gardiner, S.L., McMullin, E. & Fisher, C.R. (2001) *Seepiophila jonesi*, a new genus and species of vestimentiferan tube worm (Annelida: Pogonophora) from hydrocarbon seep communities in the Gulf of Mexico. *Proceedings of the Biological Society of Washington*, 114, 694–707.
Gaurav, V., Lohman, D.J. & Rudolf, M. (2011) SequenceMatrix: concatenation software for the fast assembly of multi-gene datasets with character set and codon information. *Cladistics*, 27 (2), 171–180.
https://doi.org/10.1111/j.1096-0031.2010.00329.x
Gebruk, A., Galkin, S., Vereshchaka, A., Moskalev, L. & Southward, A. (1997) Ecology and biogeography of the hydrothermal vent fauna of the Mid-Atlantic Ridge. *Advances in Marine Biology*, 32, 93–144.
https://doi.org/10.1016/S0065-2881(08)60016-4
Goffredi, S.K., Johnson, S., Tunnicliffe, V., Caress, D., Clague, D., Escobar, E., Lundsten, L., Paduan, J.B., Rouse, G., Salcedo, D.L., Soto, L.A., Spelz-Madero, R., Zierenberg, R. & Vrijenhoek, R. (2017) Hydrothermal vent fields discovered in the southern Gulf of California clarify role of habitat in augmenting regional diversity. *Proceedings of the Royal Society B: Biological Sciences*, 284, 1–10.
https://doi.org/10.1098/rspb.2017.0817
Guindon, S. & Gascuel, O. (2003) A simple, fast and accurate method to estimate large phylogenies by maximum-likelihood. *Systematic Biology*, 52 (5), 696–704.
https://doi.org/10.1080/10635150390235520
Halanych, K.M., Feldman, R.A. & Vrijenhoek, R.C. (2001) Molecular evidence that *Sclerolinum brattstromi* is closely related to vestimentiferans, not to frenulate pogonophorans (Siboglinidae, Annelida). *Biological Bulletin*, 201, 65–75.
https://doi.org/10.2307/1543527
Han, X., Suess, E., Sahling, H. & Wallmann, K. (2004) Fluid venting activity on the Costa Rica margin: New results from authigenic carbonates. *International Journal of Earth Sciences*, 93, 596–611.
https://doi.org/10.1007/s00531-004-0402-y
Hasegawa, M., Kishino, H. & Yano, T.A. (1985) Dating of the human-ape splitting by a molecular clock of mitochondrial DNA. *Journal of Molecular Evolution*, 22, 160–174.
https://doi.org/10.1007/BF02101694
Jones, M.L. (1981) *Riftia pachyptila*, new genus, new species, the vestimentiferan worm from the Galápagos Rift geothermal vents. *Biological Society of Washington*, 93, 1295–1313.
Jones, M.L. (1985) On the Vestimentifera, new phylum: six new species, and other taxa, from hydrothermal vents and elsewhere. *Bulletin of the Biological Society of Washington*, 6, 117–158.
Karaseva, N.P., Rimskaya-Korsakova, N.N., Galkin, S.V. & Malakhov, V.V. (2016) Taxonomy, geographical and bathymetric distribution of vestimentiferan tubeworms (Annelida, Siboglinidae). *Biology Bulletin*, 43, 937–969.
https://doi.org/10.1134/S1062359016090132
Katoh, K. & Standley, D.M. (2013) MAFFT multiple sequence alignment software version 7: Improvements in performance and usability. *Molecular Biology and Evolution*, 30, 772–780.
https://doi.org/10.1093/molbev/mst010
Kenk, V. & Wilson, B. (1985) A new mussel (Bivalvia, Mytilidae) from hydrothermal vents, in the Galapagos Rift zone. *Malacologia*, 26, 253–271.
Kobayashi, G., Miura, T. & Kojima, S. (2015) *Lamellibrachia sagami* sp. nov., a new vestimentiferan tubeworm (Annelida: Siboglinidae) from Sagami Bay and several sites in the northwestern Pacific Ocean. *Zootaxa*, 4018 (1), 97–108.
https://doi.org/10.11646/zootaxa.4018.1.5
Kojima, S., Ohta, S., Yamamoto, T., Miura, T., Fujiwara, Y. & Hashimoto, J. (2001) Molecular taxonomy of vestimentiferans of the western Pacific and their phylogenetic relationship to species of the eastern Pacific. I. Family Lamellibrachiidae. *Marine Biology*, 139, 211–219.
https://doi.org/10.1007/s002270100581
Kojima, S., Watanabe, H., Tsuchida, S., Fujikura, K., Rowden, A., Takai, K. & Miura, T. (2006) Phylogenetic relationships of a tube worm (*Lamellibrachia juni*) from three hydrothermal vent fields in the South Pacific. *Journal of the Marine Biological Association of the United Kingdom*, 86, 1357–1361.
https://doi.org/10.1017/S002531540601438X
Kudenov, J.D. (1991) A new family and genus of the order Amphinomida (Polychaeta) from the Galapagos Hydrothermal vents. *Ophelia*, Supplement 5 (Systematics, Biology and Morphology of World Polychaeta), 11–120.
Levin, L.A., Mendoza, G.F., Grupe, B.M., Gonzalez, J.P., Jellison, B., Rouse, G., Thurber, A.R. & Waren, A. (2015) Biodiversity on the rocks: Macrofauna inhabiting authigenic carbonate at Costa Rica methane seeps. *PLoS ONE*, 10, e0131080.
https://doi.org/10.1371/journal.pone.0131080
Levin, L.A., Orphan, V.J., Rouse, G.W., Rathburn, A.E., Ussler, W., Cook, G.S., Goffredi, S.K., Perez, E.M., Waren, A., Grupe,

B.M., Chadwick, G. & Strickrott, B. (2012) A hydrothermal seep on the Costa Rica margin: middle ground in a continuum of reducing ecosystems. *Proceedings of the Royal Society B: Biological Sciences*, 279, 2580–2588. https://doi.org/10.1098/rspb.2012.0205

Li, Y., Kocot, K.M., Schander, C., Santos, S.R., Thornhill, D.J. & Halanych, K.M. (2015) Mitogenomics reveals phylogeny and repeated motifs in control regions of the deep-sea family Siboglinidae (Annelida). *Molecular Phylogenetics and Evolution*, 85, 221–229. https://doi.org/10.1016/j.ympev.2015.02.008

Li, Y., Kocot, K.M., Whelan, N.V., Santos, S.R., Waits, D.S., Thornhill, D.J. & Halanych, K.M. (2017) Phylogenomics of tubeworms (Siboglinidae, Annelida) and comparative performance of different reconstruction methods. *Zoologica Scripta*, 46, 200–213. https://doi.org/10.1111/zsc.12201

Mañe-Garzón, F. & Montero, R. (1985) Sobre una nueva forma de verme tubicola *Lamellibrachia victori* n. sp. (Vestimentifera) proposicion de un nuevo phylum: mesoneurophora. *Revista de Biología del Uruguay*, 8, 1–28. https://doi.org/10.1364/AO.6.002125

Mau, S., Sahling, H., Rehder, G., Suess, E., Linke, P. & Soeding, E. (2006) Estimates of methane output from mud extrusions at the erosive convergent margin off Costa Rica. *Marine Geology*, 225, 129–144. https://doi.org/10.1016/j.margeo.2005.09.007

McMullin, E.R., Hourdez, S., Schaeffer, S.W. & Fisher, C.R. (2003) Phylogeny and biogeography of deep sea vestimentiferan tubworms and their bacterial symbionts. *Symbiosis*, 34, 1–41.

Miglietta, M.P., Hourdez, S., Cowart, D.A., Schaeffer, S.W. & Fisher, C. (2010) Species boundaries of Gulf of Mexico vestimentiferans (Polychaeta, Siboglinidae) inferred from mitochondrial genes. *Deep-Sea Research Part II: Topical Studies in Oceanography*, 57, 1916–1925. https://doi.org/10.1016/j.dsr2.2010.05.007

Miura, T. & Kojima, S. (2006) Two new species of vestimentiferan tubeworm (Polychaeta: Siboglinidae a.k.a. Pogonophora) from the Brothers Caldera, Kermadec Arc, South Pacific Ocean. *Species Diversity*, 11, 209–224. https://doi.org/10.12782/specdiv.11.209

Miura, T., Tsukahara, J. & Hashimoto, J. (1997) *Lamellibrachia satsuma*, a new species of vestimentiferan worms (Annelida: Pogonophora) from a shallow hydrothermal vent in Kagoshima Bay, Japan. *Proceedings of the Biological Society of Washington*, 110, 447–456.

Moalic, Y., Desbruyères, D., Duarte, C.M., Rozenfeld, A.F., Bachraty, C. & Arnaud-Haond, S. (2012) Biogeography revisited with network theory: Retracing the history of hydrothermal vent communities. *Systematic Biology*, 61, 127–137. https://doi.org/10.1093/sysbio/syr088

Nelson, K. & Fisher, C. (2000) Absence of cospeciation in deep-sea vestimentiferan tube worms and their bacterial endosymbionts. *Symbiosis*, 28, 1–15. https://doi.org/10.2307/25066661

Nishijima, M., Lindsay, D.J., Hata, J., Nakamura, A., Kasai, H., Ise, Y., Fisher, C.R., Fujiwara, Y., Kawato, M. & Maruyama, T. (2010) Association of thioautotrophic bacteria with deep-sea sponges. *Marine Biotechnology*, 12, 253–260. https://doi.org/10.1007/s10126-009-9253-7

O'Dea, A., Lessios, H.A., Coates, A.G., Eytan, R.I., Restrepo-Moreno, S.A., Cione, A.L., Collins, L.S., de Queiroz, A., Farris, D.W., Norris, R.D., Stallard, R.F., Woodburne, M.O., Aguilera, O., Aubry, M.-P., Berggren, W.A., Budd, A.F., Cozzuol, M.A., Coppard, S.E., Duque-Caro, H., Finnegan, S., Gasparini, G.M., Grossman, E.L., Johnson, K.G., Keigwin, L.D., Knowlton, N., Leigh, E.G., Leonard-Pingel, J.S., Marko, P.B., Pyenson, N.D., Rachello-Dolmen, P.G., Soibelzon, E., Soibelzon, L., Todd, J.A., Vermeij, G.J. & Jackson, J.B.C. (2016) Formation of the Isthmus of Panama. *Science Advances*, 2, 1–12. https://doi.org/10.1126/sciadv.1600883

Palumbi, S.R. (1996) Nucleic acid II: the polymerase chain reaction. *In*: Hillis, D.M., Moritz, C. & Mable, B.K. (Eds.), *Molecular Systematics*. Sinauer Associates, Inc, Sunderland, MA, pp. 205–247.

Patra, A.K., Kwon, Y.M., Kang, S.G., Fujiwara, Y. & Kim, S.J. (2016) The complete mitochondrial genome sequence of the tubeworm *Lamellibrachia satsuma* and structural conservation in the mitochondrial genome control regions of Order Sabellida. *Marine Genomics*, 26, 63–71. https://doi.org/10.1016/j.margen.2015.12.010

Paull, C.K., Ussler, W., Peltzer, E.T., Brewer, P.G., Keaten, R., Mitts, P.J., Nealon, J.W., Greinert, J., Herguera, J.C. & Elena Perez, M. (2007) Authigenic carbon entombed in methane-soaked sediments from the northeastern transform margin of the Guaymas Basin, Gulf of California. *Deep-Sea Research Part II: Topical Studies in Oceanography*, 54, 1240–1267. https://doi.org/10.1016/j.dsr2.2007.04.009

Pleijel, F., Dahlgren, T.G. & Rouse, G.W. (2009) Progress in systematics: from Siboglinidae to Pogonophora and Vestimentifera and back to Siboglinidae. *Comptes Rendus Biologies*, 332, 140–148. https://doi.org/10.1016/j.crvi.2008.10.007

Plouviez, S., Jacobson, A., Wu, M. & Van Dover, C.L. (2015) Characterization of vent fauna at the mid-cayman spreading center. *Deep-Sea Research Part I: Oceanographic Research Papers*, 97, 124–133. https://doi.org/10.1016/j.dsr.2014.11.011

Puillandre, N., Lambert, A., Brouillet, S. & Achaz, G. (2012) ABGD, Automatic Barcode Gap Discovery for primary species delimitation. *Molecular Ecology*, 21, 1864–1877.
https://doi.org/10.1111/j.1365-294X.2011.05239.x

Rogers, A.D., Tyler, P.A., Connelly, D.P., Copley, J.T., James, R., Larter, R.D., Linse, K., Mills, R.A., Garabato, A.N., Pancost, R.D., Pearce, D.A., Polunin, N.V.C., German, C.R., Shank, T., Boersch-Supan, P.H., Alker, B.J., Aquilina, A., Bennett, S.A., Clarke, A., Dinley, R.J.J., Graham, A.G.C., Green, D.R.H., Hawkes, J.A., Hepburn, L., Hilario, A., Huvenne, V.A.I., Marsh, L., Ramirez-Llodra, E., Reid, W.D.K., Roterman, C.N., Sweeting, C.J., Thatje, S. & Zwirglmaier, K. (2012) The discovery of new deep-sea hydrothermal vent communities in the Southern ocean and implications for biogeography. *PLoS Biology*, 10, e1001234.
https://doi.org/10.1371/journal.pbio.1001234

Ronquist, F., Teslenko, M., Mark, P. van der, Ayres, D., Darling, A., Hohna, S., Larget, B., Liu, L., Suchard, M. & Huelsenbeck, J. (2012) Efficient Bayesian phylogenetic inference and model choice across a large model space. *Systematic Biology*, 61, 539–542.
https://doi.org/10.1093/sysbio/sys029

Rouse, G.W. (2001) A cladistic analysis of Siboglinidae Caullery, 1914 (Polychaeta, Annelida): Formerly the phyla Pogonophora and Vestimentifera. *Zoological Journal of the Linnean Society*, 132, 55–80.
https://doi.org/10.1006/zjls.2000.0263

Sahling, H., Masson, D.G., Ranero, C.R., Hühnerbach, V., Weinrebe, W., Klaucke, I., Bürk, D., Brückmann, W. & Suess, E. (2008) Fluid seepage at the continental margin offshore Costa Rica and southern Nicaragua. *Geochemistry*, *Geophysics*, *Geosystems*, 9, Q05S05, 1–22.
https://doi.org/10.1029/2008GC001978

Shank, T.M., Fornari, D.J., Von Damm, K.L., Lilley, M.D., Haymon, R.M. & Lutz, R.A. (1998) Temporal and spatial patterns of biological community development at nascent deep-sea hydrothermal vents (9° 50'N, East Pacific Rise). *Deep-Sea Research II*, 45, 465–515.
https://doi.org/10.1016/S0967-0645(97)00089-1

Southward, E.C. (1991) Three new species of Pogonophora, including two vestimentiferans, from hydrothermal sites in the Lau Back-arc Basin (Southwest Pacific Ocean). *Journal of Natural History*, 25, 859–881.
https://doi.org/10.1080/00222939100770571

Southward, E.C. & Galkin, S.V. (1997) A new vestimentiferan (Pogonophora: Obturata) from hydrothermal vent fields in the Manus Back-arc Basin (Bismarck Sea, Papua New Guinea, Southwest Pacific Ocean). *Journal of Natural History*, 31, 43–55.
https://doi.org/10.1080/00222939700770041

Southward, E.C., Schulze, A. & Tunnicliffe, V. (2002) Vestimentiferans (Pogonophora) in the Pacific and Indian Oceans: A new genus from Lihir Island (Papua New Guinea) and the Java Trench, with the first report of *Arcovestia ivanovi* from the North Fiji Basin. *Journal of Natural History*, 36, 1179–1197.
https://doi.org/10.1080/00222930110040402

Southward, E.C., Tunniclife, V., Black, M.B., Dixon, D.R. & Dixon, L.R.J. (1996) segmentation and vent tube-worms (Vestimentifera) in the NE Pacific. *Geological Society, London*, *Special Publications*, 118, 211224.
https://doi.org/10.1144/GSL.SP.1996.118.01.13

Southward, E.C., Andersen, A.C. & Hourdez, S. (2011) *Lamellibrachia anaximandri* n. sp., a new vestimentiferan tubeworm (Annelida) from the Mediterranean, with notes on frenulate tubeworms from the same habitat. *Zoosystema*, 33, 245–279.
https://doi.org/10.5252/z2011n3a1

Stamatakis, A. (2014) RAxML version 8: A tool for phylogenetic analysis and post-analysis of large phylogenies. *Bioinformatics*, 30, 1312–1313.
https://doi.org/10.1093/bioinformatics/btu033

Stiller, J., Rousset, V., Pleijel, F., Chevaldonné, P., Vrijenhoek, R.C. & Rouse, G.W. (2013) Phylogeny, biogeography and systematics of hydrothermal vent and methane seep Amphisamytha (Ampharetidae, Annelida), with descriptions of three new species. *Systematics and Biodiversity*, 11, 35–65.
https://doi.org/10.1080/14772000.2013.772925

Suess, E., Carson, B., Ritger, S.D., Moore, J.C., Jones, M.L., Kulm, L.D. & Cochrane., G.R. (1985) Biological communities at vent sites along the subduction zone off Oregon. *Bulletin of the Biological Society of Washington*, 6, 475–484.

Sun, Y., Liang, Q., Sun, J., Yang, Y., Tao, J., Liang, J., Feng, D., Qiu, J.W. & Qian, P.Y. (2018) The mitochondrial genome of the deep-sea tubeworm Paraescarpia echinospica (Siboglinidae, Annelida) and its phylogenetic implications. *Mitochondrial DNA Part B: Resources*, 3, 131–132.
https://doi.org/10.1080/23802359.2018.1424576

Swofford, D.L. (2002) *Phylogenetic analysis using parsimony (*and other methods)*. 4th ed. Sinauer Associates, Inc, Sunderland, MA, v4.0a161.

Van der Land, J. & Nørrevang, A. (1975) The systematic position of *Lamellibrachia* (Annelida, Vestimentifera). *Zeitschrift für Zoologische Systematik und Evolutionsforschung*, 1, 86–101.
https://doi.org/10.1126/science.1064574

Van Dover, C.L., Humphris, S.E., Fornari, D., Cavanaugh, C.M., Collier, R., Goffredi, S.K., Hashimoto, J., Littey, M.D.,

Reysenbach, A.L., Shank, T.M., Von Damm, K.L., Banta, A., Gallant, R.M., Götz, D., Green, D., Hall, J., Harmer, T.L., Hurtado, L.A., Johnson, P., McKiness, Z.P., Meredith, C., Olson, E., Pan, I.L., Turnipseed, M., Won, Y., Young, C.R. & Vrijenhoek, R.C. (2001) Biogeography and ecological setting of Indian Ocean hydrothermal vents. *Science*, 294, 818–823. https://doi.org/10.1126/science.1064574

Watanabe, H., Fujikura, K., Kojima, S., Miyazaki, J.I. & Fujiwaram, Y. (2010) Japan: Vents and Seeps in Close Proximity. *In*: *The Vent and Seep Biota. Topics in Geobiology. Vol. 33*. Springer, Dordrecht, pp. 379–401. https://doi.org/10.1007/978-90-481-9572-5_12

Webb, M. (1969) *Lamellibrachia barhami*, gen. nov., sp. nov. (Pogonophora), from the Northeast Pacific. *Bulletin of Marine Science*, 19, 18–47.

Worsaae, K., Rimskaya-Korsakova, N.N. & Rouse, G.W. (2016) Neural reconstruction of bone-eating *Osedax* spp. (Annelida) and evolution of the siboglinid nervous system. *BMC Evolutionary Biology*, 16, 1–23. https://doi.org/10.1186/s12862-016-0639-7

3.1 Acknowledgements

Chapter 3 in full, is a reprint of the material as it appears in *Zootaxa*. McCowin, Marina F. and Rouse, Greg W. (2018). A new *Lamellibrachia* species and confirmed range extension for *Lamellibrachia barhami* (Siboglinidae, Annelida) from Costa Rica methane seeps. *Zookeys* 4504(1): 1-22. The dissertation author was the primary investigator and author of this paper.

Chapter 4

A new record of *Lamellibrachia columna* (Siboglinidae, Annelida) from cold seeps off New Zealand, and an assessment of its presence in the western Pacific Ocean

Marina F. McCowin[1], Ashley A. Rowden[2] and Greg W. Rouse[1]

[1]Scripps Institution of Oceanography, University of California San Diego, USA; [2]The National Institute of Water and Atmospheric Research, Wellington, New Zealand

McCowin *et al. Marine Biodiversity Records* (2019) 12:10
https://doi.org/10.1186/s41200-019-0169-2

Marine Biodiversity Records

MARINE RECORD Open Access

A new record of *Lamellibrachia columna* (Siboglinidae, Annelida) from cold seeps off New Zealand, and an assessment of its presence in the western Pacific Ocean

Marina F. McCowin[1*], Ashley A. Rowden[2] and Greg W. Rouse[1]

Abstract

Lamellibrachia columna Southward was originally described from hydrothermal vents of the Lau Basin, between Fiji and Tonga. This study utilizes phylogenetic and morphological analyses to confirm the collection of *Lamellibrachia columna* from cold seeps on the Hikurangi Margin off New Zealand, thereby extending its geographic range southward by approximately 1900 km. We also propose, based on molecular evidence, that specimens previously reported from vents in the Nankai Trough, Japan and seeps off southern and eastern Japan are *L. columna*. Furthermore, we suggest that *Lamellibrachia sagami* Kobayashi et al. described from cold seeps off southern and eastern Japan is a junior synonym of *Lamellibrachia columna*. Our work confirms that *L. columna* is found at two types of chemosynthetic habitat over a wide geographic range in the western Pacific Ocean.

Keywords: Vestimentifera, Deep sea, Pacific Ocean, Phylogeny, Synonymy

Background

Members of Vestimentifera (originally introduced by Jones (1985), and now one of four informal lineages within Siboglinidae Caullery, 1914 [Hilário et al. 2011; Pleijel et al. 2009]) live in chemosynthetic environments such as hydrothermal vents (Bright and Lallier 2010; Jones 1980; Shank et al. 1998), cold seeps (Bright and Lallier 2010; Levin et al. 2012; Webb 1969), and whale falls (Bright and Lallier 2010; Feldman et al. 1998), where they subsist off endosymbiotic chemoautotrophic bacteria (Bright and Lallier 2010). *Lamellibrachia* Webb, 1969 is one of the few vestimentiferan genera with a broad geographic and habitat distribution, having been reported from seeps, vents, and whale bones in the Pacific, Atlantic, Caribbean, and Gulf of Mexico (Bright and Lallier 2010; Feldman et al. 1998; Kobayashi et al. 2015; Nishijima et al. 2010; Watanabe et al. 2010). Of the nine *Lamellibrachia* species described to date, *Lamellibrachia columna* Southward, 1991 was the first to be described from the southwestern Pacific, at 1870 m in an area of diffuse venting at the Lau Back-arc Basin (Southward 1991). Since its initial discovery, *L. columna* has been reported at diffuse vents from the southwestern Pacific back-arc basin at Lau from 1832 to 1914 m (Black et al. 1997; Kojima et al. 1997, 2001; Southward 1991; Southward et al. 2011) (Fig. 1). To date, *Lamellibrachia columna* is most easily differentiated from other *Lamellibrachia* species by its numbers of sheath and branchial lamellae (Southward 1991). Other diagnostic characteristics such as obturaculum dimensions and plaque size are quite variable and overlap with those of other *Lamellibrachia* species, making DNA data and phylogenetic analyses an important part of the identification process (Kobayashi et al. 2015; McCowin and Rouse 2018; Southward 1991; Southward et al. 2011). The Japanese samples identified as *Lamellibrachia* sp. L1 and *Lamellibrachia* sp. L2 (Kojima et al. 2001) were noted as being very close to a published sequence (Black et al. 1997) of *Lamellibrachia columna* from the type locality, with L2 as the sister taxon to *L. columna.* Kojima et al. (2001) even noted that "L1 and L2 might be conspecific with *L. columna*".

* Correspondence: marruda@ucsd.edu
[1]Scripps Institution of Oceanography, University of California San Diego, La Jolla, CA, USA
Full list of author information is available at the end of the article

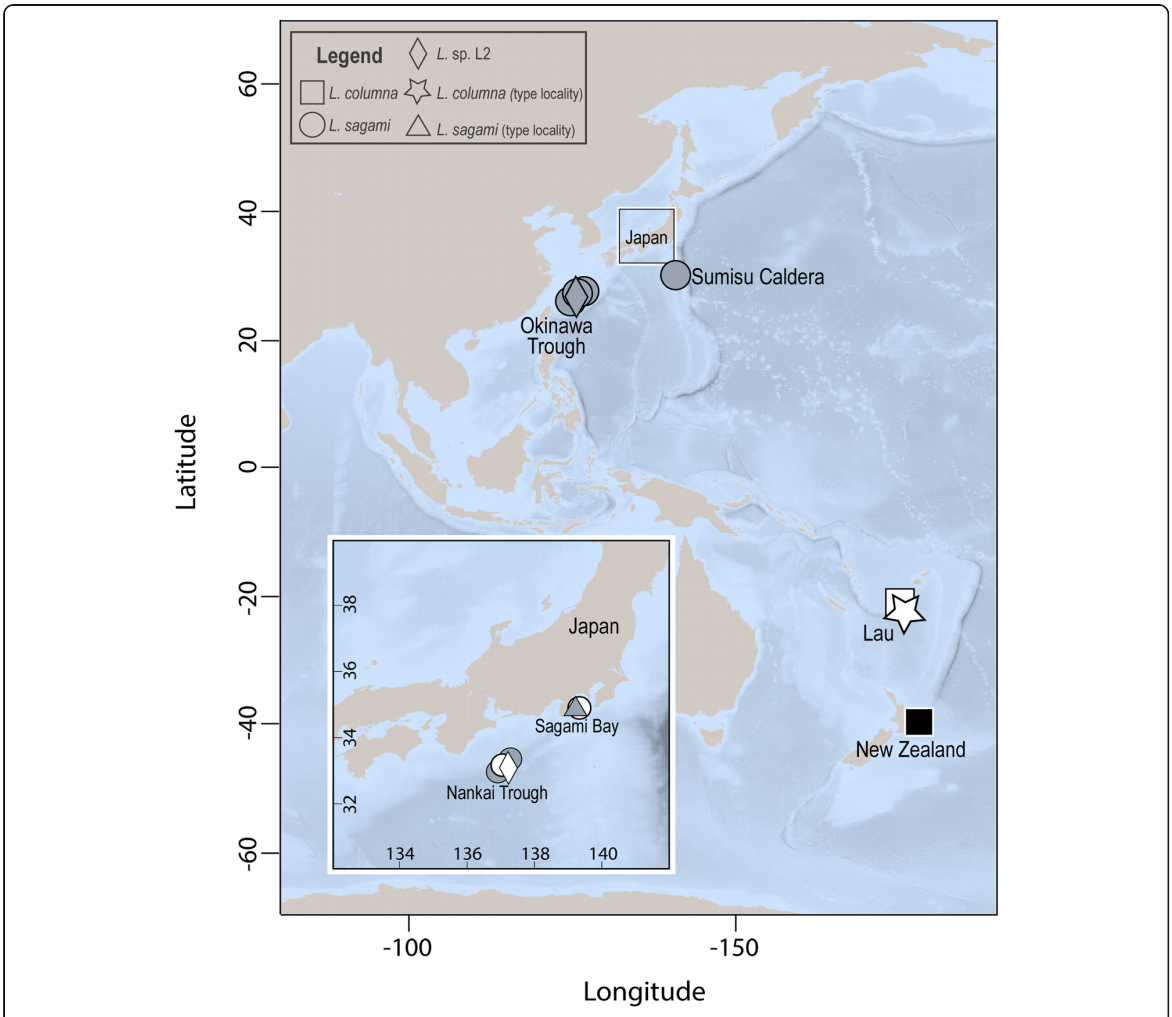

Fig. 1 Distribution of *Lamellibrachia columna* (Braby et al. 2007; Kojima et al. 2003; Kojima et al. 2001), *Lamellibrachia sagami* (Kobayashi et al. 2015; Kojima et al. 2003; Kojima et al. 2001), and *Lamellibrachia* sp. L2 (Kojima et al. 1997; Kojima et al. 2001). Squares represent *L. columna* localities, circles represent *L. sagami* localities, and diamonds represent *L.* sp. L2 localities. Symbols that are white represent localities with supporting molecular data, while symbols that are grey represent localities without molecular data. Black square represents the newly sampled *L. columna* with molecular data from this study. Star and triangle represent type localities for *L. columna* and *L. sagami*, respectively

The samples identified as *Lamellibrachia* sp. L1 in Kojima et al. 2001 were subsequently described as *Lamellibrachia sagami* Kobayashi et al 2015, with the type locality being a cold seep at 853 m in Sagami Bay, Japan. *Lamellibrachia sagami* was differentiated from other *Lamellibrachia* species by its sheath and branchial lamellae and the sizes of its vestimental and trunk plaques (Kobayashi et al. 2015). It has also been reported from other cold seeps along the eastern coast of Japan (Fig. 1) at depths of 290–2180 m (Kobayashi et al. 2015; Kojima et al. 2015; Kojima et al. 1997; Miura and Fujikura 2008). *Lamellibrachia sagami* has been found sympatrically with its close genetic relative *L.* sp. L2 (Kojima et al. 2001; Kojima et al. 1997) off the east coast of Japan at the Nankai Trough (Kobayashi et al. 2015; Kojima et al. 2003; Kojima et al. 2001; Kojima et al. 1997).

Here we report a new record of *Lamellibrachia columna* collected from cold seeps of the Hikurangi Margin off New Zealand. Phylogenetic and morphological analyses confirm the identification of specimens collected at this locality as *L. columna*, thereby extending its range southward by approximately 1900 km. We

explore other records of closely-related *Lamellibrachia* species from Japan, and discuss the resulting biogeographical implications for *Lamellibrachia columna*.

Methods

Samples (NIWA 27133) were loaned to Scripps Institution of Oceanography by New Zealand's National Institute of Water and Atmospheric Research (NIWA). These samples were from among other samples of unidentified *Lamellibrachia* specimens originally collected in 2006 from cold seeps off the east coast of the North Island of New Zealand (see Baco et al. 2010 and Bowden et al. 2013 for a full description of the habitat and locations where the tube worms were found, and their densities). The anterior and a portion of the trunk of the specimens examined here for DNA analysis, were originally fixed in 99% ethanol and later frozen (– 20 °C). These three specimens were collected from the Builder's Pencil seep site, between 810 and 817 m (NIWA 27133A, NIWA 27133B, SIO-BIC A9468). Whole specimens were photographed prior to preservation using a Nikon D70S with 90 mm Nikkor lens mounted on a fixed copy stand column. Ten plaques from the vestimentum and ten plaques from the trunk of each specimen were measured by cutting thin pieces of epidermis from the vestimentum and trunk and placing them on a glass slide with a 5% sodium hydroxide solution prior to observation. Analysis of morphological features of whole specimens was completed post-preservation and compared to morphological records of *L. columna* published by Southward (Southward 1991; Southward et al. 2011).

DNA was extracted from the vestimentum of the New Zealand specimens with the Zymo Research DNA-Tissue Miniprep kit, following the protocol supplied by the manufacturer. Approximately 1275 base pairs (bp) of mitochondrial cytochrome subunit I (COI) were amplified using the vestimentiferan *mtCOI* primer set COIf and COIr (Nelson and Fisher 2000) and up to 600 bp of 16S rRNA (16S) were amplified using the primer set 16SbrH and 16sArL (Palumbi 1996). Amplification was carried out in a thermal cycler (Eppendorf) with 12.5 µL Apex 2.0x RED DNA Polymerase Master Mix (Genesee Scientific), 1 µL each of the appropriate forward and reverse primers (10 µM), 8.5 µL water, and 2 µL eluted DNA. The vestimentiferan COI temperature profile was as follows: 95 °C/300 s – (94 °C/60s – 55 °C/60s – 72 °C/120 s) * 35 cycles – 72 °C/420 s. The 16S temperature profile was as follows: 95 °C/180 s – (95 °C/40s – 50 °C/40s – 72 °C/50s) * 35 cycles – 72 °C/300 s. The PCR products were purified with the ExoSAP-IT protocol (USB, Affymetrix), and sequencing was performed by Eurofins Genomics (Louisville, KY).

Alignments of the newly generated sequences and available sequence data from GenBank for COI and 16S (Table 1) published in the most recent siboglinid phylogenies (Black et al. 1997; Braby et al. 2007; Cowart et al. 2014; Kobayashi et al. 2015; Kojima et al. 2001; Li et al. 2017; Li et al. 2015; McCowin and Rouse 2018; McMullin et al. 2003; Miglietta et al. 2010; Sun et al. 2018), including sequences for *Lamellibrachia columna* from the type locality (Lau Back Arc Basin), were performed using MAFFT with default settings (Katoh and Standley 2013) and concatenated with SequenceMatrix v.1.6.7 (Gaurav et al. 2011). For species that showed very little variation in COI (*L. anaximandri, L.* cf. *luymesi*, *L. satsuma, L. barhami*), a single individual was chosen to represent each lineage in the phylogenetic analyses. *Lamellibrachia juni* also showed little intraspecific variation in COI, but multiple individuals were chosen to represent the lineage for comparison with the other analyses conducted in this study. This species has also been recorded in the closest geographic proximity to the species of *Lamellibrachia* examined here (i.e., hydrothermal vents of the Kermadec Arc, to the north of New Zealand – 524 km distant) (Miura and Kojima 2006). Maximum likelihood (ML) analyses were conducted on the concatenated dataset using RAxML v.8.2.19 (Stamatakis 2014) with each partition assigned the GTR + G + I model by the Akaike information criterion (AIC) in jModelTest 2 (Darriba et al. 2012; Guindon and Gascuel 2003). Node support was assessed via a thorough bootstrapping (1000 replicates). Bayesian Inference (BI) analyses were also conducted using MrBayes v.3.2.5 (Ronquist et al. 2012) with the same best-fit models assigned to their respective partitions. Maximum parsimony (MP) analyses were conducted using PAUP* v.4.0a (Swofford 2002), using heuristic searches with the tree-bisection-reconnection branch-swapping algorithm and 100 random addition replicates. Support values were determined using 100 bootstrap replicates. Uncorrected pairwise distances were calculated for the COI dataset (~ 1275 bp) with PAUP* v.4.0a (Swofford 2002). A model-corrected distance analysis for a reduced COI dataset containing the New Zealand specimens (NIWA 27133/SIO-BIC A9468), *L. columna, L.* sp. L2, and *L. sagami* (selection supported by all molecular analyses) was also conducted with the best-fit model, HKY (Hasegawa and Kishino 1985), selected via AIC in jModelTest 2. An additional model-corrected distance analysis (best-fit model HKY selected via AIC) was conducted for the *L. juni* COI dataset (all terminals available on GenBank) for comparison with the *L. columna/L.* sp. L2/*L. sagami* dataset. A haplotype network of the New Zealand specimens, *L. columna*, *L.* sp. L2, and *L. sagami* COI dataset was created with PopART v.1.7 (Bandelt et al. 1999) using the median-joining option and epsilon set at 0.

Table 1 Origin of sequenced terminals, vouchers, and GenBank accession numbers. New sequences are set in bold. *GM* Gulf of Mexico, *CR* Costa Rica, *NZ* New Zealand, *SP* South Pacific

Scientific Name	Origin	COI	16S	Voucher or Reference
Lamellibrachia anaximandri	Eastern Mediterranean	EU046616	HM746782	SMH-2007a
Lamellibrachia barhami	Jaco Scar, CR	MH670766–92	MH660399	SIO-BIC A8343
Lamellibrachia columna	Lau Back Arc Basin	U74061	–	Black et al. 1997
Lamellibrachia columna	Lau Back Arc Basin	DQ996645	FJ347646	Braby et al. 2007, Vrijenhoek et al. 2009
Lamellibrachia columna	**Hikurangi Margin, NZ**	**MK496532-34**	**MK93453-55**	**SIO-BIC A9468, NIWA 27133A, NIWA 27133B**
Lamellibrachia sp. L2	Nankai Trough, Japan	D50592	–	Kojima et al. 1997
Lamellibrachia donwalshi sp. nov.	Mound 12, CR	MH670827	MH664918	SIO-BIC A8382
Lamellibrachia juni 1	TOTO Caldera, Mariana Arc	AB264601	–	Kojima et al. 2006
Lamellibrachia juni 2	Manus Basin, SP	AB264602	–	Kojima et al. 2003
Lamellibrachia juni 3	Manus Basin, SP	AB264603	–	Kojima et al. 2006
Lamellibrachia juni 4	Brothers Caldera, Kermadec Arc, NZ	AB264604	–	Miura and Kojima 2006
Lamellibrachia juni 7	Manus Basin, SP	AB088675	–	Kojima et al. 2003
Lamellibrachia cf. *luymesi*	Green Canyon, GM	GU059225	GU068209	Miglietta et al. 2010
Lamellibrachia sagami	Sagami Bay, Japan	LC064365	–	JAMSTEC 1140043315
Lamellibrachia sagami (*L.* sp. L1)	Nankai Trough, Japan	D38029	–	JAMSTEC 1150054786
Lamellibrachia satsuma	Kagoshima Bay, Japan	KP987801	KP987801	Patra et al. 2016
Lamellibrachia sp. 1	GM	GU059165–66, GU059169, GU059227, GU059237	GU068253–54, GU068257, GU068212, GU068227	Miglietta et al. 2010
Lamellibrachia sp. 2	GM	GU059173, GU059175–77	GU068265, GU068269	Miglietta et al. 2010
Riftia pachyptila	East Pacific Rise	KJ789166	KJ789166	Li et al. 2015

Results

The ML, BI, and MP analyses (Fig. 2) were congruent, with strong support for the inclusion of the *Lamellibrachia* specimens from New Zealand within *L. columna*. An uncorrected pairwise distance analysis and an HKY-corrected distance analysis based on COI sequences showed a maximum distance of 0.50% between the *L. columna* specimens from the type locality and *L. columna* specimens from New Zealand (Table 2). The haplotype network revealed a two-base-pair divergence between the same samples (Fig. 3). Morphological analyses of the *L. columna* specimens from New Zealand revealed (Table 3) that all characteristics except the obturaculum and plaque dimensions fell within or near the expected range for *L. columna* established by Southward 1991. The number of sheath lamellae ranged from 14 to 16 (expected range 8–16 [Southward 1991]), while the number of branchial lamellae ranged from 20 to 22 (expected 21 [Southward 1991]) for each specimen. The obturaculum lengths ranged from 7 to 13 mm (expected range 15–42 mm [Southward 1991]), while obturaculum widths ranged from 5 to 8 mm (expected range 8–13 mm [Southward 1991]). The diameters of the vestimental plaques ranged from 59 to 60 μm (expected range 65–90 μm [Southward et al. 2011]), and the diameters of the trunk plaques ranged from 67 to 75 μm (expected range 70–120 μm [Southward et al. 2011]).

The phylogenetic tree also showed strong support for referring *Lamellibrachia* sp. L2 as *L. columna*. There was a maximum uncorrected distance of 0.33% in COI sequences between the *L. columna* specimens from the type locality and *L.* sp. L2 (Table 2). In addition, an HKY-corrected distance analysis based on COI sequences showed a maximum distance of 0.5% between the *L.* sp. L2 specimens from Japan and the specimens from New Zealand. The haplotype network also revealed

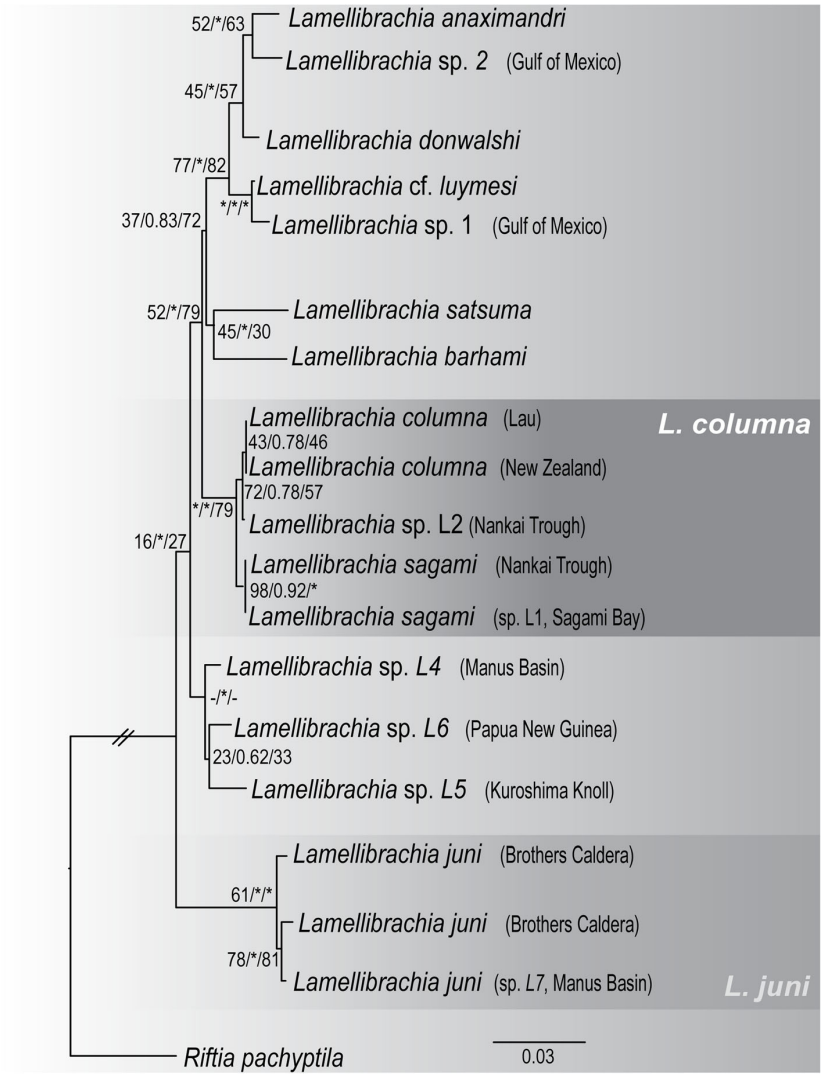

Fig. 2 Maximum likelihood trees of the combined analysis from two mitochondrial genes (16S, COI) aligned with MAFFT and then concatenated (rooted with *Riftia pachyptila*). Bootstrap support percentages from Maximum Likelihood and Maximum Parsimony analyses (separated by slashes) are followed by Bayesian posterior probabilities. Support values of 95%/0.95 or greater for each analysis are indicated by asterisks. Nodes not recovered in one of the analyses are indicated by a hyphen

minimal divergence between *L.* sp. L2 and *L. columna*. *Lamellibrachia* sp. L2 was found to differ by only two base pairs from *L. columna* (from the type locality) and shared a haplotype with the New Zealand specimens (Fig. 3).

The phylogenetic tree and both distance analyses also revealed a close relationship between *Lamellibrachia columna* and *L. sagami* (Fig. 2, Table 2). Both the uncorrected and corrected analyses based on COI sequences revealed a minimum distance of 0.95–0.98% between *L. sagami* and the *L. columna* from the type locality, 0.67–0.69% between *L. sagami* and the *L. columna* from New Zealand, and 0.64% between *L. sagami* and the *L.* sp. L2 from Japan. The HKY-corrected analysis showed a maximum distance of 1.35% between *L. sagami* and *L. columna* from their respective type localities, 0.99% between *L. sagami* and *L.* sp. L2, and 1.24% between *L. sagami* and *L. columna* from New Zealand. An HKY-corrected analysis of *L. juni* Miura and Kojima, 2006 (Miura and Kojima 2006) generated for comparison

Table 2. Uncorrected pairwise distances for COI data (all *L. columna* and *L. sagami* terminals included, non-identical *L. juni* terminals included, duplicates of other species removed), generated with PAUP*. *SB* Sagami Bay, *NT* Nankai Trough, *MA* Mariana Arc, *MB* Manus Basin, *NZ* New Zealand. Terminals comparing *L. columna*, *L. sagami*, and *L.* sp. L2 are set in bold.

	L. juni 1 (MA)	*L. juni* 2 (MB)	*L. juni* 3 (MB)	*L. juni* 4 (NZ)	*L. juni* 7 (MB)	*L.* sp. *L4*	*L.* sp. *L5*	*L.* sp. *L6*	*L. sa-gami* (SB)	*L. sa-gami* (NT)	*L. columna* (Lau 1)	*L. columna* (Lau 2)	*L.* sp. L2 (NT)	*L. columna* (NZ 1)	*L. columna* (NZ 2)	*L. columna* (NZ 3)	*L. satsuma*	*L. barhami*	*L.* cf. *luy-mesi*	*L.* sp. 1	*L.* sp. 2	*L. donwalshi*
L. juni 2 (MB)	1.18																					
L. juni 3 (MB)	1.38	0.39																				
L. juni 4 (NZ)	1.38	0.89	1.08																			
L. juni 7 (MB)	1.09	0.00	0.00	0.79	–	–	–	–	–	–	–	–	–	–	–	–	–	–	–	–	–	–
L. sp. *L4*	6.68	6.48	6.68	6.29	6.33	–	–	–	–	–	–	–	–	–	–	–	–	–	–	–	–	–
L. sp. *L5*	6.78	6.97	6.98	6.78	6.73	2.62	–	–	–	–	–	–	–	–	–	–	–	–	–	–	–	–
L. sp. *L6*	7.10	6.89	6.70	6.98	6.54	1.85	2.83	–	–	–	–	–	–	–	–	–	–	–	–	–	–	–
L. sagami (SB)	7.13	6.81	6.81	6.82	6.49	4.13	4.31	4.00	–	–	–	–	–	–	–	–	–	–	–	–	–	–
L. sagami (NT)	7.60	7.40	7.50	7.20	7.23	4.10	4.49	4.60	0.00	–	–	–	–	–	–	–	–	–	–	–	–	–
L. columna (Lau 1)	7.78	7.57	7.67	7.36	7.45	4.66	4.95	4.75	**0.98**	**1.33**	–	–	–	–	–	–	–	–	–	–	–	–
L. columna (Lau 2)	7.15	6.83	6.83	6.84	6.52	4.05	4.37	3.60	**0.95**	**0.78**	**0.00**	–	–	–	–	–	–	–	–	–	–	–
L. sp. L2 (NT)	7.49	7.29	7.39	7.09	7.13	4.09	4.29	4.40	**0.64**	**0.98**	**0.33**	**0.31**	–	–	–	–	–	–	–	–	–	–
L. columna (NZ 1)	7.61	7.41	7.51	7.21	7.31	4.21	4.60	4.51	**0.67**	**1.21**	**0.50**	**0.33**	**0.20**	–	–	–	–	–	–	–	–	–
L. columna (NZ 2)	7.65	7.46	7.56	7.25	7.35	4.23	4.62	4.54	**0.68**	**1.22**	**0.50**	**0.34**	**0.20**	**0.00**	–	–	–	–	–	–	–	–
L. columna (NZ 3)	7.68	7.48	7.58	7.28	7.38	4.25	4.64	4.55	**0.69**	**1.22**	**0.49**	**0.34**	**0.20**	**0.00**	**0.00**	–	–	–	–	–	–	–
L. satsuma	8.27	8.18	8.48	8.08	8.10	5.69	5.87	5.69	5.51	6.18	6.15	5.44	5.89	5.80	5.77	5.85	–	–	–	–	–	–
L. barhami	7.32	7.32	7.54	7.54	7.23	5.09	5.30	5.52	4.99	5.34	5.68	4.87	5.32	5.52	5.53	5.54	6.06	–	–	–	–	–
L. cf. *luymesi*	7.36	7.36	7.46	7.36	7.19	4.09	4.47	4.28	4.14	4.11	4.28	3.83	3.79	3.66	3.70	3.69	5.12	6.27	–	–	–	–
L. sp. 1 (GoM)	8.16	7.86	7.86	7.87	7.54	5.16	4.71	4.71	4.49	4.43	4.92	4.19	4.29	4.32	4.36	4.38	5.94	5.93	1.01	–	–	–
L. sp. 2 (GoM)	8.26	7.24	7.42	7.59	7.10	5.05	5.21	5.07	4.45	4.43	4.60	4.38	4.60	4.59	4.59	4.59	6.12	4.55	3.36	3.38	–	–
L. donwalshi	7.67	7.04	7.25	7.57	6.95	4.42	4.72	4.53	4.34	4.46	4.68	3.88	4.21	4.19	4.19	4.20	6.25	5.42	2.85	3.59	2.37	–
L. anaxi-mandri	8.24	7.78	7.79	7.64	7.59	5.18	4.28	4.74	4.56	4.60	5.23	4.50	4.77	4.58	4.64	4.65	6.18	5.52	2.87	2.50	2.71	2.49

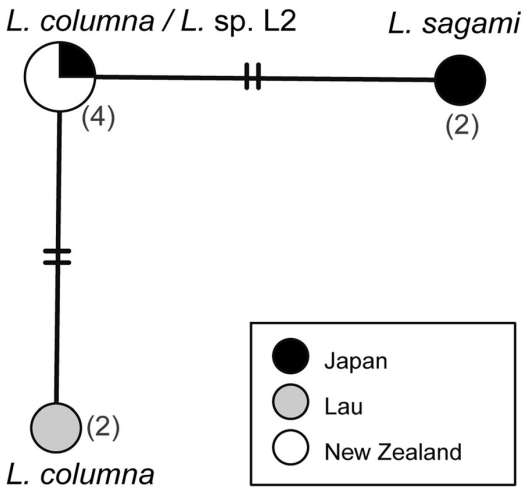

Fig. 3 Haplotype network from COI data for *Lamellibrachia columna*, *L.* sp. L2, and *Lamellibrachia sagami* sampled from New Zealand to Japan. Numbers in parentheses next to each haplotype represent the number of specimens with that haplotype

revealed a maximum distance of 1.39% among *L. juni* specimens from various localities. The minimum uncorrected COI distance between *L. juni* from the Kermadec Arc, New Zealand and the New Zealand *L. columna* specimens was 7.28%. Haplotype networks generated for the COI data from *L. columna* (type locality), the New Zealand specimens, *L.* sp. L2, and *L. sagami* (Fig. 3) showed minimal divergence between specimens (at most two base pairs between haplotypes).

The morphological characteristics of *Lamellibrachia sagami* also fall within or very close to the accepted range for *L. columna* (Kobayashi et al. 2015; Southward 1991; Southward et al. 2011) and exhibited by the New Zealand *L. columna* specimens, including obturaculum length (*L. sagami* measures 5.8–22.5 mm [Kobayashi et al. 2015]), obturaculum width (4.4–10.8 mm [Kobayashi et al. 2015]), number of branchial lamellae (19–26 [Kobayashi et al. 2015]), and vestimental and trunk plaque diameters (59–101 μm and 67–130 μm, respectively [Kobayashi et al. 2015]), Table 3. The number of sheath lamellae is the only characteristic that is not partially or completely shared by *L. sagami* and *L. columna* (ranges of sheath lamellae reported are 3–6 for *L. sagami* [Kobayashi et al. 2015] and 8–16 for *L. columna* [Southward 1991]).

Discussion

All phylogenetic analyses (Figs. 2 and 3) clearly support the inclusion of the specimens collected off New Zealand within *Lamellibrachia columna*. The minimal base pair differences shown in the haplotype networks (Fig. 3), and the low pairwise distances (corrected and uncorrected) between sequences from *L. columna* and the New Zealand specimens provide strong support for this result. Morphological measurements of the New Zealand specimens fell within or very close to the accepted ranges for diagnostic characters of *L. columna* (Southward 1991; Southward et al. 2011). This morphological similarity can be seen clearly when comparing specimens from New Zealand and Lau in Table 3 and Fig. 4. However, the measurements made of the obturaculum for the New Zealand specimens do show a slight reduction from the previous ranges recorded for this species of 15–42 mm length and 8–13 mm width (Southward 1991; Southward et al. 2011). The New Zealand specimens were below this range (7–13 mm length, 5–8 mm width) and also exhibited some variation in number of branchial lamellae, which has not been previously reported for this species. However, phenotypic plasticity is common in other Vestimentifera, such as *Ridgeia* Jones, 1985 (Southward et al. 1995), and has often been a source of past confusion in differentiation of vestimentiferan species (e.g., *Ridgeia piscesae* Jones, 1985 and its junior synonym *R. phaeophiale* Jones 1985, which exhibited stark morphological differences but no genetic differentiation [Southward et al. 1995]). Furthermore, Southward et al. (1995) suggested that phenotypic plasticity within vestimentiferan species may be a response to physical variation in their environment, and recounted major variation in tubes and various size measurements of *R. piscesae* with environmental differences (Southward et al. 1995).

Table 3 Morphological characters of *Lamellibrachia columna* and *Lamellibrachia sagami*. *OL* Obturaculum length, *OW* Obturaculum width, *BL* Number of branchial lamellae, *SL* Number of sheath lamellae, *VP* diameter of vestimental plaques, *TP* diameter of trunk plaque

Taxon	n	OL (mm)	OW (mm)	BL	SL	VP (μm)	TP (μm)	Reference
Lamellibrachia columna	13	15–42	8–13	21	8–16	65–90	70–120	Southward 1991, Southward et al. 2011
Lamellibrachia columna (New Zealand)	3	7–13	5–8	20–22	14–16	59–60	67–75	This study
Lamellibrachia sagami (holotype, Sagami Bay)	1	15.7	10.5	25	5	67–81	91–102	Kobayashi et al. 2015
Lamellibrachia sagami (paratypes, Sagami Bay)	17	5.8–22.5	4.4–10.8	19-26	3–6	59–101	67–130	Kobayashi et al. 2015
Lamellibrachia sagami (Nankai Trough)	1	10.2	6.8	23	5	58–67	70–104	Kobayashi et al. 2015

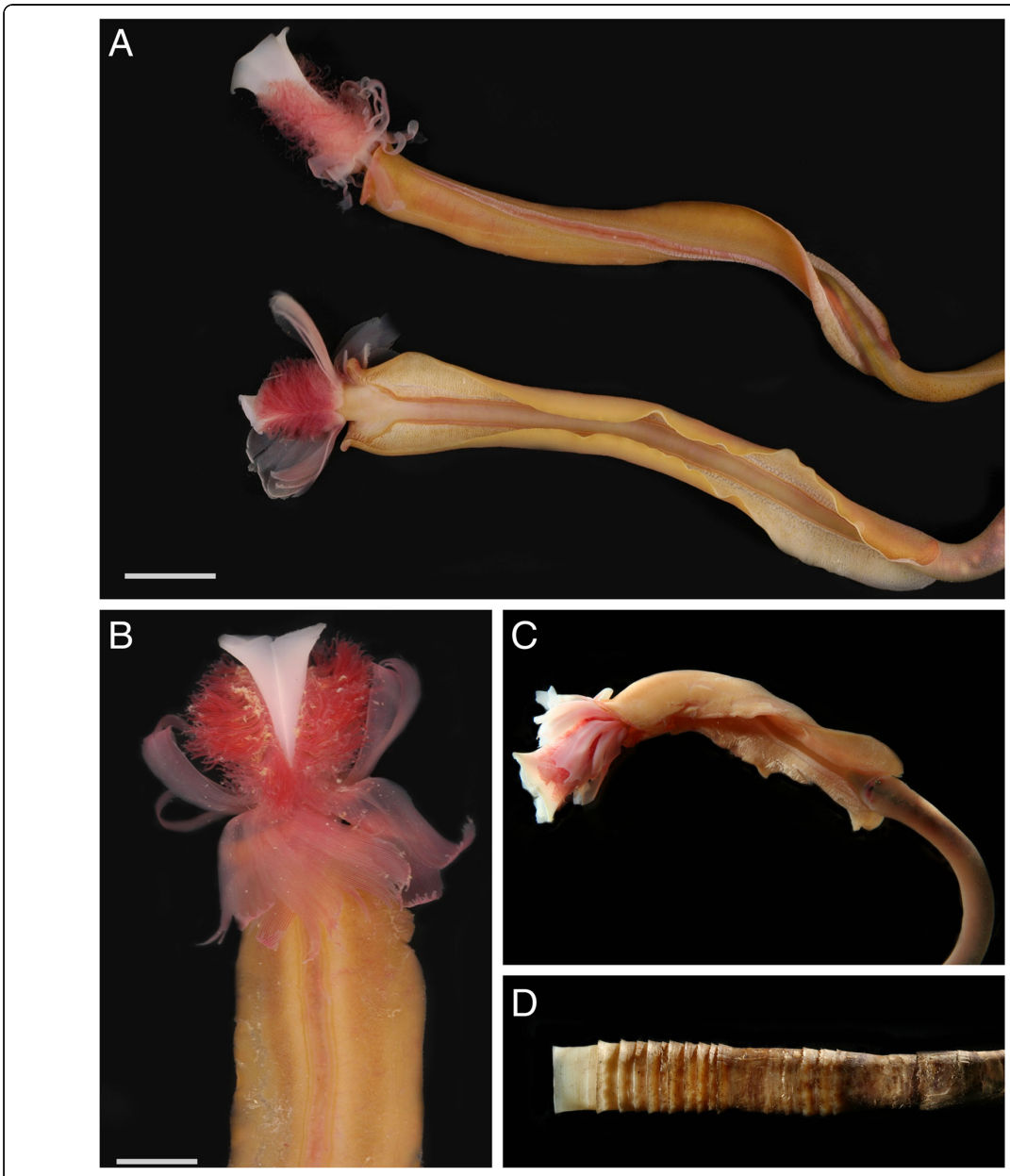

Fig. 4 In situ photographs of *Lamellibrachia columna* (New Zealand NIWA 27133/SIO-BIC A9468 and Lau specimens). **a** Ventral (top) and dorsal (bottom) anterior of two *L. columna* specimens (New Zealand, NIWA 27133/SIO-BIC A9468), scale bar represents 10 mm. **b** Ventral anterior of *L. columna* (New Zealand, NIWA 27133/SIO-BIC A9468), scale bar represents 5 mm. **c** Dorsal anterior of *L. columna* (Lau [Vrijenhoek et al. 2009]). **d** *L. columna* tube anterior (Lau [Vrijenhoek et al. 2009])

Phenotypic plasticity is clearly present within *Lamellibrachia* as well, as is made apparent by the already wide ranges of morphological characters previously established for various *Lamellibrachia* species (Gardiner and Hourdez 2003; Jones 1985; Kobayashi et al. 2015; McCowin and Rouse 2018; Miura et al. 1997; Miura and Kojima 2006; Southward 1991; Webb 1969). Thus, a slight widening of the range for a few morphological traits of *L. columna* is not surprising. We therefore designate the New Zealand *Lamellibrachia* specimens

as *L. columna,* which will extend the geographic range of *L. columna* southward by approximately 1900 km and the depth range of *L. columna* by approximately 1000 m (for a new depth range of 810–1914 m).

All phylogenetic analyses also supported the inclusion of *Lamellibrachia* sp. L2 within *L. columna* (Fig. 2). The phylogenetic tree (Fig. 2) shows a very short branch length between *L. columna* and *L.* sp. L2 that is comparable to the branch lengths within *L. juni* (Kojima et al. 2003; Kojima et al. 2001). The haplotype network (Fig. 3) and distance analyses (Table 2) also clearly show that there are few genetic differences between *L. columna* from the type locality and *L.* sp. L2. This similarity has been noted before by Kojima et al. (2001). It was reported in that study that the genetic distance between *L. columna* and *L.* sp. L2 was approximately 0.3% (Kojima et al. 2001), which is consistent with the uncorrected distances calculated in this study (Table 2). Based on the previously accepted variation within the *L. juni* clade (Kojima et al. 2003; Kojima et al. 2001) represented numerically by the small corrected and uncorrected pairwise distances of up to 1.39% between *L. juni* specimens from various localities (Table 2), *L.* sp. L2 should be considered conspecific with *L. columna*, as it exhibits similarly minute corrected and uncorrected pairwise distances (0.31–0.34%, Table 2) from *L. columna* specimens from the type locality. There is no morphological data published for *L.* sp. L2 (Kojima et al. 2003; Kojima 2002; Kojima et al. 2001), but the molecular evidence overwhelmingly supports the referral of *L.* sp. L2 sequences to *L. columna*. This will extend the depth range of *L. columna* to 3270 m (Kojima et al. 2001; Kojima et al. 1997) and its geographic range to southeastern Japan. As a result, *L. columna* will represent the most broadly distributed *Lamellibrachia* species to date, with a geographic range spanning approximately 9000 km from the coast of New Zealand to the coast of Japan and a depth range of 810–3270 m. This range extension will also result in the putative geographic sympatry of *L. columna* and *L. sagami*, since both *L.* sp. L2 and *L. sagami* have been sampled from the Nankai Trough (Kobayashi et al. 2015; Kojima et al. 2001).

Our results (Fig. 2), and those previously published (Kojima et al. 2001), showed high support for the close sister relationship between *L. sagami* and *L. columna*/*L.* sp. L2. This topology is reminiscent of the level of variation within the *L. juni* clade, which has a similar topology, suggesting that the *L. sagami/L. columna/L.* sp. L2 clade should also represent a single species. The uncorrected and corrected pairwise distances between *L. sagami* and *L. columna* provide additional support for this potential revision. The maximum HKY-corrected distance was 1.35% between *L. columna* and *L. sagami* from their respective type localities, 0.99% between the sympatric *L.* sp. L2 (*L. columna*) and *L. sagami* sequences, and 1.24% between *L. sagami* from Japan and *L. columna* from New Zealand (all uncorrected distances were smaller, Table 2). The small distances between *L. columna* and *L. sagami* and *L.* sp. L2 (*L. columna*) recovered in this study have been previously noted, and *L. sagami* (called "*L.* sp. L1" prior to its formal description in 2015) and *L.* sp. L2 (now *L. columna*) were reported as potentially "conspecific with *L. columna"* due to their small genetic distances (0.5–1.1%) from *L. columna* (Kojima et al. 2001). Other *Lamellibrachia* species in Japan and New Zealand that are geographically close to or sympatric with *L. columna* and *L. sagami*, such as *L. juni* and *L. satsuma*, are clearly genetically distinct, with uncorrected distances ranging between 5.44 and 8.48% (Table 2). The distance between *L. sagami* and *L. columna* is comparable to distances calculated within the single species *L. juni* (0–1.38% uncorrected, 0–1.39% HKY-corrected). The haplotype network (Fig. 3) of *L. sagami, L. columna*, and *L.* sp. L2 provides a visual representation of this close relationship (two base-pair distances between haplotypes) which also supports their synonymy. The referral of *L.* sp. L2 to *L. columna* in this paper also results in the sympatry of *L. columna* and *L. sagami* off the eastern coast of Japan, with records from each at the Nankai Trough (Kobayashi et al. 2015; Kojima et al. 2001, 2003; Southward 1991; Southward et al. 2011). The morphological data also reveals similarities between *L. sagami* and *L. columna*. Nearly all of the morphological characters of *L. sagami* (obturaculum length and width, plaque diameters, branchial lamellae) closely overlap with the ranges accepted for *L. columna* (Kobayashi et al. 2015; Southward 1991; Southward et al. 2011) (Table 3), except for the number of sheath lamellae, which falls in a smaller range for *L. sagami* (3-6 [Kobayashi et al. 2015]) than for *L. columna* (8–16 [Southward et al. 2011; Southward 1991]). As was made evident by Southward et al. (Southward et al. 1995), phenotypic plasticity is not uncommon in Vestimentifera and has resulted in past confusion regarding species descriptions based heavily on morphology. The molecular analyses, morphological analyses, and geographic sympatry support the synonymy of *L. sagami* with *L. columna.* Past studies have shown low levels of variation in the mitochondrial genes 16S and COI in Vestimentifera (Cowart et al. 2014; Cowart et al. 2013; McMullin et al. 2003), so further genetic data is required to elucidate more detailed patterns of gene flow in widely distributed species like *L. columna*. However, present evidence, especially the small number of base pair variations and the distance comparison with *L. juni* and other *Lamellibrachia* species, justifies the synonymy of *L. sagami* with *L. columna*. We synonymize the two here and amend the diagnosis of *L. columna* to include the additional

morphological variation represented by its junior synonym *L. sagami* (see below).

Biogeographies of hydrothermal vent fauna indicate that vent fauna of the western Pacific are generally distinct from those of the eastern Pacific (Van Dover et al. 2002; Moalic et al. 2012), but also indicate various levels of latitudinal sub-division among the vent fauna of the western Pacific (Bachraty et al. 2009; Rogers et al. 2012). These sub-divisions presumably represent evolutionary and modern-day processes that influence population connectivity (Mitarai et al. 2016), and while our finding of a high degree of relatedness among *Lamellibrachia columna* from off Japan and New Zealand does not refute the proposed sub-divisions of the overall vent faunal assemblages of the western Pacific, it provides an interesting example of at least one species of chemosynthetic environments that maintains a population across almost the entire latitudinal range of the region. Our study now confirms that *L. columna* is found at both vents and cold seep habitats, and that at the southernmost extent of its range off New Zealand it occurs at seeps, but apparently does not occur at vents off New Zealand. It is possible that environmental conditions at vent sites off New Zealand are not suitable for *L. columna*, where L. *juni* is found (Miura and Kojima 2006), or that the species is yet to be discovered at these sites. Whatever the reason may be for the apparent lack of *L. columna* at vents off New Zealand, our finding of the species at seeps is useful in terms of documenting the extent of the habitat flexibility of *Lamellibrachia*, and for developing a biogeography of cold seep fauna which is much less well-understood than for vent fauna.

Taxonomy

Siboglinidae Caullery, 1914.

Lamellibrachia Webb, 1969.

Lamellibrachia columna Southward, 1991

Lamellibrachia sp. L1 (Sagami Bay, Nankai Trough): Kojima et al. 1997 (*L.* sp. La1-4, Lc1-4, Ld1, Ld2-3, Ld4), p. 509; Kojima et al. 2001, p. 211; Kojima 2002, p. 57; Kojima et al. 2003, p. 625; Kojima et al. 2006, p. 1357; Miura and Kojima 2006, p. 209; Miura and Fujikura 2008, p. 57; Miura and Fujikura 2008, p. 153, Fig. 9.3 A–C.

Lamellibrachia sp. L2 (Nankai Trough): Kojima et al. 1997 (*L.* sp. Le1, Le2), p. 509; Kojima et al. 2001, p. 213; Kojima 2002, p. 346; Kojima et al. 2003, p. 631.

Lamellibrachia sagami **new synonym** (Sagami Bay): Kobayashi et al. 2015, p. 99. Figs. 2-5.

Material examined: Three specimens were collected from the Builder's Pencil seep site off the east coast of the North Island of New Zealand, between 810 and 817 m, using an epibenthic sled (Station TAN0616/32; 39° 32.4′ S, 178° 20.4′ W). Two of these specimens are deposited at NIWA (NIWA 27133A, NIWA 27133B), and one specimen is deposited at the Scripps Institution of Oceanography Benthic Invertebrates Collection (SIO-BIC A9468).

Diagnosis (emended): The obturaculum width ranges from 4.4–13 mm (Kobayashi et al. 2015; Southward 1991) and its length ranges from 5.8–42 mm; it is surrounded by the branchial plume (1,8), Fig. 4a–c. There are 19–26 pairs of branchial lamellae surrounding the obturaculum (Kobayashi et al. 2015; Southward 1991). There are 3–16 pairs of sheath lamellae which enclose the crown region and vary in size but are all shorter than the obturaculum, Fig. 4a–c. The smallest lamellae are near the mid-ventral line (Kobayashi et al. 2015; Southward 1991). The anterior edge of the vestimentum forms a collar with a central split (Kobayashi et al. 2015; Southward 1991). Paired dorsal ciliated genital grooves with epidermal folds occur in males (Fig. 4a, c), while females lack epidermal folds and grooves appear less obvious (Kobayashi et al. 2015; Southward 1991). Tubes are fairly straight and smooth, with an anterior diameter ranging from 14 to 20 mm (Southward 1991) (Fig. 4d). Vestimental plaques range in diameter from 58 to 101 μm, while trunk plaques range from 67 to 130 μm in diameter.

Distribution: *Lamellibrachia columna* is known from vents at the Lau Back-arc basin (Black et al. 1997; Braby et al. 2007; Southward 1991), vents and seeps along the middle Honshu coast of Japan (including, but not limited to, the Sagami Bay, Nankai Trough, and Okinawa Trough) (Kobayashi et al. 2015; Kojima et al. 2001; Kojima et al. 1997), and seeps on the Hikurangi margin east of New Zealand, at depths between 270 and 3270 m (Baco et al. 2010; Black et al. 1997; Bowden et al. 2013; Braby et al. 2007; Kobayashi et al. 2015; Kojima et al. 1997, 2001; Southward 1991).

Remarks: Southward's 1991 diagnosis of *Lamellibrachia columna* has been amended to accommodate the inclusion of specimens from New Zealand (NIWA 27133, SIO-BIC A9468), Japan (*L.* sp. L2), and its new junior synonym *L. sagami*. Phylogenetic and morphological evidence suggests that *L. columna* exhibits wider ranges of lamellae counts, plaque diameters, and obturaculum sizes than previously reported.

Acknowledgements

We would like to thank Sadie Mills and Caroline Chin (NIWA) for their curation of the samples, and for sending preserved samples to SIO, and David Bowden (NIWA) and Fredrik Pleijel (University of Gothenburg) for providing photographs of *L. columna* specimens from New Zealand and Lau, respectively. We would also like to thank the crew and scientific party of the RENEWZ I voyage (TAN0616) made using the *R/V Tangaroa*. Amy Baco

(Florida State University) helpfully provided the results of her preliminary genetic investigation of *Lamellibrachia* samples from the New Zealand cold seeps.

Authors' contributions
GWR, AR conceived the paper. AR provided specimens from New Zealand, collection data, and input regarding the manuscript. MM performed DNA extraction and amplification and morphological examination of New Zealand specimens, conducted the molecular and phylogenetic analyses, generated the figures and drafted the manuscript. GWR, AR, and MM then finalized the manuscript. All authors read and approved the final manuscript.

Funding
US National Science Foundation (NSF OCE-1634172); NOAA Ocean Exploration. Grants #NA05OAR4171076 and #NA17RJ1231/58; NIWA Science Capability Development Fund projects CRFH073 and CDSB1601.

Availability of data and materials
Sequence data generated and/or analyzed during this study are available on GenBank (accession numbers provided in Table 1) (Benson et al. 2005).

Ethics approval and consent to participate
Not applicable.

Consent for publication
Not applicable.

Competing interests
The authors declare that they have no competing interests.

Author details
[1]Scripps Institution of Oceanography, University of California San Diego, La Jolla, CA, USA. [2]The National Institute of Water and Atmospheric Research, Wellington, New Zealand.

Received: 8 February 2019 Accepted: 19 May 2019
Published online: 18 June 2019

References

Bachraty C, Legendre P, Desbruyères D. Biogeographic relationships among deep-sea hydrothermal vent faunas at global scale. Deep Res Part I Oceanogr Res Pap. 2009;56:1371–8.
Baco AR, Rowden AA, Levin LA, Smith CR, Bowden DA. Initial characterization of cold seep faunal communities on the New Zealand Hikurangi margin. Mar Geol. 2010;272(1–4):251–9Available from. https://doi.org/10.1016/j.margeo.2009.06.015.
Bandelt H, Forster P, Röhl A. Median-joining networks for inferring intraspecific phylogenies. Mol Biol Evol. 1999;16(1):37–48.
Benson DA, Karsch-mizrachi I, Lipman DJ, Ostell J, Wheeler DL. GenBank. 2005;33:D34–8.
Black MB, Halanych KM, Maas PAY, Hoeh WR, Hashimoto J, Desbruyères D, et al. Molecular systematics of vestimentiferan tubeworms from hydrothermal vents and cold-water seeps. Mar Biol. 1997;130:141–9.
Bowden DA, Rowden AA, Thurber AR, Baco AR, Levin LA, Smith CR. Cold seep Epifaunal communities on the Hikurangi margin, New Zealand: composition, succession, and vulnerability to human activities. PLoS One. 2013;8(10):20.
Braby CE, Rouse GW, Johnson SB, Jones WJ, Vrijenhoek RC. Bathymetric and temporal variation among *Osedax* boneworms and associated megafauna on whale-falls in Monterey Bay, California. Deep Res I. 2007;54(10):1773–91.
Bright M, Lallier F. The biology of Vestimentiferan tubeworms. Oceanogr Mar Biol An Annu Rev [Internet]. 2010;48:213–65 Available from: https://doi.org/10.1201/EBK1439821169-c4.
Caullery M. Sur les Siboglinidae, type nouveau d'invertébrés receuillis par l'expédition du Siboga. C R Hebd Seances Acad Sci. 1914;158:2014–7.
Cowart DA, Halanych KM, Schaeffer SW, Fisher CR. Depth-dependent gene flow in Gulf of Mexico cold seep *Lamellibrachia* tubeworms (Annelida, Siboglinidae). Hydrobiologia. 2014;736:139–54.
Cowart DA, Huang C, Arnaud-Haond S, Carney SL, Fisher CR, Schaeffer SW. Restriction to large-scale gene flow vs. regional panmixia among cold seep *Escarpia* spp. (Polychaeta, Siboglinidae). Mol Ecol. 2013;22:4147–62.
Darriba D, Taboada GL, Doallo R, Posada D. jModelTest 2: more models, new heuristics and parallel computing. Nat Methods. 2012;9(8):772 Available from: http://www.nature.com/articles/nmeth.2109.
Van Dover CL, German CR, Speer KG, Parson LM, Vrijenhoek RC. Evolution and biogeography of Deep-Sea vent and seep invertebrates. Science (80-). 2002;295(2002):1253–7.
Feldman RA, Shank TM, Black MB, Baco AR, Smith CR, Vrijenhoek RC. Vestimentiferan on a whale fall. Biol Bull. 1998;194(2):116–9 Available from: https://www.jstor.org/stable/1543041.
Gardiner SL, Hourdez S. On the occurrence of the vestimentiferan tube worm *Lamellibrachia luymesi* van der land and Norrevang, 1975 (Annelida: Pogonophora) in hydrocarbon seep communities in the Gulf of Mexico. Proc Biol Soc Washingt. 2003;116(2):380–94.
Gaurav V, LD J, Rudolf M. SequenceMatrix: concatenation software for the fast assembly of multi-gene datasets with character set and codon information. Cladistics. 2011;27:171–80 Available from: https://onlinelibrary.wiley.com/doi/abs/10.1111/j.1096-0031.2010.00329.x.
Guindon S, Gascuel O. A simple, fast, and accurate algorithm to estimate large phylogenies by maximum likelihood. Syst Biol. 2003;52(5):696–704.
Hasegawa M, Kishino H. Yano T Aki. Dating of the human-ape splitting by a molecular clock of mitochondrial DNA. J Mol Evol. 1985;22:160–74.
Hilário A, Capa M, Dahlgren TG, Halanych KM, Little CTS, Thornhill DJ, et al. New perspectives on the ecology and evolution of Siboglinid tubeworms. PLoS One. 2011;6(2):14.
Jones ML. *Riftia pachyptila*, new genus, new species, the vestimentiferan worm from the Galápagos rift geothermal vents. Proc Biol Soc Washingt [Internet]. 1980;93(4):1295–313 Available from: http://www.biodiversitylibrary.org/item/22854.
Jones ML. On the Vestimentifera, new phylum: six new species, and other taxa, from hydrothermal vents and elsewhere. Bull Biol Soc Washingt. 1985;6:117–58.
Katoh K, Standley DM. MAFFT multiple sequence alignment software version 7: improvements in performance and usability. Mol Biol Evol. 2013;30(4):772–80.
Kobayashi G, Miura T, Kojima S. *Lamellibrachia sagami* sp. Nov., a new vestimentiferan tubeworm (Annelida: Siboglinidae) from Sagami Bay and several sites in the northwestern Pacific Ocean. Zootaxa. 2015;4018(1):97–108.
Kojima S. Deep-sea chemoautosynthesis-based communities in the northwestern Pacific. J Oceanogr. 2002;58(2):343–63.
Kojima S, Ohta S, Yamamoto T, Miura T, Fujiwara Y, Hashimoto J. Molecular taxonomy of vestimentiferans of the western Pacific and their phylogenetic relationship to species of the eastern Pacific. I. Family Lamellibrachiidae. Mar Biol. 2001;139:211–9.
Kojima S, Ohta S, Yamamoto T, Yamaguchi T, Miura T, Fujiwara Y, Fujikura K, Hashimoto J. Molecular taxonomy of vestimentiferans of the western Pacific and their phylogenetic relationship to species of the eastern Pacific III. Alaysia-like vestimentiferans and relationships among families. Mar Biol. 2003;142:625-35.
Kojima S, Segawa R, Hashimoto J, Ohta S. Molecular phylogeny of vestimentiferans collected around Japan, revealed by the nucleotide sequences of mitochondrial DNA. Mar Biol. 1997;127(3):507–13.
Kojima S, Watanabe H, Tsuchida S, Fujikura K, Rowden A, Takai K, et al. Phylogenetic relationships of a tube worm (*Lamellibrachia juni*) from three hydrothermal vent fields in the South Pacific. J Mar Biol Assoc UK. 2006;86:1357–61 Available from: http://www.journals.cambridge.org/abstract_S002531540601438X.
Levin LA, Orphan VJ, Rouse GW, Rathburn AE, Ussler W, Cook GS, et al. A hydrothermal seep on the Costa Rica margin: middle ground in a continuum of reducing ecosystems. Proc R Soc B Biol Sci [Internet]. 2012;279:2580–8 Available from: http://rspb.royalsocietypublishing.org/cgi/doi/10.1098/rspb.2012.0205.
Li Y, Kocot KM, Schander C, Santos SR, Thornhill DJ, Halanych KM. Mitogenomics reveals phylogeny and repeated motifs in control regions of the deep-sea family Siboglinidae (Annelida). Mol Phylogenet Evol. 2015;85:221–9. https://doi.org/10.1016/j.ympev.2015.02.008.
Li Y, Kocot KM, Whelan NV, Santos SR, Waits DS, Thornhill DJ, et al. Phylogenomics of tubeworms (Siboglinidae, Annelida) and comparative performance of different reconstruction methods. Zool Scr. 2017;46(2):200–13.
McCowin MF, Rouse GW. A new *Lamellibrachia* species and confirmed range extension for *Lamellibrachia barhami* (Siboglinidae, Annelida) from Costa Rica methane seeps. Zootaxa. 2018;4504(1):1–22.
McMullin ER, Hourdez S, Schaeffer SW, Fisher CR. Phylogeny and biogeography of deep sea vestimentiferan tubworms and their bacterial symbionts. Symbiosis. 2003;34(1):1–41.
Miglietta MP, Hourdez S, Cowart DA, Schaeffer SW, Fisher C. Species boundaries of Gulf of Mexico vestimentiferans (Polychaeta, Siboglinidae) inferred from

mitochondrial genes. Deep Res Part II Top Stud Oceanogr. 2010;57:1916–25. https://doi.org/10.1016/j.dsr2.2010.05.007.
Mitarai S, Watanabe H, Nakajima Y, Shchepetkin AF, McWilliams JC. Quantifying dispersal from hydrothermal vent fields in the western Pacific Ocean. Proc Natl Acad Sci. 2016;113(11):2976–81 Available from: http://www.pnas.org/lookup/doi/10.1073/pnas.1518395113.
Miura T, Fujikura K. In: Fujikura K, Okutani T, Maruyama T, editors. Deep-sea life--biological observations using research submersibles. Kanagawa: Tokai University Press; 2008.
Miura T, Kojima S, editors. Two new species of Vestimentiferan tubeworm (Polychaeta: Siboglinidae a.k.a. Pogonophora) from the Brothers Caldera, Kermadec Arc, South Pacific Ocean. Species Divers. 2006;11(3):209–24 [cited 2018 May 25]; Available from: http://ci.nii.ac.jp/naid/110006794409/en/.
Miura T, Tsukahara J, Hashimoto J. *Lamellibrachia satsuma*, a new species of vestimentiferan worms (Annelida: Pogonophora) from a shallow hydrothermal vent in Kagoshima Bay, Japan Proc Biol Soc Washingt. 1997;110(3):447–56 Available from: https://archive.org/details/biostor-81167.
Moalic Y, Desbruyères D, Duarte CM, Rozenfeld AF, Bachraty C, Arnaud-Haond S. Biogeography revisited with network theory: retracing the history of hydrothermal vent communities. Syst Biol. 2012;61(1):127–37.
Nelson K, Fisher CR. Absence of cospeciation in deep-sea vestimentiferan tube worms and their bacterial endosymbionts. Symbiosis. 2000;28:1–15.
Nishijima M, Lindsay DJ, Hata J, Nakamura A, Kasai H, Ise Y, et al. Association of thioautotrophic bacteria with deep-sea sponges. Mar Biotechnol. 2010;12(3):253–60.
Palumbi SR. Nucleic acid II: the polymerase chain reaction. In: Hillis DM, Moritz C, Mable BK, editors. Mol. Syst. 2nd ed. Sunderland, MA: Sinauer associates, Inc; 1996. p. 205–47.
Patra AK, Kwon YM, Kang SG, Fujiwara Y, Kim SJ. The complete mitochondrial genome sequence of the tubeworm *Lamellibrachia satsuma* and structural conservation in the mitochondrial genome control regions of order Sabellida. Mar Genomics. 2016;26:63–71. https://doi.org/10.1016/j.margen.2015.12.010.
Pleijel F, Dahlgren TG, Rouse GW. Progress in systematics: from Siboglinidae to Pogonophora and Vestimentifera and back to Siboglinidae. C R Biol. 2009;332:140–8 [cited 2018 May 28] Available from: https://www.sciencedirect.com/science/article/pii/S1631069108003004?via%3Dihub.
Rogers AD, Tyler PA, Connelly DP, Copley JT, James R, Larter RD, et al. The discovery of new deep-sea hydrothermal vent communities in the Southern Ocean and implications for biogeography. PLoS Biol. 2012;10(1):17.
Ronquist F, Teslenko M, van der Mark P, Ayres D, Darling A, Hohna S, et al. Efficient Bayesian phylogenetic inference and model choice across a large model space. Syst Biol. 2012;61:539–42.
Shank TM, Fornari DJ, Von Damm KL, Lilley MD, Haymon RM, Lutz RA. Temporal and spatial patterns of biological community development at nascent deep-sea hydrothermal vents (9° 50′N, East Pacific rise). Deep Res II. 1998;45:465–515.
Southward EC. Three new species of Pogonophora, including two vestimentiferans, from hydrothermal sites in the Lau Back-Arc Basin (Southwest Pacific Ocean). J Nat Hist. 1991;25(4):859–81 [cited 2018 May 27] Available from: http://www.tandfonline.com/doi/abs/10.1080/00222939100770571.
Southward EC, Andersen AC, Hourdez S. *Lamellibrachia anaximandri* n. sp., a new vestimentiferan tubeworm (Annelida) from the Mediterranean, with notes on frenulate tubeworms from the same habitat. Zoosystema. 2011;33(3):245–79 [cited 2018 May 27] Available from: http://www.bioone.org/doi/abs/10.5252/z2011n3a1.
Southward EC, Tunnicliffe V, Black M. Revision of the species of *Ridgeia* from Northeast Pacific hydrothermal vents, with a redescription of *Ridgeia piscesae* Jones (Pogonophora: Obturata = Vestimentifera). Can J Zool. 1995;73(2):282–95 Available from: http://www.nrcresearchpress.com/doi/10.1139/z95-033.
Stamatakis A. RAxML version 8: a tool for phylogenetic analysis and post-analysis of large phylogenies. Bioinformatics. 2014;30(9):1312–3.
Sun Y, Liang Q, Sun J, Yang Y, Tao J, Liang J, et al. The mitochondrial genome of the deep-sea tubeworm *Paraescarpia echinospica* (Siboglinidae, Annelida) and its phylogenetic implications. Mitochondrial DNA Part B Resour. 2018;3(1):131–2. https://doi.org/10.1080/23802359.2018.1424576.
Swofford DL. Phylogenetic analysis using parsimony (*and other methods). 4th ed. Sunderland: Sinauer Associates, Inc; 2002.
Vrijenhoek RC, Johnson SB, Rouse GW. A remarkable diversity of bone-eating worms (*Osedax*; Siboglinidae; Annelida). BMC Biol. 2009;7(74):1–13.
Watanabe H, Fujikura K, Kojima S, Miyazaki JI, Fujiwara Y. Japan: vents and seeps in close proximity. In: Vent seep biota. Top. Geobiol. Vol 33. Dordrecht: Springer; 2010. p. 379–401.
Webb M. *Lamellibrachia barhami*, gen. Nov., sp. nov. (Pogonophora), from the Northeast Pacific. Bull Mar Sci. 1969;19(1):18–47.

4.1 Acknowledgements

Chapter 4 in full, is a reprint of the material as it appears in *Marine Biodiversity Records*. McCowin, Marina F., Rowden, Ashley A., and Rouse, Greg W. (2018). A new record of *Lamellibrachia columna* (Siboglinidae, Annelida) from cold seeps off New Zealand, and an assessment of its presence in the western Pacific Ocean. *Marine Biodiversity Records* 12(10): 12. The dissertation author was the primary investigator and author of this paper.

Chapter 5

Updated phylogeny of Vestimentifera (Siboglinidae, Polychaeta, Annelida) based on mitochondrial genomes, with description of a new species

Marina F. McCowin[1], Patrick C. Collins[2] and Greg W. Rouse[1]

[1]Scripps Institution of Oceanography, University of California San Diego, USA; [2]Queen's University Belfast, Belfast, Co. Antrim, BT0 5DL, Northern Ireland

5.1 Abstract

Siboglinid tubeworms are found at chemosynthetic environments worldwide and the Vestimentifera clade is particularly well known for their reliance on chemoautotrophic bacterial symbionts for nutrition. The mitochondrial genomes have been published for nine vestimentiferan species to date. This study provides new complete mitochondrial genomes for ten further Vestimentifera, including the first mitochondrial genomes sequenced for *Alaysia spiralis*, *Arcovestia ivanovi*, *Lamellibrachia barhami*, *Lamellibrachia columna*, *Lamellibrachia donwalshi*, and unnamed species of *Alaysia* and *Oasisia*. Phylogenetic analyses combining fifteen mitochondrial genes and the nuclear 18S rRNA gene recovered *Lamellibrachia* as sister to the remaining Vestimentifera and *Riftia pachyptila* as separate from the other vent-endemic taxa. Additionally, a new species of *Alaysia* is described from the Manus Basin.

5.2 Introduction

Tubeworms of the rank-free clade Vestimentifera within Siboglinidae (Annelida, Polychaeta, Siboglinidae) are found at deep-sea chemosynthetic environments such as hydrothermal vents, seeps, and organic falls (Bright and Lallier, 2010; Feldman et al., 1998; Jones, 1980; Webb, 1969). Vestimentifera, erected by Jones (1985) and later revised as an informal lineage within Siboglinidae Caullery, 1914 (Hilário et al., 2011; Pleijel et al., 2009; Rouse and Fauchald, 1997), encompasses ten currently accepted genera that are known for their reliance on symbioses with chemoautotrophic bacteria. These bacteria metabolize hydrogen sulfide, providing nutrition for the host worms, which lack a mouth and gut as adults and rely on the organic compounds provided by their endosymbionts (Bright and Lallier, 2010). Six genera are endemic to hydrothermal vents in the Pacific: *Riftia* Jones, 1981, *Ridgeia* Jones, 1985, *Tevnia* Jones, 1985, *Oasisia* Jones, 1985, *Alaysia* E. C. Southward, 1991, and *Arcovestia* Southward and Galkin, 1997 with no vent-only taxa known from other oceans.

Alaysia spiralis Southward, 1991 was originally described from the Lau Back-Arc basin

and *Arcovestia ivanovi* Southward & Galkin, 1997 from the Manus Basin (Papua New Guinea). The two are differentiated by their outer sheath lamellae (present in *Alaysia*, absent in *Arcovestia*) and obturaculum characteristics (E.C. Southward and Galkin, 1997). Photos of specimens of each species (including *Alaysia spiralis* from near the type locality) are presented in Figure 5.1. Both of these vestimentiferan species grow in low density patches at the Manus Basin vents around areas of diffuse flow and provide crucial habitat for many other organisms that contribute to the biodiversity in the basin (Samadi et al., 2015). This area has been a focus of study in recent years (Kojima et al., 2002; Samadi et al., 2015; Van Audenhaege et al., 2019; Watanabe and Kojima, 2015) because large areas have been slated for deep-sea mining, which would likely have deleterious effects on the biodiversity, connectivity, and community structure of the region, though there is a current moratorium on mining in the area (Miller et al., 2018). Sampling has been conducted in an attempt to catalog the existing biodiversity to inform management practices (Kojima et al., 2002; Samadi et al., 2015; Van Audenhaege et al., 2019). This sampling has revealed multiple species of Vestimentifera, including *Lamellibrachia* Webb, 1969, *Arcovestia*, *Alaysia*, and *Paraescarpia* Southward et al., 2002 (Samadi et al., 2015; Van Audenhaege et al., 2019), and some putative new species of *Alaysia* in this region (Kojima et al., 2003, unpublished data). Many questions remain unanswered about *Alaysia* and *Arcovestia*, including their placement in the overall phylogeny of Vestimentifera, which has not yet been established with ample molecular data. There have only been two phylogenetic studies with molecular data for *Alaysia* or *Arcovestia* to date (Kojima et al., 2003, 2002). While Kojima et al. (2002) provided identification of *Arcovestia ivanovi* sequences based on their proximity to the type locality, only tentative identifications of potential *Alaysia* species could be reported by Kojima et al. (2003) due to a lack of *A. spiralis* material from the type locality in the Lau Back-Arc Basin. Neither study confidently placed *Alaysia* or *Arcovestia* in the vestimentiferan phylogeny owing to limited taxonomic sampling and the use of only mitochondrial COI data.

The mitochondrial genomes of sixteen members of Siboglinidae have already proven valuable in resolving the siboglinid phylogeny, (Li et al., 2015; Patra et al., 2016; Sun et al., 2018).

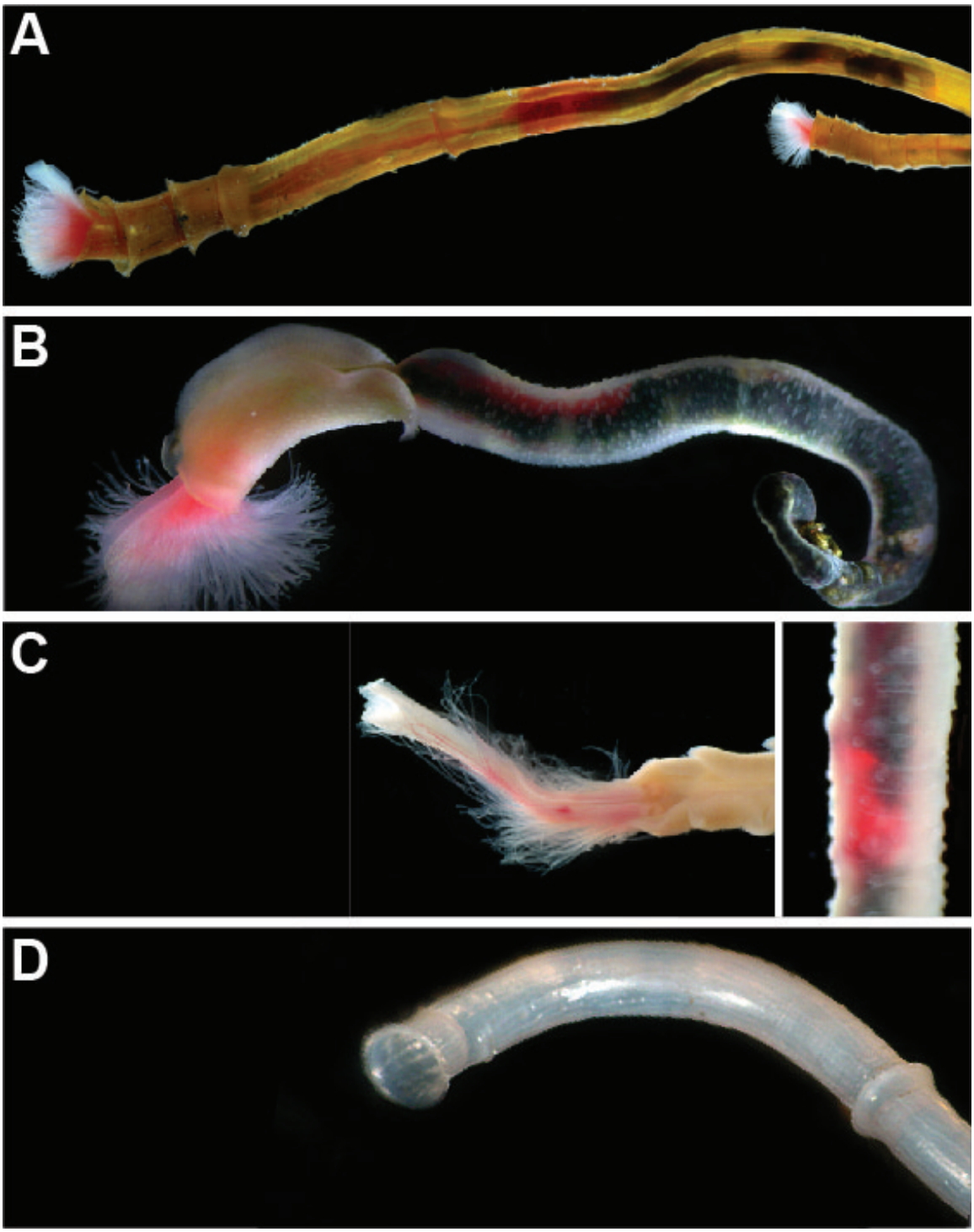

Figure 5.1. Photographs of *Arcovestia ivanovi* and *Alaysia spiralis*. (A) *Arcovestia ivanovi* (GenBank accession number FJ667530) anterior in tube. (B) *A. ivanovi* (same specimen) whole, dissected out of tube. (C) *Alaysia spiralis* (GenBank accession number FJ667536) anterior, dissected out of tube. (D) *A. spiralis* tube (animal removed).

However, the mitochondrial genomes of *Alaysia* and *Arcovestia* are missing from these datasets. This study adds the mitochondrial genomes for *Alaysia spiralis* and *Arcovestia ivanovi*, as well as eight other members of Vestimentifera, including a new species of *Alaysia*, a new species of *Oasisia*, multiple *Lamellibrachia* species, and additional samples of *Riftia pachyptila* Jones, 1981 and *Escarpia spicata* Jones, 1985. Nucleotide and amino-acid-translated phylogenies are generated from the newly sequenced mitochondrial genome data (13 protein coding genes and 2 ribosomal RNA genes) and nuclear 18S gene. Genetic data from this study reveals two putatively new species of *Alaysia* and includes a formal description for one of them.

5.3 Methods

5.3.1 Sampling and Morphological Analyses

Vestimentifera samples were collected and subsampled for DNA on various dives between 1990 and 2018. Figure 5.2 shows sampling and type localities for *Alaysia* and *Arcovestia*. Twelve *Alaysia spiralis* specimens were borrowed from the South Australian Museum (SAM) for analysis, originally collected from the ”Snowcap” and ”Satanic Mills” sites in the Manus Basin in 2000. One *Alaysia spiralis* specimen was also collected by the ROV Jason II at a vent near the species type locality in the Lau Back-Arc Basin, at 1,905 meters in 2005. While the voucher material for this specimen was lost/destroyed, photographs and sequences associated with the specimen have been made available (see Figure 5.1 and Table 5.2). Two *Arcovestia ivanovi* specimens were collected by the ROV Jason II at a vent at approximately 2,200 meters in the Lau Back-Arc Basin in 2005. Four *A. ivanovi* specimens were borrowed from SAM, originally sampled from the ”Snowcap” and ”Satanic Mills” sites in the Manus Basin in 2000 (CSIRO Binatang 2000 Expedition). Eleven specimens of a putative new species of *Alaysia* (*Alaysia* sp. nov. 2) were also collected from the ”South Su” site in the Manus Basin in 2007, and three specimens of a different putative new species of *Alaysia* (*Alaysia* sp. nov. 1) were collected from the ”Snowcap” and ”Satanic Mills” sites in the Manus Basin in 2000. Additional sampling details

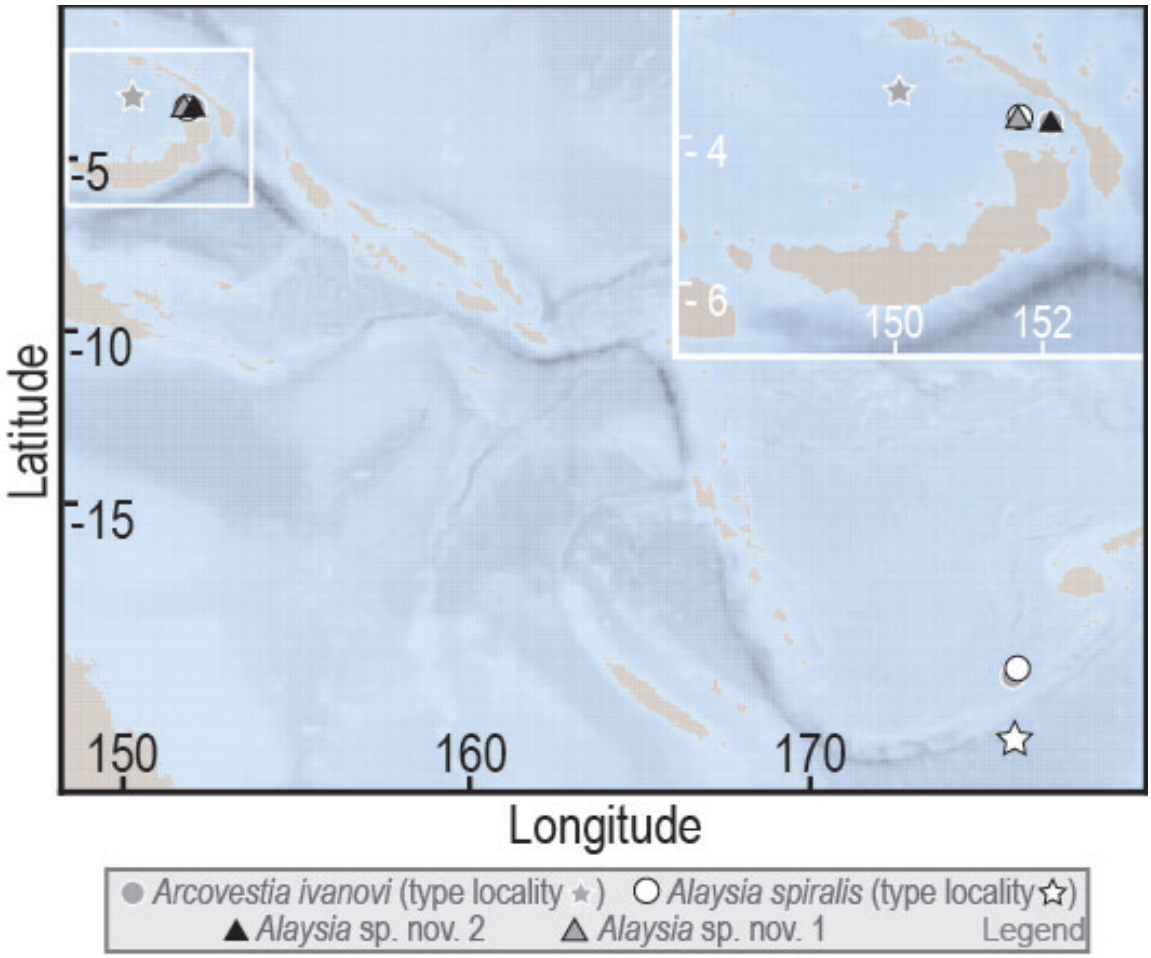

Figure 5.2. Map of sampling areas in Manus and Lau Back-Arc basins. Type localities of currently described species represented by stars. Type localities of putative new species represented by triangles. All other sampling localities represented by circles.

for these specimens and others used in genetic analysis are also listed in Table 5.1 (samples for which whole mitochondrial genomes were sequenced) and Table 5.2 (all samples used in various phylogenetic analyses). The map of Manus and Lau Basin sampling localities (Figure 5.2) was created in RStudio using R v.4.1.3 with the package marmap v.1.0.6 (Pante and Simon-Bouhet, 2013).

For molecular analyses, whole or partially whole animals were either frozen and kept at -80^{o}C or preserved in 95% ethanol in their chitinous tubes. The *Alaysia* sp. nov. 2 holotype was fixed and stored in 95% Ethanol, and later the anterior was dissected out from the tube to

Table 5.1. Sequencing information and origin of sequenced terminals, vouchers, and GenBank accession numbers for whole mitochondrial genome data. Newly sequenced mitochondrial genomes are set in bold.

Scientific Name	Locality	Depth	Latitude	Longitude	Habitat	Total Length	Average Sequencing Coverage	AT Content	GC Content	GenBank Accession Number	Voucher or Reference
Alaysia sp. nov. 2	**South Su, Manus Basin, Bismarck Sea**	**1452**	**-3.811**	**152.103**	**vent**	**14981**	**360**	**65.20%**	**34.80%**	**ON929999**	**SIO-BIC A12497**
Alaysia spiralis	**Eastern Manus Basin, Bismarck Sea**	**1645-1735**	**-3.728**	**151.669**	**vent**	**15040**	**524**	**65.54%**	**34.46%**	**ON929998**	**SAM E8131**
Arcovestia ivanovi	**South Su, Manus Basin, Bismarck Sea**	**1452**	**-3.811**	**152.103**	**vent**	**14953**	**316**	**65.75%**	**34.25%**	**ON930000**	**SIO-BIC A12501**
Escarpia "laminata"	Mississippi Canyon, US	~754	28.19	-89.8	seep	15445	232	66.09%	33.91%	KJ789161	Li et al. 2015
Escarpia spicata	**West Florida Escarpment, Gulf of Mexico**	**3314**	**26.04**	**-84.91**	**seep**	**15150**	**236**	**63.78%**	**36.22%**	**ON929994**	**SIO-BIC A12974**
Escarpia spicata	**Jaco Scar, Costa Rica Margin**	**1798-1908**	**9.12**	**-84.84**	**seep**	**15168**	**248.7**	**63.75%**	**36.25%**	**ON929996**	**SIO-BIC A8327**
Lamellibrachia barhami	**Mound Jaguar, Costa Rica Margin**	**1909**	**9.66**	**-85.88**	**seep**	**15019**	**382**	**65.03%**	**34.97%**	**ON929997**	**SIO-BIC A10173B**
Lamellibrachia columna	**Builder's Pencil, Hikurangi Margin, New Zealand**	**810-817**	**-39.54**	**178.33**	**seep**	**15115**	**358.6**	**63.50%**	**36.50%**	**ON929995**	**SIO-BIC A9468**
Lamellibrachia donwalshi	**Mound 12, Costa Rica Margin**	**990-999**	**8.93**	**-84.31**	**seep**	**14982**	**479**	**63.88%**	**35.12%**	**ON929991**	**SIO-BIC A8272**
Lamellibrachia luymesi	Mississippi Canyon, US	~754	28.19	-89.8	seep	14991	67	64.56%	35.44%	KJ89163	Li et al. 2015
Lamellibrachia satsuma	Kagoshima Bay, Japan	110	31.66	130.8	seep	15037	-	65.60%	34.40%	KP987801	Patra et al. 2016
Oasisia alvinae	East Pacific Rise	~2630	9.8	-103.94	vent	14849	39	64.92%	35.08%	KJ789164	Li et al. 2015
Oasisia sp. nov.	**Southern East Pacific Rise (32S)**	**2338**	**-31.87**	**-112.04**	**vent**	**15356**	**240**	**64.80%**	**35.20%**	**ON929992**	**SIO-BIC A11662**
Paraescarpia echinospica	Haima cold seep, soouth China Sea	1370-1390	~17	~110	seep	15280	-	64.32%	35.68%	MG462707	Sun et al. 2018
Ridgeia piscesae	Southern Explorer Ridge, northeastern Pacific	-	49.76	-130.26	vent	15002	-	57.00%	43.00%	KJ872501	Jun et al. 2016
Riftia pachyptila	East Pacific Rise	~2522	9.85	-104.29	vent	14987	71	66.76	33.24%	KJ789166	Li et al. 2015
Riftia pachyptila	**Matterhorn area, Auka Vent Field, Pescadero Basin, Gulf of California**	**3653.5**	**23.95**	**108.86**	**vent**	**16566**	**486**	**65.51%**	**34.49%**	**ON929993**	**SiO-BIC A9493**
Sclerolinum brattstromi	Storfjorden Fjord, Norway	~660	62.45	5.09	-	15383	23	64.9	35.10%	KJ789167	Li et al. 2015
Seepiophila jonesi	Mississippi Canyon, US	~754	28.19	-89.8	seep	15092	220	64.83	35.17%	KJ789168	Li et al. 2015
Tevnia jerichonana	East Pacific Rise	~2537	9.79	-104.27	vent	14891	22	64.51%	35.49%	KJ789172	Li et al. 2015

facilitate photography and measurements. Specimen tissues adhered to their semi-transparent chitinous tube walls during fixing and preservation, so photographs and measurements were taken through the semi-transparent tubes when possible, to keep the specimen intact. The specimen was photographed using a Canon T7i camera and Leica MZ12.5 stereo microscope. Measurements were made of the obturaculum, crown, vestimentum, trunk, and tube of the holotype specimen. Specimens are deposited at the South Australian Museum (SAM), Adelaide, South Australia, Australia and the Scripps Institution of Oceanography Benthic Invertebrate Collection (SIO-BIC), La Jolla, California, USA (accession numbers in Table 5.1 and Table 5.2).

5.3.2 DNA Extraction, Amplification, and Sequencing

DNA was extracted from two *Arcovestia* specimens and seventeen *Alaysia* specimens (various species) with the Zymo Research DNA-Tissue Miniprep kit (Zymo Research, Inc.), following the protocol supplied by the manufacturer. DNA was extracted from the remaining four *Arcovestia* and nine *Alaysia* specimens by the Vrijenhoek lab at the Monterey Bay Aquarium Research Institute (MBARI), Moss Landing, California, USA, before it was donated to SIO-BIC. DNA was also extracted from two *Escarpia spicata* specimens, a single *Oasisia* sp. nov. specimen, a single *Riftia pachyptila* specimen, and a single *Lamellibrachia barhami* specimen with the Zymo Research kit and protocol (for later library preparation and mitochondrial genome sequencing, see Table 5.1). Previous extractions of L. *columna* (McCowin et al., 2019), and *L. donwalshi* (McCowin and Rouse, 2018) were also utilized for library preparation and mitochondrial genome sequencing (Table 5.1).

Approximately 500 bp of the mitochondrial gene cytochrome c oxidase subunit I (COI) were amplified for each newly-extracted specimen using the vestimentiferan mtCOI primer set COIf and COIr (Nelson and Fisher, 2000) to confirm field identifications of species (see Supplementary Table B.2.1.1 for primer sequences). For a subset of *Alaysia* and *Arcovestia* samples for which COI did not amplify with these primers, two sets of designed primers targeting shorter regions of the mtCOI gene (approximately 300 bp and 400 bp) were used (Supplementary

Table 5.2. Origin of sequenced terminals, vouchers, and GenBank accession numbers for all phylogenetic analyses.

Scientific Name	Locality	Depth	Latitude	Longitude	COI	16S	18S	Voucher or Reference
Alaysia sp. A1	Off Hatsushima, Sagami Bay, Japan	830 - 1230	34.98	139.22	AB088670	-	-	Kojima et al. 2003
Alaysia sp. A2	Daiyon Yonaguni Knoll, South Okinawa Trough, Japan	1320	24.85	122.7	AB088671	-	-	Kojima et al. 2003
Alaysia sp. A3	PACMANUS site, Manus Basin	1660 - 1710	-3.73	151.67	AB088672	-	-	Kojima et al. 2003
Alaysia sp. A4	North Iheya Knoll, Mid-Okinawa Trough	1050	27.78	126.9	AB088673	-	-	Kojima et al. 2003
***Alaysia* sp. nov. 1**	**"Snowcap", Eastern Manus Basin**	**1645-1735**	**-3.728**	**151.669**	**OP125606-7**	**-**	**-**	**SIO-BIC A14184-5**
***Alaysia* sp. nov. 1**	**"Satanic Mills", Eastern Manus Basin**	**1691**	**-3.725**	**151.674**	**OP125608**	**-**	**-**	**SIO-BIC A14186**
***Alaysia* sp. nov. 2**	**"South Su", Manus Basin**	**1452**	**-3.811**	**152.103**	**OP135973-82**	**OP137205-9**	**-**	**SIO-BIC A14167A-E, A14168, A12500, A12503, A12506, A12508**
***Alaysia* sp. nov. 2**	**"South Su", Manus Basin**	**1452**	**-3.811**	**152.103**	**ON929999**	**ON929999**	**OP137200**	**SIO-BIC A12497**
Alaysia spiralis	**Lau Back-arc Basin**	**1905**	**-20.054**	**176.135**	**FJ667536**	**-**	**-**	**this study**
Alaysia spiralis	**"Snowcap", Eastern Manus Basin**	**1645-1735**	**-3.728**	**151.669**	**OP131318-26**	**-**	**-**	**SAM E8119, E8121-6, E8128-9**
Alaysia spiralis	**"Snowcap", Eastern Manus Basin**	**1645-1735**	**-3.728**	**151.669**	**ON929998**	**ON929998**	**OP137198**	**SAM E8131**
Alaysia spiralis	**"Satanic Mills", Eastern Manus Basin**	**1691**	**-3.725**	**151.674**	**OP131729**	**-**		**SAM E3632a**
Arcovestia ivanovi	**Lau Back-arc Basin**	**2719-2721**	**-20.318**	**176.137**	**OP115783-4**	**-**	**-**	**SIO-BIC A14169, A11518**
Arcovestia ivanovi	**Lau Back-arc Basin**	**2719-2721**	**-20.3178**	**176.1373**	**FJ667530**	**-**	**-**	**this study**
Arcovestia ivanovi	**"South Su", Manus Basin**	**1452**	**-3.811**	**152.103**	**OP115786-8**	**-**	**-**	**SIO-BIC A12498, A12510, A12512**
Arcovestia ivanovi	**"South Su", Manus Basin**	**1452**	**-3.811**	**152.103**	**ON930000**	**ON930000**	**OP137199**	**SIO-BIC A12501**
Arcovestia ivanovi	Fenway, PACMANUS site, Manus Basin	1665 - 1800	-3.728	151.673	MK252699	-	-	Li et al. 2018
Arcovestia ivanovi	PACMANUS site, Manus Basin	1677 - 1716	0.002	151.673 - 151.681	MK694787	-	-	Van Audenhaege et al. 2019
Arcovestia ivanovi	PACMANUS or DESMOS site, Manus Basin	1660 - 1900	-0.03	151.67 - 151.87	AB073491	-	-	Kojima et al. 2002
Escarpia "laminata"	Mississippi Canyon, US	~754	28.19	-89.8	KJ789161	KJ789161	AF168741	Li et al. 2015, Halanych & Vrijenhoek 1999
Escarpia southwardae	Worm Hole seep, West Africa	3189	-4.76	9.94	KC870958	-	-	Cowart et al. 2013

Table 5.2. (*Continued.*) Origin of sequenced terminals, vouchers, and GenBank accession numbers for all phylogenetic analyses.

Scientific Name	Locality	Depth	Latitude	Longitude	COI	16S	18S	Voucher or Reference
Escarpia spicata	**West Florida Escarpment, Gulf of Mexico**	**3314**	**26.04**	**-84.91**	**ON929994**	**ON929994**	**OP137196**	**SIO-BIC A12974**
Escarpia spicata	**Jaco Scar, Costa Rica Margin**	**1798-1908**	**9.12**	**-84.84**	**ON929996**	**ON929996**	**OP137197**	**SIO-BIC A8327**
Lamellibrachia anaximandri	Nile deep-sea fan, eastern Mediterranean	2129, 1686	32.64, 32.50	29.92, 30.26	EU046616	HM746782	-	Southward et al. 2011
Lamellibrachia barhami	**Mound Jaguar, Costa Rica Margin**	**1909**	**9.66**	**-85.88**	**ON929997**	**ON929997**	**OP137204**	**SIO-BIC A10173B**
Lamellibrachia columna	**Builder's Pencil, Hikurangi Margin, New Zealand**	**810-817**	**-39.54**	**178.33**	**ON929995**	**ON929995**	**OP137202**	**SIO-BIC A9468**
Lamellibrachia donwalshi	**Mound 12, Costa Rica Margin**	**990-999**	**8.93**	**-84.31**	**ON929991**	**ON929991**	**OP137203**	**SIO-BIC A8272**
Lamellibrachia juni	DESMOS site, Manus Basin	1900	-3.7	151.87	AB264603	-	-	Kojima et al. 2006
Lamellibrachia luymesi	Mississippi Canyon, US	~754	28.19	-89.8	KJ89163	KJ89163	-	Li et al. 2015
Lamellibrachia satsuma	Kagoshima Bay, Japan	110	31.66	130.8	KP987801	KP987801	FM995543	Patra et al. 2016, Pradillon et al. 2009
Oasisia alvinae	East Pacific Rise	2630	9.8	-103.94	KJ789164	KJ789164	AF168743	Li et al. 2014, Halanych & Vrijenhoek 1999
Oasisia fujikurai	Brother's Caldera, Kermadec Arc	1600	-34.86	179.06	AB242857	-	-	Miura & Kojima 2006
Oasisia sp. nov.	**Southern East Pacific Rise (32S)**	**2338**	**-31.87**	**-112.04**	**ON929993**	**ON929993**	**OP137195**	**SIO-BIC A11662**
Paraescarpia echinospica	Haima cold seep, soouth China Sea	1370-1390	~17	~110	MG462707	MG462707	-	Sun et al. 2018
Ridgeia piscesae	Southern Explorer Ridge, northeastern Pacific	-	49.76	-130.26	KJ872501	KJ872501	AF168744	Jun et al. 2016, Halanych & Vrijenhoek 1999
Riftia pachyptila	**Matterhorn area, Auka Vent Field, Pescadero Basin, Gulf of California**	**3653.5**	**23.95**	**108.86**	**ON929992**	**ON929992**	**OP137201**	**SIO-BIC A9493**
Riftia pachyptila	East Pacific Rise	~2522	9.85	-104.29	KJ789166	KJ789166	-	Li et al. 2015
Sclerolinum brattstromi	Storfjorden Fjord, Norway	~660	62.45	5.09	KJ789167	KJ789167	AF315061	Li et al. 2015, Halanych et al. 2000
Seepiophila jonesi	Mississippi Canyon, US	~754	28.19	-89.8	KJ789168	KJ789168	-	Li et al. 2015

Table B.2.1). For the *Alaysia* sp. nov. 2 holotype, an approximately 400 bp fragment of 16S rRNA (16S) was amplified using the primers 16sArL and 16sbrH (Palumbi, 1996). For one specimen of each *Arcovestia* and *Alaysia* species (excluding *Alaysia* sp. nov. 1) and specimens for which mitochondrial genomes were newly sequenced, approximately 1,770 bp of 18S rRNA were amplified in three fragments using the primer pairs 18S1F and 18S5R, 18Sa2.0 and 18S9R, and 18S3F and 18Sbi (Giribet et al., 1996; Whiting et al., 1997). Amplification was carried out with 12.5 L of Apex 2.0z RED DNA Polymerase Master Mix (Genesee Scientific), 1 L each of the appropriate forward and reverse primers (10 M concentration), 8.5 L of water, and 2 L of eluted DN*A*. Additional PCR reaction details (program parameters for thermal cycler) for each gene can be found in Supplementary Table B.2.1. All PCR products were purified with the ExoSAP-IT protocol (USB, Affymetrix) and sequencing was performed by Eurofins Genomics (Louisville, KY). All sequences were de novo assembled in Geneious Prime version 2022.0.2 (Biomatters Ltd.) GenBank accession numbers associated with all Sanger-sequenced individuals can be found in Table 5.2.

While samples of *Alaysia* sp. nov. 1 were successfully extracted and sequenced, the original voucher material was lost/destroyed. Due to the lack of type material, *Alaysia* sp. nov. 1 will not be described in this study, but the sequences associated with these specimens have been made available (GenBank accession numbers in Table 5.2) for future analyses.

5.3.3 Mitochondrial Genome Sequencing, Assembly, and Annotation

This study used genome skimming (shallow whole genome sequencing followed by bioinformatic separation of mitochondrial reads) to obtain mitochondrial genome data (Trevisan et al., 2019). Prior to library preparation for genome skimming, all extractions were quantified with a Qubit BR Assay kit (ThermoFisher Scientific) following the protocol supplied by the manufacturer. In addition, the quality of all extractions was assessed with gel electrophoresis. Sequencing libraries for a single high-quantity/quality extraction for a representative of *Arcovestia ivanovi*, *Alaysia spiralis*, *Alaysia* sp. nov. 2, *Lamellibrachia barhami*, L. *columna*, *L.*

donwalshi, *Oasisia* sp. nov., and *Riftia pachyptila*, and 2 extractions of *Escarpia spicata* (from different localities) were prepared and sequenced by Novogene (Sacramento, CA, USA) using their Whole Genome Sequencing (WGS) protocol and generating 2 Gb of 150 bp paired-end reads per sample.

Seqkit Version 0.13.2 (Shen et al., 2016) was used to assess read numbers and lengths before and after trimming and filtering for quality. Raw reads were trimmed to remove adapter sequences and low quality leading and trailing bases, and filtered with a 4-base sliding window (cutting where average quality per base fell below 15) with Trimmomatic Version 0.39 (Bolger et al., 2014). Reads shorter than 36 bases were removed from the dataset. Trimmed reads were then assembled with Mitofinder Version 1.4 (Allio et al., 2020) with the megahit assembler and tRNA annotation with MiTFi, and the invertebrate mitochondrial DNA genetic code translator (Elzanowski and Ostell, 2019). A reference genomes file for use with MitoFinder was compiled from annelid mitochondrial genomes from GenBank (included only sequences classified as "RefSeq"). Average coverage for each mitochondrial genome ranged between 240x and 524x (Table 5.1). The resulting annotated contigs were checked with the MITOS web server (Bernt et al., 2013) and annotations were manually checked for inaccuracies and edited in Geneious Prime to reconcile any errors. GenBank accession numbers associated with whole mitochondrial genome sequences can be found in Table 5.1.

5.3.4 Phylogenetic Analyses Using Mitochondrial Genomes

The thirteen protein-coding genes, 12S rRNA (12S), and 16S rRNA (16S) from the mitochondrial genome assemblies, nuclear 18S rRNA (18S), and data from GenBank (Table 5.1) were aligned separately with the MAFFT version 7 online server (Katoh et al., 2019) with the direction of nucleotide sequences set to adjust according to the first sequence (extremely slow) and all other settings default (nucleotide dataset). All thirteen mitochondrial protein-coding genes were also translated into amino acids in Geneious Prime (to be combined with the non-coding 12S, 16S, and 18S nucleotide data to form the amino-acid-translated dataset). Appropriate

models for each gene partition (nucleotide and amino-acid-translated separate) were chosen by ModelTest-NG v.0.1.6 under the Akaike Information Criterion (AICc) (Supplementary Table B.2.2). The datasets (nucleotide and amino-acid-translated) were then concatenated. Each of the two resulting datasets contained 13 mitochondrial protein-coding genes (either in nucleotide or amino-acid-translated format), 12S, 16S, and nuclear 18S. Maximum likelihood (ML) analyses were conducted with each of the nucleotide and amino-acid-translated datasets with the RAxML GUI interface v. 2.0.2 (Edler et al., 2020) using RAxML-ng v. 1.0.1 (Kozlov et al., 2019) with each partition assigned the appropriate model from ModelTest-NG (Supplementary Table B.2.2). An additional ML analysis was conducted for the nucleotide dataset with the third codon positions of protein coding genes partitioned separately from the first and second positions. For each ML analysis, 10 runs and a thorough bootstrapping (1000 replicates) was used to assess node support. Since topologies and support were identical for the two nucleotide datasets (original and third codon position partitioned), Bayesian Inference (BI) analyses were conducted only with the original nucleotide and amino-acid-translated datasets. Bayesian Inference analyses were conducted with MrBayes v.3.2.7a (Huelsenbeck and Ronquist, 2001; Ronquist and Huelsenbeck, 2003). Since MrBayes was unable to incorporate the same models as RAxML-NG, the most similar model that could be accommodated by MrBayes was assigned to each gene partition instead (see Supplementary Table B.2.2). For the amino-acid-translated dataset, a single fixed model was chosen for all amino-acid-translated partitions (MTMAM, based on the most frequent model chosen by ModelTest-NG), with the non-coding genes assigned the same models as in the nucleotide-only analysis (Supplementary Table B.2.2). For both the nucleotide and amino-acid-translated datasets, BI analyses were carried out with Markov chain Monte Carlo (MCMC) for 20 million generations with 4 chains and trees sampled every 1000 generations. Burn-in was determined to be 5% using Tracer v.1.7 (Rambaut et al., 2018). Maximum parsimony (MP) analyses were also conducted with PAUP* v.4.0a168 (Swofford, 2003) for the nucleotide and amino-acid-translated datasets using heuristic searches with the tree-bisection-reconnection branch-swapping algorithm and 1000 random addition replicates. For MP analyses, support

values were determined with 1000 bootstrap replicates.

Since the nucleotide and amino-acid-translated datasets produced slightly different topologies regarding the reciprocal monophyly of *Alaysia* and *Arcovestia*, an approximately unbiased (AU) test was conducted to test whether the reciprocal monophyly of *Alaysia* and *Arcovestia* was significantly better than a paraphyletic *Alaysia*. For the nucleotide dataset, a constrained tree forcing paraphyly of *Alaysia* and *Arcovestia* (placing *Arcovestia* sister to *Alaysia* sp. nov. 2) was made using Mesquite 3.70 (Maddison and Maddison, 2018) and RAxML-NG. The AU test was conducted in IQ-Tree v.1.6.12 (Chernomor et al., 2016) with 20,000 replicates to generate likelihood scores and p-values for the constrained and unconstrained (ML nucleotide) trees. For the amino-acid-translated dataset, a constrained tree forcing reciprocal monophyly of *Alaysia* and *Arcovestia* was made using Mesquite and RAxML-NG. An AU test was then conducted in IQ-Tree with 20,000 replicates for the constrained and unconstrained (ML amino-acid-translated) trees.

To test for substitution saturation in the third codon position of the protein-coding genes, the index of substitution saturation (I_{ss}) was assessed with DAMBE 5 (Xia, 2013), following the protocol laid out in Xia and Lemey, 2012. Whole alignments of each protein-coding gene were assessed using the proportion of invariant sites calculated by ModelTest-NG first. The proportion of invariant sites was then calculated for third codon positions using the ML nucleotide tree for estimation in DAMBE 5. For each protein-coding gene, the whole alignment and the third codon position only were tested for substitution saturation using the Xia et al. test (as in Xia and Lemey, 2012), and calculations of I_{ss} and I_{ssc} were compared to determine saturation. Additional ML, BI, and MP analyses were conducted with the nucleotide dataset with genes that appeared to be saturated (I_{ss} greater than I_{ssc}) omitted from the analyses (all parameters for each analysis otherwise the same as the previous analyses of the nucleotide dataset).

Since the nucleotide and amino-acid-translated datasets produced a topology with a placement of *Riftia pachyptila* that differs from its placement in some recent studies, an approximately unbiased test was also conducted to test whether the alternative topology (grouping *Riftia pachyp-*

tila with the other vent-endemic taxa) was not significantly different than the topology recovered in all ML, BI, and MP analyses in this study. A constrained tree placing *Riftia pachyptila* with the clade containing the other vent-endemic taxa (*Ridgeia*, *Tevnia*, *Oasisia*, *Alaysia*, *Arcovestia*) was made using Mesquite and RAxML-NG. The AU test was conducted with IQ-Tree with 20,000 replicates to generate likelihood scores for the constrained and unconstrained (ML nucleotide) trees.

An ancestral state reconstruction (ASR) of habitat was conducted utilizing the whole mitochondrial genome dataset (nucleotide) with the addition of COI (and 16S and 18S when possible) sequences from GenBank for the following taxa (for which whole mitochondrial genomes have not been sequenced): *Oasisia fujikurai*, *Escarpia laminata*, *Escarpia southwardae*, *Lamellibrachia anaximandri*, and *Lamellibrachia juni* (Table 5.2). Another Maximum Likelihood analysis was conducted in RAxML-NG with models re-assessed with ModelTest-NG for genes with new data (COI, 16S, 18S) (Supplementary Table B.2.2). The ancestral state reconstruction was conducted using this ML topology and a matrix of habitat types (vent, seep, organic fall; used &-coding for taxa known to inhabit multiple environments). The ASR was conducted in RStudio using R v.4.1.3, and the packages phytools v.1.0-1 (Revell, 2012) and corHMM v.2.7 (Beaulieu et al., 2013) were used to fit hidden Markov models of discrete character evolution. The AIC criterion determined the best model, "ER" (all rates equal) for the reconstruction.

5.3.5 Phylogenetic Analyses of *Alaysia* and *Arcovestia*

Separate phylogenetic analyses were conducted with the newly sequenced COI, 16S, and 18S data for *Alaysia spiralis*, *Arcovestia ivanovi*, the two putative new species of *Alaysia*, and previously sequenced *Alaysia* and *Arcovestia* data from GenBank (Table 5.2). This data was combined with sequences for outgroups *Tevnia jerichonana*, *Oasisia alvinae*, and *Ridgeia piscesae*, available on GenBank (Table 5.2). The outgroups chosen for phylogenetic analyses were informed by the placement of *Alaysia* and *Arcovestia* in the 16-gene analyses (nucleotide and amino-acid-translated datasets agreed). The COI, 16S, and 18S datasets were aligned

separately with MAFFT and tested with ModelTest-NG for the best-fit models under the AICc prior to concatenating (models assigned to each partition are listed in Supplementary Table B.2.2). A Maximum Likelihood analysis was conducted with RAxML-NG with each partition assigned its appropriate model from ModelTest-NG, and a thorough bootstrapping (1000 replicates) was used to assess node support. A Bayesian Inference analysis was conducted for the same concatenated dataset in MrBayes. Since MrBayes was unable to incorporate the same models as RAxML-NG, the most similar models that could be accommodated by MrBayes were assigned to each gene partition instead (see Supplementary Table B.2.2). The BI analysis was carried out with Markov chain Monte Carlo (MCMC) for 20 million generations with 4 chains and trees sampled every 1000 generations. Burn-in was determined to be 5% using Tracer. An additional ML analysis was run with the same models as those implemented in MrBayes to assess whether differences in topologies produced by the two analyses were due to model selection differences (same settings as previous ML analysis, except for each gene partition being assigned the same models as those used for the BI analysis). A Maximum Parsimony (MP) analysis was also conducted with PAUP* for the same concatenated dataset using heuristic searches with the tree-bisection-reconnection branch-swapping algorithm and 1000 random addition replicates. For the MP analysis, support values were determined with 1000 bootstrap replicates.

The newly generated COI sequences for *Alaysia* and *Arcovestia* from this study were combined with available *Alaysia* and *Arcovestia* GenBank sequences to calculate uncorrected and model-corrected inter- and intra-specific distances. For model-corrected distances for each species, models for each COI dataset (separated by species) were selected using the AICc criterion in jModelTest2 v.2.1.10 (Darriba et al., 2012) since PAUP* was unable to incorporate models from ModelTest-NG. Haplotype networks were also created using these COI datasets (terminals listed in Table 5.2) for *Alaysia spiralis*, *Arcovestia ivanovi*, *Alaysia* sp. nov. 1 and *Alaysia* sp. nov. 2. Owing to some short sequences limiting the total sequence alignment length for haplotype network analyses, multiple haplotype network versions were created with various alignment lengths (omitting sequences that were very short) for comparison (for the *Arcovestia*

ivanovi, *Alaysia spiralis*, and *Alaysia* sp. nov. 2 networks; not necessary for the *Alaysia* sp. nov. 1 network since there were only three sequences of roughly equal length). Differences between networks were small, but side-by-side comparisons of each network are available in Supplementary Figure B.1.1.1.

5.4 Results

5.4.1 Mitochondrial Genome Sequencing and Composition

Gene order and direction was conserved among the newly sequenced taxa (*Alaysia spiralis* and *Alaysia* sp. nov. 2, *Arcovestia ivanovi*, *Escarpia spicata* (Costa Rica) and *Escarpia spicata* (Gulf of Mexico), *Oasisia* sp. nov., *Lamellibrachia barhami*, *Lamellibrachia columna*, *Lamellibrachia donwalshi*, and *Riftia pachyptila*) and the available vestimentiferan mitochondrial genomes from GenBank. The newly sequenced mitochondrial genomes also had similar total lengths compared to previously sequenced mitochondrial genomes for other members of Vestimentifera, ranging from 14,981-16566 bp (Table 5.1). AT and GC content were also like other Vestimentifera, ranging from 63.50%-65.75% and 36.50%-34.35% respectively (Table 5.1).

5.4.2 Sixteen-gene Phylogenetic Analyses

The 16-gene Maximum Likelihood (ML), Bayesian Inference (BI), and Maximum Parsimony (MP) analyses of both the nucleotide and amino-acid-translated datasets produced similar topologies with similarly high levels of support at most nodes (Figure 5.3). All analyses of the nucleotide dataset produced congruent topologies, and all analyses of the amino-acid-translated dataset produced congruent topologies (topologies produced from the nucleotide and amino-acid-translated datasets differed slightly from each other, discussed in additional detail below). All analyses of both datasets recovered well-supported clades of *Lamellibrachia*, *Escarpia* and *Oasisia*, and supported the *Lamellibrachia* clade as sister to the remaining Vestimentifera. All

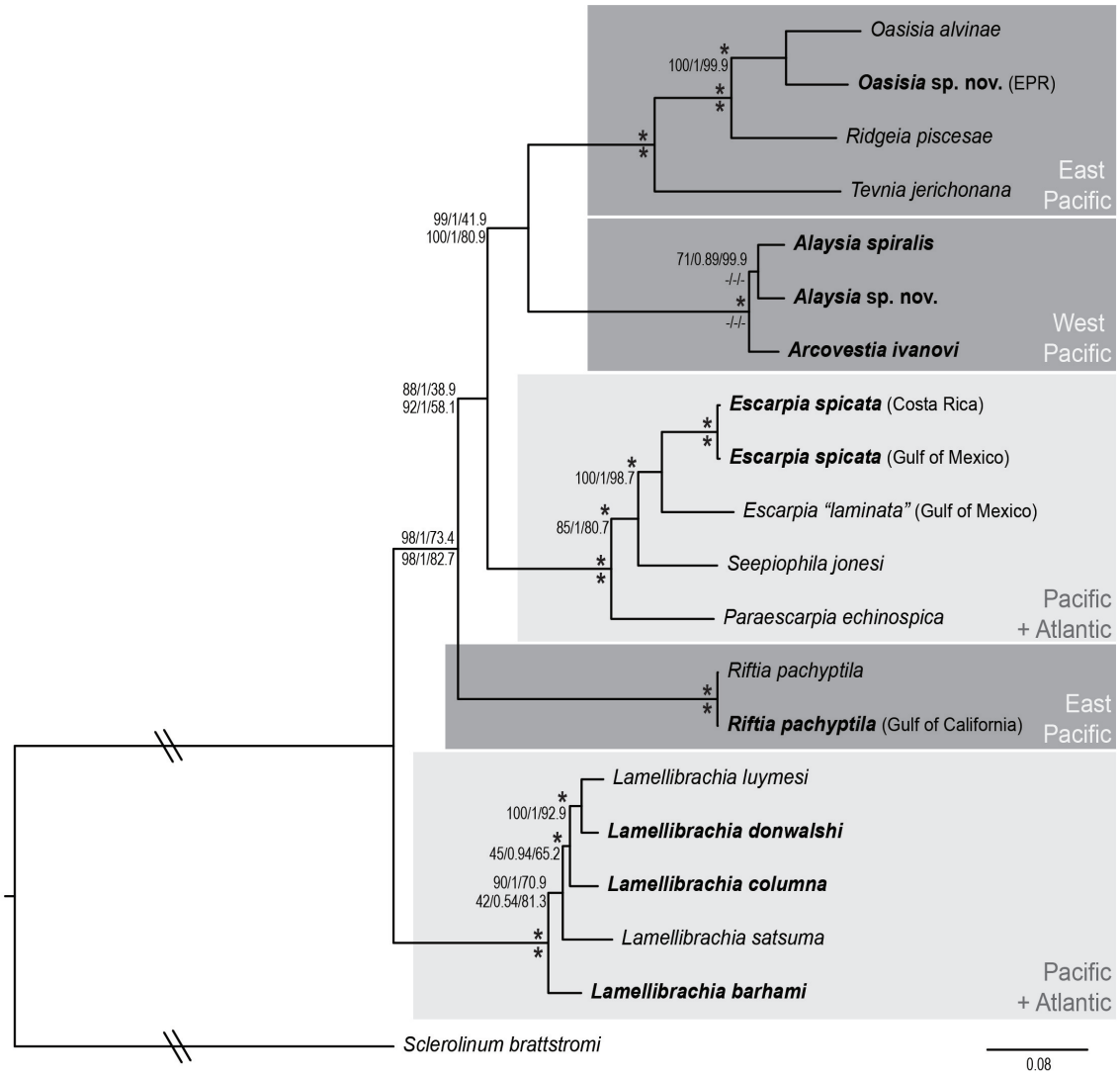

Figure 5.3. Maximum Likelihood tree of the concatenated 16-gene nucleotide data. Support values above nodes are from nucleotide-only dataset, support values below nodes are from amino-acid-translated dataset. Bootstrap support percentages from the ML analysis are listed first, followed by Bayesian posterior probabilities and bootstrap support percentages from the Maximum Parsimony analysis. Stars indicate maximal support from all three analyses. Nodes not recovered by an analysis are indicated by a hyphen.

analyses also supported a clade of Pacific vent-endemic taxa (consisting of *Oasisia*, *Ridgeia*, *Tevnia*, *Alaysia*, and *Arcovestia*) that excluded *Riftia pachyptila*. *Riftia pachyptila* was instead placed sister to the remaining Vestimentifera (excluding *Lamellibrachia*) in all analyses. The placement of *Escarpia spicata* was also notable (and identical in all analyses). While two newly sequenced *Escarpia spicata* mitochondrial genomes (one from the East Pacific off Costa Rica

and one from the Gulf of Mexico) grouped together with a very short branch length, the existing mitochondrial genome referred to as *Escarpia spicata* from GenBank (also from the Gulf of Mexico) was clearly separate from the others and is referred to here as *Escarpia* "*laminata*" (discussed in additional detail below).

As noted above, tree topologies differed slightly between the ML, BI, and MP analyses derived from the nucleotide dataset versus the analyses derived from the amino-acid-translated dataset. All analyses derived from the nucleotide dataset produced identical topologies in which *Alaysia* and *Arcovestia* were recovered as reciprocally monophyletic (Figure 5.3). All analyses derived from the amino-acid-translated dataset produced congruent topologies in which *Alaysia* and *Arcovestia* were recovered as paraphyletic, with *Arcovestia* nested inside *Alaysia* (*Arcovestia* sister to *Alaysia* sp. nov. 2) (Supplementary Figure B.1.2). No other differences were observed between the tree topologies produced by the nucleotide and amino-acid-translated datasets.

Each protein-coding gene was tested for substitution saturation in DAMBE using the nucleotide alignment for that gene. Each nucleotide alignment was tested both as a whole alignment and at the third codon position to assess potential substitution saturation at that position (Table 5.4). Of the thirteen protein-coding genes, three exhibited an index of substitution saturation (I_{ss}) value that was significantly greater than the critical index of substitution saturation (I_{ssc}) value at the third codon position, thus indicating saturation in those genes (ATP8, ND4L, ND6). Additional ML, BI, and MP analyses of the nucleotide dataset excluding the saturated genes produced identical topologies to the original nucleotide dataset analyses (Supplementary Figure B.1.3).

Since the potential reciprocal monophyly of *Alaysia* and *Arcovestia* differed between the nucleotide and amino-acid-translated datasets, an Approximately Unbiased (AU) test was conducted for each dataset to compare the two potential topologies. For the nucleotide dataset, the ML topology (Figure 5.3, *Alaysia* and *Arcovestia* reciprocally monophyletic) was compared with a constrained tree in which *Alaysia* was paraphyletic (*Arcovestia* sister to *Alaysia* sp. nov.). The p-values for the ML (monophyly) and constrained (paraphyly) trees were 0.878 and 0.122,

Table 5.3. Index of substitution saturation (I_{ss}) and critical index of substitution saturation (I_{ssc}) values for third codon position and whole alignments of protein-coding genes. Bold values are significant (p-value less than 0.05).

	Position 3		**Whole Alignment**	
Gene	**I_{ss}**	**I_{ssc} (Sym)**	**I_{ss}**	**I_{ssc} (Sym)**
ATP6	0.6484	0.6247	0.5003	**0.743**
ATP8	0.6466	**0.3209**	0.5067	0.5693
COX1	0.5361	**0.7167**	0.4482	**0.7853**
COX2	0.5172	**0.6247**	0.4304	**0.743**
COX3	0.5933	0.6416	0.4461	**0.7519**
CYTB	0.6171	**0.6858**	0.469	**0.7725**
ND1	0.5976	**0.6629**	0.4703	**0.7621**
ND2	0.6357	0.6669	0.4969	**0.7639**
ND3	0.5389	**0.6748**	0.5182	**0.6748**
ND4L	0.6325	**0.4751**	0.4715	**0.6557**
ND4	0.6113	**0.7023**	0.4986	**0.7799**
ND5	0.6284	**0.7259**	0.4932	**0.7877**
ND6	0.6434	**0.5672**	0.509	**0.707**

respectively. For the amino-acid-translated dataset, the ML topology (Supplementary Figure B.1.2, *Alaysia* paraphyletic with *Arcovestia* sister to *Alaysia* sp. nov.) was compared with a constrained tree in which *Alaysia* and *Arcovestia* were reciprocally monophyletic. The p-values for the ML (paraphyly) and constrained (monophyly) trees were 0.866 and 0.134, respectively. Neither AU test conducted in IQ-Tree recovered a significant difference between trees.

Since the placement of *Riftia pachyptila* in this study differed from its placement in some other recent publications, an AU test was also conducted to compare the topology recovered in this study with an alternative placement of *R. pachyptila* within the clade of Pacific vent-endemic taxa. The test compared the ML topology (Figure 5.3) with a tree that constrained *R. pachyptila* within a clade of vent-endemic taxa (*Oasisia*, *Ridgeia*, *Tevnia*, *Alaysia*, *Arcovestia*). The AU test conducted in IQ-Tree did not recover a significant difference between the ML and constrained trees, with p-values of 0.923 and 0.0767, respectively.

A likelihood ancestral state reconstruction (ASR) of habitat (vent, seep, and/or organic fall) was conducted on the ML tree topology (including additional vestimentiferan species with available GenBank data, not just those with whole mitochondrial genomes). The ASR revealed that a vent origin was most likely for the most recent common ancestor of the Vestimentifera

clade. It also revealed two potential origins of seep-dwelling taxa: one for the *Lamellibrachia* clade and one leading to the most recent common ancestor of the *Paraescarpia* + *Seepiophila* + *Escarpia* clade (Figure 5.4).

5.4.3 Three-gene Phylogenetic Analyses of *Alaysia* and *Arcovestia*

Phylogenetic analyses of *Alaysia* and *Arcovestia* were also conducted with a three-gene (COI, 16S, 18S) concatenated dataset. While various outgroup choices for the concatenated three-gene phylogenetic analyses resulted in differing topologies with varied and poor support, the results of the much larger 16-gene datasets placed the *Alaysia* + *Arcovestia* clade sister to the vent-endemic taxa *Tevnia jerichonana*, *Oasisia alvinae*, and *Ridgeia piscesae* regardless of the dataset used. Based on this result, all three of these vent-endemic taxa were chosen as outgroups for the three-gene phylogeny of *Alaysia* and *Arcovestia*. The ML, BI, and MP analyses of this concatenated three-gene dataset all consistently recovered *Alaysia spiralis* as sister to *Alaysia* sp. A3 with a very short branch length. These and other phylogenetic analyses (see below) indicate that *Alaysia* sp. A3 is *Alaysia spiralis*. At the time of its publication, there was not molecular data available for *A. spiralis*, so it was tentatively referred to as *Alaysia* sp. A3 (Kojima et al., 2003). The *A. spiralis* clade was also recovered by all analyses to be sister to a clade consisting of *Alaysia* sp. A1 and *Alaysia* sp. A2. However, the remaining terminals varied in position between analyses, and many relationships within the trees were poorly supported (Figure 5.5, Supplementary Figure B.1.4). The ML analysis (Figure 5.5, Supplementary Figure B.1.4A) produced a topology with reciprocally monophyletic *Alaysia* and *Arcovestia* clades. Within the *Alaysia* clade, *Alaysia* sp. nov. 2 was placed sister to *Alaysia* sp. A4 (from the Mid Okinawa Trough) and *Alaysia* sp. nov. 1 was placed sister to the remaining *Alaysia* species (*Alaysia spiralis*, *A.* sp. A1, *A.* sp. A2, and *A.* sp. A3). The BI analysis (Supplementary Figure B.1.4B) also recovered a clade that included *Alaysia spiralis*, *A.* sp. A1, *A.* sp. A2, and *A.* sp. A3. However, the BI analyses did not recover reciprocally monophyletic *Alaysia* and *Arcovestia* clades. Instead, *Arcovestia ivanovi* was nested inside a grade of *Alaysia* species (Supplementary

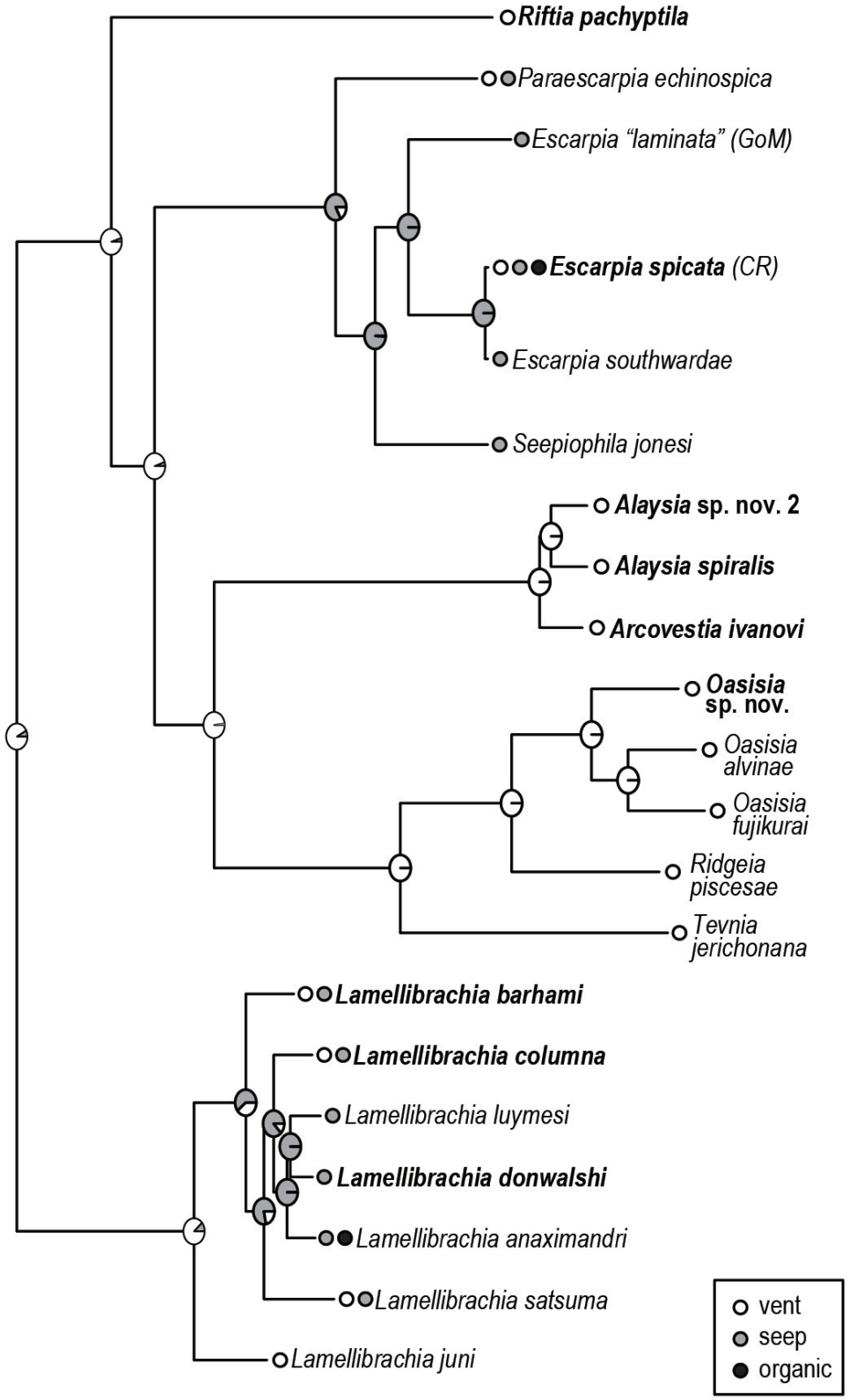

Figure 5.4. Ancestral state reconstruction of habitat (vent, seep, organic fall) mapped onto the Maximum Likelihood phylogeny generated from the 16-gene concatenated nucleotide data.

Figure B.1.4B). An additional ML analysis of the same dataset with the same models that were applied in MrBayes (instead of those chosen by ModelTest-NG and implemented in RAxML-NG) resulted in the same topology as the BI analysis. The MP analysis (Supplementary Figure B.1.4C) also recovered a clade containing *Alaysia spiralis*, *A.* sp. A1, *A.* sp. A2, and *A.* sp. A3. However, while the MP analysis did also recover a grade of *Alaysia* species with *Arcovestia ivanovi* nested inside, as in the BI analysis, the placement of the various *Alaysia* species in this grade in the MP analysis differed from that of the BI analysis (Supplementary Figure B.1.4).

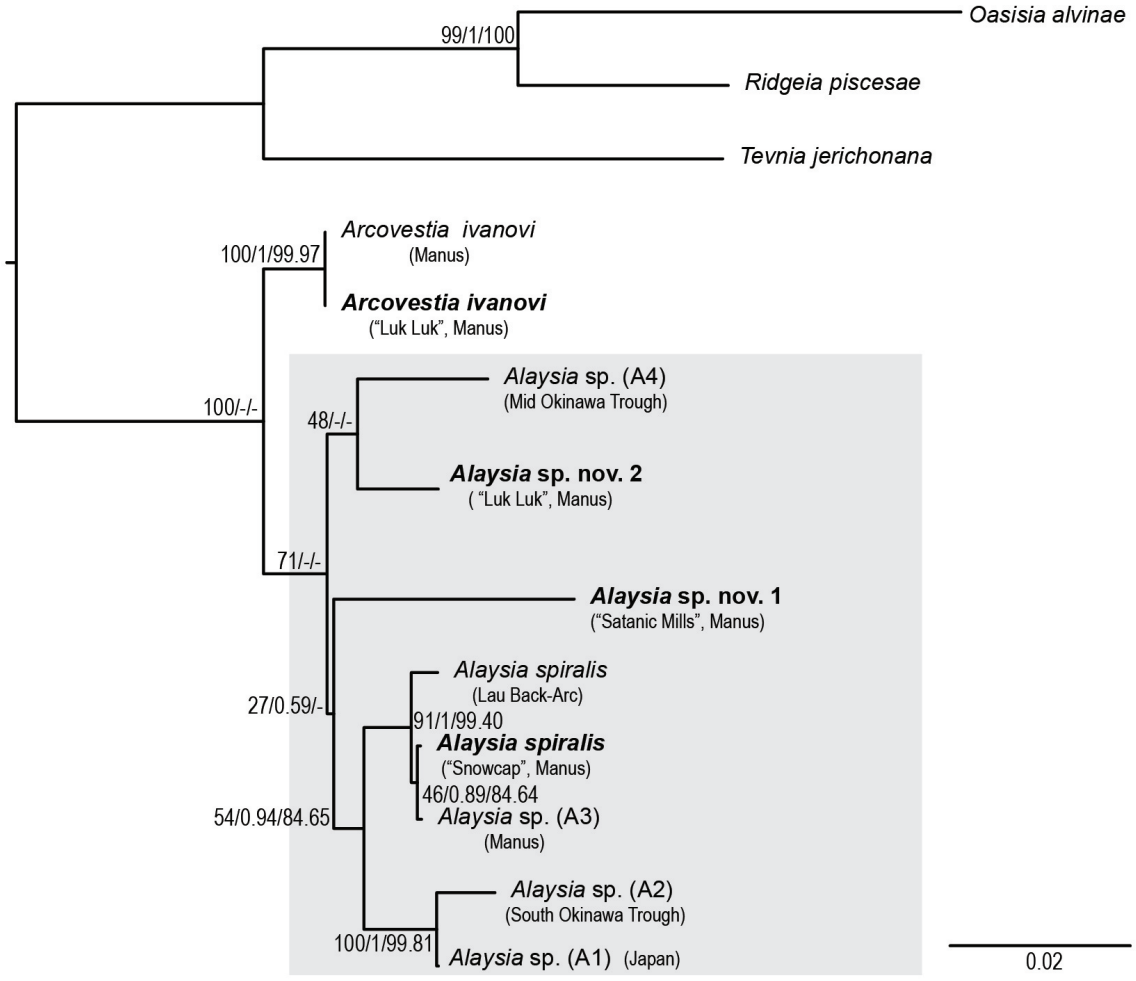

Figure 5.5. Maximum Likelihood tree of the concatenated three-gene nucleotide data. Bootstrap support percentages from the ML analysis are listed first, followed by Bayesian posterior probabilities and bootstrap support percentages from the Maximum Parsimony analysis. Nodes not recovered by an analysis are indicated by a hyphen. *Alaysia* clade indicated in grey box.

Table 5.4. Summary of uncorrected and corrected pairwise distances for Alaysia and Arcovestia COI data. Model listed for corrected pairwise distances.

TAXA	MODEL	MINIMUM INTRASPECIFIC DISTANCE		MAXIMUM INTRASPECIFIC DISTANCE		MINIMUM INTERSPECIFIC DISTANCE	
Species	For Corrected Analyses	Uncorrected	Corrected	Uncorrected	Corrected	Uncorrected	Closest Taxon
Arcovestia ivanovi	HKY	0	0	1.39%	1.47%	4.51%	Alaysia spiralis
Alaysia spiralis	HKY	0	0	1.24%	1.37%	2.48%	Alaysia sp. A1
Alaysia sp. nov. 2	F81	0	0	0.09%	0.09%	3.38%	Alaysia sp. A4
Alaysia sp. nov. 1	HKY	0.31%	0.31%	0.62%	0.64%	6.02%	Alaysia sp. A1
Alaysia sp. A1	-	-	-	-	-	1.28%	Alaysia sp. A2
Alaysia sp. A3	-	-	-	-	-	0.10%	Alaysia spiralis

An uncorrected pairwise distance analysis for the COI dataset revealed low intraspecific distances within *Alaysia* and *Arcovestia*, with maximum intraspecific distances ranging from 0.09% (*Alaysia* sp. nov. 2) to 1.39% (*Arcovestia ivanovi*) (Table 5.3). Corrected intraspecific distances for each species revealed similar results (*Alaysia* sp. nov. 2: 0-0.09%, *Alaysia* sp. nov. 1: 0.31-0.64%, *Alaysia spiralis*: 0-1.37%, *Arcovestia ivanovi*: 0-1.47%). The minimum interspecific pairwise distance between *Arcovestia ivanovi* and *Alaysia spiralis* (*A. ivanovi*'s closest relative) was 4.51% (uncorrected) to 5.84% (corrected). The minimum interspecific pairwise distance between *Alaysia spiralis* and *Alaysia* sp. A3 was 0.10% (uncorrected and corrected), which also supports the conclusion that *Alaysia* sp. A3 is *A. spiralis*. The minimum interspecific distance between *A. spiralis* and its closest relative, *Alaysia* sp. A1, was 2.48% (uncorrected) to 2.81% (corrected). The minimum interspecific pairwise distance between *Alaysia* sp. nov. 2 and its closest relative, *Alaysia* sp. A4, was 3.38% (uncorrected) to 3.86% (corrected). The minimum interspecific pairwise distance between *Alaysia* sp. nov. 1 and its closest relative, *Alaysia* sp. A1, was 6.02% (uncorrected) to 8.22% (corrected).

Haplotype networks generated for the COI dataset revealed low haplotype diversity

within species (Figure 5.6). Because missing data could not be accommodated in haplotype network analyses, multiple networks were created to compare haplotype diversity with various total alignment lengths for comparison (excluding taxa with short sequences as needed). The differences between these networks were negligible (Supplementary Figure B.1.1), and the networks with the greatest haplotype diversity are shown in Figure 5.6. The majority of *Arcovestia ivanovi* specimens (Figure 5.6A) specimens shared a single common haplotype regardless of locality and differed by up to 5 base pairs. *Alaysia spiralis* (Figure 5.6B) specimens followed a similar pattern with a single common haplotype, with a specimen from the type locality differing from the most common haplotype by 3 base pairs. *Alaysia* sp. nov. 2 (Figure 5.6C) showed the lowest haplotype diversity (just a single common haplotype) and *Alaysia* sp. nov. 1 (Figure 5.6D) also showed relatively low haplotype diversity, with specimens differing by at most 4 base pairs (note that the number of specimens sequenced for *Alaysia* sp. nov. 1 is lower than for the other species).

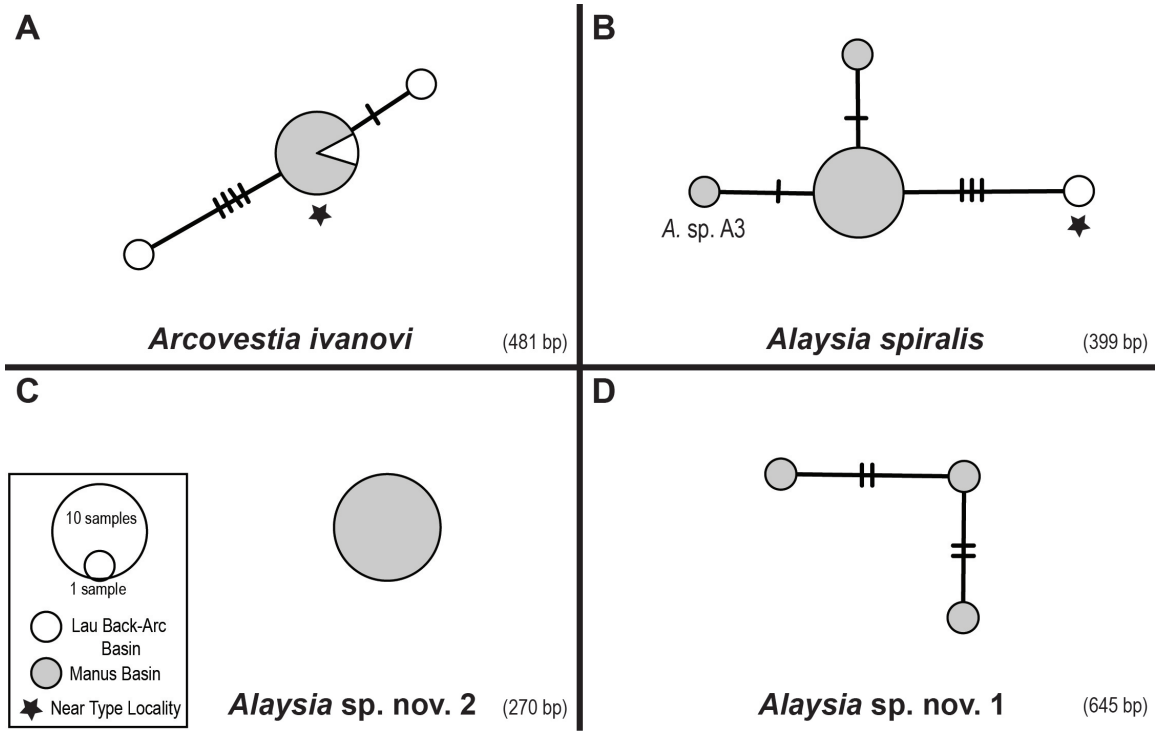

Figure 5.6. Haplotype networks from COI data for (A) *Arcovestia ivanovi*, (B) *Alaysia spiralis*, (C) *Alaysia* sp. nov. 2, and (D) *Alaysia* sp. nov. 1. Color-coded according to locality.

5.5 Taxonomy

This section is not intended to act as an official description or publication of the new species under the International Code of Zoological Nomenclature (ICZN).

Family - Siboglinidae Caullery, 1914

Alaysia Southward, 1991

Type species: *Alaysia spiralis* Southward, 1991

Alaysia sp. nov. 2

(Figure 5.7)

Type Locality. South Sulu, Manus Basin, vent site known as ”South Su”, approximately 1,452 meters depth; -3.811 S, 152.103 E.

Material Examined. Holotype: SIO-BIC A14168 (1 individual), collected on April 15 2007 from ”South Su” vent site, South Sulu, Manus Basin at 1,452 m depth; -3.811 S, 152.103 E. Collected by Patrick Collins and Carol Logan. Fixed and preserved whole (within chitinous tubes) in 95% ethanol. Paratypes: SIO-BIC A14167A-N (14 specimens), collected on April 15 2007 from ”South Su” vent site, South Sulu, Manus Basin at 1,452 m depth; -3.811 S, 152.103 E. Collected by Patrick Collins and Cindy Van Dover. Fixed and preserved whole (within chitinous tubes) in 95% ethanol.

Description. Anterior crown (branchial plume) plus obturaculum length of holotype specimen 1.0 mm, crown diameter 1.0 mm. Vestimentum length 1.0 cm, vestimentum diameter 1.0 mm (Figure 5.7A, Figure 5.7B). Obturaculum with dorsal groove and slightly cup-shaped top. Outer sheath lamellae emerge from vestimentum in a pair, clear median split with no lamellae at the center of the dorsal side, obturaculum visible through that split (Figure 5.7C, Figure 5.7D). Branchial lamellae also emerge from vestimentum and appear to be fused at the base, with a longer free portion at the anterior tip with pinnules (Figure 5.7D). Paired genital grooves appear to run the length of the vestimentum on the dorsal side (Figure 5.7A, Figure 5.7C). Outer

surface of vestimentum and trunk are dotted with small papillae likely carrying cuticular plaques (Figure 5.7E, Figure 5.7F). All specimens lacking opisthosoma. Tubes observed for holotype and multiple paratype specimens. Tubes are smooth and stiff, often semi-transparent (Figure 5.7G). Anterior part of tube is often curved or coiled (Figure 5.7G). Tube is thin and appears to lack distinct collars, approximate diameter (holotype specimen) 1.1 mm, approximate length 12.1 cm.

Distribution. *Alaysia* sp. nov. 2 has been recovered from two diffuse flow vent sites in close proximity in the Manus Basin (within 0.083 decimal degrees of latitude and 0.434 decimal degrees of longitude).

Remarks. *Alaysia* sp. nov. 2 has notable similarities to the type species *Alaysia spiralis*, including similar shape/size of obturaculum, similar arrangement of branchial and sheath lamellae, presence of paired genital grooves on the dorsal side of the vestimentum, and small papillae on the vestimentum and trunk. However, the *Alaysia* sp. nov. 2 holotype appears to have a smaller crown and vestimentum diameter, and tubes of holotypes and paratypes are curved but not always coiled like a corkscrew as in the original description of *A. spiralis* (E. C. Southward, 1991). *Alaysia* sp. nov. 2 differs genetically from *Alaysia spiralis* and other currently undescribed putative new species of *Alaysia*.

5.6 Discussion

5.6.1 Sixteen-gene Phylogenetic Analyses

This study provides the most complete mitogenomic phylogeny of Vestimentifera to date, with ten new mitochondrial genomes and nuclear 18S included and including representatives of all genera. All analyses (Maximum Likelihood, Bayesian Inference, and Maximum Parsimony) of both nucleotide and amino-acid-translated datasets show very similar topologies and high support at most nodes. Similar topologies have been found in previous studies (Li et al., 2017, 2015; Patra et al., 2016) with some differences in the placement of *Riftia pachyptila* (Li et

Figure 5.7. Photographs of *Alaysia* sp. nov. 2 holotype (SIO-BIC A14168). (A) Dorsal anterior. (B) Lateral anterior. (C) Close-up of dorsal anterior. (D) Close-up of lateral anterior. (E) Close-up of lateral vestimentum and trunk. (F) Close-up of trunk. (G) Chitinous tube.

al., 2017, 2015; Sun et al., 2018), which will be discussed in more detail below. All analyses recovered well-supported monophyletic clades of *Lamellibrachia*, *Escarpia*, and *Oasisia*, with the *Lamellibrachia* clade recovered as sister to the remaining Vestimentifera. This result is consistent with all recent phylogenies of Vestimentifera that utilize whole mitochondrial genome data and/or transcriptome data (Li et al., 2017, 2015; Patra et al., 2016; Sun et al., 2018). The placement of various *Escarpia spicata* terminals calls into question the identification of the *E. spicata* specimen available on GenBank from the Gulf of Mexico. The type locality of *E. spicata* lies in the East Pacific (Jones, 1985) and there is additional genetic data to support its existence there; therefore, it seems most likely that the *E. spicata* specimen from Costa Rica (also from the East Pacific) is a true *E. spicata*. The previously identified *E. spicata* specimen from the Gulf of Mexico, which is separated by a considerable branch length from the Costa Rica *E. spicata*, may therefore be *E. laminata*, which has been morphologically identified in the Gulf of Mexico (Cowart et al., 2013). The specimen is currently labeled *E.* "*laminata*" with quotations indicating the uncertainty of its identity until it can be confirmed with morphological or additional molecular data (morphological data and/or a voucher specimen associated with this sequence were not reported by Li et al. (2015)) The potential of this specimen as *E. laminata* is further corroborated by the additionally sequenced *E. spicata* specimen from the Gulf of Mexico from this study, which clearly groups with the *E. spicata* from Costa Rica suggesting this species has a very wide distribution.

This study places *Alaysia* and *Arcovestia* within the larger Vestimentifera phylogeny for the first time. While the placement of these taxa sister to the other Pacific vent-endemic taxa *Oasisia*, *Ridgeia*, and *Tevnia* is well-supported in all analyses, the reciprocal monophyly of *Alaysia* and *Arcovestia* varied between the nucleotide and amino-acid translated datasets. The Approximately Unbiased (AU) test conducted with both the nucleotide and amino-acid-translated datasets to compare these two possible topologies (reciprocally monophyletic versus paraphyletic *Alaysia* and *Arcovestia*) did not produce any significant results. Tests for substitution saturation in DAMBE (Table 5.4) revealed three potentially saturated genes in the dataset, so

phylogenetic analyses (ML, BI, MP) were repeated with those genes (ATP8, ND4L, ND6) removed. The analyses produced phylogenies identical to the original nucleotide analyses, indicating that saturation was not the cause of the differing topologies. This is unsurprising given that substitution saturation is often suggested to affect mostly deep nodes and branches in a phylogeny (Xia and Lemey, 2012) as has been shown in some major arthropod groups (Xia et al., 2003), while the relationship between *Alaysia* and *Arcovestia* is fairly shallow in this phylogeny. Given that some clades within Vestimentifera, such as *Escarpia* and *Lamellibrachia* have been known to exhibit low diversity in various mitochondrial and nuclear genes such as COI, cytochrome B, and 18S (Cowart et al., 2013; Miglietta et al., 2010), and exhibit small genetic distances between species (Cowart et al., 2013; McCowin et al., 2019; Miglietta et al., 2010), it may be possible that the already limited phylogenetic signal in the nucleotide data is being lost in the amino-acid-translated dataset for *Alaysia* and *Arcovestia*. If this is the case, the nucleotide dataset and phylogeny may be a more accurate representation of the data until more nuclear loci can be obtained for *Alaysia* and *Arcovestia* for a better-supported phylogeny. We therefore maintain Alasyia and *Arcovestia* as separate genera.

While the 16-gene analyses in this study produced topologies that are similar to multiple previous studies utilizing similar datasets (Li et al., 2017, 2015; Patra et al., 2016), some studies report a notable difference in the placement of *Riftia pachyptila* (Li et al., 2017, 2015; Sun et al., 2018). Those studies report *R. pachyptila* as sister to the other vent-endemic taxa, a contrast to the result in this study that placed *R. pachyptila* sister to a clade composed of the rest of the Vestimentifera (excluding *Lamellibrachia*). Past studies often report middling support for the placement of *R. pachyptila*, regardless of its placement in the phylogeny (Li et al., 2017, 2015; Patra et al., 2016), while its placement away from the other vent-endemic taxa in this study is well-supported. Interestingly, this placement may be supported by morphological data. Jones noted some major morphological differences between *R. pachyptila* and the other vent endemic taxa in 1988 which led him to hypothesize that *Riftia* was sister to the remaining Vestimentifera (Jones, 1988). Jones noted such morphological differences as the locations of afferent and

efferent plume vessels and branchial lamellae (axial in *R. pachyptila* and basally situated in all other Vestimentifera), the composition of dorsal and ventral mesenteries (separated by a central structure containing gonad and trophosome in *R. pachyptila*, containing major longitudinal blood vessels in other Vestimentifera), and *Riftia*'s particularly large size compared to other members of Vestimentifera (Jones, 1988). However, *R. pachyptila* does share some morphological traits with the other vent-endemic taxa as well, such as paired excretory pores (Jones, 1988). An AU test was conducted to assess whether the topology recovered by this study was better supported than a constrained topology in which *R. pachyptila* is forced to remain in a clade with the other vent-endemic Vestimentifera. Though the AU test did not produce significant results, the constrained tree was notably close to rejection (p-value was 0.0767, trees are rejected when a p ¡ 0.05) compared to the unconstrainted (ML) tree (p-value of 0.923). While further analysis with more data is desirable to remove any ambiguity about the placement of *R. pachyptila* within Vestimentifera, both the phylogenetic evidence from this study and morphological evidence from past studies point away from a strong affinity between *R. pachyptila* and the other vent-endemic members of Vestimentifera.

The phylogenetic tree topology recovered by the 16-gene analyses in this study has interesting implications for the ancestral habitat of Vestimentifera. The likelihood ancestral state reconstruction (ASR) based on the maximum likelihood nucleotide phylogeny (which placed *Lamellibrachia* sister to all remaining Vestimentifera, followed by *Riftia* sister to the rest) revealed that a vent origin was most likely for the most recent common ancestor of Vestimentifera. This is a stark contrast to Black et al.'s (1997) hypothesis that a seep Vestimentifera ancestor invaded vents, which was based on a tree topology that depicted a grade of seep to vent Vestimentifera. Past studies that showed conflicting topologies were often not well-supported, but the now well-supported phylogeny and ASR from this study suggest a vent ancestral origin for the whole group. In addition, the ASR shows two potential origins of seep taxa within Vestimentifera. One potential seep origin occurs at the most recent common ancestor for the clade composed of *Escarpia*, *Paraescarpia*, and *Seepiophila*, and one potential seep origin occurs origin within the

Lamellibrachia clade (after *Lamellibrachia* juni diverged from the other *Lamellibrachia* species). Contrary to Black et al.'s (1997) hypothesis, this suggests a vent ancestral Vestimentifera colonized seeps. When considering the biogeography of this group, a Pacific origin seems likely given that all major clades include at least some Pacific-dwelling taxa (Figure 5.3). However, none of the vent-endemic taxa of the Pacific (including *Riftia*) have been reported from vents in any other oceans. Some taxa in the Atlantic are known to inhabit multiple habitats including vents, such as various *Lamellibrachia* species, but no Atlantic taxa are known only from vents. *Lamellibrachia* sp. 2, which has been noted from both seeps in the Gulf of Mexico and vents in the Caribbean at the Mid-Cayman Rise (Plouviez et al., 2014), is likely an example of a secondary colonization of vents. *Paraescarpia echinospica* Southward et al., 2002 is the only vestimentiferan species known to inhabit seeps in the Indian Ocean (Java Trench) and has been reported from both vents and seeps in the Pacific (originally as tentative species *Escarpia* sp. E2 by Kojima et al. in 2002 , later identified as *Paraescarpia echinospica* by Kojima et al. in 2003). We therefore hypothesize that an ancestral Pacific/vent Vestimentifera colonized seeps and dispersed across the Atlantic Ocean, perhaps through the South American Seaway prior to the closure of the Panama Isthmus.

5.6.2 Three-gene Phylogenetic Analyses of *Alaysia* and *Arcovestia*

The three-gene (COI, 16S, 18S) phylogenetic analyses (ML, BI, MP) of *Alaysia* and *Arcovestia* showed a well-supported close relationship between *Alaysia spiralis* and *Alaysia* sp. A3 (with a very short branch length) in all analyses, plus a very small intraspecific distance (0.10%) between the two terminals, indicating that the two are conspecific. This small distance between *A. spiralis* and *A.* sp. A3 is also displayed in the haplotype networks (Figure 5.6B: 1 bp between *A.* sp. A3 and other *A. spiralis* specimens, and 4 bp between *A.* sp. A3 and *A. spiralis* from near the type locality). Neither morphological analyses nor vouchers of *A.* sp. A3 were provided by Kojima et al. (2003), but all molecular evidence (branch lengths, distances, networks) support *A.* sp. A3 as another *A. spiralis* specimen. All analyses also consistently

recovered *A. spiralis* (+ *A.* sp. A3) as sister to a clade consisting of *Alaysia* sp. A1 and *Alaysia* sp. A2. *Alaysia* sp. A1 is of particular interest as it was reported by Kojima et al. (2003) to be from a seep off Hatsushima in Japan and may therefore represent the first *Alaysia* record from a seep. All analyses (including distances and networks) also supported the inclusions of *Arcovestia ivanovi* and *Alaysia spiralis* samples from outside their type localities within their respective species (Figures 5.5, 5.6).

The remaining nodes recovered by these ML, BI, and MP analyses seemed unstable and not well-supported, differing widely by method (Figure 5.5, Supplementary Figure B.1.4). While the ML analysis recovered reciprocally monophyletic *Alaysia* and *Arcovestia* clades, neither the BI nor the MP analyses did. However, it should be noted that the ML analysis implemented more nuanced models (e.g., more substitution schemes) than the BI analysis, and when reduced to the same simpler models as the BI analysis, produced an identical topology to the BI analysis. The MP analysis produced a different topology altogether, with very poor support, especially at nodes that differed from the other two analyses (Supplementary Figure B.1.4). While the original ML analysis of this dataset still has some poorly supported nodes, given that the models implemented are likely an improvement on the other two analyses and the result matches the well-supported 16-gene nucleotide phylogeny, the ML analysis is likely the best hypothesis for the relationships between various *Alaysia* species and *Arcovestia ivanovi* given the available data.

While the three-gene phylogenetic analyses are not particularly well-supported at all nodes, there is still clear support for the existence of two new *Alaysia* species, *Alaysia* sp. nov. 1 and *Alaysia* sp. nov. 2. Branch lengths between the new species and their closest relatives are like those between other *Alaysia* species (Figure 5.5). Additionally, minimum uncorrected pairwise distances between the two new *Alaysia* species and their respective closest relatives are similar to or larger than the distances between other putative new *Alaysia* species, excluding *A.* sp. A3 (Kojima et al., 2003, 2002). *Alaysia* sp. nov. 2 has a minimum distance of 3.38% from its closest relative, *A.* sp. A4 (and 4.51% to *A. spiralis*), and *A.* sp. nov. 1 has a minimum distance of 6.02% to its closest relative, *Alaysia* sp. A1 (Table 5.3). While interspecific distances are

low, they are on par or larger than those exhibited by different species in other vestimentiferan genera, such as *Lamellibrachia* (distances on the order of 2% accepted between species) and *Escarpia* (Cowart et al., 2013; McCowin and Rouse, 2018). There also appears to be a clear gap between maximum intraspecific and minimum interspecific distances within this *Alaysia* species: maximum uncorrected distances within each new species are very low (less than 1%, which is slightly less than the variation within *Alaysia* (maximum corrected distances of up to 1.37%). While exact placement of the new species within the *Alaysia* phylogeny is poorly supported and may change with additional data, all molecular data still supports the existence of two new species from the Manus Basin.

5.7 Conclusions

This study provides the most complete mitogenomic phylogeny of Vestimentifera to date, with the addition of ten newly sequenced mitochondrial genomes, including those for *Alaysia spiralis* and *Arcovestia ivanovi*, for which very little genetic data has been previously available. While the phylogenetic analyses presented in this study are largely consistent with other recent mitogenomic analyses of this group, the placement of *Riftia pachyptila* as sister to the rest of the Vestimentifera (excluding *Lamellibrachia*) with high support is notable. This placement has major implications for the habitat evolution of Vestimentifera, as a likelihood ancestral state reconstruction suggests that the most recent common ancestor of all Vestimentifera inhabited vents.

A new species of *Alaysia*, *Alaysia* sp. nov. 2 is also described from the Manus Basin, and molecular data is provided for another putative new species from the same area. The presence of multiple new species in an area previously slated for deep-sea mining highlights the importance of collecting biodiversity data in the deep sea. Without this crucial baseline data, management of these important deep-sea environments would be impossible.

5.7.1 Acknowledgements

Many thanks to Cindy Van Dover, the Duke University Principal Investigator for the 2007 Luk Luk expedition, to Robert Vrijenhoek and Shannon Johnson at the Monterey Bay Aquarium Research Institute, and to the crews of the CSIRO Binatang 2000 Expedition, R/V Melville, and the ROV Jason II. Thanks also to Charlotte Seid for collection management at SIO-BIC and Shirley Sorokin and the south Australian Museum (SAM) for curation and loan of samples. We would also like to thank Jonathan Mesulam and the Alliance of Solwara Warriors for their assistance in choosing a name for the newly described Alaysia species. Thanks also to the TAWNI program of the Chemosynthetic Ecosystems Project (ChEss) of the Census of Marine Life for further support.

Chapter 5 is being prepared for publication. McCowin, Marina F., Collins, Patrick C., and Rouse, Greg W. The dissertation author was the primary investigator and author of the material.

References

Allio, R., Schomaker-Bastos, A., Romiguier, J., Prosdocimi, F., Nabholz, B., Delsuc, F., 2020. MitoFinder: Efficient automated large-scale extraction of mitogenomic data in target enrichment phylogenomics. Mol. Ecol. Resour. 20, 892–905. https://doi.org/10.1111/1755-0998.13160

Beaulieu, J.M., O'Meara, B.C., Donoghue, M.J., 2013. Identifying hidden rate changes in the evolution of a binary morphological character: The evolution of plant habit in campanulid angiosperms. Syst. Biol. 62, 725–737. https://doi.org/10.1093/sysbio/syt034

Bernt, M., Donath, A., Jühling, F., Externbrink, F., Florentz, C., Fritzsch, G., Pütz, J., Middendorf, M., Stadler, P.F., 2013. MITOS: Improved *de novo* metazoan mitochondrial genome annotation. Mol. Phylogenet. Evol. 69, 313–319. https://doi.org/10.1016/j.ympev.2012.08.023

Bolger, A.M., Lohse, M., Usadel, B., 2014. Trimmomatic: a flexible trimmer for Illumina sequence data. Bioinformatics 30, 2114–2120. https://doi.org/10.1093/bioinformatics/btu170

Bright, M., Lallier, F., 2010. The Biology of Vestimentiferan Tubeworms. Oceanogr. Mar. Biol. An Annu. Rev. 48, 213–265. https://doi.org/10.1201/EBK1439821169-c4

Caullery, M., 1914. Sur les Siboglinidae, type nouveau d'invertébrés receuillis par l'expédition

du Siboga. C. Hebd. Seances Acad. Sci. 158, 2014–2017.

Chernomor, O., Von Haeseler, A., Minh, B.Q., 2016. Terrace Aware Data Structure for Phylogenomic Inference from Supermatrices. Syst. Biol. 65, 997–1008. https://doi.org/10.1093/sysbio/syw037

Cowart, D.A., Huang, C., Arnaud-Haond, S., Carney, S.L., Fisher, C.R., Schaeffer, S.W., 2013. Restriction to large-scale gene flow vs. regional panmixia among cold seep *Escarpia* spp. (Polychaeta, Siboglinidae). Mol. Ecol. 22, 4147–4162. https://doi.org/10.1111/mec.12379

Darriba, D., Taboada, G.L., Doallo, R., Posada, D., 2012. jModelTest 2: more models, new heuristics and parallel computing. Nat. Methods 9, 772–772. https://doi.org/10.1038/nmeth.2109

Edler, D., Klein, J., Antonelli, A., Silvestro, D., 2020. raxmlGUI 2.0: A graphical interface and toolkit for phylogenetic analyses using RAxML. Methods Ecol. Evol. 12, 373–377. https://doi.org/10.1111/2041-210X.13512

Elzanowski, A., Ostell, J., 2019. The Genetic Codes [WWW Document]. NCBI.

Feldman, R.A., Shank, T.M., Black, M.B., Baco, A.R., Smith, C.R., Vrijenhoek, R.C., 1998. Vestimentiferan on a Whale Fall. Biol. Bull. 194, 116–119.

Giribet, G., Carranza, S., Baguna, J., Riutort, M., Ribera, C., 1996. First molecular evidence for the existence of a Tardigrada plus Arthropoda clade. Mol. Biol. Evol. 13, 76–84. https://doi.org/10.1093/oxfordjournals.molbev.a025573

Hilário, A., Capa, M., Dahlgren, T.G., Halanych, K.M., Little, C.T.S., Thornhill, D.J., Verna, C., Glover, A.G., 2011. New Perspectives on the Ecology and Evolution of Siboglinid Tubeworms. PLoS One 6, e16309. https://doi.org/10.1371/journal.pone.0016309

Huelsenbeck, J.P., Ronquist, F., 2001. MrBayes: Bayesian inference of phylogeny. Bioinformatics 17, 754–5. https://doi.org/DOI: 10.1093/bioinformatics/17.8.754

Jones, M.L., 1988. The Vestimentifera, their biology, systematic and evolutionary patterns, in: Oceanologica Acta. pp. 69–82.

Jones, M.L., 1985. On the Vestimentifera, new phylum: six new species, and other taxa, from hydrothermal vents and elsewhere. Bull. Biol. Soc. Washingt. 117–158.

Jones, M.L., 1981. *Riftia pachyptila*, new genus, new species, the vestimentiferan worm from the Galápagos Rift geothermal vents. Biol. Soc. Washingt. 93, 1295–1313.

Katoh, K., Rozewicki, J., Yamada, K.D., 2019. MAFFT online service: Multiple sequence alignment, interactive sequence choice and visualization. Brief. Bioinform. 20, 1160–1166.

https://doi.org/10.1093/bib/bbx108

Kojima, S., Ohta, S., Yamamoto, T., Miura, T., Fujiwara, Y., Fujikura, K., Hashimoto, J., 2002. Molecular taxonomy of vestimentiferans of the western Pacific and their phylogenetic relationship to species of the eastern Pacific II. Families escarpiidae and arcovestiidae. Mar. Biol. 141, 57–64. https://doi.org/10.1007/s00227-002-0818-5

Kojima, S., Ohta, S., Yamamoto, T., Ymaguchi, T., Miura, T., Fujiwara, Y., Fujikura, J., Hashimoto, J., 2003. Molecular taxonomy of vestimentiferans of the western Pacific and their phylogenetic relationship to species of the eastern Pacific III. *Alaysia*-like vestimentiferans and relationships among families. Mar. Biol. 142, 625–635. https://doi.org/10.1007/s002270100581

Kozlov, A.M., Darriba, D., Flouri, T., Morel, B., Stamatakis, A., 2019. RAxML-NG: A fast, scalable and user-friendly tool for maximum likelihood phylogenetic inference. Bioinformatics 35, 4453–4455. https://doi.org/10.1093/bioinformatics/btz305

Li, Y., Kocot, K.M., Schander, C., Santos, S.R., Thornhill, D.J., Halanych, K.M., 2015. Mitogenomics reveals phylogeny and repeated motifs in control regions of the deep-sea family Siboglinidae (Annelida). Mol. Phylogenet. Evol. 85, 221–229. https://doi.org/10.1016/j.ympev.2015.02.008

Li, Y., Kocot, K.M., Whelan, N. V., Santos, S.R., Waits, D.S., Thornhill, D.J., Halanych, K.M., 2017. Phylogenomics of tubeworms (Siboglinidae, Annelida) and comparative performance of different reconstruction methods. Zool. Scr. 46, 200–213. https://doi.org/10.1111/zsc.12201

Maddison, W.P., Maddison, D.R., 2018. Mesquite: a modular system for evolutionary analysis. Version 3.51.

McCowin, M.F., Rouse, G.W., 2018. A new *Lamellibrachia* species and confirmed range extension for *Lamellibrachia barhami* (Siboglinidae, Annelida) from Costa Rica methane seeps. Zootaxa 4504, 1–22. https://doi.org/10.11646/zootaxa.4504.1.1

McCowin, M.F., Rowden, A.A., Rouse, G.W., 2019. A new record of *Lamellibrachia columna* (Siboglinidae, Annelida) from cold seeps off New Zealand, and an assessment of its presence in the western Pacific Ocean. Mar. Biodivers. Rec. 12, 12. https://doi.org/10.1186/s41200-019-0169-2

Miglietta, M.P., Hourdez, S., Cowart, D.A., Schaeffer, S.W., Fisher, C., 2010. Species boundaries of Gulf of Mexico vestimentiferans (Polychaeta, Siboglinidae) inferred from mitochondrial genes. Deep. Res. Part II Top. Stud. Oceanogr. 57, 1916–1925. https://doi.org/10.1016/j.dsr2.2010.05.007

Miller, K.A., Thompson, K.F., Johnston, P., Santillo, D., 2018. An Overview of Seabed Mining Including the Current State of Development, Environmental Impacts, and Knowledge Gaps. Front. Mar. Sci. 4. https://doi.org/10.3389/fmars.2017.00418

Nelson, K., Fisher, C.R., 2000. Absence of cospeciation in deep-sea vestimentiferan tube worms and their bacterial endosymbionts. Symbiosis 28, 1–15. https://doi.org/10.2307/25066661

Palumbi, S.R., 1996. Nucleic acid II: the polymerase chain reaction, in: Hillis, D.M., Moritz, C., Mable, B.K. (Eds.), Molecular Systematics. Sinauer Associates, Inc, Sunderland, MA, pp. 205–247.

Pante, E., Simon-Bouhet, B., 2013. marmap: A Package for Importing, Plotting and Analyzing Bathymetric and Topographic Data in R. PLoS One 8, e73051. https://doi.org/10.1371/journal.pone.0073051

Patra, A.K., Kwon, Y.M., Kang, S.G., Fujiwara, Y., Kim, S.J., 2016. The complete mitochondrial genome sequence of the tubeworm *Lamellibrachia satsuma* and structural conservation in the mitochondrial genome control regions of Order Sabellida. Mar. Genomics 26, 63–71. https://doi.org/10.1016/j.margen.2015.12.010

Pleijel, F., Dahlgren, T.G., Rouse, G.W., 2009. Progress in systematics: from Siboglinidae to Pogonophora and Vestimentifera and back to Siboglinidae. C. R. Biol. 332, 140–148. https://doi.org/10.1016/J.CRVI.2008.10.007

Plouviez, S., Jacobson, A., Wu, M., Van Dover, C.L., 2014. Characterization of vent fauna at the mid-cayman spreading center. Deep. Res. Part I Oceanogr. Res. Pap. 97, 124–133. https://doi.org/10.1016/j.dsr.2014.11.011

Rambaut, A., Drummond, A.J., Xie, D., Baele, G., Suchard, M.A., 2018. Posterior summarization in Bayesian phylogenetics using Tracer 1.7. Syst. Biol. 67, 901–904. https://doi.org/10.1093/sysbio/syy032

Revell, L.. J., 2012. phytools: An R package for phylogenetic comparative biology (and other things). Methods Ecol. Evol. 3, 217–223.

Ronquist, F., Huelsenbeck, J.P., 2003. MRBAYES 3: Bayesian phylogenetic inference under mixed models. Bioinformatics 19, 1572–1574.

Rouse, G.W., Fauchald, K., 1997. Cladistics and Polychaetes. Zool. Scr. 26, 139–204. https://doi.org/10.1111/j.1463-6409.1997.tb00412.x

Samadi, S., Puillandre, N., Pante, E., Boisselier, M.C., Corbari, L., Chen, W.J., Maestrati, P., Mana, R., Thubaut, J., Zuccon, D., Hourdez, S., 2015. Patchiness of deep-sea communities in Papua New Guinea and potential susceptibility to anthropogenic disturbances illustrated

by seep organisms. Mar. Ecol. 36, 109–132. https://doi.org/10.1111/maec.12204

Shen, W., Le, S., Li, Y., Hu, F., 2016. SeqKit: A Cross-Platform and Ultrafast Toolkit for FASTA/Q File Manipulation. PLoS One 11, e0163962. https://doi.org/10.1371/journal.pone.0163962

Southward, E.; Galkin, S., 1997. A new vestimentiferan (Pogonophora: Obturata) from hydrothermal vent fields in the Manus Back-arc Basin (Bismarck Sea, Papua New Guinea, Southwest Pacific Ocean). J. Nat. Hist. 31, 43–55.

Southward, E. C., 1991. Three new species of pogonophora, including two vestimentiferans, from hydrothermal sites in the lau back-arc basin (Southwest pacific ocean). J. Nat. Hist. 25, 859–881. https://doi.org/10.1080/00222939100770571

Southward, E. C., Galkin, S. V., 1997. A new vestimentiferan (Pogonophora: Obturata) from hydrothermal vent fields in the manus back-arc basin Bismarck Sea, Papua New Guinea, Southwest Pacific Ocean). J. Nat. Hist. 31, 43–55. https://doi.org/10.1080/00222939700770041

Southward, E.C., Schulze, A., Tunnicliffe, V., 2002. Vestimentiferans (Pogonophora) in the Pacific and Indian Oceans: A new genus from Lihir Island (Papua New Guinea) and the Java Trench, with the first report of *Arcovestia ivanovi* from the North Fiji Basin. J. Nat. Hist. 36, 1179–1197. https://doi.org/10.1080/00222930110040402

Sun, Y., Liang, Q., Sun, J., Yang, Y., Tao, J., Liang, J., Feng, D., Qiu, J.-W., Qian, P.-Y., 2018. The mitochondrial genome of the deep-sea tubeworm *Paraescarpia echinospica* (Siboglinidae, Annelida) and its phylogenetic implications. Mitochondrial DNA Part B 3, 131–132. https://doi.org/10.1080/23802359.2018.1424576

Swofford, D.L., 2003. PAUP *. Phylogenetic Analysis Using Parsimony (* and Other Methods); Version 4.

Trevisan, B., Alcantara, D.M.C., Machado, D.J., Marques, F.P.L., Lahr, D.J.G., 2019. Genome skimming is a low-cost and robust strategy to assemble complete mitochondrial genomes from ethanol preserved specimens in biodiversity studies. PeerJ 7, e7543. https://doi.org/10.7717/peerj.7543

Van Audenhaege, L., Fariñas-Bermejo, A., Schultz, T., Lee Van Dover, C., 2019. An environmental baseline for food webs at deep-sea hydrothermal vents in Manus Basin (Papua New Guinea). Deep. Res. Part I Oceanogr. Res. Pap. 148, 88–99. https://doi.org/10.1016/j.dsr.2019.04.018

Watanabe, H., Kojima, S., 2015. Subseafloor Biosphere Linked to Hydrothermal Systems: TAIGA Concept, in: Ishibashi, J., Okino, K., Sunamura, M. (Eds.), Subseafloor Biosphere Linked to Hydrothermal Systems: TAIGA Concept. Springer Japan, Tokyo, pp. 449–459.

https://doi.org/10.1007/978-4-431-54865-2

Webb, M., 1969. *Lamellibrachia barhami*, gen. nov., sp. nov. (Pogonophora), from the Northeast Pacific. Bull. Mar. Sci. 19, 18–47.

Whiting, M.F., Carpenter, J.C., Wheeler, Q.D., Wheeler, W.C., 1997. The Stresiptera Problem: Phylogeny of the Holometabolous Insect Orders Inferred from 18S and 28S Ribosomal DNA Sequences and Morphology. Syst. Biol. 46, 1. https://doi.org/10.2307/2413635

Xia, X., 2013. DAMBE5: A comprehensive software package for data analysis in molecular biology and evolution. Mol. Biol. Evol. 30, 1720–1728. https://doi.org/10.1093/molbev/mst064

Xia, X., Lemey, P., 2012. Assessing substitution saturation with DAMBE. Phylogenetic Handb. 615–630. https://doi.org/10.1017/cbo9780511819049.022

Xia, X., Xie, Z., Salemi, M., Chen, L., Wang, Y., 2003. An index of substitution saturation and its application. Mol. Phylogenet. Evol. 26, 1–7. https://doi.org/10.1016/S1055-7903(02)00326-3

Conclusion

The main objective of this dissertation was to delimit and describe various new species of deep-sea annelids and mollusks from chemosynthetic habitats and investigate their evolutionary history and biogeography in the Pacific Ocean.

In Chapter 1, we described three new species of *Bathymodiolus* mussels and confirmed the presence of *B. thermophilus* at seeps along the Costa Rica Margin in the East Pacific Ocean. We also showed some stratification by depth of these mussel species. This work underlined the importance of molecular data for future biological and ecological studies. Without molecular data, the number of species in this area, the depth stratification of those species, and the resulting hypotheses about their evolution and biogeography would have been lost.

In Chapter 2, we utilized molecular and morphological data to describe a new species of iphionid scaleworm, *Thermiphione rapanui*, from hydrothermal vents near Rapa Nui (Easter Island). We also demonstrated the paraphyly of *Thermiphione* with molecular data (*Iphionella risensis* nested within *Thermiphione*). We resolved this paraphyly by placing *I. risensis* within *Thermiphione* and emending the diagnosis for *Thermiphione*.

In Chapter 3, we used molecular and morphological data to describe a new species of vestimentiferan tube worm, *Lamellibrachia donwalshi*, from cold seeps along the Costa Rica margin. Despite its close geographic proximity to *Lamellibrachia barhami*, the new species was most closely related to *Lamellibrachia* species from the Atlantic, suggesting a vicariant event may have occurred as the Panama Isthmus began to close nine to twelve million years ago. We also provided sequence data to confirm reports of *L. barhami* at the Costa Rica margin, thereby expanding its known range (now confirmed with molecular data from Vancouver Island to Costa

Rica).

In Chapter 4, we investigated various *Lamellibrachia* samples from the Hikurangi Margin off New Zealand, and identified *Lamellibrachia columna* there. We also revealed close genetic affinities between *L. columna*, some previously undescribed putative new species of *Lamellibrachia* from the West Pacific, and *Lamellibrachia sagami*, and suggested their synonymy under *L. columna*.

In Chapter 5, we described a new species of the vent-endemic vestimentiferan tube worm *Alaysia*, and utilized whole mitochondrial genome data to elucidate the relationships between *Alaysia* and its sister taxon *Arcovestia*, as well as phylogenetic relationships between other members of Vestimentifera. We sequenced a total of ten new mitochondrial genomes to provide additional clarity and resolution for the phylogeny of Vestimentifera as a whole, effectively doubling the number of available whole mitochondrial genomes for the group. Our analyses also revealed that the vent-endemic tube worm *Riftia pachyptila* is likely not as closely affiliated with other vent-endemic Vestimentifera as previously thought. In addition, an ancestral state reconstruction of habitat suggested that the most recent common ancestor of Vestimentifera was a vent-inhabitant, and that seeps were likely colonized at two separate times during the evolution of the group.

Chemosynthetic environments are filled with unique assemblages of organisms; they are essential contributors to the biodiversity of the deep sea and provide many valuable functions, from biogeochemical services to genetic and evolutionary resources (Levin & Sibuet, 2012; Ramirez-Llodra et al., 2010). However, they are also threatened by climate change, deep-sea mining, and other anthropogenic impacts (Levin et al., 2016, 2020; Miller, Thompson, Johnston, & Santillo, 2018). Human impacts are expanding in the deep-sea, yet environmental and biological baselines are lacking (Amon et al., 2022). If we are to properly manage these environments, learn and benefit from their many services, we must create a baseline of genetic biodiversity data that reveals what species are present. My hope is that this work has improved our knowledge of potential endemic species that play crucial roles in their chemosynthetic

habitats, such as *Lamellibrachia donwalshi* and *Alaysia* sp. nov. 2, which is essential to properly inform management practices and protect these ecosystem engineers and their environments from damage. Future directions of this work include further molecular data collection and investigation of the various *Alaysia* species from the Manus and Lau Back-Arc basins (essential to resolving the relationships among them) and establishing a connectivity baseline for one of the foundational species that occurs at chemosynthetic environments along the continental margin in the eastern Pacific: *Lamellibrachia barhami*. While *L. barhami* inhabits a variety of chemosynthetic habitats and exhibits a wide geographic range (Bright & Lallier, 2010; Feldman et al., 1998; Kobayashi & Araya, 2018; Watanabe H., Fujikura K., Kojima S., Miyazaki JI., 2010), little is known about how habitat differences, geographic distance, and barriers to dispersal might affect its distribution. I believe it's likely that high-throughput sequencing approaches that include many nuclear markers will provide a great deal of insight into other members of Vestimentifera as well, especially those that exhibit low levels of diversity in mitochondrial markers.

References

Amon, D. J., Gollner, S., Morato, T., Smith, C. R., Chen, C., Christiansen, S., … Pickens, C. (2022). Assessment of scientific gaps related to the effective environmental management of deep-seabed mining. Marine Policy, 138. https://doi.org/10.1016/j.marpol.2022.105006

Bright, M., & Lallier, F. (2010). The Biology of Vestimentiferan Tubeworms. Oceanography and Marine Biology: An Annual Review, 48, 213–265. https://doi.org/10.1201/EBK1439821169-c4

Feldman, R. A., Shank, T. M., Black, M. B., Baco, A. R., Smith, C. R., & Vrijenhoek, R. C. (1998). Vestimentiferan on a Whale Fall. Biological Bulletin, 194(2), 116–119. Retrieved from https://www.jstor.org/stable/1543041

Kobayashi, G., & Araya, J. F. (2018). Southernmost records of *Escarpia spicata* and *Lamellibrachia barhami* (Annelida: Siboglinidae) confirmed with DNA obtained from dried tubes collected from undiscovered reducing environments in northern Chile. PLoS ONE, 13(10), 1–13. https://doi.org/10.1371/journal.pone.0204959

Levin, L. A., Mengerink, K., Gjerde, K. M., Rowden, A. A., Lee, C., Dover, V., … Brider, J. (2016). Defining "serious harm" to the marine environment in the context of deep-seabed mining. Marine Policy, 74, 245–259. https://doi.org/10.1016/j.marpol.2016.09.032

Levin, L. A., & Sibuet, M. (2012). Understanding Continental Margin Biodiversity: A New Imperative. Annual Review of Marine Science, 4(1), 79–112. https://doi.org/10.1146/annurev-marine-120709-142714

Levin, L. A., Wei, C. L., Dunn, D. C., Amon, D. J., Ashford, O. S., Cheung, W. W. L., … Yasuhara, M. (2020). Climate change considerations are fundamental to management of deep-sea resource extraction. Global Change Biology, 26(9), 4664–4678. https://doi.org/10.1111/gcb.15223

Miller, K. A., Thompson, K. F., Johnston, P., & Santillo, D. (2018). An Overview of Seabed Mining Including the Current State of Development, Environmental Impacts, and Knowledge Gaps. Frontiers in Marine Science, 4(January 2018). https://doi.org/10.3389/fmars.2017.00418

Ramirez-Llodra, E., Brandt, A., Danovaro, R., De Mol, B., Escobar, E., German, C. R., … Vecchione, M. (2010). Deep, diverse and definitely different: Unique attributes of the world's largest ecosystem. Biogeosciences, 7(9), 2851–2899. https://doi.org/10.5194/bg-7-2851-2010

Watanabe H., Fujikura K., Kojima S., Miyazaki JI., F. Y. (2010). Japan: Vents and Seeps in Close Proximity. In The Vent and Seep Biota. Topics in Geobiology, vol 33 (pp. 379–401). https://doi.org/https://doi.org/10.1007/978-90-481-9572-5$_1$2

Appendix A

Appendix for Chapter 1

Supplementary Files: Supplementary Files from published works are included as separate documents. See List of Supplementary Files and/or list of supplementary file names below.

A.1 Supplementary Figure 1

mccowin_concat_A1.pdf: Maximum likelihood trees from concatenated mitochondrial and nuclear datasets

A.2 Supplementary Figure 2

mccowin_mito_A2.pdf: Maximum likelihood trees from individual mitochondrial genes

A.3 Supplementary Figure 3

mccowin_nuclear_A3.pdf: Maximum likelihood trees from individual mitochondrial genes

A.4 Supplementary Figure 4

mccowin_BI_A4.pdf: Complete Bayesian Inference tree with molecular dating analyses conducted in BEAST

A.5 Supplementary Figure 5

mccowin_schematic_A5.pdf: Schematic drawings of the internal views of single valves from
new mussel species

A.6 Supplementary Table 1

mccowin_accessions_A6.xlsx: Sampling data and GenBank accession numbers (COI only) for all sequenced terminals from Costa Rica

A.7 Supplementary Table 2

mccowin_distances_A7.xlsx: Uncorrected and corrected minimum distances for COI data

A.8 Supplementary Table 3

mccowin_measurements_A8.xlsx: Morphological measurements for new *Bathymodiolus* species from Costa Rica and *Bathymodiolus thermophilus* from Costa Rica and the East Pacific Rise

Appendix B

Appendix for Chapter 5

B.1 Supplementary Figures

B.1.1 Supplementary Figure 1

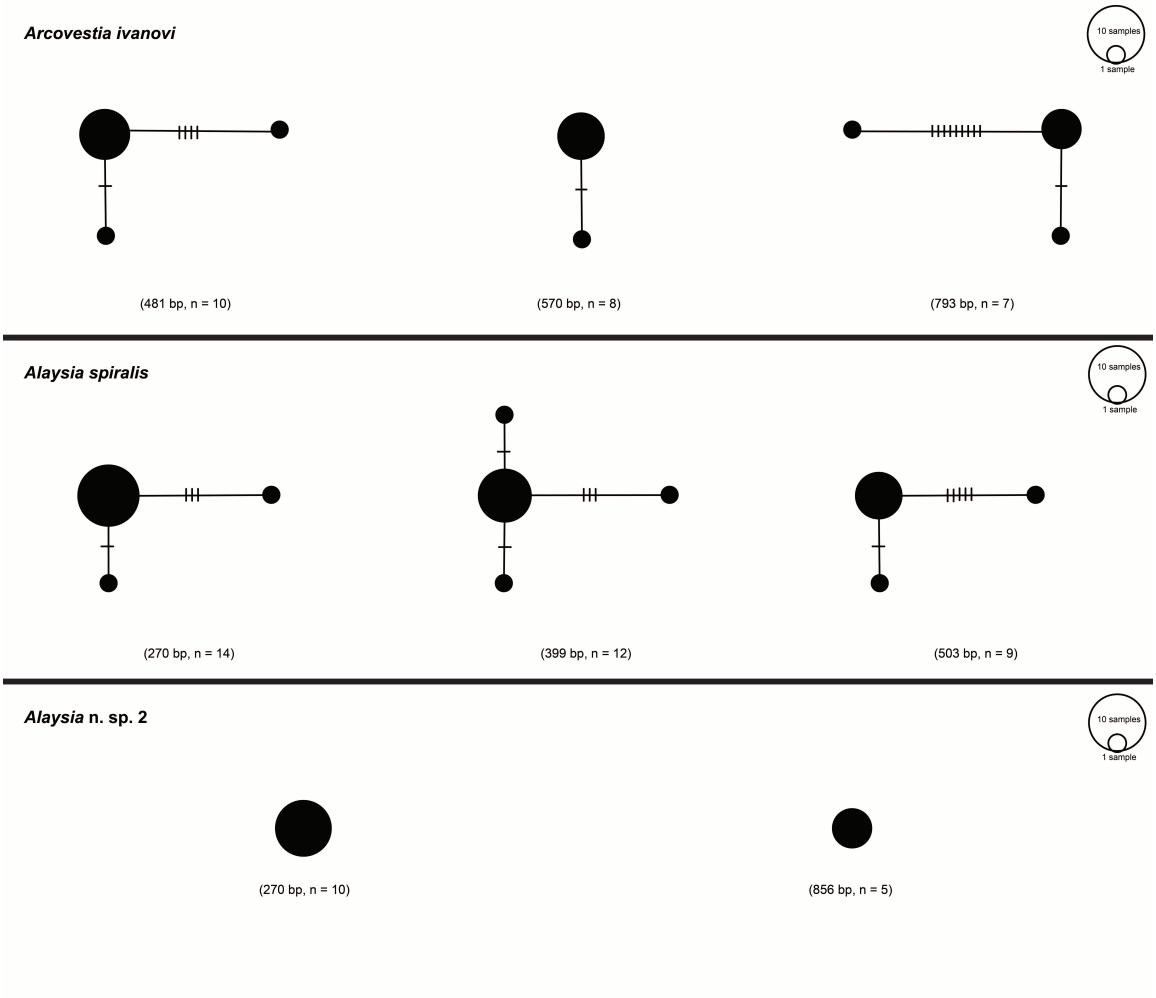

Haplotype networks from COI data for *Arcovestia ivanovi*, *Alaysia spiralis*, and *Alaysia* sp. nov 2. Each panel shows networks created from various alignment lengths and numbers of sequences.

B.1.2 Supplementary Figure 2

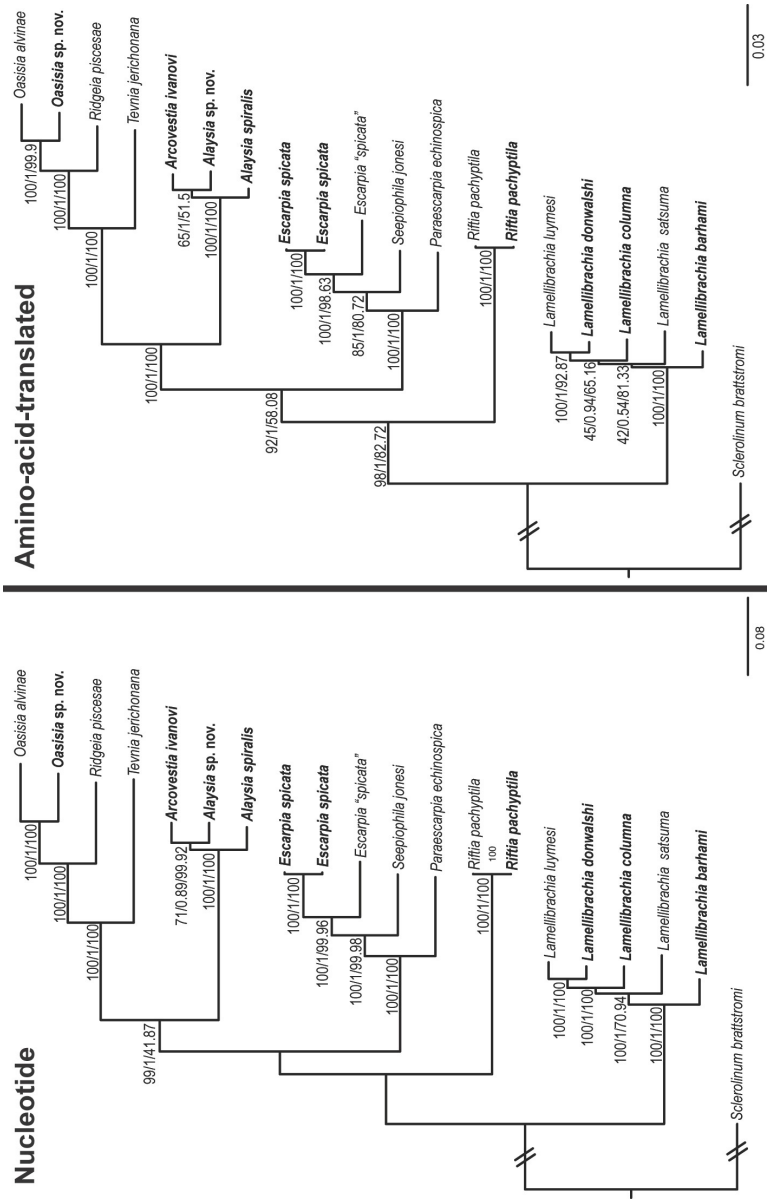

Maximum Likelihood tree of the concatenated 16-gene amino-acid-translated (protein-coding genes only) data. Bootstrap support percentages from the ML analysis are listed first, followed by Bayesian posterior probabilities and bootstrap support percentages from the Maximum Parsimony analysis. Stars indicate maximal support from all three analyses. Nodes not recovered by an analysis are indicated by a hyphen.

B.1.3 Supplementary Figure 3

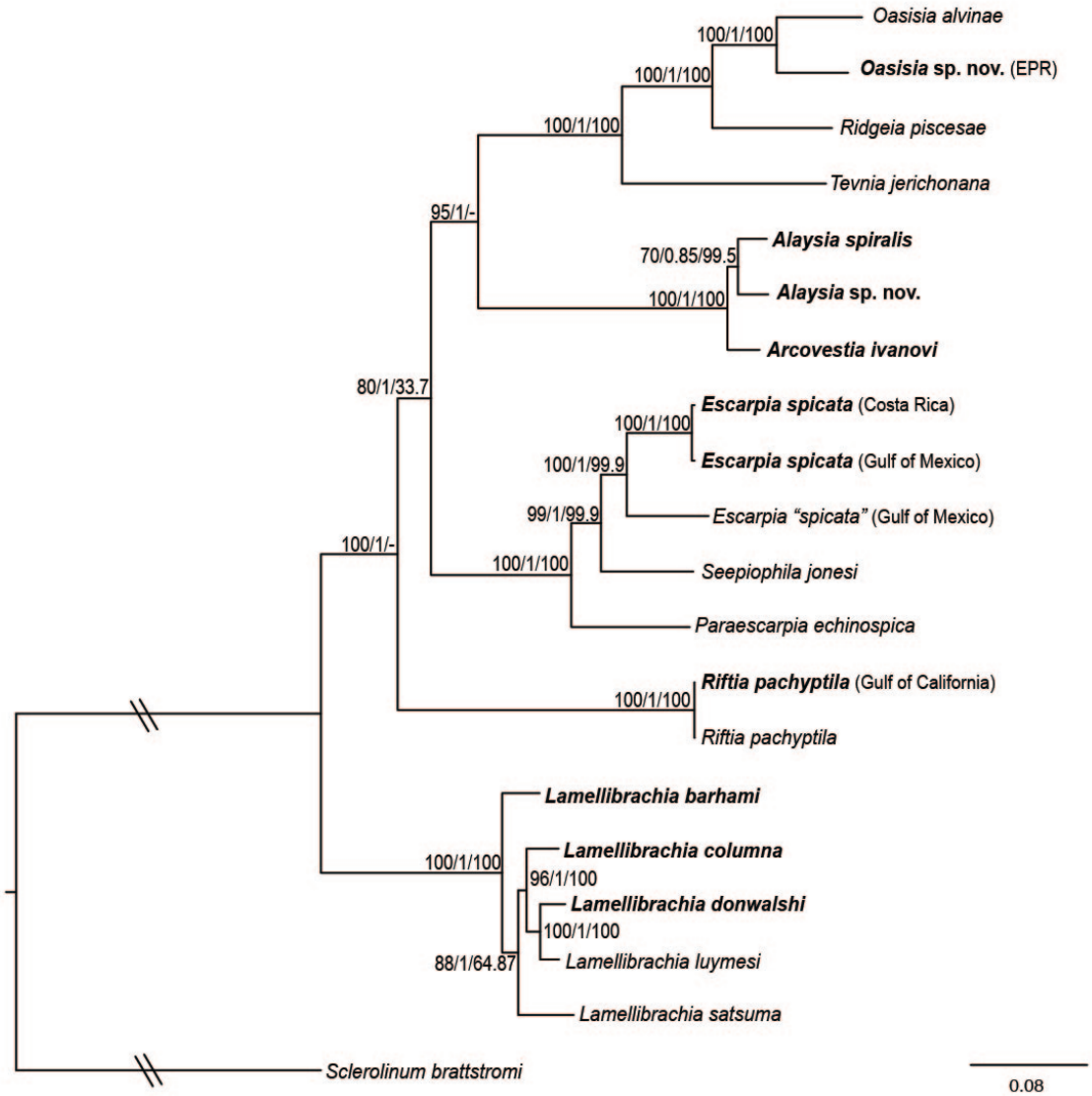

Maximum Likelihood tree of the concatenated 13-gene nucleotide data (saturated genes removed). Bootstrap support percentages from the ML analysis are listed first, followed by Bayesian posterior probabilities and bootstrap support percentages from the Maximum Parsimony analysis. Stars indicate maximal support from all three analyses. Nodes not recovered by an analysis are indicated by a hyphen.

B.1.4 Supplementary Figure 4

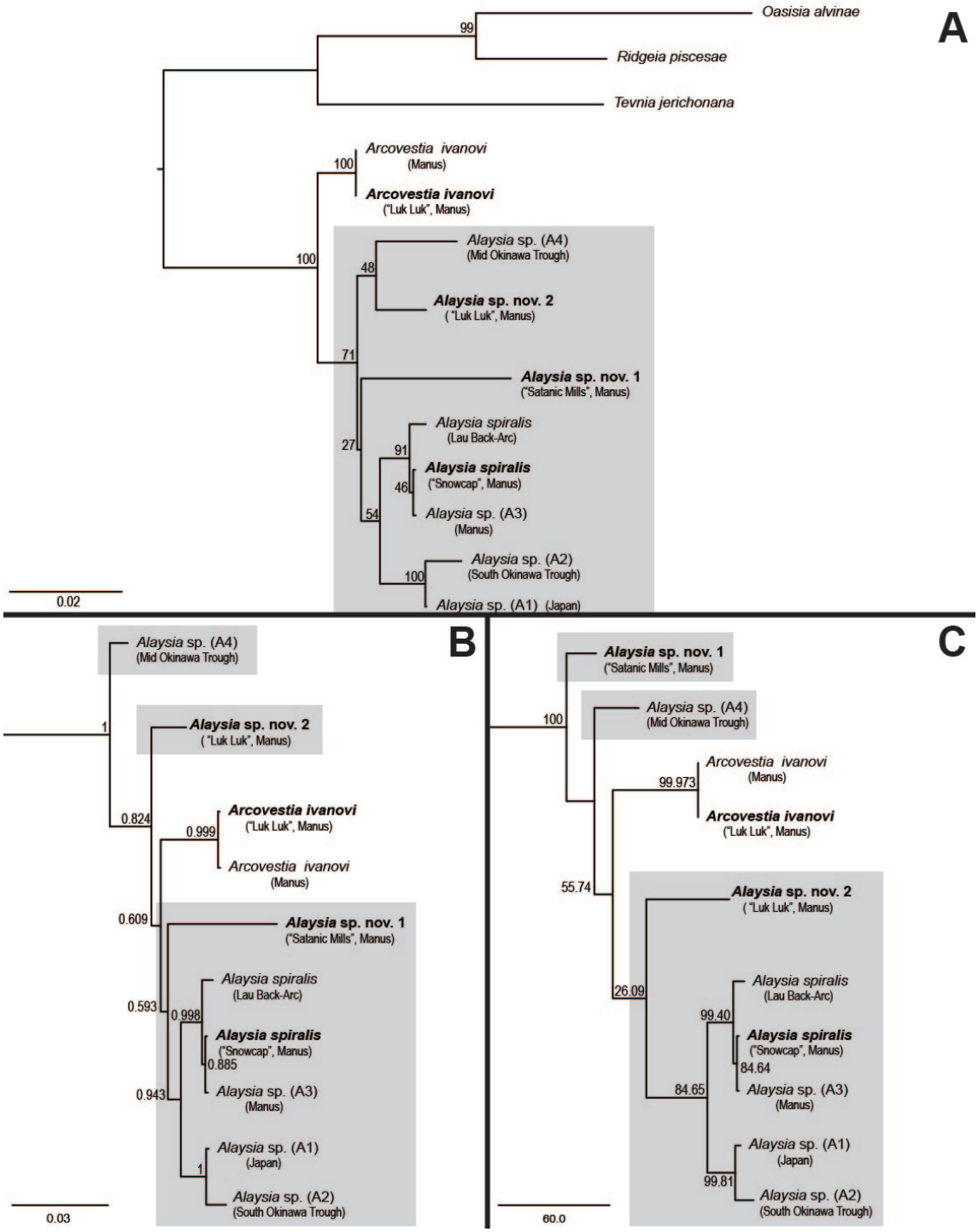

(A) Maximum Likelihood, (B) Bayesian Inference, and (C) Maximum Parsimony trees of the concatenated three-gene nucleotide data. Outgroups are identical for all analyses, but omitted from B and C panels in the figure to conserve space.

B.2 Supplementary Tables

B.2.1 Supplementary Table 1

Primer names, sequences, associated thermal cycler programs, and origins.

Primer Name	Primer Sequence	Approx. Fragment Size (bp)	PCR Program	Reference
Alaysia-51F	AGG AGG GTT TGG AAA CTG GTT	400	94 °C/180 s – (94 °C/30s – 66.6-51.6 °C/45s – 72 °C/ 60 s) * 35 cycles total (TD) – 72 °C/300 s	designed for this study
Alaysia-450R	ATA GTG AGC CCT CCA GCT AGA	400	94 °C/180 s – (94 °C/30s – 66.6-51.6 °C/45s – 72 °C/ 60 s) * 35 cycles total (TD) – 72 °C/300 s	designed for this study
Alaysia-181F	GAA AAG GGA GCC GGT ACA GG	300	94 °C/180 s – (94 °C/30s – 65-50 °C/45s – 72 °C/ 60 s) * 35 cycles total (TD) – 72 °C/300 s	designed for this study
Alaysia-480R	GAA GTG TTT AGG TTT CGG TCT GT	300	94 °C/180 s – (94 °C/30s – 65-50 °C/45s – 72 °C/ 60 s) * 35 cycles total (TD) – 72 °C/300 s	designed for this study
COIf	TCM ACT AAT CAY AAR GAY ATT GGN AC	500	95 °C/300 s – (94 °C/60s – 55 °C/60s – 72 °C/ 120 s) * 35 cycles – 72 °C/420 s	Nelson and Fisher 2000
COIr	CCD CTT AGW CCT ARR AAR TGT TGT TGN GG	500	95 °C/300 s – (94 °C/60s – 55 °C/60s – 72 °C/ 120 s) * 35 cycles – 72 °C/420 s	Nelson and Fisher 2000
16SarL	CGC CTG TTT ATC AAA AAC AT	400	95 °C/180 s – (95 °C/40s – 50 °C/ 40s – 72 °C/50s) * 35 cycles – 72 °C/300 s	Palumbi 1996
16SbrH	CCG GTC TGA ACT CAG ATC ACG T	400	95 °C/180 s – (95 °C/40s – 50 °C/ 40s – 72 °C/50s) * 35 cycles – 72 °C/300 s	Palumbi 1996
18S 1F	TAC CTG GTT GAT CCT GCC AGT AG	595	94 °C/180 s – (94 °C/30s – 49 °C/ 30s – 72 °C/60s) * 35 cycles – 72 °C/480 s	Giribet etl al. 1996, Whiting et al. 1997
18S 5R	CTT GGC AAA TGC TTT CGC	595	94 °C/180 s – (94 °C/30s – 49 °C/ 30s – 72 °C/60s) * 35 cycles – 72 °C/480 s	Giribet etl al. 1996, Whiting et al. 1997
18S 3F	GTT CGA TTC CGG AGA GGG A	595	94 °C/180 s – (94 °C/30s – 49 °C/ 30s – 72 °C/60s) * 35 cycles – 72 °C/480 s	Giribet etl al. 1996, Whiting et al. 1997
18S Bi	GAG TCT CGT TCG TTA TCG GA	595	94 °C/180 s – (94 °C/30s – 49 °C/ 30s – 72 °C/60s) * 35 cycles – 72 °C/480 s	Giribet etl al. 1996, Whiting et al. 1997
18S a2.0	ATG GTT GCA AAG CTG AAA C	590	95 °C/180 s – (94 °C/30s – 52 °C/ 30s – 72 °C/90s) * 35 cycles – 72 °C/480 s	Giribet etl al. 1996, Whiting et al. 1997
18S 9R	GAT CCT TCC GCA GGT TCA CCT AC	590	95 °C/180 s – (94 °C/30s – 52 °C/ 30s – 72 °C/90s) * 35 cycles – 72 °C/480 s	Giribet etl al. 1996, Whiting et al. 1997

B.2.2 Supplementary Table 2

Models chosen for phylogenetic analyses.

		NUCLEOTIDE MODELS		AMINO ACID MODELS	
Dataset	**Gene**	**ML**	**BI**	**ML**	**BI**
mt genomes	12S	TIM2+I+G	GTR+I+G	TIM2+I+G	GTR+I+G
mt genomes	16S	GTR+G	GTR+G	GTR+G	GTR+G
mt genomes	18S	HKY+I+G	HKY+I+G	HKY+I+G	HKY+I+G
mt genomes	ATP6	HKY+I+G	HKY+I+G	MTMAM+G	MTMAM
mt genomes	ATP8	TN93+G	GTR+G	MTREV+G	MTMAM
mt genomes	COX1	GTR+I+G	GTR+I+G	MTZOA+I+G	MTMAM
mt genomes	COX2	TIM2+I+G	GTR+I+G	MTMAM+G	MTMAM
mt genomes	COX3	TIM2+I+G	GTR+I+G	MTZOA+G	MTMAM
mt genomes	CYTB	TIM2+I+G	GTR+I+G	MTMAM+I+G	MTMAM
mt genomes	ND1	TN93+I+G	GTR+I+G	MTMAM+G	MTMAM
mt genomes	ND2	TIM2+I+G	GTR+I+G	MTMAM+G	MTMAM
mt genomes	ND3	HKY+I+G	HKY+I+G	MTMAM+G	MTMAM
mt genomes	ND4	TIM1+I+G	GTR+I+G	MTMAM+G+F	MTMAM
mt genomes	ND4L	TIM2+I+G	GTR+I+G	MTMAM	MTMAM
mt genomes	ND5	TIM3+I+G	GTR+I+G	MTMAM+G	MTMAM
mt genomes	ND6	TIM2+I+G	GTR+I+G	MTMAM+G	MTMAM
3-gene	COX1	TIM3+I	GTR+I	-	-
3-gene	16S	TIM2+I	GTR+I	-	-
3-gene	18S	HKY+G	HKY+G	-	-
ASR	12S	TIM2+I+G	-	-	-
ASR	16S	GTR+G	-	-	-
ASR	18S	TN93+I+G	-	-	-
ASR	ATP6	TPM3uf+I+G	-	-	-
ASR	ATP8	GTR+I+G	-	-	-
ASR	COX1	GTR+I+G	-	-	-
ASR	COX2	TIM2+I+G	-	-	-
ASR	COX3	TIM2+I+G	-	-	-
ASR	CYTB	TIM2+I+G	-	-	-
ASR	ND1	TN93+I+G	-	-	-
ASR	ND2	TIM2+I+G	-	-	-
ASR	ND3	TN93+I+G	-	-	-
ASR	ND4	GTR+I+G	-	-	-
ASR	ND4L	TIM2+I+G	-	-	-
ASR	ND5	TIM3+I+G	-	-	-
ASR	ND6	TIM2+I+G	-	-	-